UNIVERSIDAD NACIONAL AUTÓNOMA DE MÉXICO

MAESTRÍA Y DOCTORADO EN CIENCIAS BIOQUÍMICAS

Caracterización de los factores que favorecen la expresión alotópica del gen mitocondrial *cox2* en *Saccharomyces cerevisiae*

TESIS

QUE PARA OPTAR POR EL GRADO DE:

Doctor en Ciencias

PRESENTA:

M. en C. Christian Felipe Nieto Panqueva

TUTOR PRINCIPAL:

Dr. Diego González-Halphen
Instituto de Fisiología Celular, UNAM

MIEMBROS DEL COMITÉ TUTOR:

Dra. Sobeida Sánchez Nieto
Facultad de Química, UNAM

Dr. Leonardo Peraza Reyes
Instituto de Fisiología Celular, UNAM

Ciudad de México. Abril, 2024

PROTESTA UNIVERSITARIA DE INTEGRIDAD Y HONESTIDAD ACADÉMICA Y PROFESIONAL
(Graduación con trabajo escrito)

De conformidad con lo dispuesto en los artículos 87, fracción V, del Estatuto General, 68, primer párrafo, del Reglamento General de Estudios Universitarios y 26, fracción I, y 35 del Reglamento General de Exámenes, me comprometo en todo tiempo a honrar a la Institución y a cumplir con los principios establecidos en el Código de Ética de la Universidad Nacional Autónoma de México, especialmente con los de integridad y honestidad académica.

De acuerdo con lo anterior, manifiesto que el trabajo escrito titulado:

Caracterización de los factores que favorecen la expresión alotópica del gen mitocondrial *cox2* en *Saccharomyces cerevisiae*

que presenté para obtener el grado de ------Doctorado------es original, de mi autoría y lo realicé con
el rigor metodológico exigido por mi programa de posgrado, citando las fuentes de ideas, textos, imágenes, gráficos u otro tipo de obras empleadas para su desarrollo.

En consecuencia, acepto que la falta de cumplimiento de las disposiciones reglamentarias y normativas de la Universidad, en particular las ya referidas en el Código de Ética, llevará a la nulidad de los actos de carácter académico administrativo del proceso de graduación.

Atentamente

M. en C. Christian Felipe Nieto Panqueva
Cuenta UNAM 51504880-9

(Nombre, firma y Número de cuenta de la persona alumna)

HONORABLE JURADO

PRESIDENTE: Dr. Felipe Cruz García

SECRETARIO/A: Dra. Alexa Villavicencio Queijeiro

VOCAL: Dra. Gloria Hernández Alcántara

VOCAL: Dra. Xochitl Pérez Martínez

VOCAL: Dr. Sebastian Poggio Ghilarducci

RECONOCIMIENTOS

El presente trabajo se realizó bajo la dirección del Dr. Diego González-Halphen en el laboratorio 324 Norte del Departamento de Genética Molecular de la División de Investigación Básica del Instituto de Fisiología Celular de la UNAM.

El Comité tutor que asesoró el desarrollo de esta tesis estuvo conformado por:

La Dra. Sobeida Sánchez Nieto de la Facultad de Química, UNAM

El Dr. Leonardo Peraza Reyes del Instituto de Fisiología Celular, UNAM

El Dr. Diego González-Halphen del Instituto de Fisiología Celular, UNAM

Este trabajo forma parte del proyecto de investigación apoyado por donativos del Consejo Nacional de Ciencia y Tecnología (CONACyT), con el número de proyecto CF2019-21856 y el Programa de Apoyo a Proyectos de Investigación e Innovación Tecnológica (PAPIIT) de la Dirección General de Asuntos del Personal Académico (DGAPA, UNAM), número IN207023.

Al Consejo Nacional de Ciencia y Tecnología (CONACyT) por la beca otorgada para realizar los estudios de doctorado (CVU 700670).

Al Programa de Maestría y Doctorado en Ciencias Bioquímicas de la UNAM, en especial a Julio Ignacio Palacio Ordoñez, Adelina González Pérez y a la M. en C. Norma Trejo Medina.

Al Programa de Apoyo a los Estudios de Posgrado (PAEP), por el apoyo económico que me permitió asistir al a XXXIII Congreso Nacional de Bioquímica, así como a la estancia de investigación en el laboratorio del Dr. Patrice Hamel en el Departamento de Genética Molecular de la Universidad Estatal de Ohio, EU en 2021.

Al Dr. Patrice Hamel de la Universidad Estatal de Ohio, EE. UU., a la Dra. Marie-France Giraud del Instituto de Bioquímica y Genética Celular, UMR5095 de la Universidad de Burdeos, Francia, y al Dr. Benjamín Podbilewicz del Instituto de

Tecnología Technion, Israel, cuyas valiosas ideas, sugerencias y continuas recomendaciones ayudaron a enriquecer este trabajo.

A la Q.P.B. Miriam Vázquez Acevedo por la ayuda técnica brindada durante el desarrollo de este trabajo.

Al laboratorio de la Dra. Soledad Funes del Instituto de Fisiología Celular, en especial a la Dra. Ariann Elizabeth Mendoza Martínez y a la Dra. María Clara Avendaño Monsalve por su continua e invaluable orientación durante el desarrollo de este trabajo.

Al laboratorio del Dr. Roberto Coria del Instituto de Fisiología Celular, en especial a la Dra. Laura Kawasaki y a la M. en C. Yaisa Castillo Casaña, por su generoso apoyo en la implementación de técnicas de biología molecular y facilitar el uso de equipos.

Al laboratorio del Dr. Salvador Uribe Carvajal del Instituto de Fisiología Celular, en especial a la Dra. Natalia Chiquete Félix, y a la M. en C. Carolina Ricardez García por facilitar el uso de equipos.

Al laboratorio de la Dra. Xochitl Pérez Martínez del Instituto de Fisiología Celular, en especial a la Dra. Yolanda Camacho Villasana, y al M. en C. Ulrik Hiram Pedroza por el valioso aporte de reactivos, cepas y anticuerpos.

A la Dra. Laura Ongay Larios, a la Biol. Guadalupe Códiz Huerta y a la M. en C. Minerva Mora Cabrera, quienes forman parte de la Unidad de Biología Molecular del Instituto de Fisiología Celular de la UNAM, por llevar a cabo la síntesis de desoxioligonucleótidos y secuenciación de DNA requeridas para este trabajo.

A María del Rosario Villaseñor Ávila y Gabriela Valdés Silva, asistentes ejecutivas de los Departamentos de Biología Celular y del Desarrollo y de Genética Molecular del IFC, por su apoyo e invaluable ayuda técnica.

AGRADECIMIENTOS

A mi familia.

Este doctorado representa el fruto de una semilla plantada por mi madre, Ana Silvia Panqueva, en tiempos en los que la genética, la biología molecular y la bioquímica eran conceptos desconocidos para mí. Su cariño y visión han trascendido nuestros diferentes tiempos y espacios. Este logro es un tributo a ella y al legado que su perspectiva nos ha garantizado. Lo que se describe a continuación es un reflejo de sus enseñanzas, que me ha enfatizado que el verdadero significado de la vida radica en la apreciación del tiempo y el esfuerzo consciente.

En esta etapa de mi vida, he sido acompañado por el inquebrantable apoyo de mi pareja, Lina Rivera Cantillo. Agradezco profundamente a Lina por transmitirme su amor y alegría, que me han hecho sentir ligero y renovado para enfrentar los retos que este y otros procesos de la vida suponen. Sus aspiraciones iluminan constantemente mi camino hacia la automejora como ser humano, y su forma de compartir su vida conmigo es mi continuo recordatorio de que el futuro más prometedor se forma únicamente a través del amor.

Con mi hermana, Karol Nieto Panqueva atesoro muchos momentos que en nuestra infancia fueron formativos y definitorios para los caminos que emprenderíamos en nuestras vidas. Su perseverante lucha por labrarse un lugar fuera de nuestro hogar ha sido una de las inspiraciones más asiduas que he tenido durante la realización de este trabajo.

El apoyo brindado por Hector Paez Gutiérrez ha sido un fundamental para mi formación profesional. A él le agradezco su confianza y credibilidad en mí y por compartir, desde que el momento en que nos conocimos, su paciencia, su cariño y su inconfundible alegría.

A mi asesor.

Agradezco a Diego Gonzalez-Halphen por aceptarme como su alumno y por ofrecerme, a cambio de mi trabajo, su empatía, su continua escucha y comprensión de mis circunstancias personales, respaldándome durante todo este proceso. Además de sus invaluables enseñanzas científicas y académicas, le agradezco por compartir constantemente su fluidez, experiencia y alegres anécdotas de vida.

A los miembros de mi laboratorio e instituto.

Agradezco a Miriam Vázquez-Acevedo sus contribuciones y aportes a este proyecto. Su experiencia y conocimientos han sido fundamentales para finalizarlo satisfactoriamente.

A mis compañeros de laboratorio Diana, Juan, Héctor, Marcos, Sergio, y José Luis por sus enseñanzas, consejos y opiniones, los cuales han mejorado mi forma de abordar este proyecto.

A Cristopher, Alejandra y Till, mi sincero agradecimiento, por su colaboración y disposición para trabajar en equipo complementando diversas partes de este proyecto.

A Soledad Funes Argüello y sus estudiantes por sus amistad y camaradería. Agradezco todas las veces que me hicieron sentir como parte de su equipo, involucrándome en sus reuniones y convivencias.

A Sandra, Paula y Amin, quienes siempre me recibieron con una sonrisa cuando los encontraba en los pasillos.

A mis amigos.

Agradezco a mis amigos, tanto los actuales como aquellos que han estado presentes en las diferentes etapas de mi vida que me trajeron hasta aquí. A Zaide, Sebastian, Juan Camilo, Zamy “Cosme”, Carlos, Italo, Julian, Guillermo, MariaCamila, Raymon, Julio Cesar, Diana, Matías, Juan David, Bryan, Jesús, Yan Wong Ching, Tanya, Cristian, Alexander, Irene, Facundo, Adrián, Lee Dong Jin, Mariel, Hector, Marcos, Sergio, Amin, Micah, Mary, Emma, Mitch, Ankita y Kate. Su amistad es un regalo inestimable que atesoro con gratitud.

DEDICATORIA

Para Lina y Río quienes con su amor han transformado instantes de soledad, frustración y ansiedad en momentos de luz, alegría y serenidad.

"To go wrong in one's own way is better than to go right in someone else's. In the first case, you are a man; in the second you are no better than a bird".

Fyodor Dostoevsky

Prelude In E Minor - Gerry Mulligan Sextet

ÍNDICE

RESUMEN

El término expresión alotópica hace referencia a la reubicación artificial de un gen desde un organelo celular, como la mitocondria o el cloroplasto, al núcleo. En investigaciones previas, se produjo alotópicamente a la subunidad 2 de la enzima citocromo *c* oxidasa (COX) en la levadura *Saccharomyces cerevisiae* (Supekova et al., 2010). El precursor $Cox2^{W56R}$, sintetizado en el citosol celular, restauró el crecimiento de una cepa mutante nula *Δcox2* en sustratos no fermentativos, aunque solamente se recuperó un 60% de la actividad de COX en comparación con una cepa silvestre (wt) (Cruz-Torres et al., 2012). En este estudio, utilizando cepas que sintetizan $Cox2^{W56R}$ a partir de un gen integrado a un cromosoma nuclear y cepas que producen $Cox2^{W56R}$ a partir de un plásmido episomal de alto número de copias, exploramos si la sobreexpresión de determinados genes, relacionados directa o indirectamente con la importación, internalización, maduración y ensamblaje de $Cox2^{W56R}$, podría incrementar la importación de esta proteína alotópica al interior de la mitocondria, facilitando así el crecimiento de la levadura en medios respiratorios. Nuestra estrategia experimental se basó en tres enfoques principales: 1) un análisis de supresores multicopia; 2) una predicción fundamentada, donde se sobreexpresaron genes conocidos; y 3) la exploración del papel de la subunidad Mgr2 del translocador TIM23, un factor que modula la translocación y liberación lateral de precursores hidrofóbicos.

En el primer enfoque experimental, al transformar la cepa de integración nuclear con una biblioteca de supresores multicopia, se identificaron tres genes, *TYE7*, *RAS2* y *COX12*, cuya sobreexpresión favoreció la internalización de la subunidad alotópica a la mitocondria. En el segundo enfoque, se seleccionaron genes conocidos cuyos productos proteicos participan en la importación de proteínas a la mitocondria, para ser sobreexpresados. La sobreproducción de Cox20, Oxa1 y Pse1 aumentó el crecimiento de la cepa que produce $Cox2^{W56R}$ en alto número de copias, indicando que estos factores de alguna manera favorecen la internalización de la subunidad alotópica en la mitocondria. En el tercer enfoque, se investigó el papel de Mgr2, un factor encargado de modular la distribución de proteínas por el translocador TIM23 (Gebert et al., 2012). Se encontró que la sobreproducción de Mgr2 afecta negativamente los niveles de la proteína alotópica $Cox2^{W56R}$, a la vez que la eliminación del gen correspondiente *MGR2*, disminuyó significativamente los niveles de $Cox2^{W56R}$. Esto ocurrió bajo los dos

escenarios de expresión explorados: constitutivamente o en alto número de copias. En conjunto, todos estos hallazgos nos llevaron a proponer un modelo detallado de la biogénesis de la proteína alotópica $Cox2^{W56R}$.

INTRODUCCIÓN

Las mitocondrias

Las mitocondrias son organelos que están presentes en la mayoría de los organismos eucariotas. Aunque su principal función es la fosforilación oxidativa, también contribuyen a la biosíntesis de las pirimidinas, los aminoácidos, los fosfolípidos, los nucleótidos, las coenzimas de folato, el grupo hemo y la urea, entre otros metabolitos (Attardi y Schatz, 1988). La síntesis de las proteínas que conforman a este organelo involucra una extensa cooperación del genoma nuclear con el mitocondrial. Además, implica la operación de mecanismos especializados para la importación de proteínas y el ordenamiento intramitocondrial de proteínas, fosfolípidos y probablemente RNAs sintetizados *ex situ* (Rinehart et al., 2005; Salinas-Giegé et al., 2015).

Estructura de la mitocondria

Las mitocondrias presentan una forma tubular, y generalmente se encuentran ubicadas a lo largo de la membrana plasmática o del núcleo, aunque su disposición puede variar en diferentes tipos celulares y en diversas condiciones fisiológicas. El número de mitocondrias en una célula es variable y tiene una estrecha dependencia de las condiciones metabólicas de la misma (Hackenbrock, 1966; Pon y Schatz, 1991). Eventos continuos de fusión y fisión, tienden a formar una red mitocondrial altamente dinámica que mantiene la funcionalidad y adaptabilidad del organelo (Nunnari et al., 1997).

Morfológicamente, la mitocondria está constituida por una bicapa lipídica denominada membrana interna mitocondrial (MIM), que incluye cardiolipina y diversos fosfolípidos, la cual encapsula una matriz acuosa (Fig. 1). La MIM presenta regiones yuxtapuestas a la membrana externa y otras que sobresalen en forma de pliegues, denominadas crestas (*cristae,* G. Palade, 1956), las cuales se proyectan internamente hacia la matriz mitocondrial. Las crestas aumentan la superficie de la membrana interna y son el sitio donde se lleva a cabo la fosforilación oxidativa. Rodeando a esta bicapa invaginada, la membrana externa (MEM) funciona como la frontera del organelo, delimitándolo del

citosol celular. Entre ambas membranas se genera un espacio continuo que también es acuoso y que se denomina espacio intermembranal (EIM) (Frey y Manella, 2000).

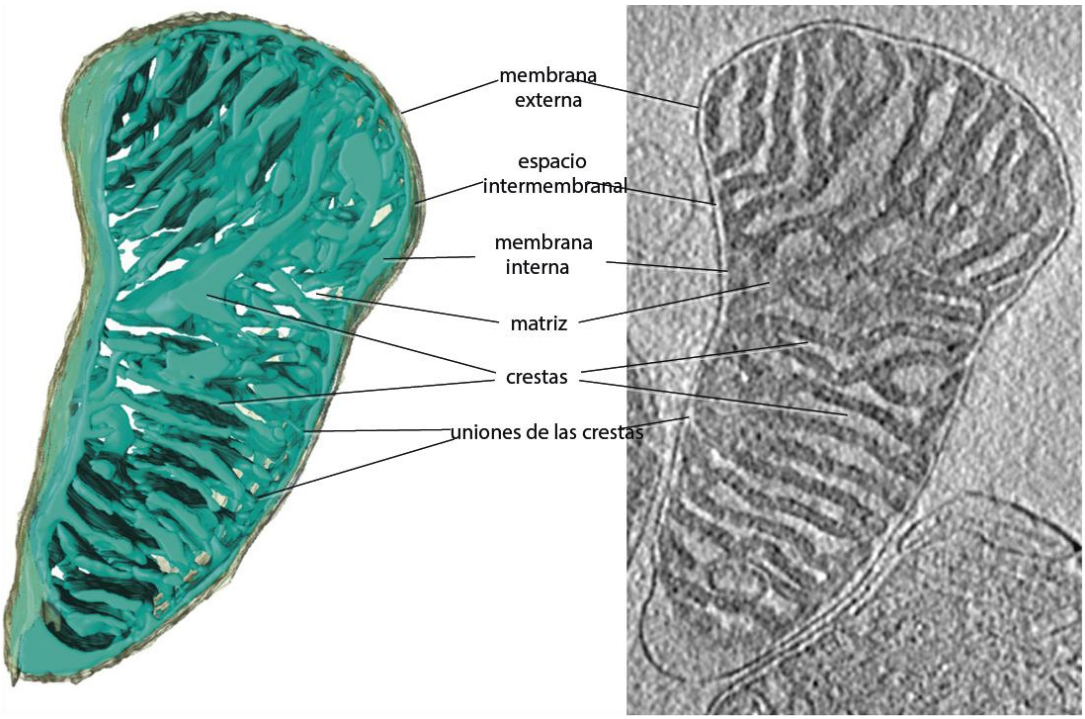

Figura 1. Estructura tridimensional de una mitocondria de corazón de ratón determinado mediante crío-tomografía electrónica. La membrana externa (gris-verde) envuelve a la membrana interna (azul claro). La membrana interna está separada de la membrana externa por solo ~20 nm y está plegada en crestas laminares, que cruzan la matriz. La membrana interna gira bruscamente en las uniones donde empiezan a formarse las crestas mitocondriales (Figura modificada de Kühlbrandt, 2015. *BMC Biology* 13:89).

Biogénesis de la mitocondria

La biogénesis mitocondrial, también conocida como mitocondriogénesis, involucra dos procesos distintos: la síntesis y formación de las membranas mitocondriales, así como los compartimentos que estas delimitan. También implica el ensamblaje y organización espacial de los complejos que llevan a cabo la fosforilación oxidativa y demás

reacciones enzimáticas (Mitchell 1961, Green y Tzagaloff, 1966). En el primer proceso, a pesar de que las membranas biológicas no se forman *de novo* y derivan del crecimiento y división de membranas preexistentes, es necesario garantizar ciertos pasos para asegurar su adecuada compartimentalización dentro de la célula, los cuales dependen principalmente de genes nucleares. En cuanto al segundo proceso, su control está regido tanto por genes mitocondriales como nucleares (Roger et al., 2017). La razón por la cual la síntesis de componentes mitocondriales implica dos genomas distintos se debe al origen endosimbiótico de este organelo.

Origen genético dual de los complejos mitocondriales

Se piensa que las mitocondrias son el resultado de un evento endosimbiótico entre una bacteria ancestral de vida libre perteneciente a la rama de las alfa-proteobacterias (Andersson et al., 1998; Karlberg et al., 2000; Williams et al., 2007; Martjin, 2018) y un ancestro de arqueas pertenecientes al phylum Lokiarchaeota (Spang et al., 2015; Zaremba-Niedzwiedzka et al., 2017). Probablemente, el arqueón hospedero tenía la capacidad de realizar glucólisis anaerobia y fermentación, mientras que el huésped bacteriano ya contaba con un sistema de transporte de electrones cuyo aceptor final era el oxígeno. Ambos procariontes debieron contar con mecanismos para replicar y transcribir DNA, sintetizar proteínas y realizar biosíntesis de lípidos para formar membranas. Las enzimas del ciclo de Krebs también pueden haber estado presentes en ambos organismos e interconvertir compuestos de carbono de cadena corta y aminoácidos (Müller et al., 2012). El fenómeno de endosimbiosis fue un evento de gran relevancia evolutiva, que dio lugar a la eucariogénesis y posteriormente a la aparición de eucariontes complejos en la tierra (Alberts et al., 2022). Esta asociación simbiótica pudo conducir a cierta redundancia en la información genética, la cual comenzó a transferirse funcionalmente desde la proto-mitocondria al proto-núcleo del hospedero o, simplemente, a perderse. No obstante, a pesar de esta migración masiva de genes, una porción de ellos fue retenida y ha permanecido hasta ahora en la gran mayoría de los genomas mitocondriales (Gray et al., 1998). Aunque existe una amplia diversidad en el número de genes que existen en el genoma mitocondrial de eucariontes, casi siempre está presente un subconjunto específico de genes que codifican subunidades de los

complejos de la fosforilación oxidativa y en ocasiones, factores necesarios para la expresión o ensamblaje de dichas subunidades (Attardi y Schatz, 1988; Gray et al., 1999). También están presentes genes que codifican a varios rRNAs y tRNAs. La presencia de un mismo subconjunto de genes en los genomas mitocondriales de diversas especies apoya la hipótesis de que la mitocondria tiene un origen monofilético (todas las mitocondrias provienen de un ancestro común único) y que la diversidad de los genes que contiene, es el producto de pérdidas de genes al azar en los diversos linajes de eucariontes.

El DNA pudo migrar de la mitocondria al núcleo por diversos mecanismos, dentro de los que se incluyen; eventos de fusión y fisión mitocondrial, el rompimiento de las membranas mitocondriales debido al estrés celular, la digestión del organelo por lisosomas o vacuolas (Berg y Kurkland, 2000; Brennicke et al., 1993; Kurkland y Andersson, 2000) o a la migración de transcritos de RNA que por un proceso de transcripción reversa se integraron al DNA cromosomal (Thorsness y Weber, 1996). Se ha reportado que una vez que llegan al núcleo, los ácidos nucleicos se pueden integrar al genoma nuclear por eventos de rompimiento y reparación de doble hebra (Ricchetti et al., 1999), o por procesos de unión de extremos no-homólogos (Blanchard and Schmidt, 1996).

Transferencia de genes de la mitocondria al núcleo

La transferencia de genes de la proto-mitocondria al núcleo ha ocurrido de manera variable en diferentes organismos, a través de procesos aleatorios. A lo largo de la historia evolutiva, parece haber una presión de selección que ha llevado a la reducción del genoma mitocondrial hasta alcanzar un mínimo en cuanto al número de genes. Esto ha provocado que las mitocondrias de los metazoos presenten la mayor densidad posible de genes por unidad de longitud de DNA (Adams y Palmer, 2003; Karakaidos 2020). Esta presión de selección se ha vinculado con la alta tasa de mutación que exhiben algunos genomas mitocondriales. Los genes mitocondriales que fueron transferidos al núcleo tienen una mayor probabilidad de estar protegidos de la acción de mutágenos debido a la presencia de histonas, y a la vez, están menos expuestos a radicales libres (Allen et al., 1996). Además, los genes transferidos al núcleo pueden asegurar su

herencia transgeneracional por eventos de reproducción sexual y recombinación (Rubio et al., 2008). Se ha descrito que los genes conservados en la mitocondria corresponden a proteínas que poseen una alta hidrofobicidad. Por lo tanto, si fueran sintetizados en el citosol, la importación de dichas proteínas a través de las membranas mitocondriales y su correcto ensamblaje dentro del organelo serían factores limitantes (Popot y de Vitry, 1990; Nieto-Panqueva et al., 2023). Como consecuencia, algunos de estos genes se localizan invariablemente en el genoma mitocondrial y no se encuentran en el genoma nuclear de ningún organismo, como es el caso de *nd1*, *nd2*, *nd4*, *nd5*, *nd6*, *cox1* y *cob* (Claros et al., 1995; Flegontov et al., 2015; Formaggioni et al., 2021).

En cuanto a los genes mitocondriales que fueron transferidos al núcleo, se precisó de su activación para que fuesen funcionales, lo que implicó modificaciones en el código genético y en el uso de codones. Además, los genes que fueron relocalizados al núcleo eventualmente incorporaron promotores y otros elementos reguladores que controlan su expresión. De especial importancia son las secuencias nucleotídicas que codifican presecuencias, las cuales dirigen a los productos proteicos adyacentes hacia la mitocondria (Fox, 2012). La migración de genes mitocondriales al núcleo requirió asimismo elementos celulares citosólicos y membranales tanto del hospedero arqueón como del endosimbionte bacteriano, por ejemplo, chaperonas, receptores de membrana y reguladores transcripcionales, que dieron origen a los sistemas de importación mitocondrial, tal como se conocen hoy en día (de Grey, 2005).

Sistemas de importación de proteínas a la mitocondria

Las proteínas mitocondriales sintetizadas en el citosol, también conocidas como precursores, constituyen aproximadamente el 95% del proteoma mitocondrial en eucariontes modernos (Vögtle et al., 2017). Estas proteínas son sintetizadas en ribosomas citosólicos y llevan consigo señales específicas que las dirigen hacia las maquinarias translocadoras localizadas en los distintos compartimentos mitocondriales. A la fecha, se han identificado al menos cinco vías de importación (Fig. 2), las cuales dependen de diferentes maquinarias conocidas como complejos de importación (Chacinska et al., 2009). Dado que las proteínas son importadas en una configuración

intrínsecamente desestructurada, chaperonas tanto citosólicas como mitocondriales, junto con otros factores de ensamblaje, desempeñan un papel crucial en el proceso de internalización. Su función principal radica en preservar la competencia de los precursores durante la importación, al mismo tiempo que participan activamente guiando y uniendo estos precursores a las proteínas receptoras en la superficie de la MEM (Hansen y Herrmann, 2019).

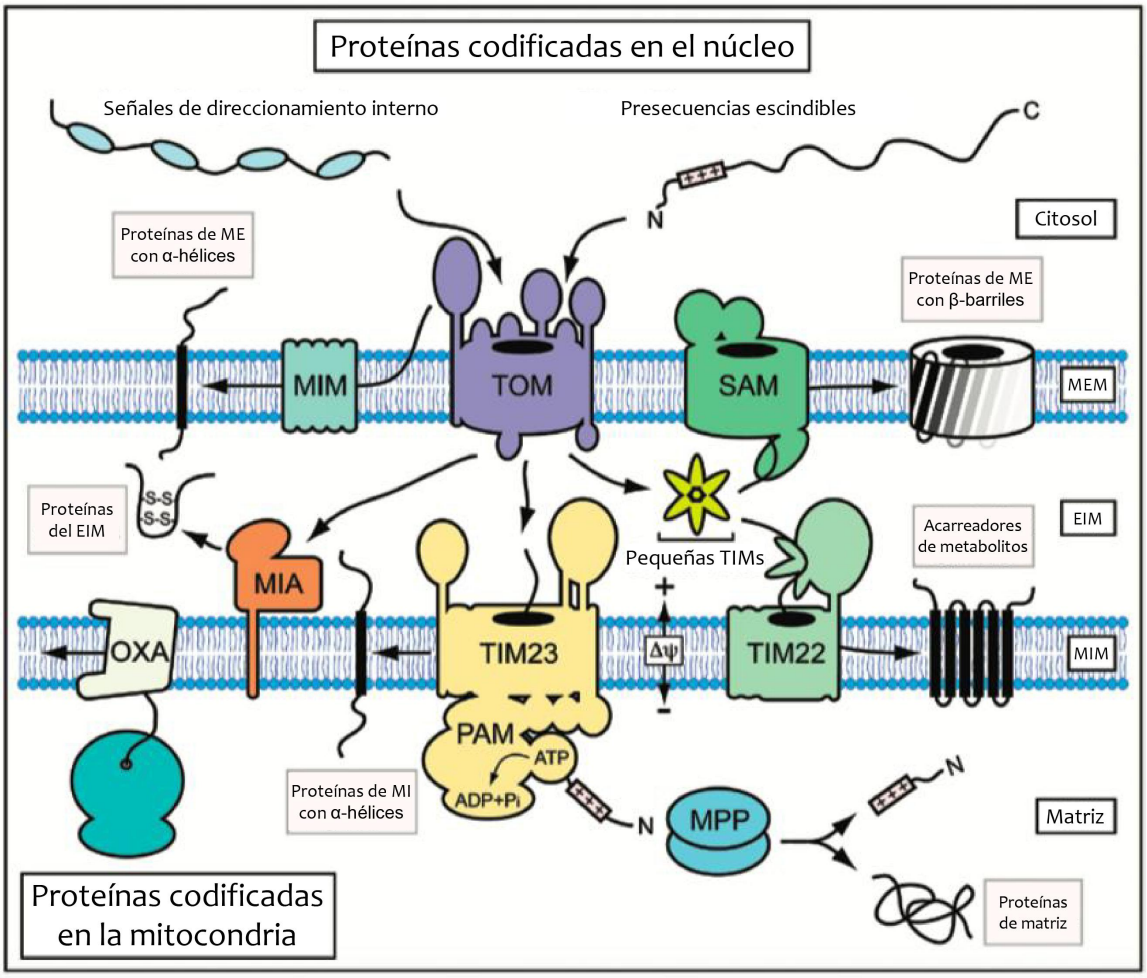

Figura 2. Vías de biogénesis de proteínas mitocondriales. Las proteínas codificadas en el genoma mitocondrial se insertan cotraduccionalmente a la membrana interna por la acción conjunta de los ribosomas mitocondriales y de la translocasa Oxa1. En contraste, la mayoría de las proteínas mitocondriales que se sintetizan en el citosol son importadas por la translocasa de la membrana externa (TOM). Las maquinarias de translocación de las membranas interna y externa son las responsables de distribuir a las proteínas precursoras en los diversos compartimentos intramitocondriales. Algunas proteínas de membrana externa de tipo α-hélice pueden pasar por alto el canal TOM y se insertan en la membrana externa mediante el complejo de importación mitocondrial (MIM). La maquinaria de importación y ensamblaje del espacio intermembranal mitocondrial (MIA) promueve la importación y oxidación de proteínas mediante la formación de enlaces disulfuro. La translocasa de presecuencias de la membrana interna (TIM23) puede insertar lateralmente a proteínas precursoras en la membrana interna o, en cooperación con el motor asociado a translocasa de presecuencias (PAM) internalizarlas en la matriz mitocondrial. La peptidasa de procesamiento mitocondrial (MPP) escinde las presecuencias N-terminales, dando lugar a las proteínas maduras. Por su parte, las pequeñas chaperonas TIM en el espacio intermembranal, entregan los precursores de los barriles-β a la maquinaria de clasificación y ensamblaje

(SAM) de la membrana externa y también distribuyen a proteínas de membrana hacia la translocasa transportadora de membrana interna (TIM22). El potencial de membrana ($\Delta\psi$) impulsa la translocación de proteínas tanto por TIM23 como por TIM22. (Figura tomada de Straub et al., 2016. *Biol. Chem.*; 397(11): 1097–1114).

La vía más caracterizada de ingreso a la mitocondria, conocida como la vía de transporte de las presecuencias, es responsable de la importación de aproximadamente el 60% de los precursores mitocondriales. En esta vía, las proteínas se sintetizan con una presecuencia de direccionamiento mitocondrial escindible (MTS, por sus siglas en inglés) en su extremo N-terminal (Roise y Schatz, 1988; Vögtle et al., 2009). Estas secuencias se caracterizan por tener entre 8 y 80 aminoácidos, siendo ricas en residuos hidroxilados como serinas y treoninas, y en general, carecen de residuos cargados negativamente. Además, forman α-hélices anfipáticas que exhiben una cara cargada positivamente y otra con residuos hidrofóbicos, que facilitan su ingreso a través de TOM y su distribución por TIM23. Estas secuencias suelen encontrarse en proteínas de matriz y de la MIM, aunque en algunos casos también pueden estar presentes en proteínas del EIM e incluso en algunas de la MEM (Doyle et al., 2013; Huang et al., 2009). Un grupo amplio de proteínas con múltiples cruces transmembranales (TMS, por sus siglas en inglés), especialmente los transportadores mitocondriales y los componentes centrales de las translocasas de la MIM, carecen de señales de direccionamiento en el extremo N-terminal. En su lugar, utilizan señales internas que se encuentran próximas a los TMS.

Las MTS son reconocidas por los receptores del complejo de translocación de la membrana externa (TOM, por sus siglas en inglés), específicamente por las subunidades Tom20 y Tom22 (Araiso et al., 2019; Sayyed et al., 2022). Por otro lado, Tom70, junto con su parálogo en levadura, Tom71, se asocian de manera más laxa al complejo TOM. Ambas subunidades reconocen preferentemente a las señales internas de direccionamiento de las proteínas sin MTS (Liu et al., 2023). Indistintamente, los receptores de TOM, al poseer motivos de repetición de tetratricopéptidos (TPR) reconocen también chaperonas de los sistemas Hsp70 y Hsp90, y en conjunto con ellas, mantienen a los sustratos en un estado desplegado competente para su importación,

evitando su agregación y asistiendo en las etapas iniciales del proceso de internalización en el organelo (Backes et al., 2021).

Una vez que los sustratos han cruzado el poro de translocación principal conformado por la subunidad de tipo barril-β Tom40, reciben asistencia por parte de Tom5, quien los orienta hacia el EIM. Allí son reconocidos por dos grandes complejos de translocación funcional y estructuralmente diferentes de la MIM (TIM, por sus siglas en inglés): TIM23, encargado de translocar a los precursores con MTS y TIM22, que transloca proteínas con señales de direccionamiento internas, como la que presentan varios acarreadores mitocondriales de 6 TMS.

El complejo de translocación TIM23

El cruce de las proteínas precursores a través del canal de importación de la MIM depende de varios factores y de la presencia de fuentes de energía: la fuerza protón motriz ($\Delta\psi$), el ΔpH, la afinidad de la MTS por el lado *cis* sobre el *trans* de la membrana, y la hidrólisis de ATP. Las MTS cargadas positivamente hacen que el $\Delta\psi$ ejerza un efecto electroforético sobre las proteínas, facilitando su paso a través de TIM23. El complejo TIM23 está embebido en la MIM y existe en forma de complejo heterotrimérico. Se compone de una dupla de subunidades centrales conformado por las proteínas Tim17 y Tim23, las cuales constituyen el sitio de translocación (Fig. 3A). Tim17 y Tim23 están compuestos por 4 TMS, organizados de una forma inclinada, y se asocian en un arreglo "espalda-con-espalda" para formar dos cavidades opuestas que están expuestas hacia la fase lipídica (Sim et al., 2023). Además, cuenta con el receptor Tim50. Estas subunidades en conjunto dan origen a una forma central del complejo conocida como $TIM23_{CORE}$.

En la transferencia de proteínas de TOM a TIM23, Tim50 interactúa con Tom22 y Tom21, asegurando el correcto direccionamiento de precursores a través del EIM. La translocación de los precursores a través de TIM23 sucede a través de una cavidad, que presenta regiones cargadas negativamente en la periferia y zonas hidrofóbicas en el centro. La alteración de estas características estructurales, modifican la eficiencia y

fidelidad del mecanismo de translocación (Sim et al., 2023; Fielden et al., 2023). Como se describe a continuación, el complejo TIM23 establece una estrecha cooperación con los complejos de la cadena de transporte de electrones III y IV, así como con el motor de importación de proteínas con presecuencias (PAM, por sus siglas en inglés), localizado en la matriz mitocondrial. En cada caso, esto da lugar a dos formas transitorias del translocador conocidas como $TIM23_{SORT}$ y $TIM23_{MOTOR}$, respectivamente.

$TIM23_{SORT}$. Junto con las unidades centrales Tim17-Tim23 y Tim50, la conformación $TIM23_{SORT}$, también incluye las subunidades Mgr2 y Tim21 (Fig. 3B). A través de esta última, se asocia con los complejos de la cadena respiratoria, *bc1* (complejo III) y citocromo *c* oxidasa (complejo IV). Esta configuración es de particular importancia para el ordenamiento y la liberación lateral de proteínas dentro de la MIM. Estas proteínas contienen una señal de paro/transferencia (del inglés stop-transfer), es decir, una región adyacente a la presecuencia de ~20 aminoácidos que es rica en residuos hidrofóbicos flanqueados por residuos cargados. Esta señal de paro/transferencia es probablemente reconocida por el factor modulador Mgr2. Bajo la acción de Mgr2, la translocación se detiene en la MIM y se induce una apertura lateral en el complejo TIM23, liberando la proteína directamente al interior de la bicapa lipídica (Ieva et al., 2013; Ieva et al., 2014; Mirzalieva et al., 2019; Lee et al., 2020; Mata et al., 2020). Mgr2 se considera, entonces, un factor que mantiene el control de calidad sobre el complejo translocador TIM23, ayudando a determinar qué proteínas deben ser completamente translocadas hasta la matriz mitocondrial y cuáles deben ser liberadas lateralmente dentro de la MIM.

$TIM23_{MOTOR}$. La forma conocida como $TIM23_{MOTOR}$, encargada de importar proteínas hasta la matriz mitocondrial, implica la asociación de $TIM23_{CORE}$ con el motor de proteínas PAM (Fig. 3B). Esta unión se lleva a cabo a través de la subunidad de andamiaje Tim44, que recluta a la proteína mtHsp70 al canal de importación (Liu et al., 2003; Craig et al., 2018). Además de mtHsp70, PAM está compuesto por las subunidades Pam18, Pam16, Mge1 y Pam17. La chaperona mtHsp70 es dependiente de ATP y es determinante para el funcionamiento del complejo motor. mtHsp70 posee un dominio de unión a nucleótidos en su extremo N-terminal y un dominio de unión a péptidos en su extremo C-terminal, a través del cual facilita el movimiento

unidireccional de las proteínas entrantes. Pam18 y Pam16 son subunidades asociadas a la MIM, que contienen dominios J, que regulan la actividad ATPasa de mtHsp70. Pam18 estimula esta actividad, mientras que Pam16 la antagoniza (Frazier et al., 2004; Li et al., 2004). Una vez que mtHsp70 se une al polipéptido en translocación, la co-chaperona Pam18, hidroliza el ATP unido, lo que provoca un cambio conformacional en mtHsp70 de abierto a cerrado, previniendo el deslizamiento del polipéptido que está siendo translocado (Mapa et al., 2010; Callegari et al., 2020). Pam17, una subunidad específica de levaduras, facilita la translocación de proteínas de matriz que son hipersensibles al potencial de membrana (Caurmont-Sarcos et al., 2020). La interacción de mtHsp70 con Tim44, es dependiente de la unión de ATP o ADP, por lo que una vez que el ATP es hidrolizado, mtHsp70 se disocia de Tim44 (Slutsky-Leiderman et al., 2007). Mge1, que actúa como regulador de mtHsp70 al ser un factor de intercambio de nucleótidos, promueve el cambio de ADP a ATP en mtHsp70 (Bolliger et al., 1994). Pam18 es el único componente del motor que tiene un segmento que atraviesa la membrana y que se une en ambos lados con otros componentes de la translocasa. Durante la translocación de un polipéptido, el motor de importación no es una entidad estable, sino que puede experimentar un intercambio activo de subunidades (Schulz y Rehling, 2014; Schendzielorz et al., 2018).

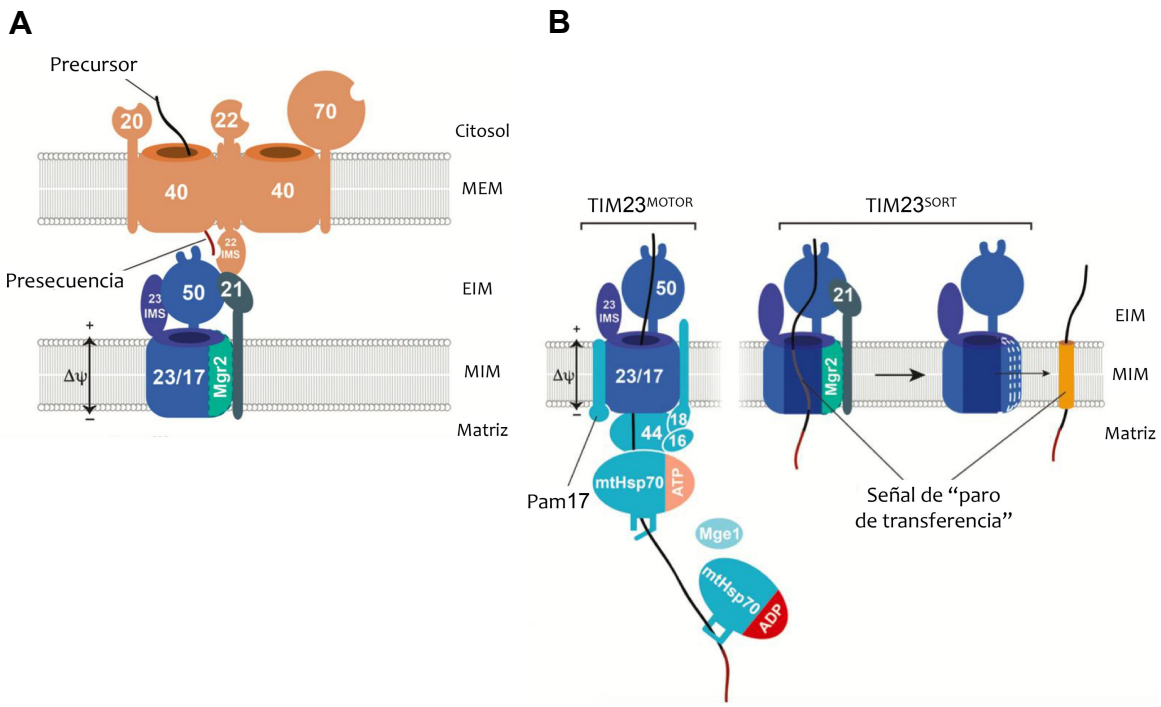

Figura 3. Mecanismo de entrega y translocación de precursores vía TIM23. A) El precursor que contiene la presecuencia se coloca en el sitio de salida del complejo TOM. Los complejos TOM y TIM23 se asocian mediante interacciones entre Tom22 y Tim21 y entre Tim23 y Tim50. Luego, Tim50 reconoce y captura a la presecuencia. B) El complejo TIM23 existe en dos estados estructurales/funcionales. $TIM23_{MOTOR}$ es la forma asociada al motor que transloca a las proteínas precursoras destinadas a la matriz mitocondrial. En contraste, $TIM23_{SORT}$ está especializado en la liberación lateral de proteínas precursoras de membrana interna que tienen un TMS y una señal hidrofóbica de "stop-transfer" después de la presecuencia (Figura tomada de Callegari et al., *Biol. Chem*. 2020; 401(6–7): 709–721).

Las presecuencias de los precursores hidrofóbicos que se liberan lateralmente a la MIM y de las proteínas cuyo destino final es la matriz mitocondrial, son removidas por la proteasa de procesamiento mitocondrial (MPP, por sus siglas en inglés), una peptidasa heterodimérica localizada en la matriz mitocondrial (Hawklitschek et al., 1988; Fukasawa et al., 2015; Wiedeman y Pfanner, 2017). El procesamiento proteolítico por MPP no está estrictamente vinculado a la translocación y puede ocurrir desde el momento en que la MTS queda expuesta en la matriz mitocondrial. Los péptidos de la presecuencia son posteriormente degradados por las proteasas de presecuencias, PreP, o

Cym1 conocidas en conjunto como el peptidasoma de la matriz mitocondrial (Johnson et al., 2006; Mossman et al., 2014). Las subunidades de MPP muestran una alta similitud con las dos unidades periféricas del complejo respiratorio III, Core1 y Core2 (Schulte et al., 1989), y en algunos organismos, dichas proteasas se encuentran totalmente integradas en ese complejo. Por lo tanto, el procesamiento ocurre en cercanía a la MIM, aunque es un proceso independiente de la transferencia de electrones que tiene lugar en el complejo III (Dessi et al., 2000).

Las mitocondrias como generadoras de la energía celular

Entender la compartimentalización de la mitocondria es de gran importancia para a la vez poder comprender los procesos bioquímicos que tienen lugar en su interior. Las enzimas responsables de la oxidación de ácidos grasos y del ciclo de los ácidos tricarboxílicos, a excepción de la enzima succinato deshidrogenasa, se encuentran en el medio acuoso de la matriz mitocondrial. Por otro lado, las enzimas responsables de la oxidación del NADH y del transporte de electrones hacia el oxígeno (deshidrogenasas, flavoproteínas, centros hierro-azufre y citocromos, respectivamente) son proteínas oligoméricas de membrana que están asociadas a las crestas mitocondriales de la MIM (Scheffler, 2008). Estas enzimas desempeñan un papel crucial en la fosforilación oxidativa, proceso que utiliza los equivalentes reductores generados durante el ciclo de Krebs para producir ATP. La cantidad de ATP generada por la fosforilación oxidativa es mucho mayor que la que se sintetiza durante la glucólisis.

La fosforilación oxidativa

La fosforilación oxidativa genera la mayoría del ATP celular en organismos no fotosintéticos y representa la principal fuente de energía para el metabolismo celular (Nelson et al., 2021). Este proceso implica una serie de reacciones que aprovechan la energía derivada de la transferencia de electrones a lo largo de la cadena respiratoria. El acoplamiento del transporte de electrones al bombeo de protones genera un gradiente electroquímico a través de la MIM, el cual es utilizado por la ATP sintasa para fosforilar el ADP (adenosina difosfato) y generar ATP (Mitchell, 1961).

La cadena de transporte de electrones (ETC) se encuentra asociada a la MIM y comprende una serie de complejos proteicos (I, II, III y IV) y transportadores móviles, organizados para funcionar secuencialmente como donadores y aceptores de electrones (Vercellino y Sazanov, 2022). El proceso comienza con la transferencia de electrones del NADH (nicotinamida adenina dinucleótido reducido) y el $FADH_2$ (dinucleótido de flavina adenina reducido) a los complejos I y II, respectivamente. Estos electrones a su vez se transfieren a los complejos restantes (III y IV) a través de una serie de reacciones redox. Al final de la ETC, el oxígeno molecular (O_2) actúa como el aceptor final de electrones, que, al combinarse con protones, forma agua (H_2O). Este último paso asegura el flujo continuo de electrones a través de la ETC.

A medida que los electrones fluyen a través de los complejos proteicos, se libera energía que se utiliza para bombear protones (H+) desde la matriz hacia el EIM, generando un gradiente electroquímico a través de la MIM. Este gradiente representa una forma de energía quimiosmótica, que será utilizada por la enzima oligomérica ATP-sintasa, para generar ATP a partir de ADP y fosfato inorgánico (Pi) (Lehninger, 1944; Kennedy y Lehninger, 1950). La ATP-sintasa funciona como un nanomotor rotatorio que promueve la síntesis de ATP en sus tres sitios catalíticos (Kühlbrandt, 2019).

La citocromo c oxidasa

El complejo IV, también conocido como citocromo *c* oxidasa (COX) (EC 1.9.3.1), es el aceptor final de la cadena de transferencia de electrones en las mitocondrias. Cataliza la reducción de oxígeno acoplada al bombeo de protones desde la matriz hacia el EIM (Yoshikawa et al., 2011). Esta enzima es dimérica y cada uno de los monómeros está constituido por 13 subunidades en humanos y 11 en levaduras (Fig. 4). Su biogénesis implica la asociación de polipéptidos codificados tanto en el genoma nuclear como en el mitocondrial. Su núcleo catalítico está compuesto por las tres subunidades más grandes, que están codificadas en los genes mitocondriales *cox1*, *cox2* y *cox3*, que se expresan en el interior del organelo. Las ocho subunidades adicionales están codificadas en el núcleo y por lo tanto son sintetizadas en el citosol antes de ser importadas a la mitocondria (Tsukihara et al., 1996). El complejo IV tiene cuatro centros metálicos con actividad redox: dos grupos hemos (citocromos *a* y *a_3)* y dos centros de cobre (Cu_A y Cu_B), que

participan en el transporte de electrones. En este proceso, los electrones se transfieren desde el citocromo *c* soluble al centro de cobre binuclear Cu_A, al hemo *a* y al segundo centro binuclear compuesto por hemo a_3 y Cu_B. Finalmente, el O_2 se une al hemo a_3 reducido para formar agua (Hill, 1994; Tsukihara et al., 1995).

El ensamblaje de COX no es trivial debido al origen genético dual de sus subunidades e implica coordinar la expresión de genes del núcleo y de la mitocondria, fenómeno en el cual participan otros factores de ensamblaje y vías de señalización. Esto permite controlar la abundancia de las subunidades y los cofactores metálicos, así como separar el proceso formando primero tres subcomplejos o módulos que se van ensamblando hasta formar una enzima funcional (Fontanesi et al., 2006). Las tres subunidades del núcleo catalítico, Cox1, Cox2 y Cox3, son proteínas integrales de membrana, altamente hidrofóbicas. En el presente estudio nos enfocamos en la subunidad II o Cox2, por lo que a continuación se darán detalles de esta subunidad en particular.

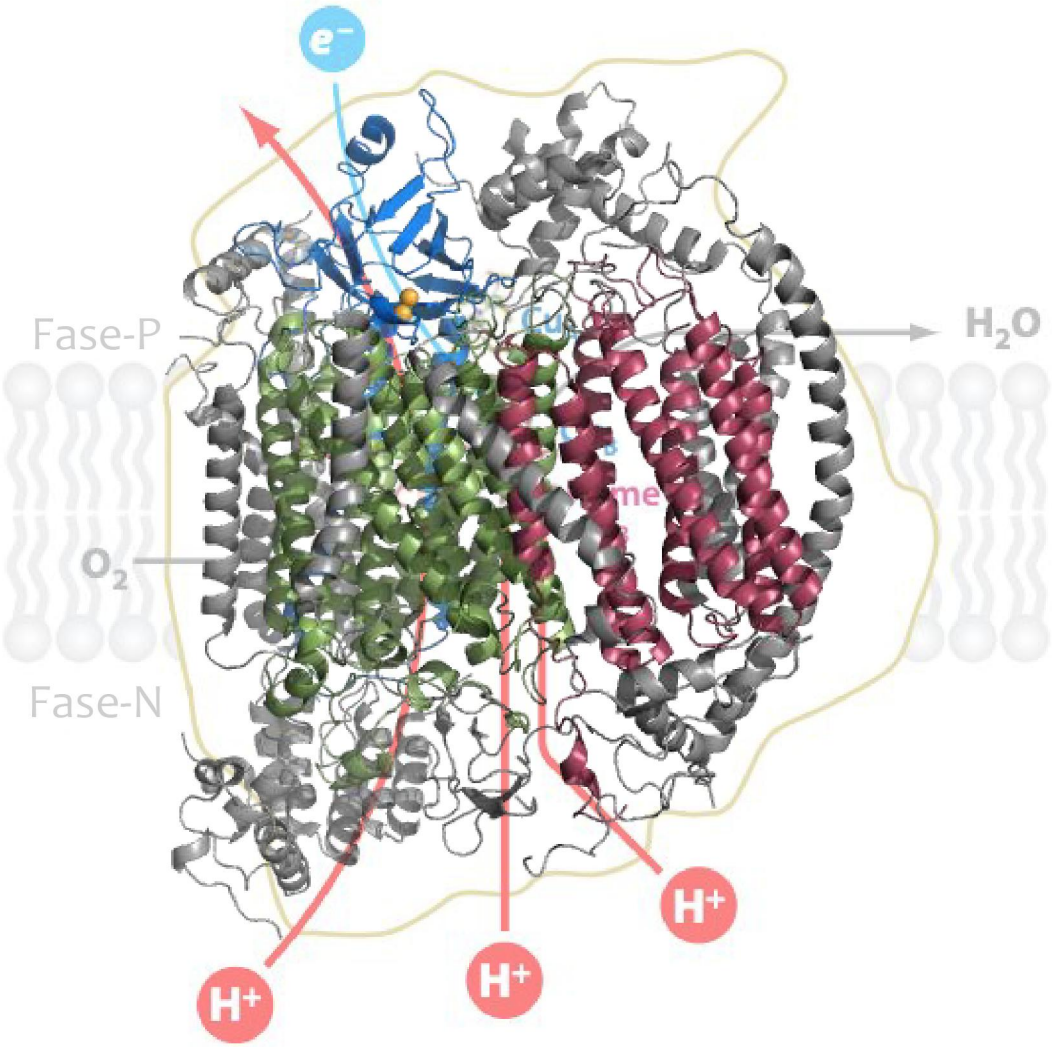

Figura 4. Estructura y posicionamiento en la MIM de la enzima citocromo *c* oxidasa. Las subunidades del núcleo catalítico y codificadas en el mtDNA se muestran en color, Cox1 en verde; Cox2 en azul y su centro binuclear de cobre en dorado; Cox3 en carmín. Se denotan las posibles vías de transporte de protones (rojo), O_2 y agua (gris) y electrones (azul claro). (Figura modificada de Yoshikawa et al., 2011. *Annu. Rev. Biophys*. 40:205-223).

Biogénesis de la subunidad Cox2

Como proteína integral de membrana, la biogénesis de Cox2 implica su inserción co-traduccional en la MIM. Este proceso cuenta con la participación de proteínas

especializadas y se sigue de un complejo proceso de maduración. Cox2 se compone de dos TMS de tipo α-hélice y una región globular hidrofílica que se extiende hacia el EIM, donde se aloja el centro binuclear de Cu_A (Soto et al., 2012). Presenta una topología N-afuera/C-afuera, lo que significa que tanto el dominio N-terminal como el dominio C-terminal de la proteína están expuestos hacia el EIM.

La síntesis de Cox2 requiere la participación de Pet111, un activador transcripcional que interactúa con la región 5-UTR del mRNA de cox*2* (Mulero y Fox, 1993; Poutre y Fox, 1987). Inicialmente, el anclaje de los ribosomas mitocondriales o mitoribosomas a la MIM es mediado por las proteínas mL45 y Letm1 en mamíferos, o sus homólogos Mba1 y Mdm38 en levadura. Estas proteínas, alinean y estabilizan la unión entre el túnel de salida del ribosoma y regiones altamente densas en proteínas de la MIM (Preuss et al., 2001; Ott et al., 2006; Pfeffer et al., 2015), donde se encuentra el resto de la maquinaria necesaria para la internalización de Cox2. La subunidad Cox2 es sintetizada como una proteína precursora que incluye un péptido líder (LP) en el extremo N-terminal, compuesto por quince aminoácidos, que facilitan su interacción con la insertasa Oxa1. La presencia del LP es una característica distintiva de Cox2 en levadura y no está presente en esta subunidad en otros organismos (He y Fox, 1997; Bonnefoy et al., 2001). Una vez que el N-terminal de Cox2 alcanza el EIM, el LP es procesado por la peptidasa Imp1 (Graef et al., 2007) que cataliza su remoción proteolítica (Nunnari et al., 1993; Schneider et al., 1994). Este paso es esencial para que la porción ya insertada de la proteína sea reconocida por la chaperona Cox20 (Hell et al., 2000), la cual estabiliza el extremo N-terminal de Cox2 mientras que se completa la síntesis del C-terminal y el ribosoma se desprende por completo de la subunidad recién sintetizada. Seguidamente, en un proceso dependiente del potencial de membrana, Cox18, en conjunto con las proteínas Mss2 y Pnt1, promueven la exportación de la región C-terminal de Cox2 hasta el EIM. Una vez que ambos TMS de Cox2 se han integrado a la membrana, la chaperona Sco1, que está anclada a la MIM mediante una α-hélice transmembranal, llevará a cabo la unión de los átomos de cobre, uno a la vez, al dominio globular de tipo β-barril de Cox2 (Lode et al., 2000; Banci et al., 2006). Esta unión implica la formación de un pliegue simétrico de grupos tioles con potencial redox en forma de horquilla β, donde Sco1 reduce el enlace disulfuro para integrar el cobre (Carr et al., 2005; Banci et al., 2007).

Las enfermedades mitocondriales

Las enfermedades mitocondriales son un grupo de trastornos genéticos que, típicamente, resultan en defectos en las proteínas que participan en la fosforilación oxidativa (OXPHOS). Además, pueden causar disfunción en el ciclo de Krebs, en el metabolismo del folato, así como causar la disminución de intermediarios enzimáticos y la acumulación de sustancias tóxicas (Gorman et al., 2016). Constituyen el grupo más común de trastornos metabólicos hereditarios y se encuentran entre las formas más comunes de trastornos neurológicos hereditarios. Desde el punto de vista clínico, se manifiestan con un amplio espectro de síntomas que pueden presentarse a cualquier edad, afectando múltiples órganos con una alta demanda energética, como nervios, corazón, músculos, riñones, hígado y glándulas del sistema endocrino (McFarland et al., 2010).

Estas enfermedades son causadas por mutaciones tanto en el genoma nuclear (nDNA) como en el mitocondrial (mtDNA). La patofisiología de estas enfermedades es compleja, ya que pueden presentar cualquier patrón de herencia, incluyendo herencia autosómica recesiva y ligada al cromosoma X para las mutaciones en el nDNA, y herencia materna para las mutaciones en el mtDNA. La complejidad aumenta en pacientes con mutaciones en el mtDNA, debido a la presencia de múltiples copias de mtDNA en una célula individual, lo que resulta en una mezcla de genomas normales y mutantes, conocida como heteroplasmia. El nivel de heteroplasmia es crucial para determinar la extensión de la disfunción celular causada por la enfermedad mitocondrial (DiMauro y Schon, 2003).

Las mutaciones del mtDNA se dividen en tres categorías: mutaciones en genes que codifican proteínas; mutaciones en RNA (tRNA y rRNA) y reordenamientos del mtDNA a gran escala (ablaciones y duplicaciones). Dado que este trabajo se centra en el gen Cox2 del complejo IV, se destacan especialmente las enfermedades asociadas a mutaciones en este gen, como la Neuropatía Óptica Hereditaria de Leber (LHON); Miopatía mitocondrial, Encefalopatía, Acidosis Láctica y Episodios similares a un accidente cerebrovascular (MELAS); Neurodegeneración con Acumulación de Hierro en el Cerebro (NBIA); Cardiomiopatía Hipertrófica (HCM); Pérdida Auditiva

NeuroSensorial (SNHL); Glaucoma Pseudoexfoliativo (PEG); el Síndrome de Médula-Páncreas de Pearson; el Síndrome Kearns–Sayre; el Síndrome de Alpers-Huttenlocher; ataxia cerebelar; rabdomiólisis; astenozoospermia; atresia biliar; entre otras (MITOMAP, 2023).

Con el avance de las técnicas para manipular el genoma mitocondrial, se han propuesto diversas estrategias para el desarrollo de terapias genéticas dirigidas a tratar estas enfermedades mitocondriales (Kyriakouli et al., 2008; Cwerman-Thibault et al., 2010). Estas estrategias abarcan desde la entrega localizada de ácidos nucleicos a la matriz mitocondrial, hasta la inhibición del mtDNA mutante mediante enzimas de restricción que lo digieren selectivamente sin alterar el mtDNA sano, así como la edición directa del mtDNA mutado y la expresión alotópica (Di Donfrancesco et al., 2022).

Expresión alotópica como posible estrategia para el tratamiento de las enfermedades mitocondriales

El término expresión alotópica hace referencia a la activación funcional en el núcleo de un gen que normalmente reside en un organelo celular, como la mitocondria. En esencia, la expresión alotópica consiste en trasladar una copia natural del gen mitocondrial afectado al núcleo y dirigir la proteína correspondiente hacia el organelo con el fin de sustituir a la proteína mitocondrial defectuosa. El proceso implica la expresión del gen desde el núcleo, la síntesis de la proteína precursora correspondiente en el citosol, su internalización en el organelo, su maduración proteolítica y la correcta localización en su compartimento mitocondrial de destino (Nagley et al., 1988; Nagley y Devenish, 1989). Este proceso se considera una estrategia prometedora para desarrollar tratamientos para enfermedades mitocondriales, ya que busca restaurar los defectos en la OXPHOS causados por mutaciones genéticas mitocondriales (Kyriakouli et al., 2008; Tischner & Wenz, 2015). Sin embargo, es importante destacar que, en este proceso, las proteínas altamente hidrofóbicas con varios TMS, a pesar de contar con una MTS, pueden ser dirigidas erróneamente al retículo endoplásmico (RE) cuando han sido expresadas *ex organello* (von Heijne, 1986; Vitali et al., 2018).

Expresión alotópica del gen cox2

La levadura *Saccharomyces cerevisiae* se ha utilizado como organismo modelo en muchos estudios de expresión alotópica. Su genoma está completamente secuenciado y bien anotado, y es posible modificarlo mediante técnicas de biología molecular clásica. Además, la levadura es un organismo anaerobio facultativo, lo que significa que puede producir ATP mediante respiración aeróbica cuando hay oxígeno disponible, pero también puede recurrir a la fermentación en ausencia de oxígeno. Esta característica permite que una cepa de levadura con genes mitocondriales de OXPHOS defectuosos o eliminados pueda crecer en fuentes de carbono fermentables y ser seleccionada en fuentes no-fermentables después de modificaciones, reparaciones o restituciones del gen defectuoso.

En una cepa mutante de *S. cerevisiae*, que carece del gen mitocondrial *cox2* (*Δcox2*) que codifica a la proteína homónima, se expresó el mismo gen desde el núcleo (Supekova et al., 2010). La construcción del gen alotópico codifica a la MTS de la proteína mitocondrial Oxa1, fusionada al LP de 15 aminoácidos de Cox2, seguida de la secuencia primaria de la subunidad Cox2, recodificada con el uso de codones nuclear, que además contiene la sustitución W56R en el TMS1 ($Cox2^{W56R}$). La MTS permite que el precursor sea reconocido por los receptores de TOM, y posteriormente, se entregue al translocador de la membrana interna TIM23. La sustitución W56R disminuye sustancialmente la hidrofobicidad promedio del TMS1, facilitando su movimiento a través de TIM23 y su completa translocación hasta la matriz mitocondrial. Una vez que el TMS1 se expone a la matriz mitocondrial, la MTS es removida y el LP permite que la translocasa Oxa1 inserte al cruce transmembrana en la MIM. De este modo, la cepa complementada *Δcox2* + $COX2^{W56R}$, puede crecer en fuentes de carbono no fermentables, restaurando parcialmente la capacidad respiratoria de la cepa mutante. Sin embargo, la transformante exhibe una menor capacidad respiratoria, mostrando únicamente el 60% de los niveles de COX en comparación con la cepa silvestre (wt) (Cruz-Torres et al., 2012). Un análisis bioquímico más detallado reveló que tanto $Cox2^{W56R}$ como $Cox2^{WT}$ mostraban secuencias N-terminales idénticas, lo que indica que tanto la MTS como el LP fueron escindidos durante la internalización de Cox2 alotópica. Como se describió anteriormente, Cox2 se procesa proteolíticamente una vez durante su

biogénesis (eliminación del LP), mientras que Cox2^{W56R} expresado alotópicamente se procesa dos veces (eliminación de la MTS y del péptido señal). La menor hidrofobicidad de TMS1 permite su translocación completa a la MIM, mientras que la hidrofobicidad de TMS2 provoca que TIM23 lo libere lateralmente a la membrana. La eliminación del LP se lleva a cabo en Cox2^{W56R} de la misma manera que sucede con la proteína Cox2^{WT} sintetizada *in organello*.

Para investigar la causa de la disminución de los niveles de actividad COX de Cox2 expresada de forma alotópica, Rubalcava-Gracia et. al (2018), generaron una cepa que produce una subunidad Cox2^{W56R} idéntica, pero dentro de la matriz mitocondrial, con el fin de reproducir las mismas condiciones naturales de biogénesis de una cepa wt. La comparación de la mutante mitocondrial *cox2^{W56R}* con la cepa silvestre reveló que ambas levaduras presentaban tasas de crecimiento similares en fuentes de carbono no fermentables y niveles de actividad de COX idénticos. Esto sugiere que la disminución en los niveles de COX no se debe a la mutación W56R en sí misma, sino que deben existir factores que afecten a la subunidad Cox2 durante su proceso de importación, maduración y ensamblaje cuando se produce de forma alotópica. El hecho de que la Cox2 alotópica siga una ruta de biogénesis diferente a la de su contraparte de tipo silvestre, respalda esta hipótesis.

El gen *COX2^{W56R}* puede expresarse a partir de un plásmido episomal multicopia de 2μ o de manera constitutiva, en un bajo número de copias, cuando se inserta en algún cromosoma nuclear o en un vector centromérico. Cuando se expresa a través de un vector multicopia con un promotor fuerte, como el promotor *PGK* de la enzima 3-fosfoglicerato cinasa, el precursor de la subunidad Cox2^{W56R} (*e*Cox2^{W56R}) tiende a acumularse en la superficie de las mitocondrias, siendo mínima la porción que se internaliza y que se procesa correctamente. En contraste, cuando la expresión proviene del gen insertado en el núcleo, se observan niveles más altos de la subunidad Cox2^{W56R} madura (*n*Cox2^{W56R}). Se ha sugerido que cuando la tasa de síntesis de la subunidad citosólica Cox2^{W56R} excede la tasa de importación, el precursor tiende a acumularse y agregarse en la superficie mitocondrial (Rubalcava-Gracia et al., 2019).

PLANTEAMIENTO DEL PROYECTO

Como se describió anteriormente, la cepa mutante *Δcox2,* transformada con un gen mitocondrial *cox2* que produce la subunidad homónima con la sustitución W56R, puede crecer tan bien como una cepa wt en sustratos no-fermentables. Esto indica que la mutación no tiene un efecto detectable ni sobre la estructura ni sobre la función de la COX ensamblada (Rubalcava-Gracia et al., 2018). Por lo anterior, la observación de que la complementación respiratoria de una cepa nula *Δcox2* es parcial cuando la subunidad $Cox2^{W56R}$ se sintetiza en el citosol, sugiere la existencia de un proceso o factor limitante, posiblemente vinculado al transporte del precursor a través del translocador TIM23. El gen $COX2^{W56R}$ puede expresarse a partir de un plásmido episomal multicopia de 2μ o de manera constitutiva en un bajo número de copias cuando se inserta en el núcleo o se expresa desde un plásmido centromérico. Cuando se utiliza un vector multicopia con un promotor fuerte, el precursor de la subunidad $Cox2^{W56R}$, denominado en lo sucesivo *e*$Cox2^{W56R}$, tiende a acumularse en la superficie de las mitocondrias, con una mínima fracción que se internaliza y procesa correctamente. En contraste, cuando la expresión proviene del gen insertado en el núcleo, se observan niveles más bajos de acumulación del precursor de la subunidad $Cox2^{W56R}$, designado en lo sucesivo *n*$Cox2^{W56R}$. Se planteó previamente que cuando la tasa de síntesis de $Cox2^{W56R}$ citosólica supera la velocidad de importación, el precursor tiende a acumularse y agregarse en la superficie mitocondrial (Rubalcava-Gracia et al., 2019). Con el objetivo de identificar los factores que limitan la capacidad de complementación total de $Cox2^{W56R}$ en una mutante nula *Δcox2,* en este estudio se propuso evaluar si la sobreexpresión de genes relacionados directa o indirectamente con la internalización del precursor, son capaces de incrementar el crecimiento respiratorio de la cepa *Δcox2* + $COX2^{W56R}$.

PREGUNTA DE INVESTIGACIÓN

¿La sobreexpresión de algunos genes que codifican proteínas involucradas en la importación de proteínas mitocondriales, favorecerá la internalización de la proteína alotópica $Cox2^{W56R}$?

HIPÓTESIS

La sobreproducción de ciertas proteínas en la levadura *S. cerevisiae*, podría facilitar la internalización de la proteína alotópica $Cox2^{W56R}$ en la mitocondria y su posterior ensamblaje en el complejo de la citocromo *c* oxidasa. Dado que, se ha planteado previamente que el paso limitante de la importación de la proteína producida alotópicamente ocurre durante su paso por el translocador TIM23, la eliminación o sobreproducción de Mgr2, un factor que participa en el control de liberación lateral de precursores hidrofóbicos por TIM23, permitirá comprender la naturaleza del paso limitante en la internalización de $Cox2^{W56R}$ alotópica.

OBJETIVO GENERAL

Determinar si la sobreexpresión de alguna de las proteínas implicadas en la importación de proteínas a la mitocondria puede facilitar la internalización de la proteína alotópica $Cox2^{W56R}$ en este organelo. Además, se evaluará el papel de Mgr2, una subunidad implicada en el control de la liberación lateral de precursores hidrofóbicos por TIM23, en el proceso de importación de $Cox2^{W56R}$ y se buscará identificar la naturaleza del paso limitante de dicha importación.

OBJETIVOS PARTICULARES

1. Utilizando una genoteca de fragmentos cromosómicos de levadura clonados en un vector de sobreexpresión, identificar y caracterizar aquellos supresores multicopia

que aumenten el crecimiento en medios respiratorios de una cepa de levadura que produzca alotópicamente a la proteína $Cox2^{W56R}$.

2. Seleccionar una serie de genes cuyos productos proteicos participan en la importación de proteínas a la mitocondria y estudiar el efecto de su sobreexpresión sobre la importación de la subunidad $Cox2^{W56R}$.

3. Explorar el efecto de eliminar y sobreexpresar el gen *MGR2* sobre la importación de la subunidad Cox2 producida alotópicamente.

4. Identificar cual es el paso limitante en la importación de la proteína alotópica Cox2.

MATERIALES Y MÉTODOS

Cepas de levadura y construcciones genéticas

En este estudio, se utilizaron cepas de la levadura *Saccharomyces cerevisiae* derivadas de la cepa parental D273-10B (laboratorio Fred Sherman, ATCC® 24657™). La cepa NB40-36A (MATα lys2 arg8::hisG, leu2-3, 112 ura3-52 [rho+]), (Pérez-Martínez et al., 2003) y la cepa EHW154 (MATa arg8::hisG ura3-52 leu 2-3, 112 his3-ΔHindIII [rho+] cox2(1,89-91)::ARG8m) (Williams y Fox, 2003) corresponden a la cepa silvestre y a la mutante nula *Δcox2*, respectivamente. Las cepas de levadura utilizadas en este estudio se enlistan en la Tabla 1.

Tabla 1. Cepas de levadura utilizadas en este trabajo.

Cepa	Genotipo	Referencia o procedencia
NB40-36A	*MATα lys2 leu2-3,112 arg8::hisG ura3-52 [rho+]*	Pérez-Martínez et al., 2003
EHW154	*MATa arg8::hisG his3-ΔHindIII leu 2-3,112 lys2 ura3-52 [rho+] cox2(1,89-91)::ARG8m*	Williams y Fox, 2003
DRG102	*EHW154 ura3-52::hphNT1 PGK5 MTSOXA1 COX2W56R PGK3*	Rubalcava-Gracia et al., 2019
FNY101	*NB40-36A mgr2Δ::KanMX6*	Este trabajo
FNY102	*EHW154 mgr2Δ::KanMX6*	Este trabajo

Para lograr la expresión alotópica de $Cox2^{W56R}$ en la mutante *Δcox2*, se introdujo el vector de integración pRS306H (Rubalcava-Gracia et al., 2019). Este vector contiene un casete de resistencia a higromicina (*B*), y facilita la inserción de la construcción a través de recombinación homóloga en el locus *URA3*, lo que resulta en la cepa denominada *Δcox2* + $nCOX2^{W56R}$. Además, se empleó el plásmido multicopia episomal de 2μ pFL61, que porta el marcador de auxotrofía *URA3*, para generar la cepa denominada *Δcox2* +

eCOX2^{W56R}. Estos dos sistemas de expresión nos permitieron obtener niveles bajos (*n*) y altos (*e*) de la subunidad Cox2^{W56R} producida alotópicamente.

Las cepas nulas de Mgr2 (*Δmgr2*) se generaron reemplazando el locus *MGR2* (*YPL098C*) mediante recombinación homóloga. Para este propósito se usó el casete *kanMX6* del plásmido pFA6a-kanMX6 (Bähler et al., 1998), el cual confiere resistencia al antibiótico G418. El casete kanMX6 se amplificó utilizando los desoxioligonucleótidos mgr2-kanMX6: 5′-TAGCACAAATAGCGCAACAGCTTCAAGTCCAATATTAAGATATACCAGCTGAAGCTTCGTACGC-3′ y 5′-GAAAACGATGGGGAAGCGTAAATATATGCAAAATTTCCCCCATCGATGAATTCGAGCTCGTT-3′, diseñados para incluir regiones homólogas que flanquean aproximadamente 20 pb (nucleótidos subrayados) río arriba y río abajo del locus *MGR2*. La región amplificada resultante reemplaza completamente el marco de lectura abierto de *MGR2*.

Las cepas de levadura que sobreexpresan *MGR2* (*MGR2*↑) se generaron mediante la introducción del vector episomal de alto número de copias pMK2, un derivado de pFL61. Este plásmido, que contiene el marcador seleccionable *LEU2* en lugar de *URA3* (Minet et al., 1992), presenta un promotor de 3-fosfoglicerato cinasa (*PGK*), que quedó localizado río arriba del locus *MGR2* de tipo silvestre. El proceso de clonación implicó amplificar el gen *MGR2* utilizando los cebadores MGR2OE: directo, 5′-GCGCGGCCGCATGCCTCCTCTTCCACA-3′; y reverso, 5′-GCGCGGCCGCTCAGTCCTTACGTACCGT-3′. Estos desoxioligonucleótidos se diseñaron para incluir secuencias de sitios de restricción *Not1*, que permitieron la clonación de *MGR2* en el sitio de inserción múltiple del mismo vector.

Genoteca de supresores multicopia

Buscando ampliar el espectro de proteínas cuya sobreexpresión podría incrementar el crecimiento respiratorio de la cepa que expresa alotópicamente al gen *COX2*^{W56R}, se transformó a la cepa *Δcox2* + *nCOX2*^{W56R} con una genoteca de levadura clonada en el vector pFL44L (Chevalier et al., 1980; Bonneaud et al., 1991). Tras una selección

inicial, se realizó una segunda selección de aquellas colonias que mostraban un mayor tamaño y crecían más rápido en sustratos no fermentables, principalmente etanol y glicerol a pH 7.0. Experimentos subsecuentes de co-segregación mostraron que el incremento en su capacidad respiratoria había sido conferido por el plásmido proveniente de la genoteca. Los plásmidos de cada cepa seleccionada fueron obtenidos mediante el método de *extracción de DNA plasmídico*, que se describe más adelante, y fueron recuperados en células competentes MR32 para su posterior caracterización molecular.

Sobreexpresión de candidatos seleccionados.

Para determinar si la sobreproducción de algunas proteínas implicadas en la importación de proteínas a la mitocondria facilita la internalización de $Cox2^{W56R}$ en este organelo, se seleccionaron proteínas candidato, cuyos genes correspondientes fueron introducidos en las cepas *Δcox2 + nCOX2*^{W56R} y *Δcox2 + eCox2*^{W56R}. Para esto, obtuvimos plásmidos que sobreexpresan genes candidatos, y genes que codifican las subunidades de los complejos de translocación TIM22 y TIM23 de la colección de mosaicos genómicos de levadura *"yeast genomic tilling collection"* (Jones et al., 2008). Los plásmidos seleccionados, designados por sus respectivos identificadores, incluyeron: *COX20 (YGPM21k21), OXA1 (YGPM14c18)*, *SDH2 (YGPM20g17)*, *TOM70 (YGPM33c09), CIS1 (YGPM8p09), MSP1 (YGPM30f06), HSP104 (YGPM12e18), PSE1 (YGPM18p15), RRP5 (YGPM5p05), TIM22 (YGPM17f03), SDH3 (YGPM317i06), TIM18 (YGPM17d04), TIM54 (YGPM20p13), TIM9 (YGPM25o01), TIM12 (YGPM32o08), TIM10 (YGPM30n09), TIM17 (YGPM4a13), TIM23 (YGPM23p01), MGR2 (YGPM5l18)* y *TIM21 (YGPM21l20)*. Estos plásmidos se generaron mediante la clonación de fragmentos cromosómicos que abarcan a los genes seleccionados, en el vector plasmídico de alto número de copias pGP564. La presencia de dichos genes en todos los plásmidos utilizados en este estudio fue confirmada mediante la secuenciación de los bordes del inserto o mediante PCR diagnóstico.

Condiciones de cultivo y almacenamiento de levaduras

Las cepas de levadura se cultivaron en medio líquido o sólido (agar al 2.0%) a 30 ºC y 37 ºC, de acuerdo con lo especificado en cada resultado. Los medios empleados en este estudio incluyeron medios fermentables (glucosa: YPDA), no fermentables (etanol/glicerol: YPEG, etanol: YPE, lactato: YPLac), de selección (mínimo glucosa: SD, mínimo galactosa: SGal) y en combinación con antibióticos, que se describen en la sección *Medios de cultivo de levaduras*. El crecimiento se controló midiendo la densidad óptica a 600 nm (D.O. $_{600}$) usando un espectrofotómetro BioScreen C (Growth Curves, EE. UU.). Para su almacenamiento, las cepas se cultivaron en medios líquidos hasta superar la fase exponencial. Luego, se lavaron con agua destilada esterilizada y se almacenaron en crioviales a -70 ºC en una solución esterilizada de glicerol al 30%. Para su posterior recuperación, se empleó un palillo de madera estéril para extraer una porción de la solución congelada y sembrarla en cajas de Petri con el medio de selección adecuado.

Medios de cultivo de levaduras

YPDA: Extracto de levadura 1% p/v, bactopeptona 2% p/v, glucosa 2% p/v y adenina 0,002% p/v.

YPEG: Extracto de levadura 1% p/v, bactopeptona 2% p/v, etanol 3% p/v y glicerol 3% p/v.

YPE: Extracto de levadura 1% p/v, bactopeptona 2% p/v, y etanol 3%.

YPLac: Extracto de levadura 3% p/v, KH_2PO_4 1% p/v, NH_4Cl 1%, $CaCl_2 \cdot 2H_2O$ 0.5% p/v, NaCl 0.5% p/v, $MgSO_4 \cdot 7H_2O$ 1,1% p/v, $FeCl_3$ 0,003% p/v, ácido láctico 2% v/v. Ajustar pH 5,5 con KOH.

YPGal: Extracto de levadura 1 % p/v, bactopeptona 2% p/v y galactosa 2% p/v.

YPGly: Extracto de levadura 1% p/v, bactopeptona 2% p/v, etanol 3% p/v y glicerol 2% p/v.

SD (medio mínimo): Base nitrogenada YNB sin aminoácidos ni $(NH_4)_2SO_4$ 0,17 % p/v, $(NH_4)_2SO_4$ 0,5 % p/v, glucosa 2% y aminoácidos y nucleótidos.

SGal (medio mínimo): Base nitrogenada YNB sin aminoácidos ni $(NH_4)_2SO_4$ 0,17 % p/v, $(NH_4)_2SO_4$ 0,5 % p/v, galactosa 2% y aminoácidos y nucleótidos.

Los medios en estado sólido incluyen agar desde el 1.5% hasta el 2% p/v.

Transformación de levaduras

Las transformaciones de levadura se llevaron a cabo mediante modificaciones de los protocolos de transformación de levadura de *"un solo paso"* de Chen et al., (1992), o bien utilizando CH_3Li, DNA monocatenario como acarreador (SSDNA) y polietilenglicol (PEG) de acuerdo con lo reportado (Gietz y Woods, (2002); Gietz y Schiestl, (2007).

En el protocolo de "*un solo paso*", se prepararon tubos de 1.5 mm con 90 µl de amortiguador 1S (CH_3Li 0.2 N, PEG 3350 40% (m/v) y ditiotreitol (DTT) 100 mM ajustado a pH 5.0 esterilizado por filtración), a los cuales se añadieron 5 µl de DNA de esperma de salmón o arenque (10 mg [ml^{-1}]), desnaturalizado durante 15 minutos a 100 ºC y mantenido en hielo. A esta mezcla se agregaron 100 µl de un cultivo líquido de células en fase estacionaria, aproximadamente $5x10^7$ células, y 3 µl del plásmido de interés (500 ng [μl^{-1}]). Los tubos con la mezcla se incubaron durante 1 hora a 45 ºC y luego se estrió la mezcla en cajas de Petri con medio sólido de selección.

Para el procedimiento de CH_3Li, SSDNA y PEG, se inoculó una colonia de células en 5 ml de medio líquido y se incubó durante 16 horas a 30 ºC. Luego, el cultivo se diluyó a una $D.O._{600}$ 0.1 y se incubó hasta alcanzar una $D.O._{600}$ 0.7 - 1.0. Las células de 1.5 ml de este cultivo se recolectaron por centrifugación a 4500 x g durante 3 minutos, y se lavaron con agua estéril. El precipitado se resuspendió en 1 ml de $C_2H_3LiO_2$ 0.1 M y se incubó durante 10 minutos. Posteriormente, se recolectaron las células repitiendo el paso de centrifugación, y tras eliminar el sobrenadante, se agregaron 240 µl de PEG 3500 50 % (m/v), 36 µl de $C_2H_3LiO_2$ 1 M, 10 µl de DNA de esperma de salmón (10 mg [ml^{-1}]), desnaturalizado durante 5 minutos a 100 ºC, 5 µl del plásmido de interés (500 ng

[μl^{-1}] y 69 µl de agua estéril. La mezcla se homogenizó en un agitador tipo vórtex y se incubó a 42 ºC durante 45 minutos para transformaciones episomales o 75 minutos para transformaciones integrativas. Posteriormente, se recolectaron las células por centrifugación a 4500 x g durante 2 minutos, se eliminó el sobrenadante y el precipitado resultante se resuspendió en 100 µl de agua estéril. La mezcla fue estriada en cajas de Petri conteniendo medio sólido de selección.

Mutagénesis de levaduras por radiación ultravioleta

Se seleccionaron colonias respiratorias revertantes inducidas por UV de la cepa EHW154, que contenía a $Cox2^{WT}$ integrado en el núcleo (Rubalcava-Gracia et al., 2019). La reversión se indujo por radiación UV sobre un cultivo de levaduras que había alcanzado la fase estacionaria en medio líquido YPDA, el cual se estrió en cajas de Petri con medio sólido YPDA. Las cajas se incubaron a 4 ºC durante 16 horas previas al proceso de mutagénesis. La irradiación se llevó a cabo utilizando una fuente de UV con emisión a 245 nm, colocada a 12 cm de las cajas. Esto se produjo en ausencia de otro tipo de luz, durante 10 segundos, y luego las cajas fueron incubadas durante 3 días a 30 ºC. Posteriormente, se hicieron réplicas en cajas con medio sólido YPEG. *De entre estas últimas, se recuperaron las colonias revertantes, es decir, aquellas capaces de crecer en este medio respiratorio. Ya que el proceso en sí tiene un 30% de letalidad, solamente se recuperó una colonia revertante por cada* $2x10^9$ *células irradiadas.* El DNA genómico de la cepa se extrajo utilizando métodos que se describen más adelante. El ORF de *COX2* integrado en el núcleo se amplificó utilizando los desoxioligonucleótidos PGK-F: 5'-CAGATCATCAAGGAAGTAATTATC-3' y PGK-R: 5'-CTATTATTTTAGCGTAAAGGATG-3'. El amplicón correspondiente se secuenció y se corroboró la presencia de la mutación puntual que da lugar a la sustitución W56R.

Prueba de crecimiento mediante diluciones seriadas

Una colonia de células tomada con un asa bacteriológica se inoculó y cultivó durante 16 horas en 3.0 ml de medio líquido YPDA a 30 ºC, con agitación constante. Después de este tiempo, los cultivos se diluyeron hasta alcanzar la fase exponencial ($D.O._{600}$ 1,0), lo

que equivale aproximadamente a $2.5x10^7$ células [ml^{-1}]). Las células se colectaron mediante centrifugación a 8600 x *g* y se lavaron una vez con 1,0 ml de agua estéril. A la suspensión celular de cada cepa se le hicieron cinco diluciones secuenciales 1:10 utilizando placas de 96 pozos. Se depositaron gotas de aproximadamente 3.5 µl en cajas de Petri conteniendo medios sólidos fermentables (YPDA) y no fermentables (YPEG, YPE, YPLAC) utilizando una pipeta multicanal. Luego, las cajas de Petri se incubaron a 30 ºC o 37 ºC durante 4 a 7 días, según se indica en los resultados.

Mediciones de consumo de oxígeno

El consumo de oxígeno se evaluó mediante un ensayo polarográfico de célula completa, las cuales previamente habían sido sometidas a un ayuno en agua estéril durante 4 a 6 horas. El ensayo se llevó a cabo en una solución que contiene ácido 2-morfolinoetanosulfónico monohidrato (MES) 20 mM, con un pH de 6.0 ajustado con trietanolamina, y etanol 50 mM como sustrato oxidable. Al final del ensayo, se añadió NaCN 200 µM, para inhibir la actividad de COX (Estabrook, 1967). Las mediciones del consumo de oxígeno se efectuaron utilizando un medidor de oxígeno *Warner/Strathkelvin Instruments* equipado con un electrodo tipo Clark, en una cámara de 1.0 ml con camisa de agua mantenida a 30 ºC. Los datos fueron adquiridos mediante el software 782 *Oxygen System de Warner/Strathkelvin Instruments.*

Extracción de DNA genómico

La extracción de ADN genómico de levadura se realizó siguiendo un protocolo modificado de Hoffman y Winston, (1987). Se inoculó una colonia de células y se cultivó durante 16 horas en 3.0 ml de medio líquido YPDA a 30 ºC, con agitación constante. Las células fueron lavadas con agua destilada y recuperadas por centrifugación a 13,200 x *g* durante 1 minuto. El precipitado resultante se resuspendió en 500 µl de amortiguador de lisis (Triton X-100 2% v/v, SDS 20% 1 ml, NaCl 100 mM, Tris-HCl 100 mM pH 8.0, EDTA-Na 1 mM pH 8.0). Luego se añadieron 500 µl de fenol-cloroformo-alcohol isoamílico (25:24:1) y la mezcla se agitó manualmente durante 3 minutos. Después, se centrifugó a 13,200 x g durante 5 minutos a 4 ºC. El

sobrenadante se transfirió a un nuevo tubo con una mezcla de 1/10 volúmenes de $NaC_2H_3O_2$ 3.0 M pH 5.3 y 3/10 volúmenes de etanol al 100% enfriado a -20 ºC, e incubado a -20 ºC durante 10 minutos. A continuación, se centrifugó a 13,200 x g durante 10 minutos a 4 ºC, y el precipitado resultante se resuspendió en 1 ml de etanol al 70% enfriado a -20 ºC. Posteriormente, se centrifugó a 13,200 x g durante 1 minuto a 4 ºC, y se eliminó completamente el sobrenadante. El precipitado se secó dando vuelta al tubo boca abajo durante 10 minutos a temperatura ambiente y finalmente se resuspendió en 50 µl de agua estéril.

Extracción de DNA plasmídico

Este proceso se llevó a cabo con un protocolo adaptado de Robzyk y Kassir, (1992). Se inició con la recuperación de la pastilla celular de un cultivo de 4 ml de YPDA de levaduras en fase estacionaria mediante centrifugación a 13,200 x *g*. Tras lavar la pastilla con agua destilada, ésta se resuspendió en 200 µl de amortiguador STET (sacarosa 8% p/v, Tritón X-100 5% v/v, EDTA 50 mM, Tris-HCl 50 mM pH 8,0), al cual se le añadieron aproximadamente 0.4 g de perlas de vidrio de 0.45 mm. Tras someter a un mezclado vigoroso en un agitador tipo vórtex durante 5 minutos, se agregaron 200 µl adicionales de STET, seguido de una breve homogenización y se incubó en un baño de agua a punto de ebullición durante 3 minutos, asegurándose de usar tapas en el tubo para evitar su apertura durante la ebullición. Tras enfriar en hielo, la mezcla se centrifugó a 13,200 x g durante 10 minutos a 4 ºC. Se desechó el sobrenadante y se incubó el precipitado con 10 µl de RNAasa (10 mg [ml^{-1}]) durante 20 minutos a temperatura ambiente. Se transfirieron 250 µl del sobrenadante a un nuevo tubo con 125 µl de $C_2H_7NO_2$, y se incubó durante 1 hora más a -20 ºC. Luego, se colectó el precipitado centrifugando a 13,200 x g durante 20 minutos a 4 ºC. En este punto, el DNA cromosomal residual, las especies grandes de RNA y las potenciales impurezas que podrían interferir con la transformación del plásmido en células competentes, se habían precipitado. Luego, 200 µl del sobrenadante se agregaron a un nuevo tubo con 400 µl de etanol enfriado a -20 ºC. La mezcla se centrifugó a 13,200 x g durante 10 minutos, el precipitado fue lavado con 1 ml de etanol al 70% enfriado a -20 ºC, y el paso de centrifugado durante 5 minutos fue repetido. El precipitado final se secó

en un bloque de calentamiento para tubos de 1.5 ml a 70 ºC durante 5 minutos, para después ser resuspendido en 25 µl de agua estéril. Se utilizaron volúmenes de 1, 5 y 10 µl para transformar células competentes MR32.

Obtención de extractos proteicos totales

La extracción de proteínas se llevó a cabo utilizando el método de tratamiento alcalino de células completas de levadura descrito por Kushnnirov, (2000). Un inóculo de levaduras se cultivó en 20 ml de medio líquido SGal hasta alcanzar la fase estacionaria ($D.O._{600}$ 2.5). Posteriormente, las células se colectaron en una microcentrífuga a 2800 x *g* durante 3 minutos y se lavaron con 500 µl de una solución que contiene fluoruro de fenil-metil-sulfonilo (PMSF) a una concentración de 1.0 mM y N-α-tosil-L-lisil clorometil cetona (TLCK) a una concentración 50 µM. Al precipitado resultante se le agregaron 100 µl de NaOH 0.2 M y se incubó durante 5 minutos a temperatura ambiente, tras lo cual se centrifugó nuevamente. El nuevo precipitado se resuspendió en 50 µl de amortiguador de muestra de Laemmli (Tris-HCl 60 mM pH 6.8, glicerol 10% v/v, SDS 2% p/v, β-mercaptoetanol 5% y azul de bromofenol 0.02% p/v), y se hirvió durante 3 minutos. Después de una centrifugación adicional, se cargaron 10 µl del sobrenadante resultante en pozos de 1.5 mm de geles desnaturalizantes de poliacrilamida (12 % de acrilamida y 0.2 % de bis-acrilamida).

Fraccionamiento celular

Se inocularon cepas de levadura en medios líquidos SGal y YPLac, que se describen en la sección *Medios de cultivo de levaduras,* en matraces de 125 ml hasta alcanzar una $D.O._{600}$ entre 1.0 y 1.5. Las células se recolectaron por centrifugación a 2,500 x g durante 5 minutos, y se lavaron con agua destilada. Posteriormente, se resuspendieron en 10 ml de amortiguador TD (Tris 100 mM, DTT 10 mM) durante 10 minutos a 30 ºC. La centrifugación fue repetida para después incubar el precipitado resultante en amortiguador de zimoliasa (sorbitol 1.2 mM, KH_2PO_4 20 mM a pH 7.4 y 5 mg de zimoliasa [g^{-1}] de peso húmedo) durante 1 hora a 30 ºC con agitación constante. El precipitado se recolectó centrifugando a 2,500 x g durante 5 minutos a 4 ºC, y se

homogeneizó en 1 ml de amortiguador Dounce (sorbitol 0.6 M, Tris 10 mM a pH 7.4, EDTA 1 mM, albúmina sérica bovina al 0.2 %, PMSF 1 mM) con 30 movimientos sucesivos de un homogeneizador Dounce estrecho a 4 ºC. Las muestras se transfirieron a tubos de 1.5 ml y se centrifugaron a 2,500 x g durante 5 minutos a 4 ºC. El sobrenadante se recuperó en tubos nuevos y se centrifugó a 13,500 x g durante 10 min a 4°C. El sobrenadante, conteniendo la fracción citosólica, se recuperó en tubos nuevos, mientras que el precipitado, la fracción mitocondrial, se resuspendió en 100 µl de amortiguador SH (sorbitol 0.6 M, HEPES 20 mM a pH 7.4). Ambas fracciones se almacenaron a -70 °C para su uso posterior.

Solubilización de fracciones para electroforesis nativa

Una vez aislada la fracción mitocondrial, se lavó dos veces con una solución de sorbitol 250 mM y BisTris 50 mM ajustado a pH 7.0 con HCl, a 4 ºC. La mezcla se centrifugó a 13,500 x g durante 2 minutos, y el precipitado se resuspendió en 55 µl de solución de ácido amino-caproico 750 mM y BisTris 50 mM ajustado a pH 7.0 con HCl.

De acuerdo con la cantidad de proteína en la fracción, determinada mediante el método de Lowry, se agregaron 2 g de n-dodecil β-D-maltósido (DDM) para disociar complejos mitocondriales o 2 g de digitonina para mantener supercomplejos intactos. La muestra se solubilizó invirtiendo el tubo repetidamente y se dejó incubar durante 30 minutos a 4 ºC. Luego, la mezcla se centrifugó a 100,000 x g durante 30 minutos a 4 ºC.

El sobrenadante se mezcló con 5 µl de amortiguador de carga (ácido amino-caproico 750 mM, Bis Tris 25 mM y Coomassie Serva Blue G 35050 al 5%) y de esta mezcla, se cargaron 30 µl en pozos de 1.5 mm de geles nativos con un gradiente de poliacrilamida del 5 a 12%.

Electroforesis desnaturalizante e inmunodetección

La electroforesis en gel se llevó a cabo utilizando un sistema SDS-tricina (Schägger, 1994). Después de la electroforesis, las proteínas corridas en los geles se transfirieron a membranas de nitrocelulosa. Estas membranas se bloquearon con gelatina de piel

bovina tipo B (Marca Sigma) al 3%, se lavaron con amortiguadores de lavado TBS y TBST y se sometieron a inmunodetección. Se utilizó el anticuerpo monoclonal anti-Cox2 (Marca Abcam: 4B12A5) en una dilución 1:9,000 y el anticuerpo policlonal anti-Zwf1 (Marca Sigma-Aldrich: A9521) en una dilución 1:10,000 como control de carga, cuyos niveles permanecen invariantes (Fujiwara et al., 2016). Para el sondaje secundario, los anticuerpos anti-conejo de cabra y anti-ratón de cabra conjugados con fosfatasa alcalina se incubaron durante 4 h. Se formaron precipitados de color púrpura oscuro en forma de bandas después de la adición de cloruro de nitro-azul de tetrazolio (NBT) y sal de p-toluidina de 5-bromo-4-cloro-3'-indolil fosfato (BCIP). Las imágenes de las bandas se capturaron utilizando un escáner de imágenes HP Scanjet G4050, y la intensidad de las bandas se estimó utilizando el software GelAnalyzer 23.1 (http://www.gelanalyzer.com), desarrollado por Istvan Lazar Jr., PhD e Istvan Lazar Sr., PhD, CSc.

Preparación de células competentes

Para experimentos de clonación y propagación de plásmidos, las cepas de *Escherichia coli* DH5α (F^- *endA1 glnV44 thi-1 recA1 relA1 gyrA96 deoR nupG purB20 φ80dlacZ*ΔM15 Δ(*lacZYA-argF*)U169, hsdR17(rK^-mK^+), λ^-) y MR32, un derivado recA– de MC1061 (str. K-12 F^- λ^- Δ*(ara-leu)7697* [*araD139*]B/r Δ*(codB-lacI)3 galK16 galE15* e14$^-$ *mcrA0 relA1 rpsL150*(Str^R) *spoT1 mcrB1 hsdR2(r–m+)*) fueron preparadas como células quimiocompetentes, siguiendo el método de Hanahan, (1983). Se cultivaron bacterias *E. coli* en 2 ml de medio LB (descrito al final de este texto), durante 16 horas a 37 ºC con agitación constante. Luego, el cultivo resultante se inoculó en 100 ml de medio LB, el cual se incubó a 37 ºC hasta alcanzar una $D.O._{600}$: 0.2 - 0.4. Después, el cultivo se enfrió en hielo durante 15 minutos y las células se recolectaron centrifugando a 4,500 x g durante 15 minutos a 4 ºC. El precipitado se resuspendió en 33 ml de solución RF1 (RbCl 100 mM, $MnCl_2 \cdot 4H_2O$ 50 mM, $C_2H_3KO_2$ 30 mM, $CaCl_2 \cdot 2H_2O$ 10 mM, glicerol 15% p/v ajustando el pH a 5.8 con ácido acético 0.2 M filtrado por esterilización) y se incubó durante 90 minutos en hielo. Posteriormente, las células se centrifugaron a 4,500 x g durante 15 minutos, se eliminó el sobrenadante y se volvieron a resuspender en 8 ml de solución RF2 (RbCl 10 mM, $CaCl_2 \cdot 2H_2O$ 75 mM,

MOPS 10 mM glicerol 15% p/v ajustando el pH a 6.8 con NaOH) durante 15 minutos en hielo. Se hicieron alícuotas de 200 µl de la solución en tubos de 1.5 ml para ser congelados en nitrógeno líquido y almacenados a -80 ºC para su uso posterior. *Medios de cultivo* LB: Extracto de levadura 5% p/v, triptona 10% p/v y NaCl 10% p/v. Ajustar pH 7.0 con NaOH 5N.

RESULTADOS

Utilizando cepas con dos fondos genéticos distintos, Cox2^{W56R} producida a partir de la expresión de un gen integrado a un cromosoma nuclear (*nCOX2*^{W56R}) y Cox2^{W56R} producida desde un plásmido episomal de alto número de copias (*eCOX2*^{W56R}), intentamos identificar los factores que limitan que la proteína producida de manera alotópica en el citosol pueda complementar totalmente una mutante nula del gen mitocondrial *cox2*. Abordamos este problema con tres enfoques experimentales distintos, para determinar si el cambio en la expresión de ciertos genes, relacionados directa o indirectamente con la importación, internalización, maduración y ensamblaje de Cox2^{W56R}, podrían incrementar los niveles de esta proteína alotópica al interior de la mitocondria. Los tres enfoques son: 1) identificación de supresores multicopia de una genoteca de sobreexpresión; 2) llevar a cabo una "conjetura fundamentada", que implicó la sobreexpresión de genes identificados previamente cuyos productos proteicos se relacionan de alguna manera con la importación de proteínas a la mitocondria; y 3) exploración del papel de la subunidad Mgr2 del translocador TIM23, encargada de la correcta translocación y liberación lateral de precursores hidrofóbicos.

PRIMERA ESTRATEGIA EXPERIMENTAL: Obtención y caracterización de supresores multicopia

En el primer enfoque experimental, la cepa de integración nuclear, *n*Cox2^{W56R}, la cual es reconocida por su notable recuperación del fenotipo respiratorio (Rubalcava-Gracia et al., 2019), fue sometida a transformación con una biblioteca de supresores multicopia, basada en el vector pFL44L. Este vector contiene el marcador prototrófico *URA3*, que permite la selección de transformantes en ausencia de este aminoácido. De alrededor de 307,000 transformantes generadas, 55 colonias presentaron un crecimiento aumentado en medios respiratorios. Tras una tercera selección y de la eliminación de duplicados, el número de transformantes se redujo a 10. Estas 10 colonias exhibieron un incremento conspicuo en su capacidad para crecer en sustratos respiratorios (Fig. 5A), particularmente cuando se usó glicerol como fuente de carbono a un pH de 7.0.

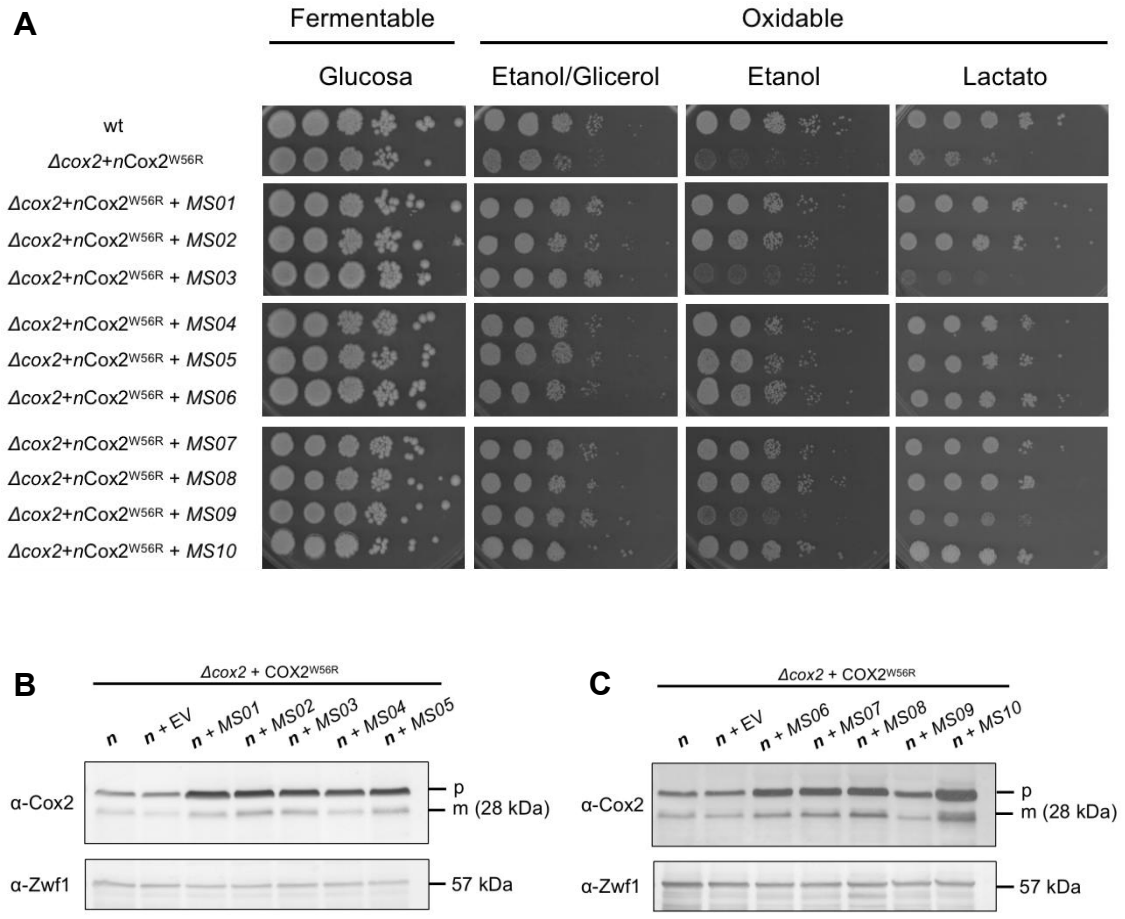

Figura 5. Diez transformantes, *MS01* a *MS10*, mostraron un incremento significativo en su crecimiento respiratorio y mayores niveles de subunidad Cox2^{W56R} madura. A) Diluciones seriadas a 30˚C que muestran el fenotipo de crecimiento fermentativo (glucosa) y respiratorio (etanol/glicerol, etanol y lactato) de una cepa silvestre (wt), la cepa de integración nuclear (nCox2^{W56R}) y las 10 cepas (*MS01* a *MS10*) obtenidas tras la transformación con la genoteca multicopia. Las fotografías se obtuvieron en el cuarto día de crecimiento. B y C) Se utilizaron anticuerpos contra Cox2 y Zwf1 para inmunodetectar las proteínas correspondientes en extractos celulares totales de las cepas de levadura indicadas: la cepa nCox2^{W56R}, la cepa control transformada con un vector vacío (n + EV), y las transformantes B) MS01 a MS05, y C) MS06 a MS10. Se indican las formas precursora (p) y madura (m) de Cox2^{W56R}. El anticuerpo anti-Zwf1 reacciona contra una banda de 57 kDa que se utilizó como control de carga.

El análisis de las inmunodetecciones reveló que, en cada una de las colonias, la sobreexpresión de los 10 plásmidos incrementó los niveles de la proteína madura

Cox2^{W56R} (ya procesada proteolíticamente) y de su precursor (conteniendo aún su presecuencia) (Fig. 5B y 5C), en comparación con una cepa que únicamente fue transformada con el vector vacío (n + EV).

En experimentos de co-segregación, donde se estudió la tendencia de las cepas a perder los plásmidos, se observó que, al resembrar las colonias que habían perdido el plásmido, éstas ya no mostraban mayor crecimiento en sustratos respiratorios. Esto indica que son precisamente los vectores de la genoteca de sobreexpresión los que le habían conferido a la levadura la capacidad de crecer más en sustratos no fermentables (Fig. 6).

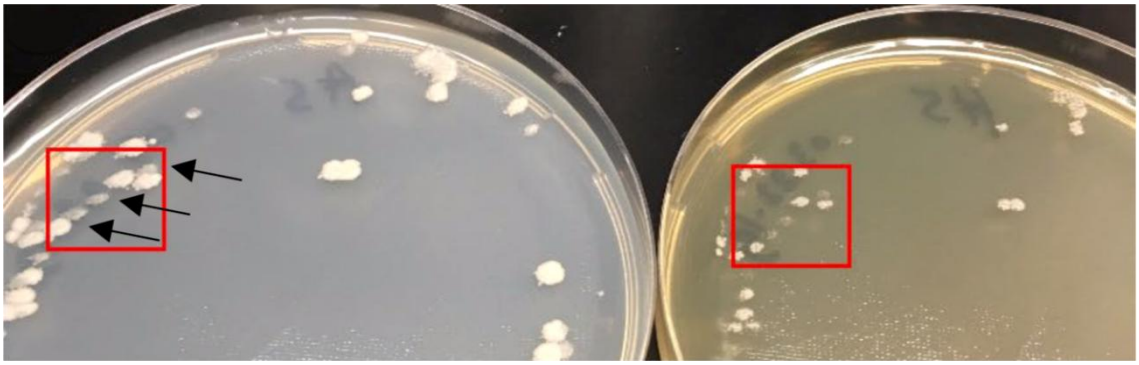

Figura 6. Experimentos de co-segregación. Se sembraron las 10 colonias que mostraban crecimiento respiratorio aumentado en un medio sólido fermentable (YPDA), y se realizaron réplicas en medios de selección SD-ura (izquierda), y en medios oxidables YPGly (derecha). En los recuadros de ambas cajas de Petri, se muestra una porción de la réplica. Se puede observar que las mismas colonias que crecen predominantemente en el medio de selección son también las que crecen más en el medio conteniendo sustratos respiratorios. Las flechas negras indican, las colonias auxótrofas para *URA3*, cuyo crecimiento respiratorio se encuentra disminuido.

El DNA plasmídico de 9 de las 10 colonias fue recuperado y analizado mediante perfiles de digestión con las enzimas de restricción *Sal*I, *Sph*I y *Bgl*II, cuyos sitios flanquean el lugar de inserción de DNA dentro del plásmido. Los perfiles de digestión caracterizados se agruparon en tres grupos diferentes. En el primer grupo, se incluyeron los supresores *MS01*, *MS02*, *MS03*, *MS08* y *MS05*, mientras que el segundo grupo

comprendió los supresores *MS06* y *MS07*. El supresor *MS09*, se encontró en el tercer grupo, exhibiendo un perfil único. A pesar de múltiples intentos, nunca se logró recuperar el DNA plasmídico del supresor *MS10*.

Se secuenciaron los extremos de los insertos contenidos en dos supresores de cada uno de los grupos de 1 y 2, así como el único supresor del tercer grupo (Fig. 7). Se identificaron los fragmentos cromosómicos que se describen a continuación: En el primer grupo, se identificó un inserto genómico de ~6.5 kb del cromosoma XV (chrXV: 976066 - 982119), cuyas coordenadas genómicas nos permitieron inferir la existencia de 5 marcos de lectura abiertos (ORFs) adyacentes intactos, entre los que se encuentra *TYE7* (YOR344C) (chrXV:977194 - 978069). En el segundo perfil de digestión, se obtuvo un inserto genómico de ~5.8 kb correspondiente al cromosoma XIV (chrXIV: 438453 - 444288), dentro del cual se identificaron 6 ORF adyacentes intactos, entre los que se encuentra *RAS2* (YNL098C) (chrXIV:439602 - 440570). En el tercer perfil de digestión, se obtuvo un inserto genómico de ~1.5. kb correspondiente al cromosoma XII (chrXII: 223901 - 226780), dentro del cual se encontró solamente 1 ORF intacto, correspondiente al gen *COX12* (YLR038C).

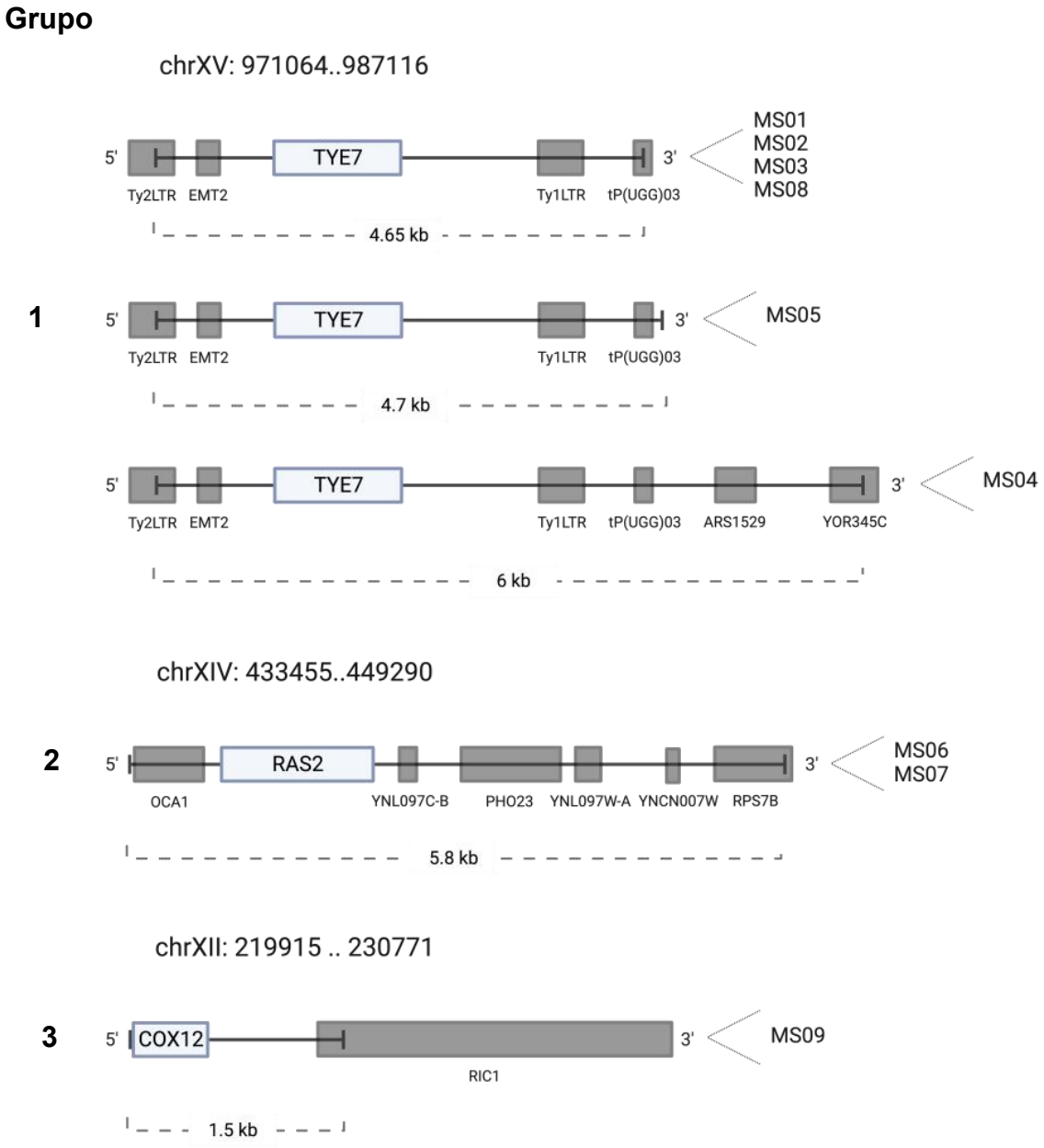

Figura 7. Los supresores *MS01* a *MS09* contienen tres fragmentos cromosómicos. El esquema representa los fragmentos genómicos de los cromosomas XV, XIV y XII con sus correspondientes coordenadas, insertados en el plásmido pFL44L de la genoteca de sobreexpresión y los ORFs presentes en cada uno de ellos (cuadros grises y celestes). Los tres ORFS seleccionados para análisis posteriores, *TYE7*, *RAS2* y *COX12*, se muestran en color celeste.

Para determinar si los tres genes propuestos eran efectivamente los responsables de generar el fenotipo observado, se clonaron los tres ORFs en un vector multicopia de la familia de pFL (Bonneaud et al., 1991; Minet et al., 1992), que contiene el promotor fuerte *PGK*. Este plásmido denominado pMK2, permitió generar una transformación independiente de la cepa original *nCox2*^{W56R} con los tres genes propuestos.

Inicialmente y al contrario de lo que se esperaba, ninguna de las sobreexpresiones en la cepa control incrementó el crecimiento de la levadura en medios respiratorios. Por lo tanto, decidimos producir una nueva cepa que expresara al gen *COX2*^{W56R} desde el núcleo. Para esto, una cepa que ya tenía integrado el gen *COX2*^{WT}, fue sometida a mutagénesis por radiación UV. Las colonias que crecieron en medios respiratorios después del proceso fueron secuenciadas. Se encontró que las colonias, consistentemente con el estudio previamente reportado (Supekova et al., 2010), presentaban la mutación W56R. En esta cepa (n^{UV}Cox2^{W56R}), generada de manera independiente, transformamos nuestros genes propuestos. Observamos que la sobreexpresión de los genes *TYE7*, *RAS2* y *COX12* condujo a una restauración notable del crecimiento en medios respiratorios (Fig. 8A).

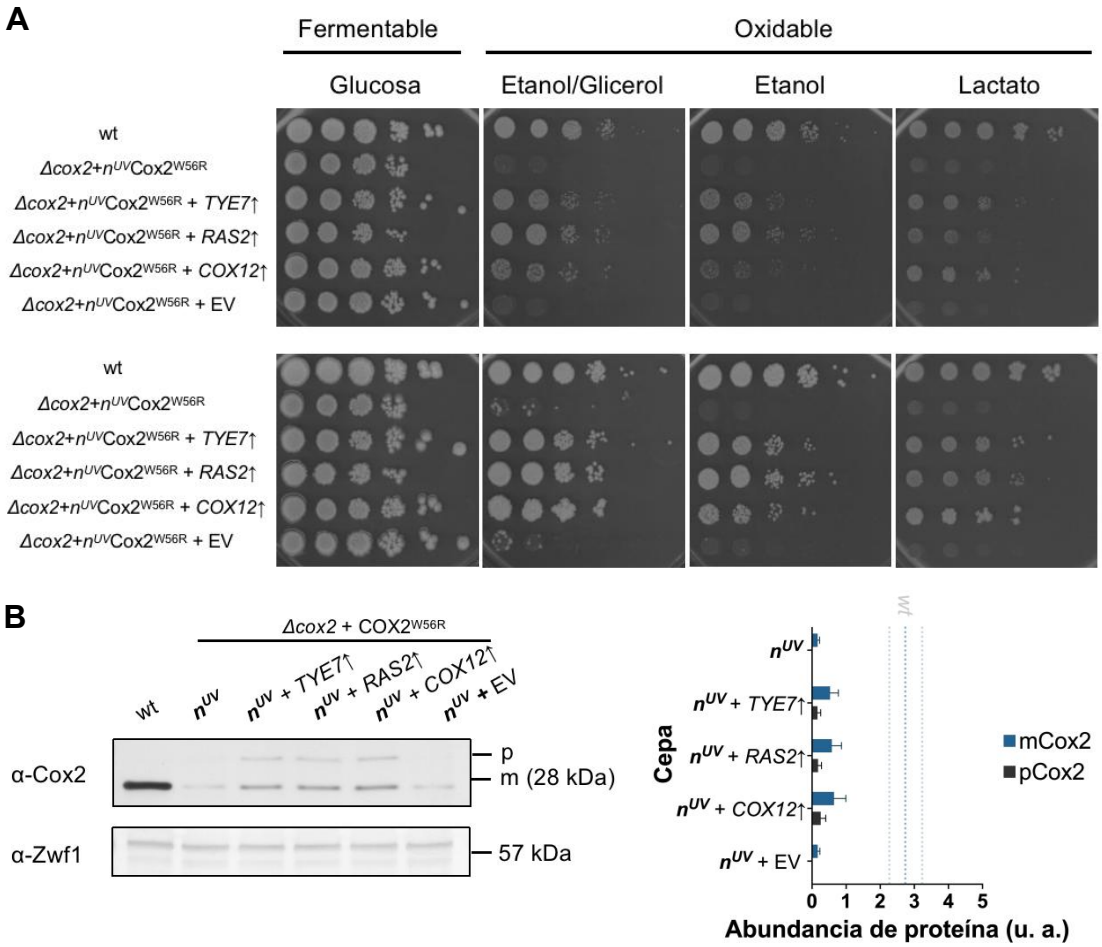

Figura 8. La sobreexpresión de los genes *TYE7*, *RAS2* y *COX12* incrementan el crecimiento de una cepa que expresa el gen *COX2*^{W56R} desde el núcleo. A) Diluciones seriadas a 30 ºC que muestran el fenotipo de crecimiento fermentativo (glucosa) y oxidable-respiratorio (etanol/glicerol, etanol y lactato) de una cepa silvestre (wt), la cepa de expresión alotópica obtenida por mutagénesis UV (n^{UV}Cox2^{W56R}) y las cepas sobreexpresando (↑) el gen indicado o, en su caso, portando el vector vacío (EV). Las fotografías se tomaron el cuarto día (paneles superiores) y séptimo día de crecimiento (paneles inferiores). B) Se utilizaron anticuerpos contra las proteínas Cox2 y Zwf1 para inmunodetectar a las proteínas correspondientes en extractos celulares totales de las cepas de levadura indicadas: tipo silvestre (wt); la cepa que produce la subunidad n^{UV}Cox2^{W56R} (n^{UV}), las tres cepas que sobreexpresan el gen indicado (↑) y la cepa de control transformada con un vector vacío (n^{UV} + EV). Se indican las formas precursora (p) y madura (m) de Cox2 y Cox2^{W56R} (28 kDa). El anticuerpo anti-Zwf1 reconoce una banda de 57 kDa que se utilizó como control de carga.

A pesar de que las cepas de expresión alotópica UV con los tres genes sobreexpresados mostraron mayor crecimiento en medios respiratorios, la cantidad de proteína madura (Fig. 8B) fue notablemente menor que la reportada anteriormente en nuestro laboratorio (Rubalcava-Gracia et al., 2019). Por lo tanto, en un segundo escenario, y teniendo en cuenta el precedente previamente publicado, donde un menor número de copias de Cox2 resultaba en una mayor internalización de la proteína alotópica que cuando se producía en un alto número de copias, se generó una cepa *Δcox2* transformada con un plásmido centromérico (*CEN*Cox2^{W56R}). Aunque la construcción de esta cepa también produce Cox2^{W56R} en bajo número de copias, difiere de cepa original *n*Cox2^{W56R} en que lleva consigo un plásmido con secuencias centroméricas (*CEN6)* y de replicación autónoma (*ARS4*) en levadura. Esto le permite expresar constitutivamente la construcción de Cox2^{W56R} en bajo número de copias, al tiempo que se mantiene mitóticamente estable (Sikorski y Hieter, 1989). Las cepas que sobreexpresan los genes propuestos mostraron un crecimiento mayor en medios respiratorios (Fig. 9), aún mayor que el de la cepa n^{UV}Cox2^{W56R}. Además, el análisis de inmunodetecciones, reveló que los tres genes sobreexpresados en esta cepa centromérica aumentaron los niveles de la forma madura de Cox2^{W56R} (Fig. 9B).

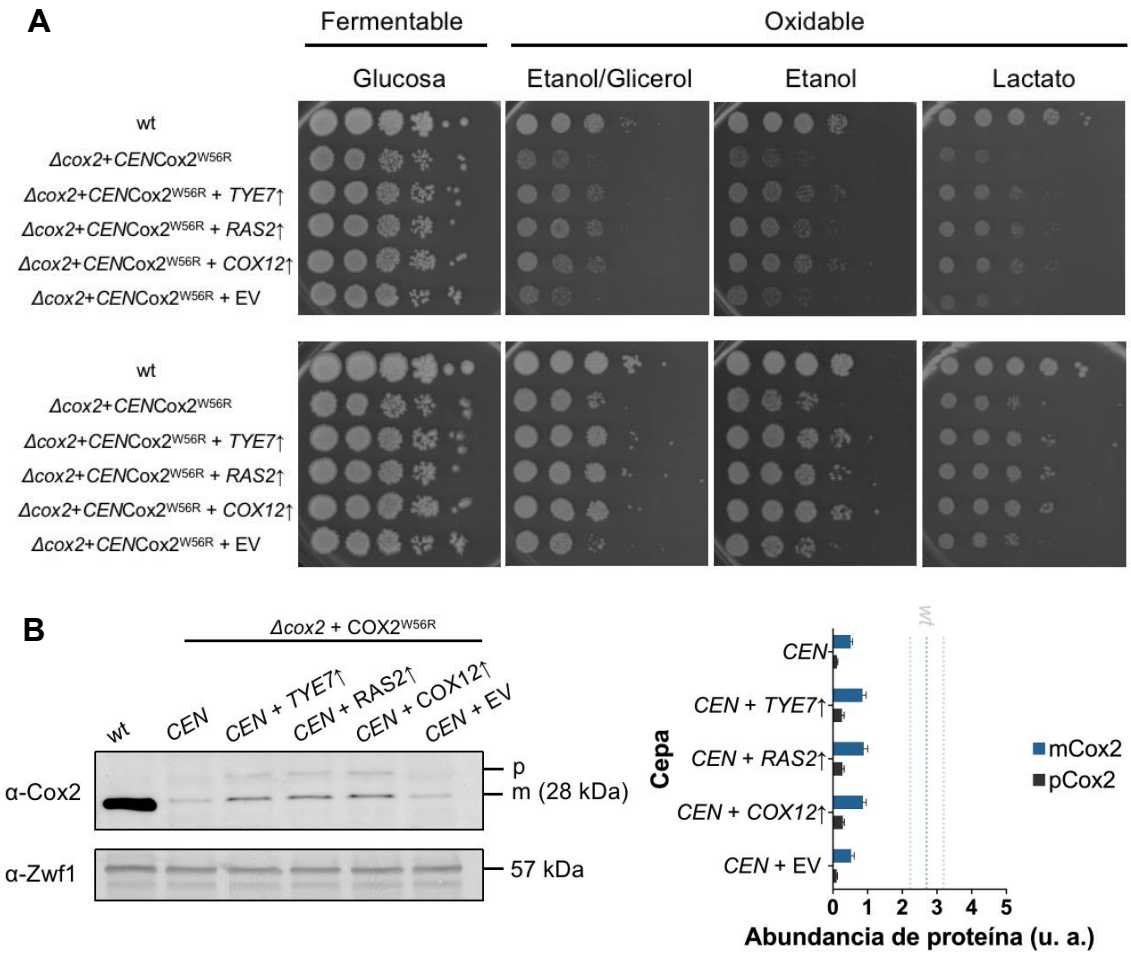

Figura 9. La sobreexpresión de los genes *TYE7*, *RAS2* y *COX12* incrementó el crecimiento en medios respiratorios en una cepa que expresa el gen *COX2*^{W56R} desde un plásmido centromérico. A) Diluciones seriadas a 30 ºC que muestran el fenotipo de crecimiento fermentativo (glucosa) y oxidable-respiratorio (etanol/glicerol, etanol y lactato) de una cepa tipo silvestre (wt), la cepa de expresión alotópica centromérica (*CEN*Cox2^{W56R}) y las cepas sobreexpresando (↑) el gen indicado o portando el vector vacío (EV). Las fotografías se tomaron el cuarto día (paneles superiores) y séptimo día de crecimiento (paneles inferiores). B) Se utilizaron anticuerpos contra Cox2 y Zwf1 para inmunodetectar las proteínas correspondientes en extractos celulares totales de las cepas de levadura indicadas: tipo silvestre (wt); la cepa *CEN*Cox2^{W56R} (*CEN*), las tres cepas que sobreexpresan el gen indicado (↑), y la cepa de control transformada con un vector vacío (*CEN* + EV). Se indican las formas precursora (p) y madura (m) de Cox2 y Cox2^{W56R} (28 kDa). El anticuerpo anti-Zwf1 reconoce una banda de 57 kDa que representa el control de carga.

Finalmente, como prueba adicional de que la sobreexpresión de los tres genes propuestos aumenta la internalización de la proteína Cox2^{W56R}, también exploramos su efecto en un sistema de expresión en alto número de copias. Existía la posibilidad de que la sobreexpresión de los tres genes propuestos se debiera a que estos genes modulaban positivamente la importación de la proteína alotópica, pero únicamente cuando era expresada en bajo número de copias. Para investigar esto, recurrimos a la cepa que produce la proteína alotópica desde un plásmido episomal de alto número de copias (*e*Cox2^{W56R}) (Fig. 10).

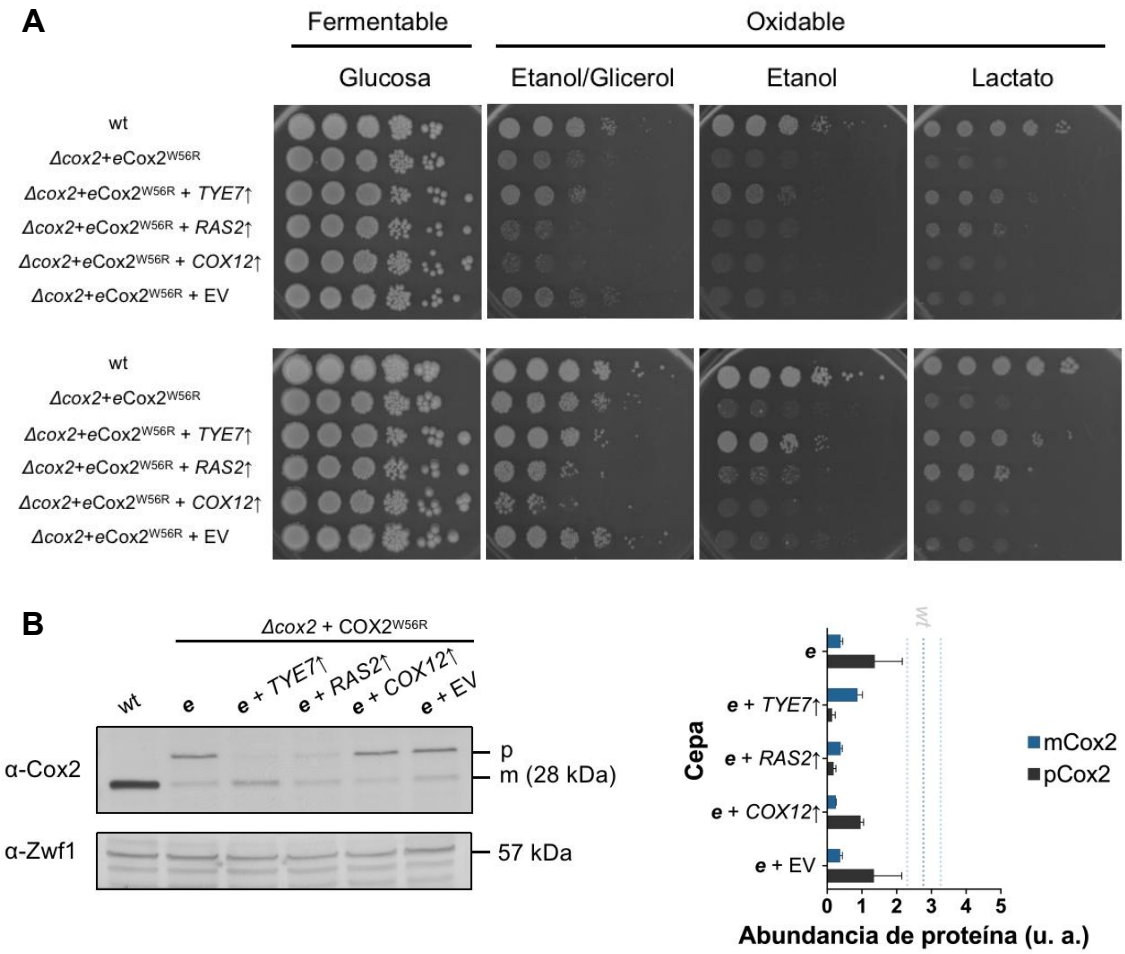

Figura 10. La sobreexpresión de los genes *TYE7*, *RAS2* y *COX12* afecta el fenotipo respiratorio de una cepa que expresa el gen *COX2^{W56R}* desde un plásmido multicopia. A) Diluciones seriadas a 30 ºC que

muestran el fenotipo de crecimiento fermentativo (glucosa) y oxidable-respiratorio (etanol/glicerol, etanol y lactato) de una cepa tipo silvestre (wt), la cepa de expresión alotópica multicopia (*e*COX2^{W56R}) y las cepas sobreexpresando (↑) el gen indicado o portando el vector vacío (EV). Las fotografías se tomaron el cuarto día (paneles superiores) y séptimo día de crecimiento (paneles inferiores). B) Se utilizaron anticuerpos contra Cox2 y Zwf1 para inmunodetectar las proteínas correspondientes en extractos celulares totales de las cepas de levadura indicadas: tipo silvestre (wt); la cepa *e*Cox2^{W56R} (*e*), las tres cepas que sobreexpresan el gen indicado (↑), y la cepa de control transformada con un vector vacío (*e* + EV). Se indican las formas precursora (p) y madura (m) de Cox2 y Cox2^{W56R} (28 kDa). El anticuerpo anti-Zwf1 reconoce una banda de 57 kDa que funciona como control de carga.

Bajo las circunstancias de expresión de *COX2^{W56R}* en alto número de copias, sólo las cepas que sobreexpresan *TYE7* y en menor medida, pero aún de manera considerable, *RAS2*, muestran un mayor crecimiento en medios respiratorios. Estos efectos son especialmente evidentes al cuarto día de crecimiento en los medios de cultivo con etanol y lactato (Fig. 10A), lo cual se correlaciona con niveles más bajos del precursor Cox2^{W56R} y niveles más altos de su forma madura (Fig. 10B).

SEGUNDA ESTRATEGIA EXPERIMENTAL: Predicción/Conjetura fundamentada

Para entender cómo otros factores influyen en la capacidad de la mitocondria para internalizar a la proteína alotópica Cox2^{W56R}, probamos sobreexpresar genes que codifican otras proteínas que participan en la importación mitocondrial. Junto con la expresión de Cox2^{W56R}, sobreexpresamos los genes que codifican las siguientes proteínas: Tom70, subunidad del complejo TOM involucrada en el reconocimiento de proteínas precursoras entrantes (Meisinger et al., 1999; Brix et al., 2000); Cox20, una chaperona esencial para la biogénesis de Cox2 y la exportación de su TMS1 a través del IMM (Hell et al., 2000); Oxa1, una insertasa de la MIM que media la exportación del extremo N-terminal de Cox2 desde la matriz mitocondrial al EIM (Hell et al., 1997, 2000). La chaperona Hsp104, una proteína citosólica de choque térmico que desensambla agregados de proteínas (Krämer et al., 2023), Msp1, una dislocasa AAA-ATPasa mitocondrial que extrae proteínas mal dirigidas para su degradación en el

proteosoma (Nakai et al., 1993; Castanzo et al., 2020), y Cis1, un factor asociado del complejo TOM que ayuda a reducir la acumulación de precursores mitocondriales al interactuar con Msp1 (Kabeya et al., 2007). Además, exploramos la sobreproducción de la proteína Pse1, una carioferina que interactúa con el complejo del poro nuclear implicado en la exportación de mRNA, y finalmente Rrp5, una proteína de unión a RNA que tiene un importante papel en la biogénesis del dominio ribosómico más grande (Venema et al., 1996). Los genes *PSE1* y *RRP5* habían sido identificados previamente en un análisis de supresores multicopia que se encontró facilitaron la importación de proteínas membranales a la mitocondria (Corral-Debrinski et al., 1999; Torchet et al., 1998). Como control, también exploramos la sobreexpresión de un gen no relacionado con la biogénesis de Cox2, por lo que se seleccionó a *SDH2*, que codifica la subunidad hierro-azufre de la enzima mitocondrial succinato deshidrogenasa (SDH o complejo II).

Cuando sobreexpresamos estos genes en la cepa que produce *n*Cox2^{W56R}, no observamos efectos significativos sobre el crecimiento en sustratos respiratorios. Sin embargo, al utilizar como fondo la cepa que produce *e*Cox2^{W56R}, notamos que *COX20*, *OXA1* y *PSE1* aumentaban el crecimiento respiratorio en comparación con la cepa que se transformó con el vector vacío. Aunque este incremento fue apenas perceptible cuando los transformantes se cultivaron a 30 ºC, fue mucho más evidente cuando las levaduras se crecieron a 37 ºC (Fig. 11). Cabe señalar también que el aumento en el crecimiento respiratorio es más pronunciado en los transformantes que expresan *COX20* y *OXA1* que en la que expresa *PSE1*.

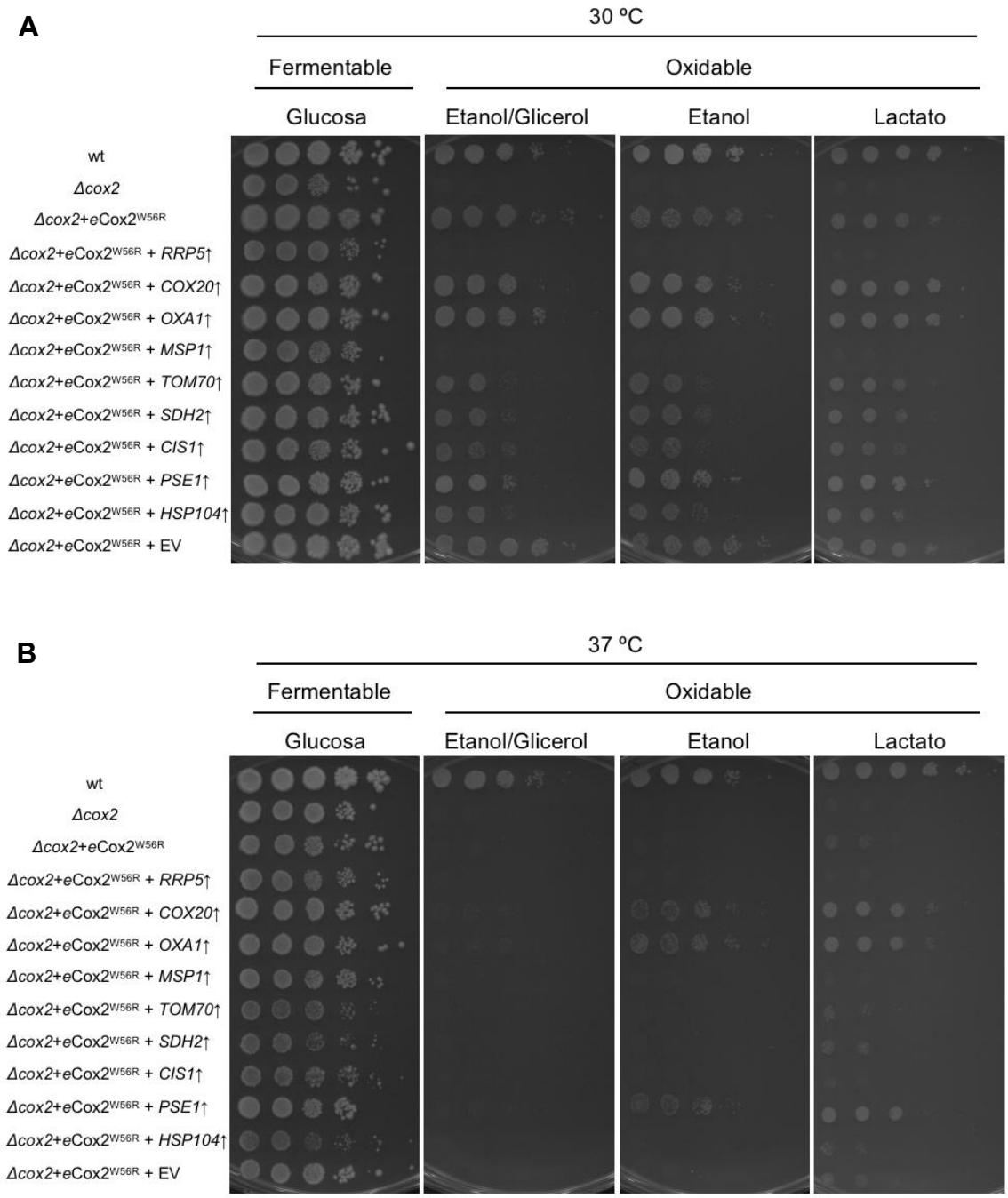

Figura 11. La sobreexpresión de los genes *OXA1, COX20* y *PSE1* aumenta el crecimiento respiratorio de una cepa que expresa el gen *COX2*^{W56R} desde un plásmido multicopia. A) Diluciones seriadas a 30 ºC que muestran el fenotipo de crecimiento fermentativo (glucosa) y oxidable-respiratorio (etanol/glicerol, etanol y lactato) de una cepa tipo silvestre (wt), la cepa de expresión alotópica multicopia (*e*COX2^{W56R}) y las cepas que sobreexpresan (↑) el gen indicado o portando el vector vacío (EV). B) Diluciones seriadas, que presentan la misma disposición de las cepas en el panel A, pero crecidas a 37 ºC. Las fotografías se tomaron el cuarto día después del inóculo inicial.

El análisis posterior de los niveles de la proteína Cox2^{W56R} de la subunidad alotópica cuando se sobreexpresan los genes *COX20*, *OXA1 y PSE1* reveló una relación positiva entre la proteína precursora y la madura. En la sobreexpresión de *COX20* y *OXA1* (Fig. 12A), se observó un aumento tanto en los niveles de la proteína madura, como del precursor, mientras que con *PSE1* (Fig. 12C), los niveles del precursor fueron menores.

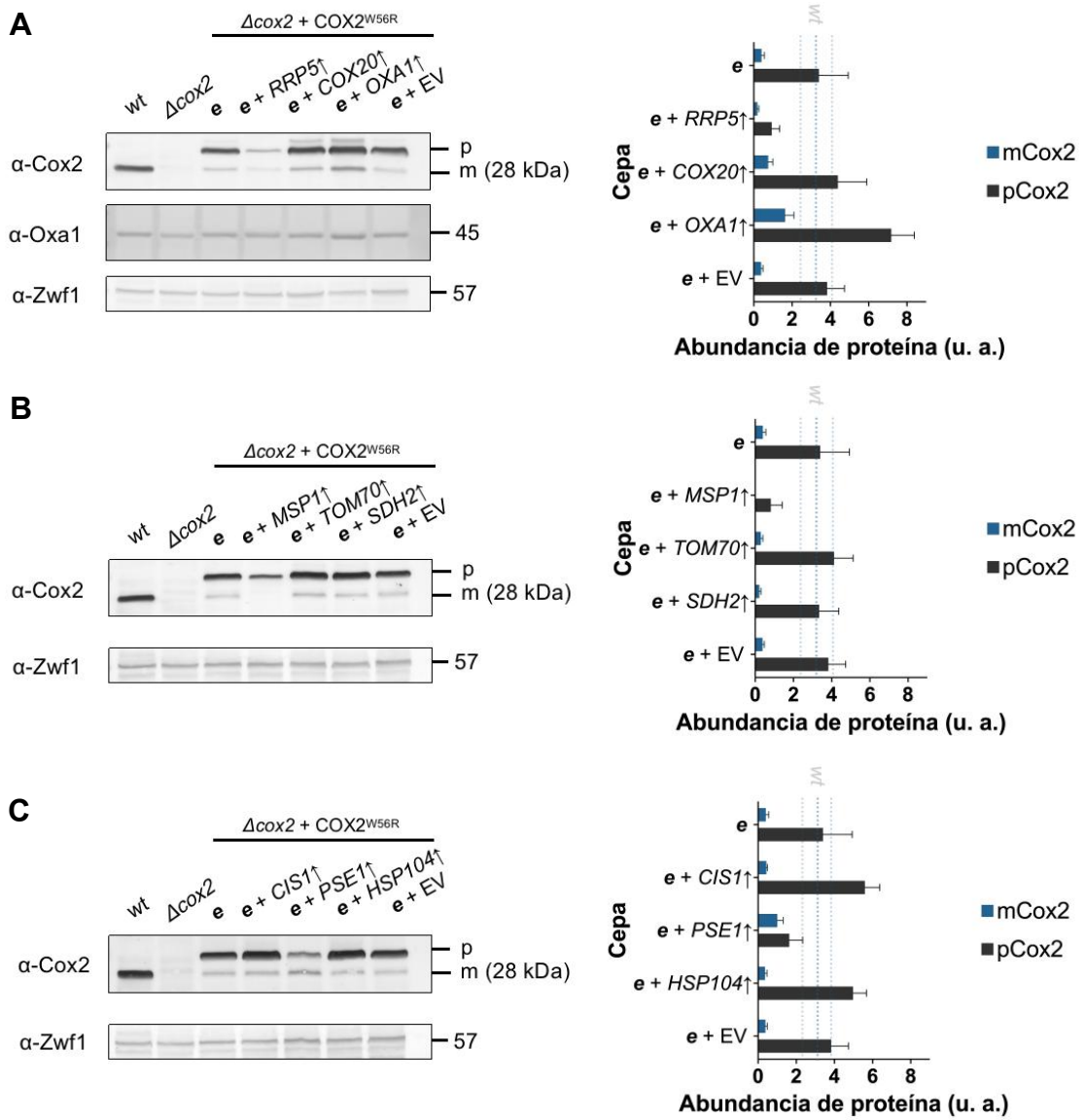

Figura 12. La sobreexpresión de los genes *OXA1, COX20* y *PSE1* incrementa la proporción de proteína madura en una cepa que expresa el gen *COX2*^{W56R} desde un plásmido multicopia. Se utilizaron anticuerpos contra Cox2, Zwf1 y Oxa1 para inmunodetectar a las proteínas correspondientes en extractos celulares totales de las cepas de levadura indicadas: tipo silvestre (wt); la cepa *e*Cox2^{W56R} (*e*), las cepas que sobreexpresan los genes: A) *RRP5*, *COX20* y *OXA1*; B) *MSP1*, *TOM70* y *SDH2*; C) *CIS1*, *PSE1* y *HSP104* (↑), y la cepa de control transformada con un vector vacío (*e* + EV). Se indican las formas precursora (p) y madura (m) de Cox2 y Cox2^{W56R} (28 kDa). El anticuerpo anti-Oxa1 reconoce a la insertasa Oxa1 (45 kDa), mientras que el anticuerpo anti-Zwf1 reconoce una banda de 57 kDa (control de carga).

Por otro lado, la sobreexpresión de *RRP5*, *MSP1*, *TOM70*, *SDH2*, *CIS1* y *HSP104* no favorece el crecimiento en medios respiratorios, siendo la sobreexpresión de *RRP5* y *MSP1* las que inhiben de manera más importante dicho crecimiento a 30 ºC (Fig. 11A). La sobreexpresión de *RRP5* y *MSP1* mantienen su efecto negativo cuando las cepas son crecidas a 37 ºC (Fig. 11B), lo cual se corroboró mediante el análisis los niveles de proteína madura de $Cox2^{W56R}$ usando inmunodetecciones (Figs. 12A y 12B). Sin embargo, no podemos llegar a la misma conclusión en cuanto al efecto de *TOM70*, *SDH2*, *CIS1* y *HSP104*.

Para corroborar que la sobreexpresión de los genes *OXA1*, *COX20* y *PSE1* inducían la sobreproducción de las proteínas correspondientes, analizamos los niveles de la proteína Oxa1 (Fig. 12A). Las cuantificaciones de las inmunodetecciones por densitometría (no mostradas), revelaron un aumento de al menos un 30% en los niveles de esta proteína en comparación con los de una cepa silvestre.

Una de las incógnitas no resueltas por trabajos anteriores era si la proteína alotópica Cox2 es internalizada en la mitocondria por el translocador TIM22 o por TIM23. En principio, se sugirió que fuese a través de TIM23, ya que es el translocador principal para todos los precursores mitocondriales que contienen una MTS. Debido a la naturaleza de su construcción genética, la proteína Cox2 alotópica cuenta con la MTS de la proteína Oxa1, cuya importación se sabe que ocurre a través de TIM23 (Herrmann et al., 1997). Sin embargo, también se ha considerado la posibilidad de que la subunidad alotópica sea insertada en la MIM por TIM22, cuyo mecanismo de acción consiste en insertar horquillas de dos cruces transmembranales en la dirección IMS hacia la matriz mitocondrial. Aunque TIM22 presenta un repertorio bien conocido de sustratos, que en su mayoría se caracterizan por presentar 6 TMS (muchos de ellos transportadores de sustancias pequeñas), se ha descrito que también puede translocar sustratos no convencionales, como el transportador mitocondrial de piruvato, la subunidad Mpc1 (Gomkale et al., 2020), que al igual que $Cox2^{W56R}$, también presenta 2 TMS. Aunque poco probable, puede considerarse la posibilidad de que TIM22 fuera la translocasa de la Cox2 alotópica. Dado que, en su topología final, Cox2 queda dispuesta con ambos dominios N-terminal y C-terminal hacia el EIM, no descartamos la posibilidad de que pueda translocarse en forma de horquilla (*hairpin*) a través de TIM22. Haciendo uso de

la misma biblioteca de sobreexpresión utilizada para observar el efecto de los genes de nuestra *predicción fundamentada*, decidimos explorar el efecto de sobreexpresar algunas de las subunidades que conforman a cada complejo de translocación. Esto nos podría proporcionar más información sobre el translocador de membrana interna que inserta a la subunidad alotópica Cox2.

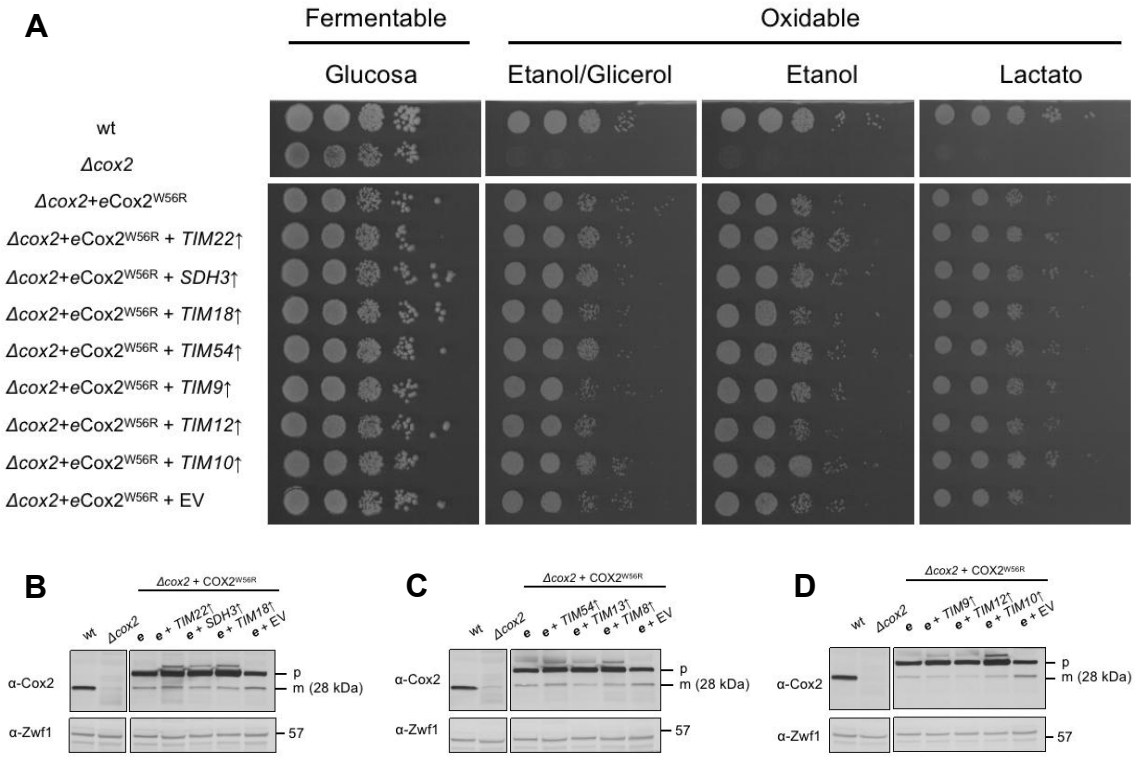

Figura 13. La sobreexpresión de genes que codifican algunas subunidades de la maquinaria de translocación TIM22 no tiene ningún efecto sobre el fenotipo respiratorio de una cepa que expresa el gen *COX2*^{W56R} desde un plásmido multicopia. A) Diluciones seriadas a 30 ºC que muestran el fenotipo de crecimiento fermentativo (glucosa) y oxidable-respiratorio (etanol/glicerol, etanol y lactato) de una cepa tipo silvestre (wt), la cepa de expresión alotópica multicopia (*e*COX2^{W56R}) y las cepas sobreexpresando (↑) el gen indicado o portando el vector vacío (EV). Las fotografías se tomaron el cuarto día de crecimiento. Se utilizaron anticuerpos contra Cox2 y Zwf1 para identificar a las proteínas correspondientes en extractos celulares totales de las cepas de levadura indicadas: tipo silvestre (wt); la cepa *e*Cox2^{W56R} (*e*), las cepas que sobreexpresan los genes: B) *TIM22*, *SDH3* y *TIM18*; B) *TIM54*, *TIM13* y *TIM8*; C) *TIM9*, *TIM12* y *TIM10* (↑), y la cepa de control transformada con un vector vacío (*e* + EV). Se indican las

formas precursora (p) y madura (m) de las proteínas Cox2 y Cox2^{W56R} (28 kDa). El anticuerpo anti-Zwf1 revela una banda de 57 kDa (control de carga).

Algunos de los componentes centrales del complejo de translocación TIM22 son las subunidades Tim18, Tim22, Tim54 y Sdh3. La sobreproducción de estas subunidades no resultó en un mayor crecimiento respiratorio en la cepa que produce eCox2^{W56R} (Fig. 13A) ni pareció incrementar los niveles en estado estacionario de Cox2^{W56R} madura (Fig. 13B, 13C). El crecimiento de las cepas que sobreexpresan a las subunidades Tim9, Tim10, Tim12 y Tim13, conocidas como "pequeñas TIM" —una familia de chaperonas que funcionan en el EIM e interactúan con proteínas de membrana hidrófobas para mantenerlas en un estado competente de importación— tampoco aumentó el crecimiento de la cepa que expresa el gen *COX2^{W56R}* (Fig. 13A, 13C, 13D). Por lo tanto, inferimos que la importación de la subunidad Cox2 alotópica probablemente no dependa del translocador TIM22.

Respecto a TIM23, al estudiar el efecto de la sobreproducción de sus subunidades, las proteínas Tim17, Tim23, Tim21 y Mgr2, reconocidas por su papel fundamental en la importación de proteínas hidrofóbicas, identificamos que la sobreexpresión de los genes *TIM21* y *TIM23* tuvo un efecto deletéreo notorio sobre el crecimiento respiratorio de la cepa *e*Cox2^{W56R} en fuentes de carbono no fermentables, mientras que la sobreexpresión de *TIM17* tuvo un efecto negativo menos pronunciado (Fig. 14A). El análisis de inmunodetecciones indicó que la sobreexpresión de *TIM17*, *TIM23*, *TIM21* y *MGR2* aumentó la acumulación del precursor eCox2^{W56R}, reduciéndose concomitantemente los niveles de la proteína madura. En particular, cuando se sobreexpresaron los genes *TIM21* y *TIM23*, la acumulación de la proteína alotópica madura disminuyó drásticamente (Fig. 14B y 14C).

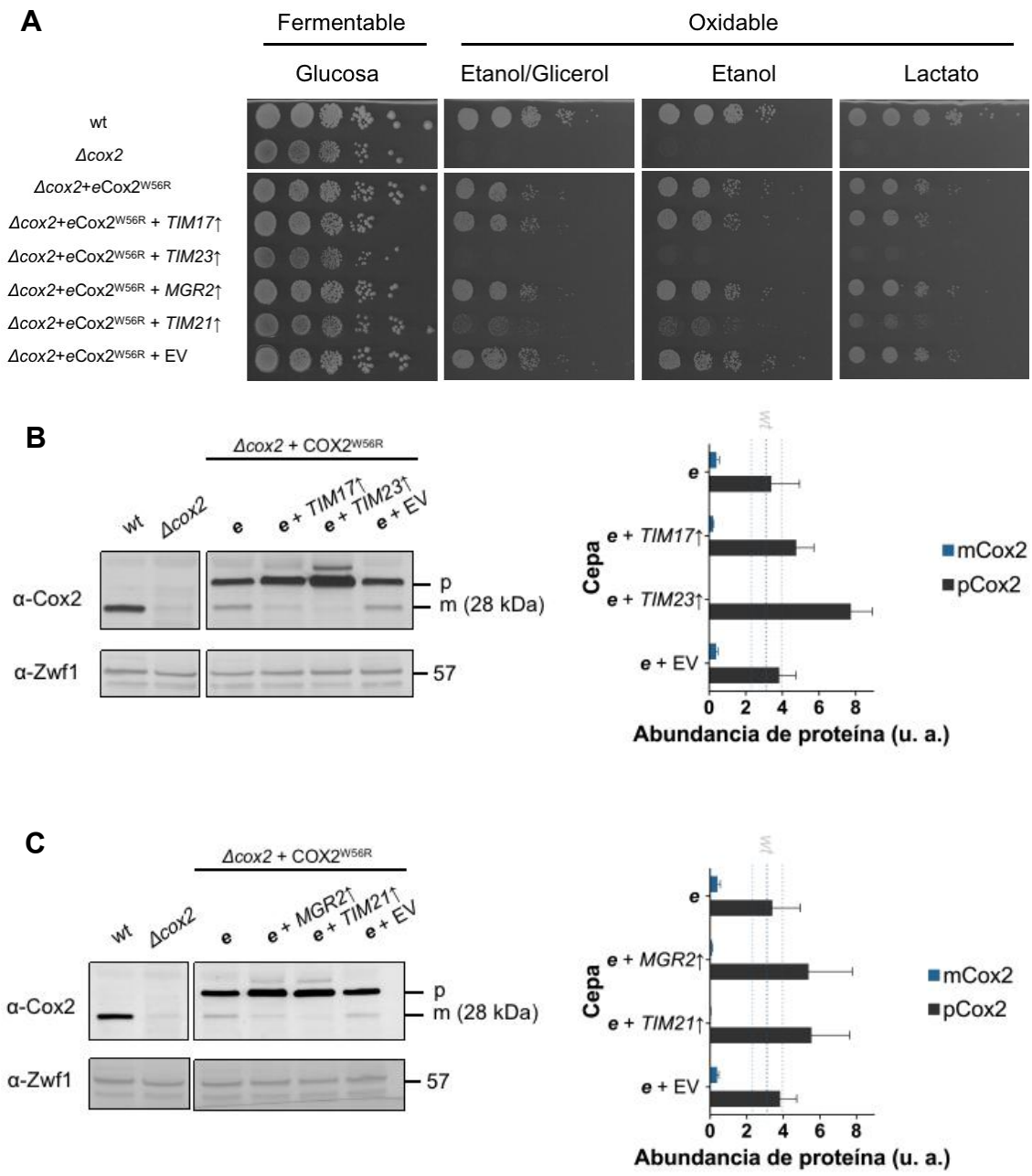

Figura 14. La sobreexpresión de genes que codifican subunidades de la maquinaria de translocación TIM23 afecta el fenotipo respiratorio de una cepa que expresa el gen *COX2*^{W56R} desde un plásmido multicopia. A) Diluciones seriadas a 30 ºC que muestran el fenotipo de crecimiento fermentativo (glucosa) y oxidable-respiratorio (etanol/glicerol, etanol y lactato) de una cepa tipo silvestre (wt), la cepa de expresión alotópica multicopia (*eCOX2*^{W56R}) y las cepas sobreexpresando (↑) el gen indicado o portando el vector vacío (EV). Las fotografías se tomaron el cuarto día de crecimiento. Se utilizaron anticuerpos contra Cox2 y Zwf1 para inmunodetectar las proteínas correspondientes en extractos celulares totales de

las cepas de levadura indicadas: tipo silvestre (wt); la cepa *e*Cox2^{W56R} (*e*), las cepas que sobreexpresan los genes: B) *TIM17* y *TIM23*; B) *MGR2* y *TIM21* (↑), y la cepa de control transformada con un vector vacío (*e* + EV). Se indican las formas precursora (p) y madura (m) de Cox2 y Cox2^{W56R} (28 kDa). El anticuerpo anti-Zwf1 se une a una banda de 57 kDa (control de carga). A la derecha de cada fotografía, los gráficos de barras representan la cuantificación de las bandas identificadas en las inmunodetecciones independientes. Los resultados se presentan como media ± DE, n = 3. La abundancia promedio y la desviación estándar de la proteína de la cepa tipo silvestre se indican mediante líneas de puntos negras y grises, respectivamente. Los resultados para *Δcox2* no se muestran, ya que siempre tuvieron un valor de cero.

El hecho de que la sobreexpresión de los componentes de TIM23 produzca un efecto deletéreo sobre el crecimiento respiratorio y la importación de *e*Cox2^{W56R}, se tomó como una indicación de que la subunidad alotópica Cox2 probablemente ingresa a las mitocondrias a través de este translocador, como ocurre con todos los precursores que contienen una MTS.

TERCERA ESTRATEGIA EXPERIMENTAL: Exploración del papel de la subunidad Mgr2 del translocador TIM23

Mgr2 se ha descrito como un regulador de TIM23 que controla la distribución de proteínas a través o dentro de la MIM, y que poseen al menos un cruce transmembranal (Gebert et al., 2012). Por lo tanto, este factor podría también participar en la importación de la proteína alotópica Cox2. Para estudiar los efectos de Mgr2 en la importación de Cox2^{W56R}, decidimos tanto eliminar como sobreexpresar el gen *MGR2*.

Al abolir la expresión del gen *MGR2* en una cepa silvestre (*Δmgr2*), no observamos ninguna alteración en su fenotipo en sustratos fermentables o respiratorios a 30 °C. Sin embargo, como se describió previamente (Matta et al., 2020), la eliminación de la función del gen *MGR2* resultó en un claro defecto en el crecimiento respiratorio a 37 °C (Fig. 15A). Por lo tanto, parece que la ausencia de Mgr2 restringe el crecimiento respiratorio en condiciones limitantes.

También examinamos el patrón polipeptídico de las mitocondrias solubilizadas aisladas de la cepa tipo silvestre y de la mutante nula *Δmgr2* cultivadas a 30 °C. Para separar a las proteínas mitocondriales, utilizamos electroforesis en geles azules nativos, seguida de la detección colorimétrica de la actividad de COX en el gel (Figura 15B). Estos experimentos revelaron claramente que la ausencia de Mgr2 disminuye los niveles estacionarios de COX.

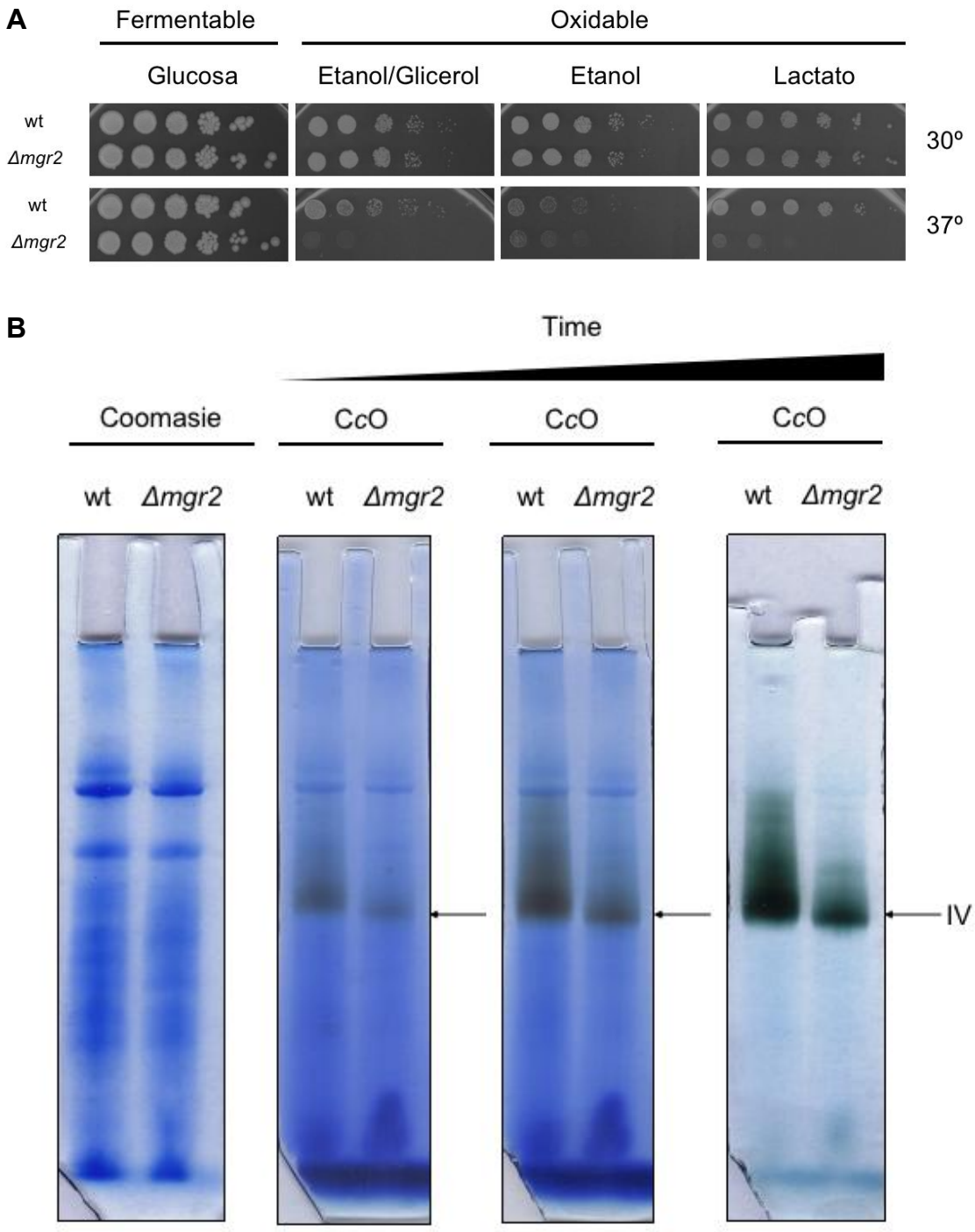

Figura 15. La eliminación del gen *MGR2* en una cepa de tipo silvestre no afecta el crecimiento respiratorio a 30 ºC, pero tiene un notable efecto negativo a 37 ºC. Diluciones seriadas a 30 ºC (paneles superiores) y a 37 ºC (paneles inferiores) que muestran el fenotipo de crecimiento fermentativo (glucosa) y respiratorio (etanol/glicerol, etanol y lactato) de una cepa tipo silvestre (wt), y una cepa cuyo gen *MGR2* fue eliminado (*Δmgr2*). Las fotografías se tomaron el cuarto día posterior al inóculo. B) Geles azules

después de electroforesis en condiciones nativas (BN-PAGE). Las mitocondrias de las cepas de tipo silvestre (wt) y de la mutante nula de Mgr2 (*Δmgr2*) se extrajeron después de cultivar las células a 30 °C. El primer gel se tiñó con azul de Coomassie y los tres siguientes muestran el curso temporal de la tinción de la actividad de la COX en el gel. La posición de la COX se indica (IV).

Ensayos polarográficos adicionales de consumo de oxígeno en células completas (Tabla 2) revelaron que al menos un 30% de la capacidad respiratoria de la cepa se ve afectada como consecuencia de la pérdida de Mgr2. Junto con la limitación del crecimiento en sustratos oxidables a 37 ºC, la disminución de la actividad de la COX y la pérdida de la actividad respiratoria, concluimos que la ausencia de Mgr2 afecta negativamente el comportamiento respiratorio de la cepa wt.

Posteriormente, exploramos el efecto de eliminar y sobreexpresar el gen *MGR2* en nuestro modelo de expresión alotópica. En el fondo de expresión en bajo número de copias (*n*Cox2^{W56R}), la eliminación del gen *MGR2* no tuvo un efecto notable sobre el crecimiento en sustratos fermentables, pero afectó sustancialmente el crecimiento respiratorio a 30 °C (Figura 16A, paneles superiores). Es importante destacar, que en esta misma cepa *n*Cox2^{W56R}, la sobreexpresión de *MGR2* desde un vector multicopia (*n*Cox2^{W56R} + *MGR2*↑) también disminuyó el crecimiento de la cepa, mientras que la transformación con el vector vacío (*n*Cox2^{W56R} + EV) no mostró ningún efecto.

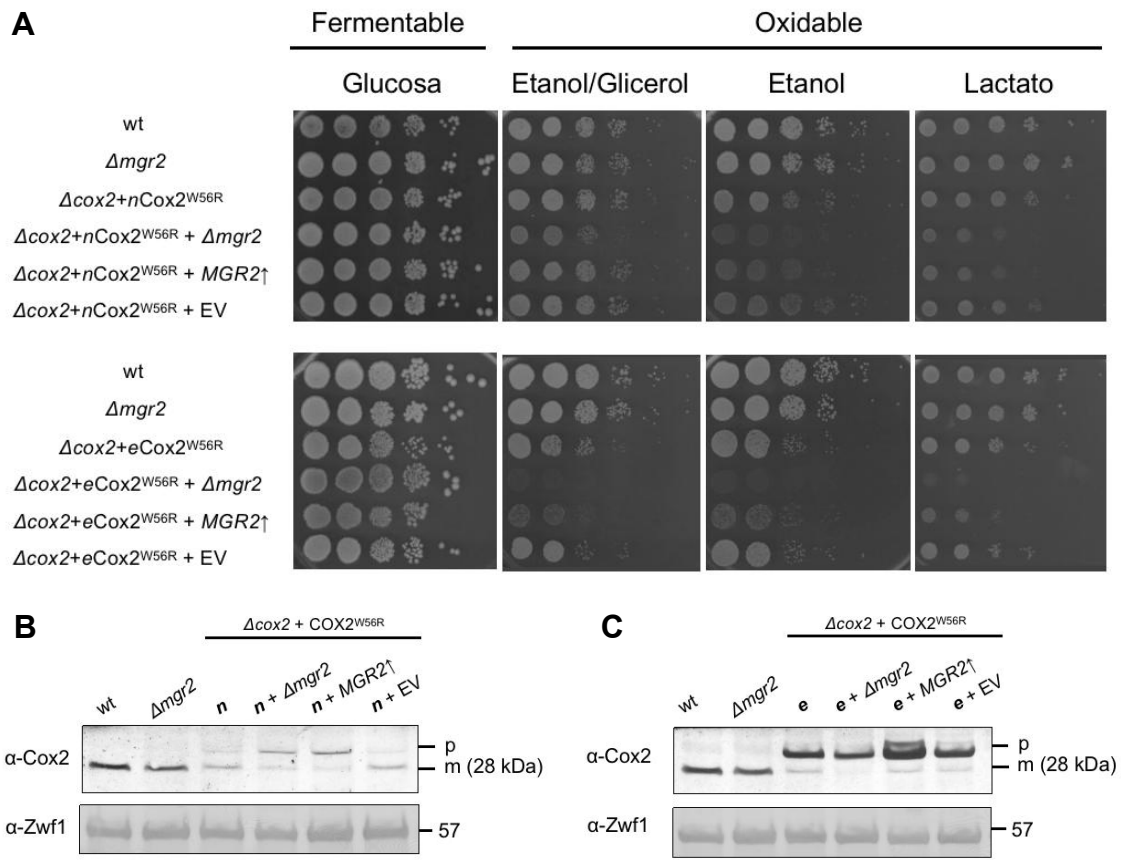

Figura 16. La eliminación y sobreexpresión del gen *MGR2* afectan el fenotipo respiratorio de cepas que expresan el gen *COX2*^{W56R} integrado en el núcleo o desde un plásmido multicopia. A) Diluciones seriadas a 30 ºC que muestran el crecimiento fermentativo (glucosa) y oxidable-respiratorio (etanol/glicerol, etanol y lactato). Se comparan una cepa silvestre (wt), una cepa sin el gen *MGR2* (*Δmgr2*) y cepas con diferentes niveles de expresión de *MGR2*, ya sea con el gen *COX2*^{W56R} integrado en el núcleo (*n*Cox2^{W56R}) (paneles superiores), o en un vector multicopia (*e*Cox2^{W56R}) (paneles inferiores). También se incluye una cepa portando el vector vacío (EV). Las fotografías fueron tomadas el cuarto día después de inocular las cajas. B) Se utilizaron anticuerpos contra Cox2 y Zwf1 para inmunodetectar las proteínas de las cepas correspondientes en extractos celulares totales de levadura. Se incluyen las siguientes cepas: la cepa tipo silvestre (wt); la cepa sin el gen *MGR2* (*Δmgr2*), la cepa *n*Cox2^{W56R}, y las cepas con diferentes niveles de expresión de *MGR2* en este fondo genético y la cepa de control transformada con un vector vacío (*e* + EV). C) Se realizó la misma serie de inmunodetecciones que en B, pero utilizando la cepa *e*Cox2^{W56R}. Se indican las formas precursora (p) y madura (m) de Cox2 y Cox2^{W56R} (28 kDa). El anticuerpo anti-Zwf1 revela una banda de 57 kDa (control de carga).

Cuando se utilizó un vector de expresión de alto número de copias para producir *e*Cox2^{W56R}, la eliminación de *MGR2* afectó aún más notablemente el crecimiento

respiratorio de la cepa, disminuyéndolo completamente (Fig. 16A). De igual manera, la sobreexpresión de *MGR2* redujo el crecimiento respiratorio de la transformante, de forma aún más pronunciada que sobre la cepa *n*Cox2^{W56R}. En conjunto, los resultados con ambos fondos genéticos sugieren que la presencia de Mgr2 es fundamental para el crecimiento respiratorio de la cepa alotópica.

Para evaluar los cambios en los niveles de proteína madura y precursora de Cox2 y Cox2^{W56R} cuando el gen *MGR2* estaba ausente o bien sobreexpresado, se analizó la acumulación de la subunidad Cox2 producida alotópicamente en extractos totales de levadura (Fig. 16B y 16C). En el contexto de *n*Cox2^{W56R}, la eliminación de *MGR2* dio lugar a un ligero aumento en los niveles del precursor y niveles disminuidos de la forma madura. Por otro lado, en el entorno de *e*Cox2^{W56R}, la ausencia de Mgr2 condujo a una importante acumulación del precursor, mientras que la presencia de la proteína madura fue casi indetectable. En ambos casos se revela que la internalización del precursor alotópico en la mitocondria está parcialmente disminuida. Además, la pérdida de la función de Mgr2 produce un fenotipo aún más grave cuando el gen alotópico *COX2^{W56R}* se expresa en copias múltiples. En contraste, cuando se sobreexpresa *MGR2*, se observa que la forma madura de la proteína correspondiente está presente, aunque se acumulan altos niveles del precursor (Fig. 16B y 16C). Esto podría estar correlacionado con el hecho de que, en ambos fondos genéticos *n*Cox2^{W56R} y *e*Cox2^{W56R}, las cepas aún mantienen la capacidad de crecer en medios respiratorios, aunque de forma limitada, como resultado de la alta acumulación de precursores.

Como se muestra en la Tabla 2, de acuerdo con el fenotipo de crecimiento respiratorio, la pérdida de la función Mgr2 en el entorno de *n*Cox2^{W56R} produce una disminución del 50% en el consumo de oxígeno, mientras que en la cepa *e*Cox2^{W56R} se produce un bloqueo completo de la respiración. En cuanto a las cepas que portan el gen alotópico *COX2^{W56R}* y a la vez sobreexpresan a *MGR2*, el consumo de oxígeno disminuye entre un 20 a 30%. En conclusión, el fenotipo de crecimiento respiratorio y el estado estacionario de Cox2^{W56R} se correlacionaron con la capacidad respiratoria de las levaduras transformadas.

Tabla 2. Mediciones del consumo de oxígeno.

Cepa	Consumo de oxígeno*	Consumo de oxígeno*	CR	% de consumo de oxígeno vs referente
	Sin sustrato	Con etanol		
wild-type	66.2 (± 8.1)	158.8 (± 0.9)	2.4	100
Δ*mgr2*	63.1 (± 6.1)	114.9 (± 2.3)	1.8	72
*n*Cox2^{W56R}	51.6 (± 1.1)	76.7 (± 0.9)	1.5	100
*n*Cox2^{W56R} + Δ*mgr2*	49.1 (± 0.5)	41.5 (± 0.9)	0.8	54
*n*Cox2^{W56R} + *MGR2*↑	65.6 (± 6.9)	60.4 (± 4.5)	1.0	79
*n*Cox2^{W56R} +EV	53.0 (± 0.3)	76.4 (± 0.6)	1.4	99.6
*e*Cox2^{W56R}	50.6 (± 5.5)	68.6 (± 3.2)	1.4	100
*e*Cox2^{W56R} + Δ*mgr2*	17.4 (± 0.6)	1.5 (± 0.03)	0.1	2
*e*Cox2^{W56R} + *MGR2*↑	46.1 (± 0.6)	46.9 (± 0.9)	1.0	68
*e*Cox2^{W56R} + EV	43.5 (± 3.1)	67.7 (± 2.7)	1.6	98.7

*expresado en ng de oxígeno atómico/min/mg de proteína mitocondrial.

Para asegurar la fiabilidad de nuestros procedimientos experimentales y descartar la posibilidad de artificios en nuestro sistema de expresión alotópica, complementamos la mutante nula *Δmgr2* con *MGR2* clonado en un plásmido multicopia; esto dio lugar a un incremento en el crecimiento respiratorio (Fig. 17A). Esta complementación no se produjo cuando el gen se insertó en dirección antisentido (3'-5') con respecto al promotor *PGK* del vector, ni cuando se transformó únicamente con el vector vacío (Fig. 17A).

Además, aislamos mitocondrias de la cepa tipo silvestre, la mutante nula *Δmgr2* y la mutante nula *Δmgr2* que sobreexpresa el gen *MGR2* (*Δmgr2* + MGR2 ↑), se solubilizaron con DDM y se sometieron a BN-PAGE (Fig. 17B). La tinción en gel de la actividad de COX reveló una actividad disminuida en la mutante nula *Δmgr2* en comparación con la cepa silvestre. Esta actividad de COX se restableció en la cepa *Δmgr2* complementada con el gen *MGR2* expresado desde un plásmido multicopia (Fig. 17B, panel central). Por el contrario, la actividad hidrolítica del complejo V (ATP sintasa) permaneció inalterada en las tres cepas (Fig. 17B, panel derecho). Finalmente, los geles azules nativos se sometieron a electroforesis de segunda dimensión de manera independiente en condiciones desnaturalizantes (2D-SDS-PAGE), y los geles resultantes se transfirieron e inmunodetectaron utilizando un anticuerpo anti-Cox2 (Fig. 17C). Se observó una disminución cercana al 50% en los niveles de Cox2 en la mutante nula *Δmgr2* en comparación con la cepa de tipo silvestre, los cuales se recuperaron parcialmente tras la complementación con el gen *MGR2* (Fig. 17C). Estos resultados indican claramente que la ausencia de Mgr2 provoca niveles disminuidos de COX, incluso cuando el crecimiento respiratorio de la mutante nula *Δmgr2* es comparable al de una cepa silvestre a 30 ˚C.

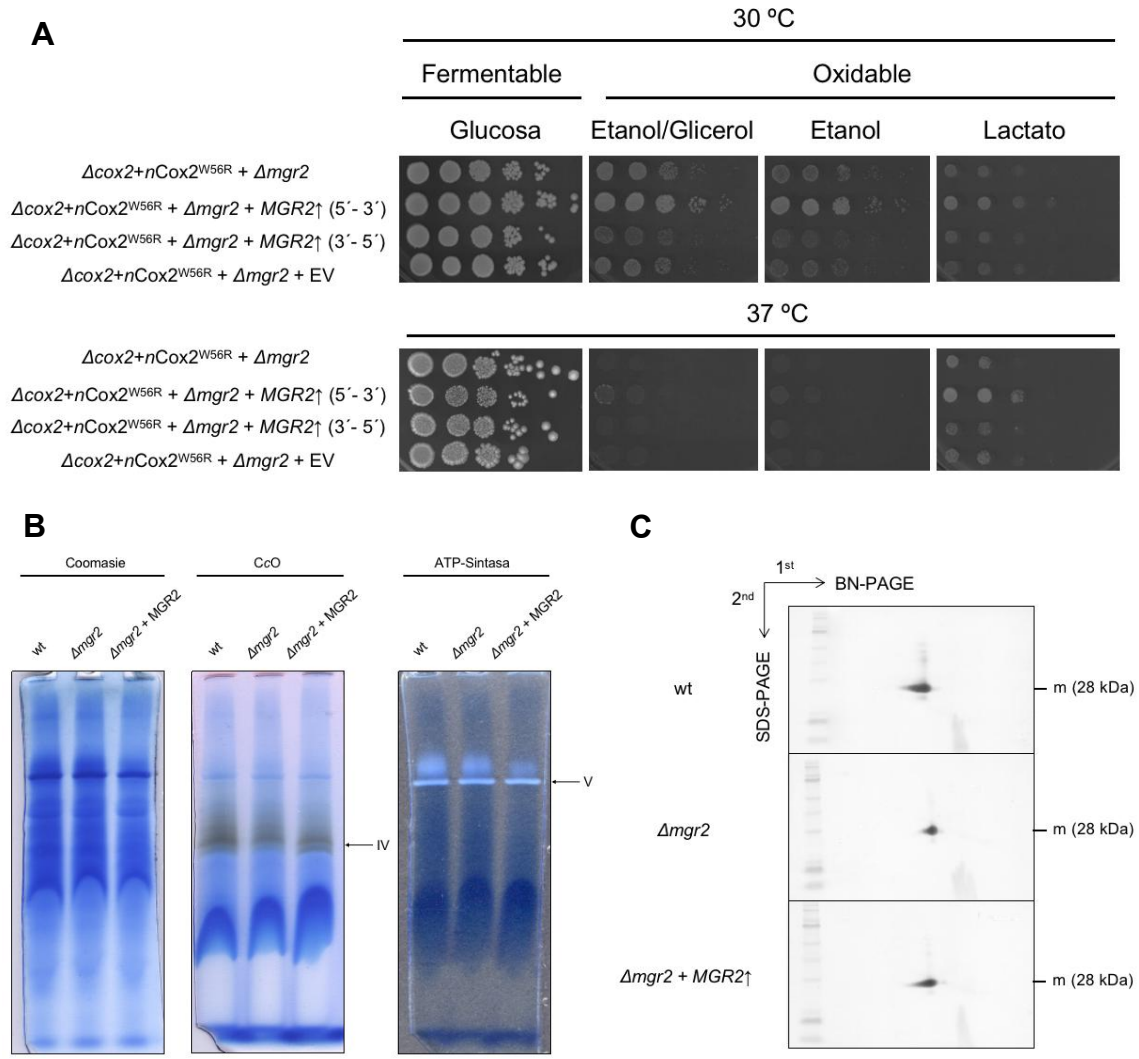

Figura 17. La expresión del gen *MGR2* complementa el defecto respiratorio en cepas de levadura como consecuencia de la ausencia de dicho gen. A) Diluciones seriadas a 30 ºC (paneles superiores) y a 37 ºC (paneles inferiores) muestran el fenotipo de crecimiento fermentativo (glucosa) y oxidable-respiratorio (etanol/glicerol, etanol y lactato) de una cepa con el gen *COX2*^{W56R} integrado en el núcleo y cuyo gen *MGR2* fue eliminado (*n*Cox2^{W56R} + *Δmgr2*), la cepas con el mismo fondo genético pero que albergan un vector multicopia portando el gen *MGR2* en la orientación 5'-3' (*n*Cox2^{W56R} + *Δmgr2* + *MGR2*↑ (5'-3')), en la orientación opuesta 3'-5' (*n*Cox2^{W56R} + *Δmgr2* + *MGR2*↑ (3'-5')), y con el vector vacío (*n*Cox2^{W56R} + *Δmgr2* + EV*)*. B) Geles azules después de electroforesis en condiciones nativas (BN-PAGE). Las mitocondrias de las cepas de tipo silvestre (wt), de la mutante nula de Mgr2 (*Δmgr2*) y de esta misma complementada con un vector expresando el gen *MGR2* desde un vector multicopia (*Δmgr2* + *MGR2*↑) se extrajeron después de cultivar las células a 30 °C. Los geles presentados, de izquierda a derecha, fueron teñidos con Coomassie Brilliant Blue (Serva), y muestran la actividad en gel de COX (precipitados color marrón) y la actividad en gel de ATPasa (precipitados blancos). La posición de la COX y ATPasa se

indica como IV y V, respectivamente. C) Se realizó una inmunodetección de los geles 2D (SDS-PAGE después de BN-PAGE). Las tiras de geles azules nativos se incubaron en presencia de SDS y se cargaron en geles desnaturalizantes de segunda dimensión. Los geles 2D resultantes se transfirieron a membranas de PVDF y se marcaron con un anticuerpo anti-Cox2. Las manchas correspondientes a las proteínas Cox2 se indican como **m** (forma madura de la proteína de 28 kDa).

DISCUSIÓN

En este trabajo, identificamos algunos genes cuya sobreexpresión promueve un mayor crecimiento respiratorio de una cepa *COX2*^{W56R}, lo cual se correlacionó con mayores niveles de la proteína alotópica Cox2^{W56R} madura dentro de las mitocondrias. A través de los tres enfoques experimentales utilizados, evidenciamos que los genes identificados son de particular relevancia en dos puntos críticos del proceso: 1) actuando como moduladores de la expresión del gen alotópico, al funcionar como activadores transcripcionales en el núcleo celular, y 2) facilitando la translocación y correcta disposición en la MIM de la proteína que se importa a la mitocondria. A continuación, sugerimos posibles mecanismos a través de los cuales los productos proteicos codificados en estos genes incrementan la internalización de la subunidad alotópica en las mitocondrias.

El gen *TYE7.* El producto de su expresión es una proteína de 33 kDa, que forma parte de una familia de proteínas ricas en residuos de serina, que contienen motivos de unión a DNA tipo bHLH (basic region/Helix-Loop-Helix/leucine-zipper, por sus siglas en inglés). Aunque no es esencial para el crecimiento, esta proteína funciona como un activador transcripcional en la expresión de genes controlados por el retrotransposon de terminación larga (LTR), Ty1 (Löhning y Ciriacy, 1994). Los retrotransposones LTR son comunes en el reino eucariota y son considerados precursores evolutivos de los retrovirus. Aunque su replicación e integración ocurren de manera similar a la de los retrovirus, estos fenómenos se llevan a cabo intracelularmente y de forma no infecciosa.

Tye7 actúa uniéndose a las cajas E de varios genes que codifican enzimas glicolíticas, como la enolasa I, la 3-fosfoglicerato cinasa, la piruvato cinasa, la gliceraldehído-3-fosfato deshidrogenasa, la fosfoglicerato mutasa y la triosafosfato isomerasa (Nishi et al., 1995; Sato et al., 1999; Robinson y Lopes, 2000). Estudios recientes utilizando la técnica de inmunodetección de cromatina con exonucleasa lambda (ChIP-exo) han revelado que Tye7 activa una serie de genes relacionados con la maquinaria de importación de proteínas mitocondriales (Horak et al., 2002; Holland et al., 2019). Estos genes incluyen a la insertasa Oxa1; a los factores Cox18, Cox20 y Coa6, implicados en la biogénesis de la proteína mitocondrial Cox2; a Tom40, un componente del complejo

TOM; a Tim50 y Ssc1, dos subunidades del complejo TIM23; así como a chaperonas de la familia HSP70, como Sse2, Ssb1 y Mdj1. Esto sugiere que la sobreexpresión de *TYE7* puede promover la internalización de $Cox2^{W56R}$ en las mitocondrias a través de un mecanismo indirecto, posiblemente activando la expresión de varios genes cuyos productos proteicos están implicados en la importación de proteínas mitocondriales.

El gen *RAS2.* La proteína Ras2 forma parte de la superfamilia Ras, que comprende más de 150 GTPasas pequeñas que median múltiples respuestas metabólicas, actuando como reguladores clave en diversas vías de señalización (Broach y Deschenes, 1990; Goitre et al., 2014), que incluyen el control de la biogénesis y función mitocondrial (Hlavatá y Nyström, 2003). Cuando la levadura crece utilizando glucosa como fuente de carbono, las proteínas Ras (las isoformas Ras1 y Ras2) se acumulan principalmente en la membrana plasmática y el núcleo. Sin embargo, en ausencia de glucosa, dichas proteínas tienden a acumularse en las mitocondrias (Broggi et al., 2013).

Se ha descrito que la eliminación del gen *RAS2* impide el crecimiento de la levadura en fuentes de carbono no fermentables (Tatchell et al., 1985). Ras2 activa la adenilil ciclasa (AC) y otras cinasas dependientes del adenosín monofosfato cíclico (cAMP), como la proteína cinasa A (PKA), que se encuentra localizada en las mitocondrias (Papa et al., 1996). La ruta de señalización Ras/cAMP está íntimamente ligada a la disponibilidad de nutrientes, desempeñando un papel crítico en el crecimiento celular de *S. cerevisiae* (Matsumoto et al., 1983). En estudios previos, se observó que, en la levadura, el cAMP revierte la represión de la glucosa en la biogénesis mitocondrial (Fang y Butow,1970) y activa genes mitocondriales que codifican subunidades que forman parte de la COX y otros componentes de la OXPHOS (Chandrasekaran y Jayaraman, 1978). Por lo tanto, junto con la PKA, el cAMP parece controlar la transcripción mitocondrial (Müller y Bandlow, 1987), actuando sobre un elemento regulador *cis* presente en el DNA mitocondrial que aún no ha sido identificado (Iqbal et al., 1996).

También se ha reportado que la sobreexpresión de *RAS2* suprime una mutación en la citrato sintasa (*CIT2*), una enzima del ciclo del glioxilato (Swiegers et al., 2006), así como una mutación en un sitio no catalítico de la subunidad alfa (atp1-2) de la ATP

sintasa mitocondrial (Mabuchi et al., 2000), ilustrando los efectos de este gen sobre enzimas mitocondriales. Además, células *RAS2*^{Val19} que exhiben una señalización hiperactiva de Ras/PKA, anulan la actividad del transportador mitocondrial de ATP/ADP (Hlavatá et al., 2007). Todos estos hallazgos parecen indicar que Ras2 induce la expresión de genes que codifican proteínas ribosomales (Neuman-Silberberg et al., 1995). Esto parece estar relacionado con una mayor tasa de transcripción de genes nucleares que codifican proteínas mitocondriales.

Por otra parte, el incremento de los niveles celulares de cAMP inducidos por Ras2 también aumenta la estabilidad del coactivador transcripcional Hap4, un regulador clave del complejo HAP (Bouchez et al., 2020). El complejo transcripcional HAP es esencial para el crecimiento de la levadura en sustratos respiratorios, ya que controla la traducción mitocondrial, reprogramando la célula para hacer la transición de fermentación a respiración y sirviendo como coordinador de la expresión entre genes mitocondriales y nucleares (Buschlen et al., 2003). En general, un aumento en la actividad de la vía de cAMP regula positivamente la biogénesis mitocondrial (Yoboue et al., 2012).

Debido a la amplia gama de efectos que las vías reguladoras de las proteínas Ras tienen en varias enzimas mitocondriales, proponemos que la sobreexpresión de *RAS2* puede promover una mayor transcripción de varios genes mitocondriales relacionados con la OXPHOS, incluidos los genes mitocondriales *cox1* y *cox3*, con un aumento concomitante en los niveles de los módulos Cox1 y Cox3 en el IMM. Estos módulos pueden incorporar fácilmente las subunidades alotópicas Cox2^{W56R} que van ingresando a la mitocondria, para formar complejos COX maduros y completamente ensamblados. Sugerimos que la incorporación preferencial de las subunidades Cox2^{W56R} producidas alotópicamente en estos módulos preformados puede formar niveles más altos de COX y a la vez promover una mayor internalización del precursor alotópico.

El gen *COX12.* Este gen codifica a la subunidad VIb de la COX en levadura. Esta subunidad es soluble, unida débilmente a la enzima y se encuentra expuesta hacia el EIM (LaMarche et al., 1992; Ing et al., 2022). Se ha reportado que Cox12 es necesario para la formación de COX activa, y su ausencia conduce al ensamblaje de una COX que

es espectroscópicamente detectable, pero que presenta una actividad enzimática notablemente reducida. Cox12 interactúa con las proteínas Rcf1 y Rcf2, las cuales participan en la formación del supercomplejo respiratorio III-IV, y facilitan el ensamblaje de subunidades adicionales en la misma COX. Esto sugiere que Cox12 tiene un papel crucial en la formación de supercomplejos, regulando además el ensamblaje y la actividad enzimática del complejo IV (Das et al., 2021). Adicionalmente, estudios genéticos recientes han revelado que junto con Coa6, Cox12 desempeña una función relevante en la inserción del centro binuclear de cobre en la COX. Mientras que la ablación de Coa6 o Cox12 puede ser rescatada mediante la suplementación con cobre, la eliminación simultánea de ambos anula completamente la biogénesis de Cox2 y la suplementación con cobre resulta insuficiente para restaurar sus niveles (Ghosh et al., 2014; 2016). Además, la sobreproducción del gen *COX12* rescata parcialmente la mutante nula *Δcoa6*. Dado que se han observado interacciones físicas entre Coa6, Cox2, Cox12 y las proteínas Sco, que participan en el suministro de cobre a Cox2, es posible que la sobreexpresión del gen *COX12* suprima la mutante nula *Δcoa6* promoviendo la formación del sitio binuclear CuA.

La inserción de cobre en el centro metálico es probablemente un paso limitante de la biogénesis de Cox2, debido a los diversos factores que participan en su formación, los cuales también podrían minimizar la producción de intermediarios reactivos de COX (Nývltová et al., 2022). Por lo tanto, sugerimos que los niveles altos de la subunidad Cox12 en el EIM podrían acelerar la entrega de cobre y el ensamblaje del centro CuA, facilitando la posterior incorporación de $Cox2^{W56R}$ en COX y aumentando simultáneamente la tasa de internalización del precursor alotópico en las mitocondrias.

El gen *OXA1*. La translocasa Oxa1 es una proteína embebida en la MIM (Hell et al., 1997, 2000; Homberg et al., 2023) que desempeña un papel crucial en la inserción de proteínas codificadas en el genoma mitocondrial (Szyrach et al., 2003). Entre estas proteínas, destacan las subunidades Cox1, Cox2 y Cox3 de la COX, componentes fundamentales de la OXPHOS (Bonnefoy et al., 1994; Herrmann y Funes, 2005). Además, Oxa1 contribuye a la inserción de los TMS de muchas proteínas de membrana codificadas en el núcleo. Se ha demostrado que Oxa1 es esencial para la inserción del TMS1 de la subunidad alotópica $Cox2^{W56R}$ (Elliott et al., 2012). Para explicar los

efectos de Oxa1 en este trabajo, proponemos que su sobreproducción puede facilitar el reconocimiento del péptido señal cercano al TMS1 de $Cox2^{W56R}$, lo que a la vez permitiría una inserción más eficiente de la proteína alotópica en la membrana interna mitocondrial. Una incorporación más eficiente de la subunidad alotópica a la MIM, a su vez podría promover la entrada de más precursores de $Cox2^{W56R}$ a la mitocondria.

El gen *COX20.* Cox20 es una proteína embebida en la MIM, que sirve como chaperona específica de Cox2 y está involucrada en varios pasos de la biogénesis de COX (Herrmann y Funes, 2005; Kumar et al., 2015; Keerthiraju et al., 2019). Junto con el receptor de membrana Mba1 que ancla al mitoribosoma a la MIM, Cox20 estabiliza el polipéptido Cox2 naciente que es sintetizado en la matriz mitocondrial y, tras la remoción del péptido líder de Cox2, entrega la subunidad a Cox18, responsable de exportar el TMS2 y la región C-terminal de Cox2, el cual contiene el sitio de unión de cobre (Lorenzi et al., 2016; Bourens et al., 2017). La unión de Cox20 a Cox2 en la cara de la MIM que está expuesta hacia el EIM, acelera la disociación de la translocasa Cox18 de la proteína Cox2 recién exportada (Elliot et al., 2012) y promueve su maduración posterior al entregar la subunidad al sistema de inserción de cobre Sco1-Sco2-Coa6 (Hell et al., 2000).

La importación de $Cox2^{W56R}$ alotópica no requiere de la participación de Cox18 (Elliot et al., 2012), lo que sugiere que la vía de biogénesis de la subunidad producida alotópicamente no implica la translocación del TMS2 hasta la matriz mitocondrial para después ser insertada en la MIM. Es posible que la sobreexpresión de *COX20* estabilice la inserción del TMS1 de la subunidad alotópica $Cox2^{W56R}$ mediada por Oxa1 y facilite la interacción de la subunidad con la maquinaria de inserción de Cu.

El gen *PSE1*. Pse1 es un miembro de la superfamilia de la carioferina β que interactúan con el complejo del poro nuclear. En estudios previos, se ha observado que la sobreexpresión de *PSE1* facilita la inserción de proteínas a la mitocondria, incluida la proteína hidrofóbica Atm1, un transportador ABC dependiente de ATP que contiene varios TMS. Atm1 exporta precursores mitocondriales que contienen grupos de hierro-azufre Fe/S al citosol (Corral-Debrinsky et al., 1999). También se ha reportado que las cepas de levadura con mutaciones en el gen *PSE1* no son capaces de crecer en medios

que contienen glicerol como fuente de carbono, y exhiben un patrón de mayor fragmentación en su red mitocondrial, además de una disminución significativa del potencial de membrana ΔΨ, en comparación con una cepa silvestre (Lord et al., 2015).

No es evidente de inmediato por qué la sobreexpresión de *PSE1* suprime el fenotipo de $Cox2^{W56R}$. Es posible que Pse1 tenga una localización dual y ejerza sus efectos tanto en el núcleo como en las mitocondrias. Sin embargo, hasta la fecha, esta localización dual no ha sido confirmada. También es posible que la sobreexpresión de *PSE1* facilite la exportación nuclear de un mRNA que codifique una chaperona necesaria para la importación mitocondrial de proteínas de membrana. Esta chaperona podría prevenir la agregación de sus TMS, manteniendo su estructura desplegada de manera conveniente para su importación. La existencia de este posible factor tampoco ha sido confirmada. Sin duda, dilucidar el mecanismo al través del cual actúa la sobreproducción de Pse1 es de gran interés y amerita estudios futuros.

Participación de Mgr2 en la biogénesis de la subunidad alotópica $Cox2^{W56R}$. Mgr2 es una pequeña proteína hidrofóbica de 12kDa, que tiene dos TMS. Fue identificada inicialmente como un factor de acoplamiento del translocador de la MIM, TIM23 (Gebert et al., 2012; Ieva et al., 2013; 2014). Se ha propuesto que Mgr2 regula el mecanismo de translocación del complejo TIM23 (Mirzalieva et al., 2019), que como ya se mencionó, puede existir en la MIM en tres formas estructural y funcionalmente distintas que se encuentran intercambiándose continuamente: $TIM23_{CORE}$, $TIM23_{MOTOR}$ y $TIM23_{SORT}$ (Popov-Celeketić et al., 2008; Bohnert et al., 2010; Chacinska et al., 2010). Varios trabajos sugieren que Mgr2 se une cerca a la apertura lateral de la cavidad de Tim17 durante la translocación de proteínas (Sim et al., 2023; Zhou et al., 2023), de alguna manera regulando la liberación lateral de ciertos precursores.

A pesar de lo anterior, Mgr2 no es esencial para el crecimiento de la levadura a una temperatura de 30 °C (Fig. 15). La no esencialidad de Mgr2 sugiere que la formación de la estructura a la que contribuye puede ser requerida selectivamente para la translocación de ciertos precursores (Ieva et al., 2014; Sim et al., 2023). También se ha descrito que Mgr2 funciona como un modulador que interactúa directamente con las α-hélices hidrofóbicas que están siendo translocadas a través de TIM23 (Matta et al.,

2020). En resumen, Mgr2 parece monitorear la hidrofobicidad de las proteínas en tránsito por TIM23, favoreciendo la apertura lateral de la cavidad de translocación y la liberación lateral de ciertas proteínas de membrana en la MIM (Gebert et al., 2012).

Por otra parte, Pam18 que es una proteína que sirve de andamiaje para la forma de la translocasa conocida como $TIM23_{MOTOR}$, es crucial para la importación de proteínas hasta la matriz mitocondrial (Mokranjac et al., 2020). Cuando Pam18 es reclutada a la translocasa, la función principal de su dominio α-hélice transmembranal es obstruir la liberación lateral de proteínas dentro de la MIM. Una vez que un TMS hidrofóbico queda arrestado en la cavidad de translocación de TIM23, Pam18 se desasocia y permite el reclutamiento de Mgr2 (Schendzielorz et al., 2018). Lo anterior implica necesariamente una transición del translocador de su forma $TIM23_{MOTOR}$ a $TIM23_{SORT}$. El rol de Mgr2 en $TIM23_{SORT}$ entonces, es discriminar qué α-hélices deben ser liberadas lateralmente dentro de la MIM o translocadas a través de la MIM. Mgr2 probablemente actúa monitoreando las señales "stop-transfer" contenidas en los TMS hidrofóbicos para que sean liberadas dentro de la membrana, mientras que las α-hélices menos hidrofóbicas cruzan a través de la cavidad de Tim17 hasta la matriz mitocondrial (Botelho et al., 2011; Lee et al., 2020).

Aunque estudios previos han mostrado que una mutante nula *Δmgr2* presenta un fenotipo de crecimiento respiratorio sensible a la temperatura (Matta et al., 2020), no se habían descrito otros efectos sobre la cadena respiratoria causadas por la ausencia de Mgr2. En este trabajo corroboramos que la ausencia de Mgr2 en un contexto silvestre no tiene un efecto deletéreo sobre el crecimiento de la levadura; sin embargo, da lugar a una disminución del 30% tanto en el consumo de oxígeno como en la actividad de COX (Fig. 15). ¿Cómo podemos explicar que una disminución importante en los niveles de COX no afecte el crecimiento de la levadura? Dado que la COX (complejo IV) y el complejo *bc1* (complejo III) se encuentran en una alta abundancia en una célula de *S. cerevisiae* (67000 y 83000 copias/célula respectivamente) (Morgenstern et al., 2017; Pfanner et al., 2019), una reducción moderada en los niveles de COX no debería afectar drásticamente el crecimiento de la levadura. Es posible que sus efectos adversos solo se manifiesten una vez que los niveles caigan por debajo de un umbral crítico.

Es muy probable que Mgr2 participe también en la biogénesis de COX, incluso cuando la subunidad Cox2 se sintetiza normalmente dentro de las mitocondrias. Es probable que Mgr2 controle el proceso de importación de algunas de las subunidades de COX codificadas en el núcleo que contienen un TMS hidrofóbico. De hecho, nueve subunidades codificadas en el núcleo están presentes en la estructura tridimensional obtenida por crio-EM del complejo COX de levadura (PDB: 6YMY; Berndtsson et al., 2020), y seis de ellas exhiben un TMS orientado con una topología N-afuera/C-afuera (Cox5, Cox7, Cox8, Cox9, Cox13 y Cox26). Para alcanzar esta topología final, $TIM23_{SORT}$ debe liberar lateralmente las seis subunidades en la MIM y muy probablemente Mgr2 modula este proceso. La ausencia de Mgr2 podría afectar la liberación lateral de estas subunidades en la MIM, disminuyendo los niveles de COX en estado estacionario. Sin embargo, consideramos que el papel de Mgr2 se vuelve crucial cuando aumenta la temperatura o bien cuando el ensamblaje de COX depende de la subunidad Cox2 producida alotópicamente.

Nuestros hallazgos revelan que la ausencia de Mgr2 afecta negativamente el crecimiento respiratorio y la internalización tanto de *n*$Cox2^{W56R}$ como de *e*$Cox2^{W56R}$. Un escenario posible es que, en ausencia de Mgr2, el TMS1 con la sustitución W56R ya no se considere menos hidrofóbico y se reconozca como una señal "*stop-transfer*". De esta manera, el TMS1 sería liberado lateralmente en la MIM en lugar de ser importado hasta la matriz mitocondrial, lo que resultaría en una proteína embebida en la membrana con una topología incorrecta (N-adentro/C-afuera en lugar de N-afuera/C-afuera). Esto está respaldado por el hecho de que en una mutante nula de Mgr2, TIM23 tiende a acelerar la liberación lateral de TMS en la MIM a través de la vía de "paro-transferencia" (Ieva et al., 2014; Lee et al., 2020).

La sobreproducción de Mgr2 también disminuyó la internalización de *n*$Cox2^{W56R}$, efecto que se hizo aún más evidente en el caso de *e*$Cox2^{W56R}$. Dado que Pam18 y Mgr2 parecen competir por el mismo sitio de unión en el complejo $TIM23_{CORE}$ (Schendzielorz et al., 2018), un escenario plausible es que la producción de altos niveles de Mgr2 tiendan a desplazar a Pam18. Esto podría afectar la función de $TIM23_{MOTOR}$ y disminuir la internalización del TMS1 de $Cox2^{W56R}$ en la matriz mitocondrial.

Además de los resultados aportados en este trabajo respecto a Mgr2, se realizó un sencillo análisis bioinformático utilizando dos aproximaciones: complexómica de alta resolución y modelos del complejo TIM23. El análisis de perfiles de complexómica de alta resolución de proteínas que comprenden el 90% del proteoma mitocondrial de levadura, ha sido generosamente puesto a disposición del público en el sitio MitCOM (Schulte et al., 2023). En dichos perfiles hemos identificados dos picos independientes relacionados con la subunidad Tim17. Estos picos corresponden a las asociaciones Tim17-Pam18 y Tim17-Mgr2, que claramente presentan distintas masas moleculares aparentes (Fig. 18). Estas asociaciones distintas podrían representar las dos formas alternas del translocador TIM23: $TIM23_{MOTOR}$ y $TIM23_{SORT}$.

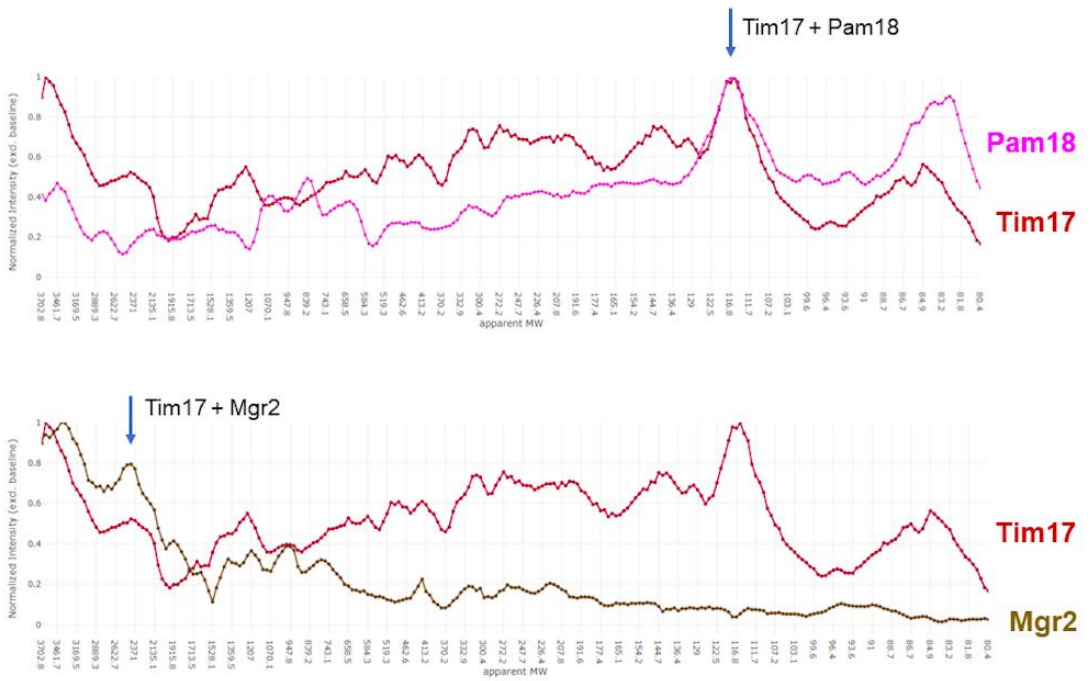

Figura 18. Perfiles de complexómica de alta resolución que muestran asociaciones independientes de Tim17 con Pam18 o Mgr2. Las flechas azules indican picos independientes para los pares Tim17/Pam18 y Tim17/Mgr2.

De forma complementaria, modelos del complejo proteico TIM23 generados mediante AlphaFold-Multimer (Jumper et al., 2021) sugieren que tanto Pam18 como Mgr2 se unen de forma independiente al mismo dominio de Tim17 (Fig. 19).

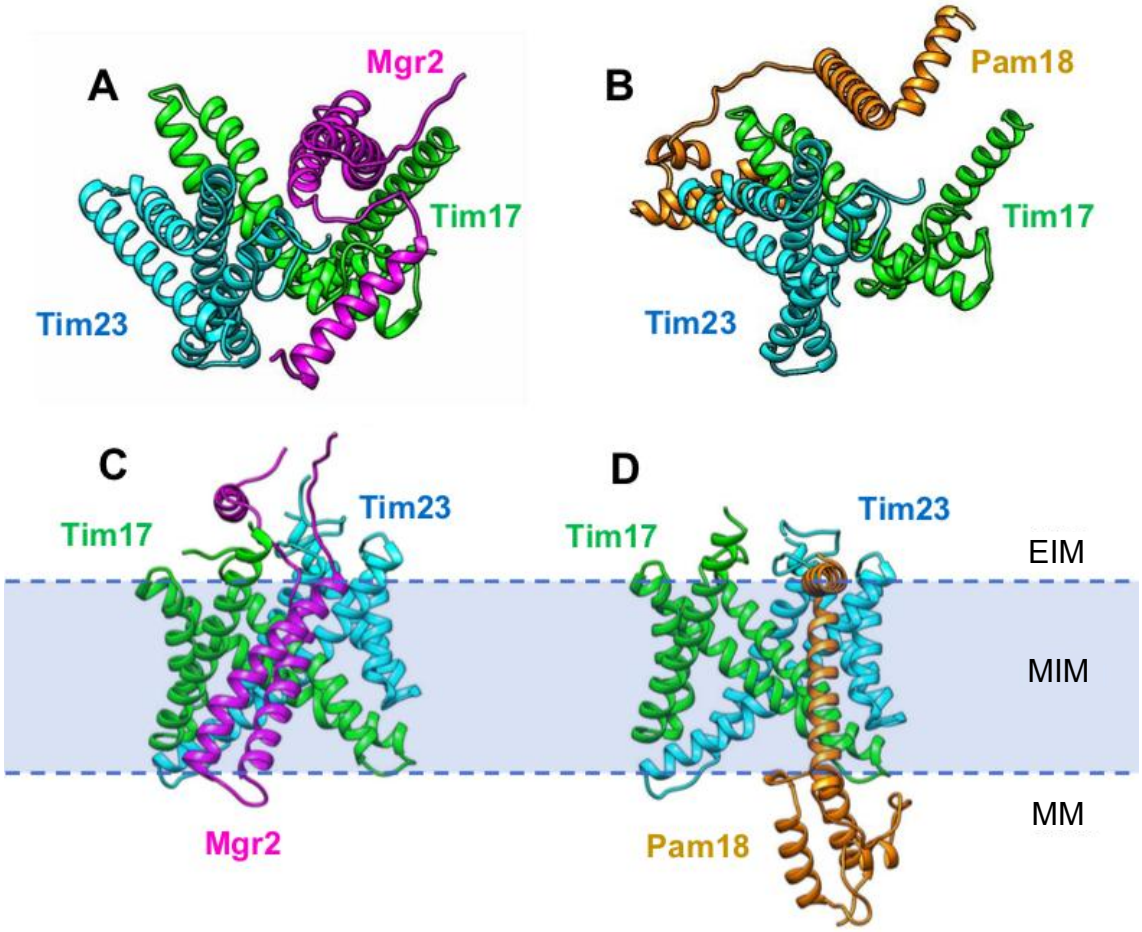

Figura 19. Modelos tridimensionales de las asociaciones Tim23/Tim17/Mgr2 y Tim23/Tim17/Pam18 obtenidos mediante AlphaFold Multimer. Paneles A y C: Dos vistas del complejo Tim23/Tim17/Mgr2. Paneles B y D: Dos vistas del complejo Tim23/Tim17/Pam18. Para mayor claridad, los modelos muestran secuencias parciales de los componentes proteicos (Tim17, de M1 a K141; Tim23, de E75 a K222; Mgr2, de M1 a D113; y Pam18, de K47 a K168). Las líneas azules discontinuas indican la membrana mitocondrial interna. EIM: espacio intermembranal: MIM: membrana interna mitocondrial; MM: matriz mitocondrial.

Un nuevo modelo de importación de $Cox2^{W56R}$. Estudios anteriores sobre la biogénesis de la subunidad alotópica $Cox2^{W56R}$ han postulado la capacidad de TIM23 de distribuir precursores a través de dos rutas diferentes: el TMS1 de la proteína se transloca hasta la matriz mitocondrial a través de la "vía conservada" (*conservative pathway*), mientras que el TMS2 se libera lateralmente a la MIM a través de la vía de paro/transferencia (*stop-transfer pathway*) (Cruz-Torres et al., 2012; Rubalcava-Gracia et al., 2018; Nieto-Panqueva et al., 2023). Aquí, el hallazgo de que Mgr2 es esencial para la importación de $Cox2^{W56R}$, nos llevó a elaborar aún más el modelo original propuesto previamente en nuestro grupo de trabajo. En esta nueva propuesta (Fig. 20), $TIM23_{MOTOR}$ transloca la MTS y el TMS1 de $Cox2^{W56R}$ hasta la matriz mitocondrial. Luego, el TMS2 será detenido debido a su alta hidrofobicidad y a la presencia de una señal de paro/transferencia. En este paso, el motor PAM debe desensamblarse de $TIM23_{MOTOR}$, lo que resulta en la formación transitoriamente de $TIM23_{CORE}$ (Tim50/Tim23/Tim17). Inmediatamente después, Mgr2, Tim21 y los complejos respiratorios III y IV pueden ser reclutados por $TIM23_{CORE}$ para ensamblar un complejo $TIM23_{SORT}$ funcionalmente competente. Con la ayuda de Mgr2, este complejo liberará lateralmente el TMS2 de $Cox2^{W56R}$ dentro de la MIM. Por lo tanto, proponemos, que la importación de la subunidad Cox2 alotópica requiere la participación secuencial de las tres formas funcionales/estructurales del translocador TIM23: $TIM23_{MOTOR}$, $TIM23_{CORE}$ y $TIM23_{SORT}$. Los análisis bioinformáticos descritos anteriormente (Fig. 18 y Fig. 19) parecen respaldar este modelo.

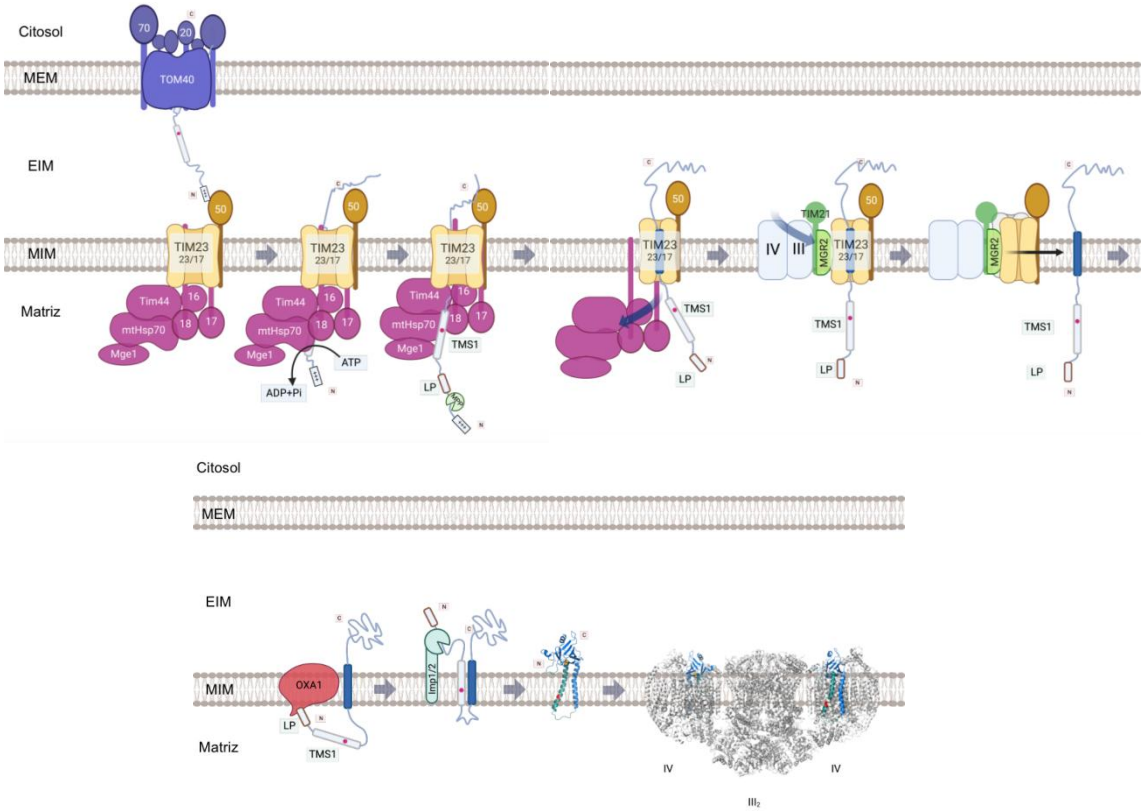

Figura 20. Nuevo modelo que describe la ruta de biogénesis que sigue la subunidad alotópica Cox2^{W56R}. En el panel superior, el complejo TOM (en color violeta) transloca el precursor alotópico de Cox2 y lo entrega a TIM23$_{MOTOR}$ (en colores amarillo y fucsia). La secuencia de direccionamiento mitocondrial (MTS), el péptido líder (LP) y el TMS1 (μΔGapp = 0.55 kcal/mol) del precursor de Cox2 (en azul claro, con una marca roja indicando la sustitución W56R) son translocados completamente por TIM23$_{MOTOR}$ hasta la matriz mitocondrial. La MTS es eliminada proteolíticamente por la proteasa de procesamiento de matriz (MPP, en verde claro). El TMS2 de Cox2 (en azul oscuro), con μΔGapp = 0.44 kcal/mol, se detiene a su paso por TIM23 debido a su alta hidrofobicidad. Lo anterior induce la disociación del motor PAM (en color fucsia) y el reclutamiento de Mgr2 (en verde claro), Tim21 (en verde) y los complejos respiratorios III y IV (en azul claro) para ensamblar TIM23$_{SORT}$. Luego, TIM23$_{SORT}$ libera lateralmente el TMS2 de la Cox2 alotópica en la MIM. Subsecuentemente, como se muestra en el panel inferior, la insertasa Oxa1 (en color rojo) reconoce el LP y lleva a cabo la inserción del TMS1 en la MIM (este paso puede ocurrir antes, simultáneamente o después de que el TMS2 se libere en la MIM). Posteriormente, la proteasa Imp1 (IMP1/2), ubicada en el EIM, elimina el LP. Postulamos que el resto de la ruta de biogénesis es idéntica a la de una proteína Cox2 sintetizada en la mitocondria: incorporación del centro de cobre binuclear, ensamblaje con los módulos Cox1 y Cox3, formación de COX maduro, y ensamblaje en el supercomplejo III_2IV_2. Los valores de μΔGapp fueron calculados como en Nieto-Panqueva et al., (2023).

En resumen, consideramos que se requiere de un intercambio dinámico entre $TIM23_{MOTOR}$ y $TIM23_{SORT}$ durante la translocación y distribución del precursor alotópico $Cox2^{W56R}$. Nuestro modelo explica por qué la ruta de biogénesis seguida por una proteína Cox2 codificada en el núcleo de forma natural (Adams et al., 1999; Daley et al., 2002) o artificial (Rubalcava-Gracia et al., 2018) es mucho más compleja que la seguida por su contraparte sintetizada en el interior de la mitocondria. Por último, el modelo sugiere que el paso limitante en la importación de $Cox2^{W56R}$ a las mitocondrias probablemente ocurre cuando Tim17 retiene su TMS2, lo que provoca el desmontaje de $TIM23_{MOTOR}$ (liberación del motor PAM), seguido del ensamblaje de un complejo $TIM23_{SORT}$ funcional. Este intercambio de la maquinaria de translocación debe ocurrir mientras se internaliza un único polipéptido $Cox2^{W56R}$, lo que implica inevitablemente una discontinuidad importante en el proceso de importación de la subunidad alotópica.

Nuestro modelo ilustra la complejidad del proceso necesario para que una subunidad $Cox2^{W56R}$ producida alotópicamente alcance su topología funcional final N-afuera/C-afuera en la MIM. También arroja luz sobre el mecanismo mediante el cual otras proteínas de membrana mitocondriales codificadas en el núcleo, que presentan una MTS, dos TMS y una topología N-afuera/C-afuera, son importadas y distribuidas por el translocador TIM23.

CONCLUSIONES

i. La sobreexpresión de los genes *TYE7*, *RAS2* y *PSE1* incrementa los niveles estacionarios de la subunidad alotópica $Cox2^{W56R}$. Cada uno de los productos proteicos correspondientes posiblemente actúa a través de mecanismos diferentes.

ii. El hecho de que los niveles elevados de Oxa1 y Cox20 incrementen el crecimiento respiratorio de $Cox2^{W56R}$ con respecto a su control, sugiere que ambas proteínas probablemente participan en un paso limitante en la biogénesis de la proteína alotópica. La sobreproducción de Oxa1 aparentemente facilita el reconocimiento del péptido señal de $Cox2^{W56R}$ y promueve la inserción del TMS1 de la proteína. Por su parte, Cox20 parece estabilizar al TMS1 en la MIM y facilitar la inserción de cobre por los factores residentes en el EIM.

iii. La sobreproducción de Cox12, subunidad de la COX expuesta al EIM, podría facilitar la incorporación del sitio binuclear de cobre mediado por el sistema Sco1-Sco2-Coa6.

iv. La subunidad alotópica $Cox2^{W56R}$ es importada por el translocador de la membrana interna TIM23. Aunque esto ya había sido predicho en trabajos previos (debido a que todos los precursores que contienen una MTS son dirigidos hacia TIM23 para su internalización), no se había demostrado formalmente. Aquí, proporcionamos evidencia formal de la participación de Mgr2 en la importación de la Cox2 alotópica, lo que a su vez indica que dicha subunidad ingresa a la mitocondria a través de TIM23.

v. La eliminación del gen *MGR2* afectó la internalización de la subunidad Cox2 producida alotópicamente. La participación de Mgr2 en la importación de $Cox2^{W56R}$ sugiere fuertemente que las dos formas del translocador TIM23, $TIM23_{MOTOR}$ y $TIM23_{SORT}$, también participan en este proceso: $TIM23_{MOTOR}$ translocando la MTS y el TMS1 de $Cox2^{W56R}$ hasta la matriz mitocondrial y $TIM23_{SORT}$, con la ayuda de Mgr2, liberando lateralmente el TMS2 de la subunidad en la MIM.

vi. La sobreexpresión del gen *MGR2* también afectó negativamente la internalización de la subunidad Cox2 alotópica. Ya que Mgr2 y Pam18 se unen al mismo dominio de la subunidad Tim17, bloqueando el acceso directo de la cavidad translocadora a

la bicapa lipídica, la sobreproducción de Mgr2 podría competir por el sitio de unión, desplazando a la subunidad Pam18.

vii. El paso limitante en la biogénesis de $Cox2^{W56R}$ se debe al intercambio de las dos formas funcionales/estructurales de la maquinaria de translocación TIM23. Ya que un polipéptido único, que es internalizado en un momento dado, no puede interactuar con dos translocadores simultáneamente, debe existir un intercambio secuencial de $TIM23_{MOTOR}$ a $TIM23_{SORT}$ durante la biogénesis de la subunidad Cox2 alotópica. El reordenamiento de $TIM23_{MOTOR}$ a $TIM23_{SORT}$ implica inevitablemente una discontinuidad importante en el proceso de importación de la subunidad alotópica. Es por esto que proponemos que el intercambio $TIM23_{MOTOR}$/$TIM23_{SORT}$ representa el paso limitante en la biogénesis de $Cox2^{W56R}$, ya que necesariamente implica el desensamble de una forma del translocador y el ensamblaje de otra forma del translocador.

PERSPECTIVAS

- Identificar, a través de ensayos de proteómica cuantitativa (SILAC-MS), si proteínas relacionadas con la biogénesis e importación mitocondrial se ven afectadas en cepas donde los genes *TYE7*, *RAS2* y *PSE1* son eliminados. Esto nos permitirá determinar si la interacción entre estas proteínas y $Cox2^{W56R}$ se origina por un segundo factor o por cambios en su expresión desde el núcleo celular antes de su importación.

- Explorar, mediante ensayos de co-inmunoprecipitación, en qué medida los componentes del complejo IV y otras proteínas mitocondriales además de Cox2, se ven afectadas en mitocondrias aisladas de células wt y deficientes de Cox20.

- Examinar si la fusión covalente de Mgr2 a la subunidad Tim17, durante la importación de proteínas de membrana con uno y varios TMS, influye en la eficiencia del proceso de liberación lateral dentro de la MIM.

- Investigar los efectos de la deleción y sobreexpresión del gen *PAM18* en nuestra cepa de expresión alotópica $COX2^{W56R}$, para corroborar si la presencia de las proteínas Mgr2 y Pam18 en el complejo de translocación TIM23 es en efecto mutuamente excluyente.

REFERENCIAS

Adams, K. L., Song, K., Roessler, P. G., Nugent, J. M., Doyle, J. L., Doyle, J. J., & Palmer, J. D. (1999). Intracellular gene transfer in action: dual transcription and multiple silencings of nuclear and mitochondrial cox2 genes in legumes. Proceedings of the National Academy of Sciences of the United States of America, 96(24), 13863–13868. https://doi.org/10.1073/pnas.96.24.13863

Adams, K. L., & Palmer, J. D. (2003). Evolution of mitochondrial gene content: gene loss and transfer to the nucleus. Molecular phylogenetics and evolution, 29(3), 380–395. https://doi.org/10.1016/s1055-7903(03)00194-5

Alberts, B., Heald, R., Johnson, A., Morgan, D., Raff, M., Roberts, K., & Walter, P. (2022). Energy Conversion and Metabolic Compartmentation: Mitochondria and Chloroplasts. In Molecular Biology of the Cell (7th ed., pp. 814–823). essay, W. W. Norton & Company.

Allen, J. F., & Raven, J. A. (1996). Free-radical-induced mutation vs redox regulation: costs and benefits of genes in organelles. Journal of molecular evolution, 42(5), 482–492. https://doi.org/10.1007/BF02352278

Andersson, S. G., Zomorodipour, A., Andersson, J. O., Sicheritz-Pontén, T., Alsmark, U. C., Podowski, R. M., Näslund, A. K., Eriksson, A. S., Winkler, H. H., & Kurland, C. G. (1998). The genome sequence of Rickettsia prowazekii and the origin of mitochondria. Nature, 396(6707), 133–140. https://doi.org/10.1038/24094

Araiso, Y., Tsutsumi, A., Qiu, J., Imai, K., Shiota, T., Song, J., Lindau, C., Wenz, L. S., Sakaue, H., Yunoki, K., Kawano, S., Suzuki, J., Wischnewski, M., Schütze, C., Ariyama, H., Ando, T., Becker, T., Lithgow, T., Wiedemann, N., Pfanner, N., … Endo, T. (2019). Structure of the mitochondrial import gate reveals distinct preprotein paths. Nature, 575(7782), 395–401. https://doi.org/10.1038/s41586-019-1680-7

Attardi, G., & Schatz, G. (1988). Biogenesis of mitochondria. Annual review of cell biology, 4, 289–333. https://doi.org/10.1146/annurev.cb.04.110188.001445

Backes, S., Bykov, Y. S., Flohr, T., Räschle, M., Zhou, J., Lenhard, S., Krämer, L., Mühlhaus, T., Bibi, C., Jann, C., Smith, J. D., Steinmetz, L. M., Rapaport, D., Storchová, Z., Schuldiner, M., Boos, F., & Herrmann, J. M. (2021). The chaperone-binding activity of the mitochondrial surface receptor Tom70 protects the cytosol against mitoprotein-induced stress. Cell reports, 35(1), 108936. https://doi.org/10.1016/j.celrep.2021.108936

Banci, L., Bertini, I., Calderone, V., Ciofi-Baffoni, S., Mangani, S., Martinelli, M., Palumaa, P., & Wang, S. (2006). A

hint for the function of human Sco1 from different structures. Proceedings of the National Academy of Sciences of the United States of America, 103(23), 8595–8600. https://doi.org/10.1073/pnas.0601375103

Banci, L., Bertini, I., Ciofi-Baffoni, S., Gerothanassis, I. P., Leontari, I., Martinelli, M., & Wang, S. (2007). A structural characterization of human SCO2. Structure (London, England : 1993), 15(9), 1132–1140. https://doi.org/10.1016/j.str.2007.07.011

Bähler, J., Wu, J. Q., Longtine, M. S., Shah, N. G., McKenzie, A., 3rd, Steever, A. B., Wach, A., Philippsen, P., & Pringle, J. R. (1998). Heterologous modules for efficient and versatile PCR-based gene targeting in Schizosaccharomyces pombe. Yeast (Chichester, England), 14(10), 943–951. https://doi.org/10.1002/(SICI)1097-0061(199807)14:10<943::AID-YEA292>3.0.CO;2-Y

Berg, O. G., & Kurland, C. G. (2000). Why mitochondrial genes are most often found in nuclei. Molecular biology and evolution, 17(6), 951–961. https://doi.org/10.1093/oxfordjournals.molbev.a026376

Berndtsson, J., Kohler, A., Rathore, S., Marin-Buera, L., Dawitz, H., Diessl, J., Kohler, V., Barrientos, A., Büttner, S., Fontanesi, F., & Ott, M. (2020). Respiratory supercomplexes enhance electron transport by decreasing cytochrome c diffusion distance. EMBO reports, 21(12), e51015. https://doi.org/10.15252/embr.202051015

Blanchard, J. L., & Schmidt, G. W. (1996). Mitochondrial DNA migration events in yeast and humans: integration by a common end-joining mechanism and alternative perspectives on nucleotide substitution patterns. Molecular biology and evolution, 13(3), 537–548. https://doi.org/10.1093/oxfordjournals.molbev.a025614

Brennicke, A., Grohmann, L., Hiesel, R., Knoop, V., & Schuster, W. (1993). The mitochondrial genome on its way to the nucleus: different stages of gene transfer in higher plants. FEBS letters, 325(1-2), 140–145. https://doi.org/10.1016/0014-5793(93)81430-8

Brix, J., Ziegler, G. A., Dietmeier, K., Schneider-Mergener, J., Schulz, G. E., & Pfanner, N. (2000). The mitochondrial import receptor Tom70: identification of a 25 kDa core domain with a specific binding site for preproteins. Journal of molecular biology, 303(4), 479–488. https://doi.org/10.1006/jmbi.2000.4120

Bohnert, M., Rehling, P., Guiard, B., Herrmann, J. M., Pfanner, N., & van der Laan, M. (2010). Cooperation of stop-transfer and conservative sorting mechanisms in mitochondrial protein transport. Current biology : CB, 20(13), 1227–1232. https://doi.org/10.1016/j.cub.2010.05.058

Bolliger, L., Deloche, O., Glick, B. S., Georgopoulos, C., Jenö, P., Kronidou, N.,

Horst, M., Morishima, N., & Schatz, G. (1994). A mitochondrial homolog of bacterial GrpE interacts with mitochondrial hsp70 and is essential for viability. The EMBO journal, 13(8), 1998–2006. https://doi.org/10.1002/j.1460-2075.1994.tb06469.x

Bonneaud, N., Ozier-Kalogeropoulos, O., Li, G. Y., Labouesse, M., Minvielle-Sebastia, L., & Lacroute, F. (1991). A family of low and high copy replicative, integrative and single-stranded S. cerevisiae/E. coli shuttle vectors. Yeast (Chichester, England), 7(6), 609–615. https://doi.org/10.1002/yea.320070609

Bonnefoy, N., Chalvet, F., Hamel, P., Slonimski, P. P., & Dujardin, G. (1994). OXA1, a Saccharomyces cerevisiae nuclear gene whose sequence is conserved from prokaryotes to eukaryotes controls cytochrome oxidase biogenesis. Journal of molecular biology, 239(2), 201–212. https://doi.org/10.1006/jmbi.1994.1363

Bonnefoy, N., Bsat, N., & Fox, T. D. (2001). Mitochondrial translation of Saccharomyces cerevisiae COX2 mRNA is controlled by the nucleotide sequence specifying the pre-Cox2p leader peptide. Molecular and cellular biology, 21(7), 2359–2372. https://doi.org/10.1128/MCB.21.7.2359-2372.2001

Botelho, S. C., Osterberg, M., Reichert, A. S., Yamano, K., Björkholm, P., Endo, T., von Heijne, G., & Kim, H. (2011). TIM23-mediated insertion of transmembrane α-helices into the mitochondrial inner membrane. The EMBO journal, 30(6), 1003–1011. https://doi.org/10.1038/emboj.2011.29

Bouchez, C. L., Yoboue, E. D., de la Rosa Vargas, L. E., Salin, B., Cuvellier, S., Rigoulet, M., Duvezin-Caubet, S., & Devin, A. (2020). "Labile" heme critically regulates mitochondrial biogenesis through the transcriptional co-activator Hap4p in Saccharomyces cerevisiae. The Journal of biological chemistry, 295(15), 5095–5109. https://doi.org/10.1074/jbc.RA120.012739

Bourens, M., & Barrientos, A. (2017). Human mitochondrial cytochrome c oxidase assembly factor COX18 acts transiently as a membrane insertase within the subunit 2 maturation module. The Journal of biological chemistry, 292(19), 7774–7783. https://doi.org/10.1074/jbc.M117.778514

Broach, J. R., & Deschenes, R. J. (1990). The function of ras genes in Saccharomyces cerevisiae. Advances in cancer research, 54, 79–139. https://doi.org/10.1016/s0065-230x(08)60809-x

Broggi, S., Martegani, E., & Colombo, S. (2013). Live-cell imaging of endogenous Ras-GTP shows predominant Ras activation at the plasma membrane and in the nucleus in Saccharomyces cerevisiae. The international journal of biochemistry & cell biology, 45(2), 384–394.

https://doi.org/10.1016/j.biocel.2012.10.013

Buschlen, S., Amillet, J. M., Guiard, B., Fournier, A., Marcireau, C., & Bolotin-Fukuhara, M. (2003). The S. Cerevisiae HAP complex, a key regulator of mitochondrial function, coordinates nuclear and mitochondrial gene expression. Comparative and functional genomics, 4(1), 37–46. https://doi.org/10.1002/cfg.254

Callegari, S., Cruz-Zaragoza, L. D., & Rehling, P. (2020). From TOM to the TIM23 complex - handing over of a precursor. Biological chemistry, 401(6-7), 709–721. https://doi.org/10.1515/hsz-2020-0101

Carr, H. S., Maxfield, A. B., Horng, Y. C., & Winge, D. R. (2005). Functional analysis of the domains in Cox11. The Journal of biological chemistry, 280(24), 22664–22669. https://doi.org/10.1074/jbc.M414077200

Castanzo, D. T., LaFrance, B., & Martin, A. (2020). The AAA+ ATPase Msp1 is a processive protein translocase with robust unfoldase activity. Proceedings of the National Academy of Sciences of the United States of America, 117(26), 14970–14977. https://doi.org/10.1073/pnas.1920109117

Caumont-Sarcos, A., Moulin, C., Poinot, L., Guiard, B., van der Laan, M., & Ieva, R. (2020). Transmembrane Coordination of Preprotein Recognition and Motor Coupling by the Mitochondrial Presequence Receptor Tim50. Cell reports, 30(9), 3092–3104.e4. https://doi.org/10.1016/j.celrep.2020.02.031

Chacinska, A., Koehler, C. M., Milenkovic, D., Lithgow, T., & Pfanner, N. (2009). Importing mitochondrial proteins: machineries and mechanisms. Cell, 138(4), 628–644. https://doi.org/10.1016/j.cell.2009.08.005

Chacinska, A., van der Laan, M., Mehnert, C. S., Guiard, B., Mick, D. U., Hutu, D. P., Truscott, K. N., Wiedemann, N., Meisinger, C., Pfanner, N., & Rehling, P. (2010). Distinct forms of mitochondrial TOM-TIM supercomplexes define signal-dependent states of preprotein sorting. Molecular and cellular biology, 30(1), 307–318. https://doi.org/10.1128/MCB.00749-09

Chandrasekaran, K., & Jayaraman, J. (1978). Effect of cyclic AMP on the biogenesis of cytochrome oxidase in yeast. FEBS letters, 87(1), 52–54. https://doi.org/10.1016/0014-5793(78)80131-8

Chen, D. C., Yang, B. C., & Kuo, T. T. (1992). One-step transformation of yeast in stationary phase. Current genetics, 21(1), 83–84. https://doi.org/10.1007/BF00318659

Chevallier, M. R., Bloch, J. C., & Lacroute, F. (1980). Transcriptional and translational expression of a chimeric bacterial-yeast plasmid in yeasts. Gene, 11(1-2), 11–19.

https://doi.org/10.1016/0378-1119(80)90082-7

Claros, M. G., Perea, J., Shu, Y., Samatey, F. A., Popot, J. L., & Jacq, C. (1995). Limitations to in vivo import of hydrophobic proteins into yeast mitochondria. The case of a cytoplasmically synthesized apocytochrome b. European journal of biochemistry, 228(3), 762–771. https://doi.org/10.1111/j.1432-1033.1995.0762m.x

Corral-Debrinski, M., Belgareh, N., Blugeon, C., Claros, M. G., Doye, V., & Jacq, C. (1999). Overexpression of yeast karyopherin Pse1p/Kap121p stimulates the mitochondrial import of hydrophobic proteins in vivo. Molecular microbiology, 31(5), 1499–1511. https://doi.org/10.1046/j.1365-2958.1999.01295.x

Craig E. A. (2018). Hsp70 at the membrane: driving protein translocation. BMC biology, 16(1), 11. https://doi.org/10.1186/s12915-017-0474-3

Cruz-Torres, V., Vázquez-Acevedo, M., García-Villegas, R., Pérez-Martínez, X., Mendoza-Hernández, G., & González-Halphen, D. (2012). The cytosol-synthesized subunit II (Cox2) precursor with the point mutation W56R is correctly processed in yeast mitochondria to rescue cytochrome oxidase. Biochimica et biophysica acta, 1817(12), 2128–2139. https://doi.org/10.1016/j.bbabio.2012.09.006

Cwerman-Thibault, H., Sahel, J. A., & Corral-Debrinski, M. (2011). Mitochondrial medicine: to a new era of gene therapy for mitochondrial DNA mutations. Journal of inherited metabolic disease, 34(2), 327–344. https://doi.org/10.1007/s10545-010-9131-5

Daley, D. O., Adams, K. L., Clifton, R., Qualmann, S., Millar, A. H., Palmer, J. D., Pratje, E., & Whelan, J. (2002). Gene transfer from mitochondrion to nucleus: novel mechanisms for gene activation from Cox2. The Plant journal : for cell and molecular biology, 30(1), 11–21. https://doi.org/10.1046/j.1365-313x.2002.01263.x

Das, S., Mukherjee, S., Bedi, M., & Ghosh, A. (2021). Mutations in the Yeast Cox12 Subunit Severely Compromise the Activity of the Mitochondrial Complex IV. Biochemistry. Biokhimiia, 86(12), 1607–1623. https://doi.org/10.1134/S0006297921120105

de Grey A. D. (2005). Forces maintaining organellar genomes: is any as strong as genetic code disparity or hydrophobicity?. BioEssays : news and reviews in molecular, cellular and developmental biology, 27(4), 436–446. https://doi.org/10.1002/bies.20209

Dessi, P., Rudhe, C., & Glaser, E. (2000). Studies on the topology of the protein import channel in relation to the plant mitochondrial processing peptidase integrated into the cytochrome bc1

complex. The Plant journal : for cell and molecular biology, 24(5), 637–644. https://doi.org/10.1046/j.1365-313x.2000.00910.x

Di Donfrancesco, A., Massaro, G., Di Meo, I., Tiranti, V., Bottani, E., & Brunetti, D. (2022). Gene Therapy for Mitochondrial Diseases: Current Status and Future Perspective. Pharmaceutics, 14(6), 1287. https://doi.org/10.3390/pharmaceutics14061287

DiMauro, S., & Schon, E. A. (2003). Mitochondrial respiratory-chain diseases. The New England journal of medicine, 348(26), 2656–2668. https://doi.org/10.1056/NEJMra022567

Doyle, S. R., Kasinadhuni, N. R., Chan, C. K., & Grant, W. N. (2013). Evidence of evolutionary constraints that influences the sequence composition and diversity of mitochondrial matrix targeting signals. PloS one, 8(6), e67938. https://doi.org/10.1371/journal.pone.0067938

Elliott, L. E., Saracco, S. A., & Fox, T. D. (2012). Multiple roles of the Cox20 chaperone in assembly of Saccharomyces cerevisiae cytochrome c oxidase. Genetics, 190(2), 559–567. https://doi.org/10.1534/genetics.111.135665

Estabrook, R.W. (1967). [7] Mitochondrial respiratory control and the polarographic measurement of ADP : O ratios. Methods in Enzymology, 10, 41-47. https://doi.org/10.1016/0076%2D6879(67)10010%2D4

Fang, M., & Butow, R. A. (1970). Nucleotide reversal of mitochondrial repression in Saccharomyces cerevisiae. Biochemical and biophysical research communications, 41(6), 1579–1583. https://doi.org/10.1016/0006-291x(70)90568-1

Flegontov, P., Michálek, J., Janouškovec, J., Lai, D. H., Jirků, M., Hajdušková, E., Tomčala, A., Otto, T. D., Keeling, P. J., Pain, A., Oborník, M., & Lukeš, J. (2015). Divergent mitochondrial respiratory chains in phototrophic relatives of apicomplexan parasites. Molecular biology and evolution, 32(5), 1115–1131. https://doi.org/10.1093/molbev/msv021

Fontanesi, F., Soto, I. C., Horn, D., & Barrientos, A. (2006). Assembly of mitochondrial cytochrome c-oxidase, a complicated and highly regulated cellular process. American journal of physiology. Cell physiology, 291(6), C1129–C1147. https://doi.org/10.1152/ajpcell.00233.2006

Formaggioni, A., Plazzi, F., & Passamonti, M. (2022). Mito-nuclear coevolution and phylogenetic artifacts: the case of bivalve mollusks. Scientific reports, 12(1), 11040. https://doi.org/10.1038/s41598-022-15076-y

Fox T. D. (2012). Mitochondrial protein synthesis, import, and

assembly. Genetics, 192(4), 1203–1234. https://doi.org/10.1534/genetics.112.141267

Frazier, A. E., Dudek, J., Guiard, B., Voos, W., Li, Y., Lind, M., Meisinger, C., Geissler, A., Sickmann, A., Meyer, H. E., Bilanchone, V., Cumsky, M. G., Truscott, K. N., Pfanner, N., & Rehling, P. (2004). Pam16 has an essential role in the mitochondrial protein import motor. Nature structural & molecular biology, 11(3), 226–233. https://doi.org/10.1038/nsmb735

Frey, T. G., & Mannella, C. A. (2000). The internal structure of mitochondria. Trends in biochemical sciences, 25(7), 319–324. https://doi.org/10.1016/s0968-0004(00)01609-1

Fujiwara, S., Kawazoe, T., Ohnishi, K., Kitagawa, T., Popa, C., Valls, M., Genin, S., Nakamura, K., Kuramitsu, Y., Tanaka, N., & Tabuchi, M. (2016). RipAY, a Plant Pathogen Effector Protein, Exhibits Robust γ-Glutamyl Cyclotransferase Activity When Stimulated by Eukaryotic Thioredoxins. The Journal of biological chemistry, 291(13), 6813–6830. https://doi.org/10.1074/jbc.M115.678953

Fukasawa, Y., Tsuji, J., Fu, S. C., Tomii, K., Horton, P., & Imai, K. (2015). MitoFates: improved prediction of mitochondrial targeting sequences and their cleavage sites. Molecular & cellular proteomics : MCP, 14(4), 1113–1126. https://doi.org/10.1074/mcp.M114.043083

Gebert, M., Schrempp, S. G., Mehnert, C. S., Heißwolf, A. K., Oeljeklaus, S., Ieva, R., Bohnert, M., von der Malsburg, K., Wiese, S., Kleinschroth, T., Hunte, C., Meyer, H. E., Haferkamp, I., Guiard, B., Warscheid, B., Pfanner, N., & van der Laan, M. (2012). Mgr2 promotes coupling of the mitochondrial presequence translocase to partner complexes. The Journal of cell biology, 197(5), 595–604. https://doi.org/10.1083/jcb.201110047

Ghosh, A., Trivedi, P. P., Timbalia, S. A., Griffin, A. T., Rahn, J. J., Chan, S. S., & Gohil, V. M. (2014). Copper supplementation restores cytochrome c oxidase assembly defect in a mitochondrial disease model of COA6 deficiency. Human molecular genetics, 23(13), 3596–3606. https://doi.org/10.1093/hmg/ddu069

Ghosh, A., Pratt, A. T., Soma, S., Theriault, S. G., Griffin, A. T., Trivedi, P. P., & Gohil, V. M. (2016). Mitochondrial disease genes COA6, COX6B and SCO2 have overlapping roles in COX2 biogenesis. Human molecular genetics, 25(4), 660–671. https://doi.org/10.1093/hmg/ddv503

Gietz, R. D., & Schiestl, R. H. (2007). High-efficiency yeast transformation using the LiAc/SS carrier DNA/PEG method. Nature protocols, 2(1), 31–34. https://doi.org/10.1038/nprot.2007.13

Gietz, R. D., & Woods, R. A. (2002). Transformation of yeast by lithium acetate/single-stranded carrier DNA/polyethylene glycol

method. Methods in enzymology, 350, 87–96. https://doi.org/10.1016/s0076-6879(02)50957-5

Goitre, L., Trapani, E., Trabalzini, L., & Retta, S. F. (2014). The Ras superfamily of small GTPases: the unlocked secrets. Methods in molecular biology (Clifton, N.J.), 1120, 1–18. https://doi.org/10.1007/978-1-62703-791-4_1

Gomkale, R., Cruz-Zaragoza, L. D., Suppanz, I., Guiard, B., Montoya, J., Callegari, S., Pacheu-Grau, D., Warscheid, B., & Rehling, P. (2020). Defining the Substrate Spectrum of the TIM22 Complex Identifies Pyruvate Carrier Subunits as Unconventional Cargos. Current biology : CB, 30(6), 1119–1127.e5. https://doi.org/10.1016/j.cub.2020.01.024

Gorman, G. S., Chinnery, P. F., DiMauro, S., Hirano, M., Koga, Y., McFarland, R., Suomalainen, A., Thorburn, D. R., Zeviani, M., & Turnbull, D. M. (2016). Mitochondrial diseases. Nature reviews. Disease primers, 2, 16080. https://doi.org/10.1038/nrdp.2016.80

Graef, M., Seewald, G., & Langer, T. (2007). Substrate recognition by AAA+ ATPases: distinct substrate binding modes in ATP-dependent protease Yme1 of the mitochondrial intermembrane space. Molecular and cellular biology, 27(7), 2476–2485. https://doi.org/10.1128/MCB.01721-06

Gray, M. W., Lang, B. F., Cedergren, R., Golding, G. B., Lemieux, C., Sankoff, D., Turmel, M., Brossard, N., Delage, E., Littlejohn, T. G., Plante, I., Rioux, P., Saint-Louis, D., Zhu, Y., & Burger, G. (1998). Genome structure and gene content in protist mitochondrial DNAs. Nucleic acids research, 26(4), 865–878. https://doi.org/10.1093/nar/26.4.865

Gray, M. W., Burger, G., & Lang, B. F. (1999). Mitochondrial evolution. Science (New York, N.Y.), 283(5407), 1476–1481. https://doi.org/10.1126/science.283.5407.1476

Green, D. E., & Tzagoloff, A. (1966). Role of lipids in the structure and function of biological membranes. Journal of lipid research, 7(5), 587–602. https://doi.org/10.1016/S0022-2275(20)39239-7.

Hackenbrock C. R. (1966). Ultrastructural bases for metabolically linked mechanical activity in mitochondria. I. Reversible ultrastructural changes with change in metabolic steady state in isolated liver mitochondria. The Journal of cell biology, 30(2), 269–297. https://doi.org/10.1083/jcb.30.2.269

Hanahan D. (1983). Studies on transformation of Escherichia coli with plasmids. Journal of molecular biology, 166(4), 557–580. https://doi.org/10.1016/s0022-2836(83)80284-8

Hansen, K. G., & Herrmann, J. M. (2019). Transport of Proteins into Mitochondria. The protein journal, 38(3), 330–342. https://doi.org/10.1007/s10930-019-09819-6

Hawlitschek, G., Schneider, H., Schmidt, B., Tropschug, M., Hartl, F. U., & Neupert, W. (1988). Mitochondrial protein import: identification of processing peptidase and of PEP, a processing enhancing protein. Cell, 53(5), 795–806. https://doi.org/10.1016/0092-8674(88)90096-7

He, S., & Fox, T. D. (1997). Membrane translocation of mitochondrially coded Cox2p: distinct requirements for export of N and C termini and dependence on the conserved protein Oxa1p. Molecular biology of the cell, 8(8), 1449–1460. https://doi.org/10.1091/mbc.8.8.1449

Hell, K., Herrmann, J., Pratje, E., Neupert, W., & Stuart, R. A. (1997). Oxa1p mediates the export of the N- and C-termini of pCoxII from the mitochondrial matrix to the intermembrane space. FEBS letters, 418(3), 367–370. https://doi.org/10.1016/s0014-5793(97)01412-9

Hell, K., Tzagoloff, A., Neupert, W., & Stuart, R. A. (2000). Identification of Cox20p, a novel protein involved in the maturation and assembly of cytochrome oxidase subunit 2. The Journal of biological chemistry, 275(7), 4571–4578. https://doi.org/10.1074/jbc.275.7.4571

Herrmann, J. M., Neupert, W., & Stuart, R. A. (1997). Insertion into the mitochondrial inner membrane of a polytopic protein, the nuclear-encoded Oxa1p. The EMBO journal, 16(9), 2217–2226. https://doi.org/10.1093/emboj/16.9.2217

Herrmann, J. M., & Funes, S. (2005). Biogenesis of cytochrome oxidase-sophisticated assembly lines in the mitochondrial inner membrane. Gene, 354, 43–52. https://doi.org/10.1016/j.gene.2005.03.017

Hill B. C. (1994). The pathway of CO binding to cytochrome c oxidase. Can the gateway be closed?. FEBS letters, 354(3), 284–288. https://doi.org/10.1016/0014-5793(94)01140-0

Hlavatá, L., & Nyström, T. (2003). Ras proteins control mitochondrial biogenesis and function in Saccharomyces cerevisiae. Folia microbiologica, 48(6), 725–730. https://doi.org/10.1007/BF02931505

Hlavatá, L., Nachin, L., Jezek, P., & Nyström, T. (2008). Elevated Ras/protein kinase A activity in Saccharomyces cerevisiae reduces proliferation rate and lifespan by two different reactive oxygen species-dependent routes. Aging cell, 7(2), 148–157. https://doi.org/10.1111/j.1474-9726.2007.00361.x

Hoffman, C. S., & Winston, F. (1987). A ten-minute DNA preparation from yeast

efficiently releases autonomous plasmids for transformation of Escherichia coli. Gene, 57(2-3), 267–272. https://doi.org/10.1016/0378-1119(87)90131-4

Holland, P., Bergenholm, D., Börlin, C. S., Liu, G., & Nielsen, J. (2019). Predictive models of eukaryotic transcriptional regulation reveals changes in transcription factor roles and promoter usage between metabolic conditions. Nucleic acids research, 47(10), 4986–5000. https://doi.org/10.1093/nar/gkz253

Homberg, B., Rehling, P., & Cruz-Zaragoza, L. D. (2023). The multifaceted mitochondrial OXA insertase. Trends in cell biology, 33(9), 765–772. https://doi.org/10.1016/j.tcb.2023.02.001

Horak, C. E., Luscombe, N. M., Qian, J., Bertone, P., Piccirrillo, S., Gerstein, M., & Snyder, M. (2002). Complex transcriptional circuitry at the G1/S transition in Saccharomyces cerevisiae. Genes & development, 16(23), 3017–3033. https://doi.org/10.1101/gad.1039602

Huang, S., Taylor, N. L., Whelan, J., & Millar, A. H. (2009). Refining the definition of plant mitochondrial presequences through analysis of sorting signals, N-terminal modifications, and cleavage motifs. Plant physiology, 150(3), 1272–1285. https://doi.org/10.1104/pp.109.137885

Ieva, R., Heißwolf, A. K., Gebert, M., Vögtle, F. N., Wollweber, F., Mehnert, C. S., Oeljeklaus, S., Warscheid, B., Meisinger, C., van der Laan, M., & Pfanner, N. (2013). Mitochondrial inner membrane protease promotes assembly of presequence translocase by removing a carboxy-terminal targeting sequence. Nature communications, 4, 2853. https://doi.org/10.1038/ncomms3853

Ieva, R., Schrempp, S. G., Opaliński, L., Wollweber, F., Höß, P., Heißwolf, A. K., Gebert, M., Zhang, Y., Guiard, B., Rospert, S., Becker, T., Chacinska, A., Pfanner, N., & van der Laan, M. (2014). Mgr2 functions as lateral gatekeeper for preprotein sorting in the mitochondrial inner membrane. Molecular cell, 56(5), 641–652. https://doi.org/10.1016/j.molcel.2014.10.010

Ing, G., Hartley, A. M., Pinotsis, N., & Maréchal, A. (2022). Cryo-EM structure of a monomeric yeast S. cerevisiae complex IV isolated with maltosides: Implications in supercomplex formation. Biochimica et biophysica acta. Bioenergetics, 1863(7), 148591. https://doi.org/10.1016/j.bbabio.2022.148591

Iqbal, J., Gérard, H. C., Rahman, M. U., & Hudson, A. P. (1996). A probable cis-regulatory element on yeast mitochondrial DNA responsible for cAMP-mediated transcription. Current genetics, 30(6), 493–501. https://doi.org/10.1007/s002940050161

Johnson, K. A., Bhushan, S., Ståhl, A., Hallberg, B. M., Frohn, A., Glaser, E., & Eneqvist, T. (2006). The closed structure of presequence protease PreP forms a unique 10,000 Angstroms3 chamber for proteolysis. The EMBO journal, 25(9), 1977–1986. https://doi.org/10.1038/sj.emboj.7601080

Jones, G. M., Stalker, J., Humphray, S., West, A., Cox, T., Rogers, J., Dunham, I., & Prelich, G. (2008). A systematic library for comprehensive overexpression screens in Saccharomyces cerevisiae. Nature methods, 5(3), 239–241. https://doi.org/10.1038/nmeth.1181

Jumper, J., Evans, R., Pritzel, A., Green, T., Figurnov, M., Ronneberger, O., Tunyasuvunakool, K., Bates, R., Žídek, A., Potapenko, A., Bridgland, A., Meyer, C., Kohl, S. A. A., Ballard, A. J., Cowie, A., Romera-Paredes, B., Nikolov, S., Jain, R., Adler, J., Back, T., … Hassabis, D. (2021). Highly accurate protein structure prediction with AlphaFold. Nature, 596(7873), 583–589. https://doi.org/10.1038/s41586-021-03819-2

Kabeya, Y., Kawamata, T., Suzuki, K., & Ohsumi, Y. (2007). Cis1/Atg31 is required for autophagosome formation in Saccharomyces cerevisiae. Biochemical and biophysical research communications, 356(2), 405–410. https://doi.org/10.1016/j.bbrc.2007.02.150

Karakaidos, P., & Rampias, T. (2020). Mitonuclear Interactions in the Maintenance of Mitochondrial Integrity. Life (Basel, Switzerland), 10(9), 173. https://doi.org/10.3390/life10090173

Karlberg, O., Canbäck, B., Kurland, C. G., & Andersson, S. G. (2000). The dual origin of the yeast mitochondrial proteome. Yeast (Chichester, England), 17(3), 170–187. https://doi.org/10.1002/1097-0061(20000930)17:3<170::AID-YEA25>3.0.CO;2-V

Keerthiraju, E., Du, C., Tucker, G., & Greetham, D. (2019). A Role for COX20 in Tolerance to Oxidative Stress and Programmed Cell Death in Saccharomyces cerevisiae. Microorganisms, 7(11), 575. https://doi.org/10.3390/microorganisms7110575

Kennedy, E. P., & Lehninger, A. L. (1950). The products of oxidation of fatty acids by isolated rat liver mitochondria. Journal of Biological Chemistry, 185(1), 275–285. https://doi.org/10.1016/s0021-9258(18)56417-6

Krämer, L., Dalheimer, N., Räschle, M., Storchová, Z., Pielage, J., Boos, F., & Herrmann, J. M. (2023). MitoStores: chaperone-controlled protein granules store mitochondrial precursors in the cytosol. The EMBO journal, 42(7), e112309. https://doi.org/10.15252/embj.2022112309

Kumar, V., Hart, A. J., Keerthiraju, E. R., Waldron, P. R., Tucker, G. A., & Greetham, D. (2015). Expression of

Mitochondrial Cytochrome C Oxidase Chaperone Gene (COX20) Improves Tolerance to Weak Acid and Oxidative Stress during Yeast Fermentation. PloS one, 10(10), e0139129. https://doi.org/10.1371/journal.pone.0139129

Kurland, C. G., & Andersson, S. G. (2000). Origin and evolution of the mitochondrial proteome. Microbiology and molecular biology reviews : MMBR, 64(4), 786–820. https://doi.org/10.1128/MMBR.64.4.786-820.2000

Kushnirov V. V. (2000). Rapid and reliable protein extraction from yeast. Yeast (Chichester, England), 16(9), 857–860. https://doi.org/10.1002/1097-0061(20000630)16:9<857::AID-YEA561>3.0.CO;2-B

Kühlbrandt W. (2015). Structure and function of mitochondrial membrane protein complexes. BMC biology, 13, 89. https://doi.org/10.1186/s12915-015-0201-x

Kühlbrandt W. (2019). Structure and Mechanisms of F-Type ATP Synthases. Annual review of biochemistry, 88, 515–549. https://doi.org/10.1146/annurev-biochem-013118-110903

Kyriakouli, D. S., Boesch, P., Taylor, R. W., & Lightowlers, R. N. (2008). Progress and prospects: gene therapy for mitochondrial DNA disease. Gene therapy, 15(14), 1017–1023. https://doi.org/10.1038/gt.2008.91

LaMarche, A. E., Abate, M. I., Chan, S. H., & Trumpower, B. L. (1992). Isolation and characterization of COX12, the nuclear gene for a previously unrecognized subunit of Saccharomyces cerevisiae cytochrome c oxidase. The Journal of biological chemistry, 267(31), 22473–22480. https://doi.org/10.1016/S0021-9258(18)41696-1

Lee, S., Lee, H., Yoo, S., Ieva, R., van der Laan, M., von Heijne, G., & Kim, H. (2020). The Mgr2 subunit of the TIM23 complex regulates membrane insertion of marginal stop-transfer signals in the mitochondrial inner membrane. FEBS letters, 594(6), 1081–1087. https://doi.org/10.1002/1873-3468.13692

Lehninger, A. L. (1944). The synthesis, some derivatives, and the metabolism of α,γ-diketo-n-octanoic acid. Journal of Biological Chemistry, 153(2), 561–570. https://doi.org/10.1016/s0021-9258(18)72000-0

Li, Y., Dudek, J., Guiard, B., Pfanner, N., Rehling, P., & Voos, W. (2004). The presequence translocase-associated protein import motor of mitochondria. Pam16 functions in an antagonistic manner to Pam18. The Journal of biological chemistry, 279(36), 38047–38054. https://doi.org/10.1074/jbc.M404319200

Liu, Q., D'Silva, P., Walter, W., Marszalek, J., & Craig, E. A. (2003). Regulated cycling of mitochondrial Hsp70 at the protein import channel. Science (New York, N.Y.), 300(5616), 139–141. https://doi.org/10.1126/science.1083379

Liu, Q., Fong, B., Yoo, S., Unruh, J. R., Guo, F., Yu, Z., Chen, J., Si, K., Li, R., & Zhou, C. (2023). Nascent mitochondrial proteins initiate the localized condensation of cytosolic protein aggregates on the mitochondrial surface. Proceedings of the National Academy of Sciences of the United States of America, 120(31), e2300475120. https://doi.org/10.1073/pnas.2300475120

Lode, A., Kuschel, M., Paret, C., & Rödel, G. (2000). Mitochondrial copper metabolism in yeast: interaction between Sco1p and Cox2p. FEBS letters, 485(1), 19–24. https://doi.org/10.1016/s0014-5793(00)02176-1

Lord, C. L., Timney, B. L., Rout, M. P., & Wente, S. R. (2015). Altering nuclear pore complex function impacts longevity and mitochondrial function in S. cerevisiae. The Journal of cell biology, 208(6), 729–744. https://doi.org/10.1083/jcb.201412024

Lorenzi, I., Oeljeklaus, S., Ronsör, C., Bareth, B., Warscheid, B., Rehling, P., & Dennerlein, S. (2016). Ribosome-Associated Mba1 Escorts Cox2 from Insertion Machinery to Maturing Assembly Intermediates. Molecular and cellular biology, 36(22), 2782–2793. https://doi.org/10.1128/MCB.00361-16

Löhning, C., & Ciriacy, M. (1994). The TYE7 gene of Saccharomyces cerevisiae encodes a putative bHLH-LZ transcription factor required for Ty1-mediated gene expression. Yeast (Chichester, England), 10(10), 1329–1339. https://doi.org/10.1002/yea.320101010

Mabuchi, T., Ichimura, Y., Takeda, M., & Douglas, M. G. (2000). ASC1/RAS2 suppresses the growth defect on glycerol caused by the atp1-2 mutation in the yeast Saccharomyces cerevisiae. The Journal of biological chemistry, 275(14), 10492–10497. https://doi.org/10.1074/jbc.275.14.10492

Mapa, K., Sikor, M., Kudryavtsev, V., Waegemann, K., Kalinin, S., Seidel, C. A., Neupert, W., Lamb, D. C., & Mokranjac, D. (2010). The conformational dynamics of the mitochondrial Hsp70 chaperone. Molecular cell, 38(1), 89–100. https://doi.org/10.1016/j.molcel.2010.03.010

Martijn, J., Vosseberg, J., Guy, L., Offre, P., & Ettema, T. J. G. (2018). Deep mitochondrial origin outside the sampled alphaproteobacteria. Nature, 557(7703), 101–105. https://doi.org/10.1038/s41586-018-0059-5

Matta, S. K., Kumar, A., & D'Silva, P. (2020). Mgr2 regulates mitochondrial preprotein import by associating with channel-forming Tim23 subunit. Molecular biology of the

cell, 31(11), 1112–1123. https://doi.org/10.1091/mbc.E19-12-0677

Matsumoto, K., Uno, I., & Ishikawa, T. (1983). Control of cell division in Saccharomyces cerevisiae mutants defective in adenylate cyclase and cAMP-dependent protein kinase. Experimental cell research, 146(1), 151–161. https://doi.org/10.1016/0014-4827(83)90333-6

McFarland, R., Taylor, R. W., & Turnbull, D. M. (2010). A neurological perspective on mitochondrial disease. The Lancet. Neurology, 9(8), 829–840. https://doi.org/10.1016/S1474-4422(10)70116-2

Meisinger, C., Brix, J., Model, K., Pfanner, N., & Ryan, M. T. (1999). The preprotein translocase of the outer mitochondrial membrane: receptors and a general import pore. Cellular and molecular life sciences : CMLS, 56(9-10), 817–824. https://doi.org/10.1007/s000180050028

Minet, M., Dufour, M. E., & Lacroute, F. (1992). Complementation of Saccharomyces cerevisiae auxotrophic mutants by Arabidopsis thaliana cDNAs. The Plant journal : for cell and molecular biology, 2(3), 417–422. https://doi.org/10.1111/j.1365-313x.1992.00417.x

Mitchell P. (1961). Coupling of phosphorylation to electron and hydrogen transfer by a chemi-osmotic type of mechanism. Nature, 191, 144–148. https://doi.org/10.1038/191144a0

Mirzalieva, O., Jeon, S., Damri, K., Hartke, R., Drwesh, L., Demishtein-Zohary, K., Azem, A., Dunn, C. D., & Peixoto, P. M. (2019). Deletion of Mgr2p Affects the Gating Behavior of the TIM23 Complex. Frontiers in physiology, 9, 1960. https://doi.org/10.3389/fphys.2018.01960

Mokranjac D. (2020). How to get to the other side of the mitochondrial inner membrane - the protein import motor. Biological chemistry, 401(6-7), 723–736. https://doi.org/10.1515/hsz-2020-0106

Morgenstern, M., Stiller, S. B., Lübbert, P., Peikert, C. D., Dannenmaier, S., Drepper, F., Weill, U., Höß, P., Feuerstein, R., Gebert, M., Bohnert, M., van der Laan, M., Schuldiner, M., Schütze, C., Oeljeklaus, S., Pfanner, N., Wiedemann, N., & Warscheid, B. (2017). Definition of a High-Confidence Mitochondrial Proteome at Quantitative Scale. Cell reports, 19(13), 2836–2852. https://doi.org/10.1016/j.celrep.2017.06.014

Mossmann, D., Vögtle, F. N., Taskin, A. A., Teixeira, P. F., Ring, J., Burkhart, J. M., Burger, N., Pinho, C. M., Tadic, J., Loreth, D., Graff, C., Metzger, F., Sickmann, A., Kretz, O., Wiedemann, N., Zahedi, R. P., Madeo, F., Glaser, E., & Meisinger, C. (2014). Amyloid-β peptide induces mitochondrial dysfunction by inhibition of preprotein maturation. Cell metabolism, 20(4), 662–669.

https://doi.org/10.1016/j.cmet.2014.07.024

Mulero, J. J., & Fox, T. D. (1993). Alteration of the Saccharomyces cerevisiae COX2 mRNA 5'-untranslated leader by mitochondrial gene replacement and functional interaction with the translational activator protein PET111. Molecular biology of the cell, 4(12), 1327–1335. https://doi.org/10.1091/mbc.4.12.1327

Müller, G., & Bandlow, W. (1987). Protein phosphorylation in yeast mitochondria: cAMP-dependence, submitochondrial localization and substrates of mitochondrial protein kinases. Yeast (Chichester, England), 3(3), 161–174. https://doi.org/10.1002/yea.320030304

Müller, M., Mentel, M., van Hellemond, J. J., Henze, K., Woehle, C., Gould, S. B., Yu, R. Y., van der Giezen, M., Tielens, A. G., & Martin, W. F. (2012). Biochemistry and evolution of anaerobic energy metabolism in eukaryotes. Microbiology and molecular biology reviews : MMBR, 76(2), 444–495. https://doi.org/10.1128/MMBR.05024-11

Nagley, P., Farrell, L. B., Gearing, D. P., Nero, D., Meltzer, S., & Devenish, R. J. (1988). Assembly of functional proton-translocating ATPase complex in yeast mitochondria with cytoplasmically synthesized subunit 8, a polypeptide normally encoded within the organelle. Proceedings of the National Academy of Sciences of the United States of America, 85(7), 2091–2095. https://doi.org/10.1073/pnas.85.7.2091

Nagley, P. & Devenish, R.J. (1989) Leading organellar proteins along new pathways: the relocation of mitochondrial and chloroplast genes to the nucleus. Trends in Biochemical Sciences, 14 (1), 31-35. https://doi.org/10.1016/0968-0004(89)90087-X.

Nakai, M., Endo, T., Hase, T., & Matsubara, H. (1993). Intramitochondrial protein sorting. Isolation and characterization of the yeast MSP1 gene which belongs to a novel family of putative ATPases. The Journal of biological chemistry, 268(32), 24262–24269. https://doi.org/10.1016/S0021-9258(20)80519-5

Nelson, D. L., Cox, M. M., Hoskins, A. A., & Lehninger, A. L. (2021). Oxidative Phosphorylation. In Lehninger Principles of biochemistry (8th ed., pp. 711–749). essay, Macmillan International Higher Education.

Neuman-Silberberg, F. S., Bhattacharya, S., & Broach, J. R. (1995). Nutrient availability and the RAS/cyclic AMP pathway both induce expression of ribosomal protein genes in Saccharomyces cerevisiae but by different mechanisms. Molecular and cellular biology, 15(6), 3187–3196. https://doi.org/10.1128/MCB.15.6.3187

Nieto-Panqueva, F., Rubalcava-Gracia, D., Hamel, P. P., & González-Halphen, D. (2023). The constraints of allotopic

expression. Mitochondrion, 73, 30–50. https://doi.org/10.1016/j.mito.2023.09.004

Nishi, K., Park, C. S., Pepper, A. E., Eichinger, G., Innis, M. A., & Holland, M. J. (1995). The GCR1 requirement for yeast glycolytic gene expression is suppressed by dominant mutations in the SGC1 gene, which encodes a novel basic-helix-loop-helix protein. Molecular and cellular biology, 15(5), 2646–2653. https://doi.org/10.1128/MCB.15.5.2646

Nunnari, J., Fox, T. D., & Walter, P. (1993). A mitochondrial protease with two catalytic subunits of nonoverlapping specificities. Science (New York, N.Y.), 262(5142), 1997–2004. https://doi.org/10.1126/science.8266095

Nunnari, J., Marshall, W. F., Straight, A., Murray, A., Sedat, J. W., & Walter, P. (1997). Mitochondrial transmission during mating in Saccharomyces cerevisiae is determined by mitochondrial fusion and fission and the intramitochondrial segregation of mitochondrial DNA. Molecular biology of the cell, 8(7), 1233–1242. https://doi.org/10.1091/mbc.8.7.1233

Nývltová, E., Dietz, J. V., Seravalli, J., Khalimonchuk, O., & Barrientos, A. (2022). Coordination of metal center biogenesis in human cytochrome c oxidase. Nature communications, 13(1), 3615. https://doi.org/10.1038/s41467-022-31413-1

Ott, M., Prestele, M., Bauerschmitt, H., Funes, S., Bonnefoy, N., & Herrmann, J. M. (2006). Mba1, a membrane-associated ribosome receptor in mitochondria. The EMBO journal, 25(8), 1603–1610. https://doi.org/10.1038/sj.emboj.7601070

Palade G. E. (1953). An electron microscope study of the mitochondrial structure. The journal of histochemistry and cytochemistry : official journal of the Histochemistry Society, 1(4), 188–211. https://doi.org/10.1177/1.4.188

Papa, S., Sardanelli, A. M., Cocco, T., Speranza, F., Scacco, S. C., & Technikova-Dobrova, Z. (1996). The nuclear-encoded 18 kDa (IP) AQDQ subunit of bovine heart complex I is phosphorylated by the mitochondrial cAMP-dependent protein kinase. FEBS letters, 379(3), 299–301. https://doi.org/10.1016/0014-5793(95)01532-9

Perez-Martinez, X., Broadley, S. A., & Fox, T. D. (2003). Mss51p promotes mitochondrial Cox1p synthesis and interacts with newly synthesized Cox1p. The EMBO journal, 22(21), 5951–5961. https://doi.org/10.1093/emboj/cdg566

Pfanner, N., Warscheid, B., & Wiedemann, N. (2019). Mitochondrial proteins: from biogenesis to functional networks. Nature reviews. Molecular cell biology, 20(5), 267–284. https://doi.org/10.1038/s41580-018-0092-0

Pfeffer, S., Woellhaf, M. W., Herrmann, J. M., & Förster, F. (2015). Organization of the mitochondrial translation machinery studied in situ by cryoelectron tomography. Nature communications, 6, 6019. https://doi.org/10.1038/ncomms7019

Pon, L., and G. Schatz. 1991. Biogenesis of Yeast Mitochondria. In The Molecular Biology of the Yeast Saccharomyces. J.R. Broach, J.R. Pringle, and E.W. Jones, editors. Cold Spring Harbor Laboratory Press, Cold Spring Harbor, NY. 334–406.

Popot, J. L., & de Vitry, C. (1990). On the microassembly of integral membrane proteins. Annual review of biophysics and biophysical chemistry, 19, 369–403. https://doi.org/10.1146/annurev.bb.19.060190.002101

Popov-Celeketić, D., Mapa, K., Neupert, W., & Mokranjac, D. (2008). Active remodelling of the TIM23 complex during translocation of preproteins into mitochondria. The EMBO journal, 27(10), 1469–1480. https://doi.org/10.1038/emboj.2008.79

Poutre, C. G., & Fox, T. D. (1987). PET111, a Saccharomyces cerevisiae nuclear gene required for translation of the mitochondrial mRNA encoding cytochrome c oxidase subunit II. Genetics, 115(4), 637–647. https://doi.org/10.1093/genetics/115.4.637

Preuss, M., Leonhard, K., Hell, K., Stuart, R. A., Neupert, W., & Herrmann, J. M. (2001). Mba1, a novel component of the mitochondrial protein export machinery of the yeast Saccharomyces cerevisiae. The Journal of cell biology, 153(5), 1085–1096. https://doi.org/10.1083/jcb.153.5.1085

Ricchetti, M., Fairhead, C., & Dujon, B. (1999). Mitochondrial DNA repairs double-strand breaks in yeast chromosomes. Nature, 402(6757), 96–100. https://doi.org/10.1038/47076

Rinehart, J., Krett, B., Rubio, M. A., Alfonzo, J. D., & Söll, D. (2005). Saccharomyces cerevisiae imports the cytosolic pathway for Gln-tRNA synthesis into the mitochondrion. Genes & development, 19(5), 583–592. https://doi.org/10.1101/gad.1269305

Robinson, K. A., & Lopes, J. M. (2000). SURVEY AND SUMMARY: Saccharomyces cerevisiae basic helix-loop-helix proteins regulate diverse biological processes. Nucleic acids research, 28(7), 1499–1505. https://doi.org/10.1093/nar/28.7.1499

Robzyk, K., & Kassir, Y. (1992). A simple and highly efficient procedure for rescuing autonomous plasmids from yeast. Nucleic acids research, 20(14), 3790. https://doi.org/10.1093/nar/20.14.3790

Roger, A. J., Muñoz-Gómez, S. A., & Kamikawa, R. (2017). The Origin and Diversification of Mitochondria. Current biology : CB, 27(21), R1177–R1192. https://doi.org/10.1016/j.cub.2017.09.015

Roise, D., & Schatz, G. (1988). Mitochondrial presequences. The Journal of biological chemistry, 263(10), 4509–4511. https://doi.org/10.1016/S0021-9258(18)68809-X

Rubalcava-Gracia, D., Vázquez-Acevedo, M., Funes, S., Pérez-Martínez, X., & González-Halphen, D. (2018). Mitochondrial versus nuclear gene expression and membrane protein assembly: the case of subunit 2 of yeast cytochrome c oxidase. Molecular biology of the cell, 29(7), 820–833. https://doi.org/10.1091/mbc.E17-09-0560

Rubalcava-Gracia, D., García-Rincón, J., Pérez-Montfort, R., Hamel, P. P., & González-Halphen, D. (2019). Key within-membrane residues and precursor dosage impact the allotopic expression of yeast subunit II of cytochrome c oxidase. Molecular biology of the cell, 30(18), 2358–2366. https://doi.org/10.1091/mbc.E18-12-0788

Rubio, M. A., Rinehart, J. J., Krett, B., Duvezin-Caubet, S., Reichert, A. S., Söll, D., & Alfonzo, J. D. (2008). Mammalian mitochondria have the innate ability to import tRNAs by a mechanism distinct from protein import. Proceedings of the National Academy of Sciences of the United States of America, 105(27), 9186–9191. https://doi.org/10.1073/pnas.0804283105

Salinas-Giegé, T., Giegé, R., & Giegé, P. (2015). tRNA biology in mitochondria. International journal of molecular sciences, 16(3), 4518–4559. https://doi.org/10.3390/ijms16034518

Sayyed, U. M. H., & Mahalakshmi, R. (2022). Mitochondrial protein translocation machinery: From TOM structural biogenesis to functional regulation. The Journal of biological chemistry, 298(5), 101870. https://doi.org/10.1016/j.jbc.2022.101870

Schägger H. (1994). Denaturing Electrophoretic Techniques, in: Separation, Detection, and Characterization of Biological Macromolecules, a Practical Guide to Membrane Protein Purification, Academic Press, Volume 2, , Pages 59-79, https://doi.org/10.1016/B978-0-08-057172-0.50010-3

Scheffler, I. E. (2008). Mitochondrial Electron Transfer and Oxidative Phosphorylation. In Mitochondria. 2nd ed. essay, Wiley-Liss. https://doi.org/10.1002/9780470191774

Schendzielorz, A. B., Bragoszewski, P., Naumenko, N., Gomkale, R., Schulz, C., Guiard, B., Chacinska, A., & Rehling, P. (2018). Motor recruitment to the TIM23 channel's lateral gate restricts polypeptide release into the inner membrane. Nature communications, 9(1), 4028. https://doi.org/10.1038/s41467-018-06492-8

Schneider, A., Oppliger, W., & Jenö, P. (1994). Purified inner membrane protease I of yeast mitochondria is a heterodimer. The Journal of biological

chemistry, 269(12), 8635–8638. https://doi.org/10.1016/S0021-9258(17)37013-8

Schulte, U., Arretz, M., Schneider, H., Tropschug, M., Wachter, E., Neupert, W., & Weiss, H. (1989). A family of mitochondrial proteins involved in bioenergetICS and biogenesis. Nature, 339(6220), 147–149. https://doi.org/10.1038/339147a0

Schulte, U., den Brave, F., Haupt, A., Gupta, A., Song, J., Müller, C. S., Engelke, J., Mishra, S., Mårtensson, C., Ellenrieder, L., Priesnitz, C., Straub, S. P., Doan, K. N., Kulawiak, B., Bildl, W., Rampelt, H., Wiedemann, N., Pfanner, N., Fakler, B., & Becker, T. (2023). Mitochondrial complexome reveals quality-control pathways of protein import. Nature, 614(7946), 153–159. https://doi.org/10.1038/s41586-022-05641-w

Schulz, C., & Rehling, P. (2014). Remodelling of the active presequence translocase drives motor-dependent mitochondrial protein translocation. Nature communications, 5, 4349. https://doi.org/10.1038/ncomms5349

Sikorski, R. S., & Hieter, P. (1989). A system of shuttle vectors and yeast host strains designed for efficient manipulation of DNA in Saccharomyces cerevisiae. Genetics, 122(1), 19–27. https://doi.org/10.1093/genetics/122.1.19

Sim, S. I., Chen, Y., Lynch, D. L., Gumbart, J. C., & Park, E. (2023). Structural basis of mitochondrial protein import by the TIM23 complex. Nature, 621(7979), 620–626. https://doi.org/10.1038/s41586-023-06239-6

Slutsky-Leiderman, O., Marom, M., Iosefson, O., Levy, R., Maoz, S., & Azem, A. (2007). The interplay between components of the mitochondrial protein translocation motor studied using purified components. The Journal of biological chemistry, 282(47), 33935–33942. https://doi.org/10.1074/jbc.M704435200

Soto, I. C., Fontanesi, F., Liu, J., & Barrientos, A. (2012). Biogenesis and assembly of eukaryotic cytochrome c oxidase catalytic core. Biochimica et biophysica acta, 1817(6), 883–897. https://doi.org/10.1016/j.bbabio.2011.09.005

Spang, A., Saw, J. H., Jørgensen, S. L., Zaremba-Niedzwiedzka, K., Martijn, J., Lind, A. E., van Eijk, R., Schleper, C., Guy, L., & Ettema, T. J. G. (2015). Complex archaea that bridge the gap between prokaryotes and eukaryotes. Nature, 521(7551), 173–179. https://doi.org/10.1038/nature14447

Straub, S. P., Stiller, S. B., Wiedemann, N., & Pfanner, N. (2016). Dynamic organization of the mitochondrial protein import machinery. Biological chemistry, 397(11), 1097–1114. https://doi.org/10.1515/hsz-2016-0145

Supekova, L., Supek, F., Greer, J. E., & Schultz, P. G. (2010). A single mutation in the first transmembrane domain of yeast COX2 enables its allotopic expression. Proceedings of the National Academy of Sciences of the United States of America, 107(11), 5047–5052. https://doi.org/10.1073/pnas.1000735107

Swiegers, J. H., Pretorius, I. S., & Bauer, F. F. (2006). Regulation of respiratory growth by Ras: the glyoxylate cycle mutant, cit2Delta, is suppressed by RAS2. Current genetics, 50(3), 161–171. https://doi.org/10.1007/s00294-006-0084-z

Szyrach, G., Ott, M., Bonnefoy, N., Neupert, W., & Herrmann, J. M. (2003). Ribosome binding to the Oxa1 complex facilitates co-translational protein insertion in mitochondria. The EMBO journal, 22(24), 6448–6457. https://doi.org/10.1093/emboj/cdg623

Tatchell, K., Robinson, L. C., & Breitenbach, M. (1985). RAS2 of Saccharomyces cerevisiae is required for gluconeogenic growth and proper response to nutrient limitation. Proceedings of the National Academy of Sciences of the United States of America, 82(11), 3785–3789. https://doi.org/10.1073/pnas.82.11.3785

Thorsness, P. E., & Weber, E. R. (1996). Escape and migration of nucleic acids between chloroplasts, mitochondria, and the nucleus. International review of cytology, 165, 207–234. https://doi.org/10.1016/s0074-7696(08)62223-8

Tischner, C., & Wenz, T. (2015). Keep the fire burning: Current avenues in the quest of treating mitochondrial disorders. Mitochondrion, 24, 32–49. https://doi.org/10.1016/j.mito.2015.06.002

Torchet, C., Jacq, C., & Hermann-Le Denmat, S. (1998). Two mutant forms of the S1/TPR-containing protein Rrp5p affect the 18S rRNA synthesis in Saccharomyces cerevisiae. RNA (New York, N.Y.), 4(12), 1636–1652. https://doi.org/10.1017/s1355838298981511

Tsukihara, T., Aoyama, H., Yamashita, E., Tomizaki, T., Yamaguchi, H., Shinzawa-Itoh, K., Nakashima, R., Yaono, R., & Yoshikawa, S. (1995). Structures of metal sites of oxidized bovine heart cytochrome c oxidase at 2.8 A. Science (New York, N.Y.), 269(5227), 1069–1074. https://doi.org/10.1126/science.7652554

Tsukihara, T., Aoyama, H., Yamashita, E., Tomizaki, T., Yamaguchi, H., Shinzawa-Itoh, K., Nakashima, R., Yaono, R., & Yoshikawa, S. (1996). The whole structure of the 13-subunit oxidized cytochrome c oxidase at 2.8 A. Science (New York, N.Y.), 272(5265), 1136–1144. https://doi.org/10.1126/science.272.5265.1136

Venema, J., & Tollervey, D. (1996). RRP5 is required for formation of both 18S and 5.8S rRNA in yeast. The EMBO journal, 15(20), 5701–5714.

https://doi.org/10.1002/j.1460-2075.1996.tb00954.x

Vercellino, I., & Sazanov, L. A. (2022). The assembly, regulation and function of the mitochondrial respiratory chain. Nature reviews. Molecular cell biology, 23(2), 141–161. https://doi.org/10.1038/s41580-021-00415-0

Vitali, D. G., Käser, S., Kolb, A., Dimmer, K. S., Schneider, A., & Rapaport, D. (2018). Independent evolution of functionally exchangeable mitochondrial outer membrane import complexes. eLife, 7, e34488. https://doi.org/10.7554/eLife.34488

Vögtle, F. N., Wortelkamp, S., Zahedi, R. P., Becker, D., Leidhold, C., Gevaert, K., Kellermann, J., Voos, W., Sickmann, A., Pfanner, N., & Meisinger, C. (2009). Global analysis of the mitochondrial N-proteome identifies a processing peptidase critical for protein stability. Cell, 139(2), 428–439. https://doi.org/10.1016/j.cell.2009.07.045

Vögtle, F. N., Burkhart, J. M., Gonczarowska-Jorge, H., Kücükköse, C., Taskin, A. A., Kopczynski, D., Ahrends, R., Mossmann, D., Sickmann, A., Zahedi, R. P., & Meisinger, C. (2017). Landscape of submitochondrial protein distribution. Nature communications, 8(1), 290. https://doi.org/10.1038/s41467-017-00359-0

von Heijne, G. (1986). The distribution of positively charged residues in bacterial inner membrane proteins correlates with the trans-membrane topology. The EMBO journal, 5(11), 3021–3027. https://doi.org/10.1002/j.1460-2075.1986.tb04601.x

Wiedemann, N., & Pfanner, N. (2017). Mitochondrial Machineries for Protein Import and Assembly. Annual review of biochemistry, 86, 685–714. https://doi.org/10.1146/annurev-biochem-060815-014352

Williams, E. H., & Fox, T. D. (2003). Antagonistic signals within the COX2 mRNA coding sequence control its translation in Saccharomyces cerevisiae mitochondria. RNA (New York, N.Y.), 9(4), 419–431. https://doi.org/10.1261/rna.2182903

Williams, K. P., Sobral, B. W., & Dickerman, A. W. (2007). A robust species tree for the alphaproteobacteria. Journal of bacteriology, 189(13), 4578–4586. https://doi.org/10.1128/JB.00269-07

Yoboue, E. D., Augier, E., Galinier, A., Blancard, C., Pinson, B., Casteilla, L., Rigoulet, M., & Devin, A. (2012). cAMP-induced mitochondrial compartment biogenesis: role of glutathione redox state. The Journal of biological chemistry, 287(18), 14569–14578. https://doi.org/10.1074/jbc.M111.302786

Yoshikawa, S., Muramoto, K., & Shinzawa-Itoh, K. (2011). Proton-pumping mechanism of cytochrome C oxidase. Annual review of biophysics, 40, 205–223. https://doi.org/10.1146/annurev-biophys-042910-155341

Zaremba-Niedzwiedzka, K., Caceres, E. F., Saw, J. H., Bäckström, D., Juzokaite, L., Vancaester, E., Seitz, K. W., Anantharaman, K., Starnawski, P., Kjeldsen, K. U., Stott, M. B., Nunoura, T., Banfield, J. F., Schramm, A., Baker, B. J., Spang, A., & Ettema, T. J. (2017). Asgard archaea illuminate the origin of eukaryotic cellular complexity. Nature, 541(7637), 353–358. https://doi.org/10.1038/nature21031

Zhou, X., Yang, Y., Wang, G., Wang, S., Sun, D., Ou, X., Lian, Y., & Li, L. (2023). Molecular pathway of mitochondrial preprotein import through the TOM-TIM23 supercomplex. Nature structural & molecular biology, 30(12), 1996–2008. https://doi.org/10.1038/s41594-023-01103-7

APÉNDICES

Artículos publicados relacionados con el proyecto de tesis.

Artículo I.

Publicado.

Nieto-Panqueva, F., Rubalcava-Gracia, D., Hamel, P. P., & González-Halphen, D. (2023). The constraints of allotopic expression. *Mitochondrion*, 73, 30–50. https://doi.org/10.1016/j.mito.2023.09.004

Mitochondrion 73 (2023) 30–50

Contents lists available at ScienceDirect

Mitochondrion

journal homepage: www.elsevier.com/locate/mito

Review

The constraints of allotopic expression

Felipe Nieto-Panqueva [a], Diana Rubalcava-Gracia [a,b], Patrice P. Hamel [c,d], Diego González-Halphen [a,*]

[a] Instituto de Fisiología Celular, Universidad Nacional Autónoma de México, Mexico City, Mexico
[b] Division of Molecular Metabolism, Department of Medical Biochemistry and Biophysics, Karolinska Institutet, Stockholm, Sweden
[c] Department of Molecular Genetics and Department of Biological Chemistry and Pharmacology, Ohio State University, Columbus, OH, USA
[d] Vellore Institute of Technology (VIT), School of BioScience and Technology, Vellore, Tamil Nadu, India

ARTICLE INFO

Keywords:
Allotopic expression
Oxidative phosphorylation
Mitochondrial complexes
Protein import
TIM23
Apparent free energy of membrane insertion
Transmembrane stretches
Membrane embedded proteins

ABSTRACT

Allotopic expression is the functional transfer of an organellar gene to the nucleus, followed by synthesis of the gene product in the cytosol and import into the appropriate organellar sub compartment. Here, we focus on mitochondrial genes encoding OXPHOS subunits that were naturally transferred to the nucleus, and critically review experimental evidence that claim their allotopic expression. We emphasize aspects that may have been overlooked before, i.e., when modifying a mitochondrial gene for allotopic expression—besides adapting the codon usage and including sequences encoding mitochondrial targeting signals—three additional constraints should be considered: *(i)* the average apparent free energy of membrane insertion ($\mu\Delta G_{app}$) of the transmembrane stretches (TMS) in proteins earmarked for the inner mitochondrial membrane, *(ii)* the final, functional topology attained by each membrane-bound OXPHOS subunit; and *(iii)* the defined mechanism by which the protein translocator TIM23 sorts cytosol-synthesized precursors. The mechanistic constraints imposed by TIM23 dictate the operation of two pathways through which alpha-helices in TMS are sorted, that eventually determine the final topology of membrane proteins. We used the biological hydrophobicity scale to assign an average apparent free energy of membrane insertion ($\mu\Delta G_{app}$) and a "traffic light" color code to all TMS of OXPHOS membrane proteins, thereby predicting which are more likely to be internalized into mitochondria if allotopically produced. We propose that the design of proteins for allotopic expression must make allowance for $\mu\Delta G_{app}$ maximization of highly hydrophobic TMS in polypeptides whose corresponding genes have not been transferred to the nucleus in some organisms.

1. Endosymbiotic origin of mitochondria and natural transfer of mitochondrial genes to the nucleus

Mitochondria perform oxidative phosphorylation (OXPHOS), a fundamental energy-conversion process (Green and Tzagoloff, 1966; Mitchell, 1961). These organelles arose from the endosymbiosis between an ancestor of an alpha proteobacterium (Andersson et al., 1998; Martin and Müller, 1998; Roger et al., 2017; Martijn et al., 2018) and an ancestor of an archaeon related to extant members of the *phylum* Lokiarchaeota (Zaremba-Niedzwiedzka et al., 2017). After establishing this association, a massive transfer of genetic material from the endosymbiont to the archaeal host occurred (Lynch 1997; Gray, 1989; Gray et al., 1998). Once a protein-encoding gene from the endosymbiont (or protomitochondrion) relocalizes to the nucleus, there is evolutionary pressure for the relocated gene to become functional (Adams and Palmer, 2003), i.e., the transferred gene requires changes in its genetic code and/or codon usage, the acquisition of transcriptional and translational regulatory sequences, and the addition of nucleotide sequences encoding mitochondrial targeting sequences (MTS) which will enable the corresponding protein products to localize to the mitochondria. As a result, contemporary mitochondrial genomes are reduced and encode between 10- and 100-times fewer genes than most alpha proteobacterial genomes (Adams and Palmer, 2003), e.g., the human mitochondrial genome (mtDNA) encodes only 2 rRNAs, 22 tRNAs, and 13 proteins required for OXPHOS (Attardi, and Schatz, 1988; Roger et al., 2017). Despite the ongoing transfer of mitochondrial genes to the nuclear genome, some genes never become activated, and remain as pseudogenes, the so called nuclear-mitochondrial DNA segments (NUMTs)

* Corresponding author at: Departamento de Genética Molecular, Instituto de Fisiología Celular, Universidad Nacional Autónoma de México, Apartado Postal 70-243, México 04510, DF, Mexico.
E-mail address: dhalphen@ifc.unam.mx (D. González-Halphen).

https://doi.org/10.1016/j.mito.2023.09.004
Received 19 January 2023; Received in revised form 28 August 2023; Accepted 18 September 2023
Available online 20 September 2023

(Wallace et al., 1997; Bensasson et al., 2001; Woischnik and Moraes, 2002; Ricchetti et al., 2004; Calabrese et al., 2017; Lutz-Bonengel et al., 2021). A recent study shows that over 99 % of 66,083 whole-genome sequences in the human population carry at least one NUMT, and that most of these NUMTs have been inserted after humans diverged from apes (Wei et al. 2022).

Mitochondrial gene transfer to the nucleus has played a central role in the evolution of the organelle (Henze and Martin, 2001). If the relocation of mtDNA to the nuclear genome results in the successful activation of all genes, then it is expected that all coding sequences could be eventually lost from the mitochondrion (Berg and Kurland, 2000). However, mitochondria from virtually all oxygen-respiring eukaryotes possess a mitochondrial genome, except for the parasitic dinoflagellate *Amoebophrya ceratii* (John et al., 2019). In this text, we focus on human mtDNA-encoded genes and their protein products, although we also include seminal discoveries on allotopic expression made using budding yeast as a model system. However, the fundamental differences between mammalian and yeast mtDNA must be considered when describing examples of allotopic expression. Mammalian mtDNA is a small, circular molecule of ~16 kb encoding intron-less genes. The mtDNA of the yeast *Saccharomyces cerevisiae* is larger (~86 kb) and encodes genes interspersed by introns. In contrast to mammalian mtDNA, yeast mtDNA is subject to homologous recombination if it is biparentally inherited after mating (Birky, 2001). Notably, there is no evidence for the functional transfer of mitochondrial tRNA or mitoribosomal RNAs encoding genes to the nucleus (Adams and Palmer, 2003; Telonis et al., 2015). Mitochondria can use nuclear-encoded tRNA genes whose gene products are imported into the mitochondria but there is no support for a mitochondrial ancestry for these genes (Salinas-Giegé et al., 2015).

Here, we review examples of natural and artificial gene transfer of mitochondrial genes to the nucleus. We formulate the main constraints to be considered in the design of constructs for allotopic expression and examine previous reports using this experimental approach.

2. Biogenesis of mtDNA-encoded OXPHOS subunits and topological arrangement in the membrane

OXPHOS results from the concerted activity of five oligomeric protein complexes (I to V) embedded in the inner mitochondrial membrane (IMM) (Saraste, 1999; Papa et al., 2012; Vercellino and Sazanov, 2022). Electron transport through complexes I, III, and IV is tightly linked to protons being vectorially translocated from the matrix into the intermembrane space (IMS), generating an electrochemical potential $\Delta\mu H+$ across the IMM that is harnessed by complex V to generate ATP (Mitchell, 1961). High-resolution 3D structural models of human OXPHOS complexes are now accessible: the membrane-bound region of complex I, the whole complexes III and IV (Guo et al., 2017; Zong et al., 2018), and the complete complex V (Lai et al., 2023). Furthermore, many 3D structures of other mammalian OXPHOS complexes are also available (Iwata et al., 1998; Inaoka et al.,2015; Fiedorczuk et al., 2016; Letts et al., 2016; Gu et al., 2019; Pinke et al., 2020; Spikes et al., 2021). Thus, we now know the exact number and folding architecture of the transmembrane segments (TMS) of all OXPHOS subunits. Based on the experimentally deduced topological arrangement, the human mtDNA encoded subunits can be classified in four groups based on the exposition of its N or C-terminus to the IMS (out) or to the matrix (in): N_{out}-C_{out}, N_{in}-C_{in}, N_{out}-C_{in} and N_{in}-C_{out} (Fig. 1).

The mitochondrial proteome is a mosaic of components with two different genetic origins, with most proteins encoded by nuclear genes (1136 in humans according to Mitocarta 3.0) (Rath et al., 2021), and a small portion by mtDNA (~1.1 %). In general, mitochondrial genomes encode ribosomal RNAs, transfer RNAs, and a subset of proteins required for OXPHOS (Attardi, and Schatz, 1988; Roger et al., 2017). In mammals, 13 out of the 89 genes encoding OXPHOS proteins reside in the mtDNA: *nd1*, *nd2*, *nd3*, *nd4*, *nd4L*, *nd5, nd6* (for complex I), *cox1*, *cox2, cox3* (for complex IV), *cytb or cob* (for complex III), *atp6,* and *atp8* (for complex V) (Anderson et al, 1981; Boore and Fuerstenberg, 1999). Complex II is typically composed only of nuclear DNA-encoded subunits, with some exceptions in land plants (Roger et al., 2017; Huang et al., 2019). Although outnumbered, mtDNA-encoded proteins reside at the core of their respective OXPHOS complexes and are highly hydrophobic, membrane-embedded polypeptides (von Heijne, 1986; Popot and de Vitry,1990, Johnston and Williams, 2016). In this review, we will focus on the human genes mentioned above and their protein products, although the gene *atp9*, which is encoded in the mitochondrial genome of yeast, is briefly discussed.

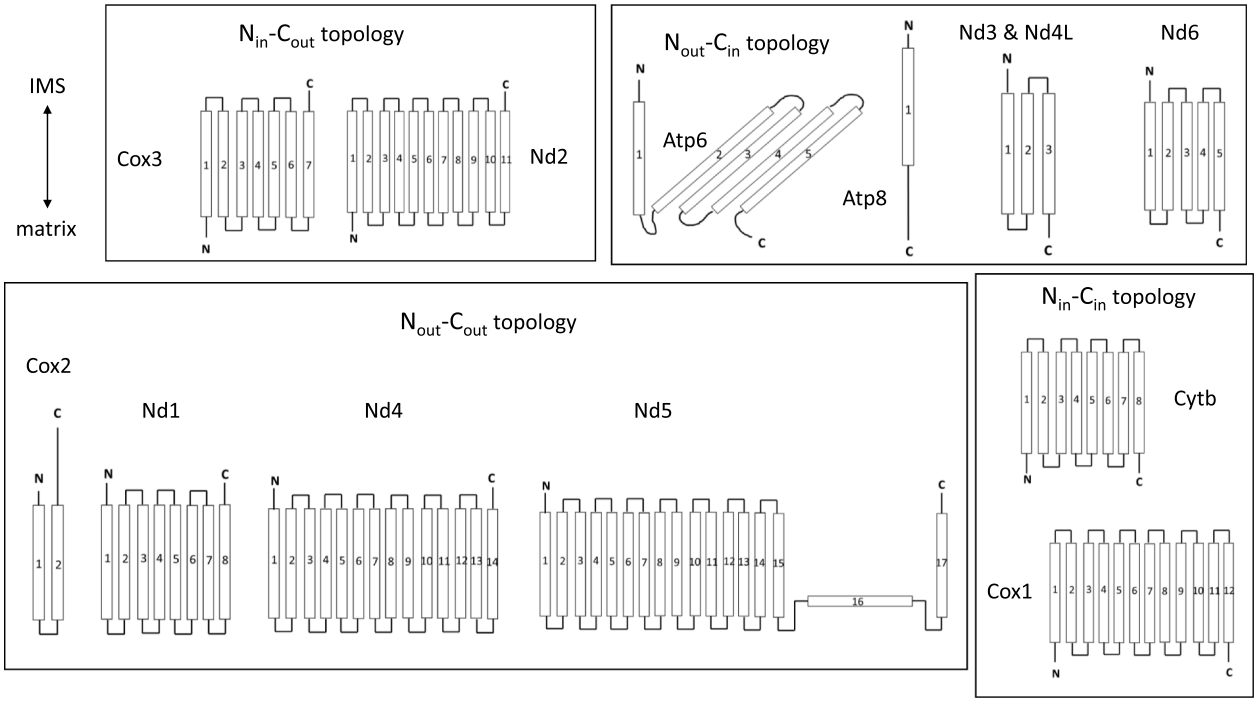

Fig. 1. The 13 human mtDNA encoded OXPHOS proteins can be classified in four different topologies.

Newly made mitochondrial polypeptides cotranslationally insert into the IMM (Dennerlein et al., 2021; Kummer and Ban, 2021), acquire prosthetic groups, and integrate into their OXPHOS complex with the aid of assembly factors (Singh et al., 2020). MtDNA-encoded subunits are synthesized by membrane-tethered mitochondrial ribosomes (mitoribosomes) and then co-translationally integrated into the IMM by Oxa1 (Oxa1L in mammals) (Bonnefoy et al., 1994; Rehling et al., 2003, Szyrach et al., 2003; Preuss et al., 2005; Ott and Herrmann, 2010; Itoh et al. 2021), an insertase belonging to a family of evolutionarily conserved membrane-embedded translocases found in bacteria and in other organelles such as the endoplasmic reticulum (ER) (McDowell et al., 2021; Güngör et al., 2022) and the chloroplasts (Wang and Dalbey, 2011). Oxa1 interacts with the N-termini of nascent polypeptides, looped segments of neighboring TMS (hairpins), and C-terminal segments of polytopic proteins (Hell et al., 2001; Szyrach et al., 2003). Human mitoribosomes are anchored to the IMM through the interaction of Oxa1L and mL45 (Mba1 in yeast), a mitoribosome subunit (Ott et al., 2006). Oxa1L also inserts proteins harboring multiple TMS, which are thought to be integrated into the membrane through hairpins (Engelman and Steitz, 1981; Herrmann et al., 1997; Herrmann and Neupert, 2003) i.e., two antiparallel, hydrophobic alpha-helices linked by a central turn. Except for Nad3 and Nad4L, all OXPHOS subunits follow a different insertion pathway into the IMM. Although details remain to be explored for each protein, we depict how the human mtDNA-encoded OXPHOS subunits may be cotranslationally inserted into the IMM, giving a representative for each of the four topological arrangements described in Fig. 1 (Suppl Figs. S1–S4).

3. Mitochondrial protein import of inner membrane proteins through TIM23

Mitochondria specialized their translocase machinery throughout evolution to allow the import of cytosol-synthesized proteins. The endosymbiont that gave rise to mitochondria probably contained core import components such as the PAM motor complex and the TOM, SAM, and OXA1 translocases at the plasma membrane, although their function was probably involved in exporting proteins (Hewitt et al., 2011; Liu et al., 2011). In addition, primitive forms of the TOM and TIM complexes, capable of importing presequence containing proteins, were most probably present in the last common ancestor of eukaryotes (Fukasawa et al., 2017).

A comprehensive description of all the import pathways of proteins targeted to mitochondrial sub-compartments and the evolution of the mitochondrial import machinery may be found in recent reviews (Pfanner et al., 2019; Grevel et al., 2020; Dimogkioka et al. 2021; Ruiz-Pesini et al., 2021; Schneider 2022). Most proteins imported into mitochondria contain an N-terminal cleavable peptide, known as mitochondrial targeting sequence (MTS), which guides them through the outer and inner membranes, and into the mitochondrial matrix. Although MTS do not have defined sequence motifs, they display some general features: they span 15–50 amino acids, tend to form positively charged, amphiphilic alpha-helices, and are rich in alanine, leucine, serine, glycine, and arginine residues, with few if any acidic residues (von Heijne et al., 1989; Chacinska et al., 2009).

MTS-containing precursors in transit to mitochondria are kept in an import-competent form by cytosolic chaperones (e.g., HSP70) and are recognized and translocated by the translocase of the outer mitochondrial membrane (TOM complex, Hartl et al., 1989; Dimogkioka et al. 2021), while others are cotranslationally imported into mitochondria (Williams et al., 2014). These precursors then cross the inner membrane through the translocase complex of the inner mitochondrial membrane, TIM23 (Callegari et al., 2020).

Proteins targeted to the IMM that lack a cleavable MTS, like the family of carriers containing six TMS, use specialized translocation machinery known as TIM22, the carrier translocase (Sirrenberg et al., 1996; Neupert, 2015; Wiedemann & Pfanner, 2017; Hansen & Herrmann, 2019; Horten et al., 2020). Aided by the membrane potential, this complex distinctively inserts multispanning, inner-membrane proteins that exhibit internal targeting signals (Rehling et al., 2004; Chacinska et al., 2009). TIM22 has a narrow, well-defined substrate repertoire (Chacinska et al., 2009): the members of the mitochondrial carrier's family with 6 TMS; the translocase components Tim23, Tim17, and Tim22 that share the same N_{out}-C_{out} topology; sideroflexins; and the Mpc2 and Mpc3 pyruvate carriers (Gomkale et al., 2020; Rampelt et al., 2020). Thus, there seems to be a clear-cut separation of protein substrates entering through TIM22 or TIM23: while TIM22 inserts hairpins of a specific group of membrane proteins in an IMS-matrix direction, TIM23 sorts MTS containing precursors (Fig. 2). Since protein import through TIM22 is not relevant to the discussion that follows, we only describe here the details of TIM23 function.

4. Mechanisms of protein sorting by TIM23 – Translocation vs. Lateral release

TIM23 exhibits the dual ability to sort TMS using either the "conservative-sorting" or the "stop-transfer" pathway (Mahlke et al., 1990; Bohnert et al. 2010) (Fig. 2). In the latter, the TMS containing a "stop-transfer" signal within their sequence stops their translocation, arrested by a TIM23 conformational state known as $TIM23^{SORT}$, which releases them laterally into the lipid phase of the IMM (Chacinska et al., 2005; van der Laan et al., 2006; 2007). In the "conservative sorting" pathway, alpha helices are fully translocated through TIM23, linked to the motor ATP-dependent presequence translocase-associated protein import motor (PAM), in a conformational state known as $TIM23^{MOTOR}$. Thus, alpha-helices get delivered into the matrix where their MTS is cleaved (by the matrix processing peptidase, MPP). If required, in a subsequent step, TMS may be inserted into the IMM by Oxa1L from the matrix side of the membrane (Omura, 1998; van der Laan et al., 2006; Mossmann et al., 2012).

Although it is not completely clear how the TIM23 complex alternates between its two distinct conformational states, incoming TMS containing stop-transfer signals will be integrated into the IMM (Glick et al., 1992). Hydrophobicity and the location of polar and aromatic residues are strong determinants of the fore-mentioned membrane insertion pathway. Alpha helices with low hydrophobicity and carrying one or more prolines, are prone to be fully translocated by $TIM23^{MOTOR}$. In contrast, TMS exhibiting high average hydrophobicity, low or null proline content, and having positively charged residues (Arg, Lys) flanking the alpha-helix (mainly on the matrix side), tend to be arrested and released laterally by $TIM23^{SORT}$ (Meier et al., 2005; Botelho et al., 2011; Osterberg et al., 2011; Lee et al., 2020). In yeast, Tim23 interacts with the Mgr2 subunit (ROMO1 in humans), which functions as a lateral gatekeeper providing quality control while binding the Tim21 subunit forming all together the $TIM23^{SORT}$ arrangement (Gebert et al., 2012; Matta et al., 2020; Richter et al. 2019; Needs et al., 2021). Since Mgr2 monitors the hydrophobicity of transiting alpha-helices, *mgr2*-null yeast strains display increased lateral release of proteins by $TIM23^{SORT}$ to the IMM (Ieva et al., 2014). Conservative sorting and stop-transfer are not mutually exclusive pathways, they represent mechanisms that may cooperate in the membrane integration of a protein (Bohnert et al., 2010). Although structurally different, $TIM23^{SORT}$ and $TIM23^{MOTOR}$ are in dynamic exchange during precursor translocation and sorting (Chacinska et al., 2010).

Pioneer work revealed that TIM23 behaves as a voltage-gated channel with an estimated diameter of 13 Å (Schwartz and Matouschek 1999; Truscott et al. 2001). An NMR-derived structure revealed dimeric Tim23 forms a pore with a width of ~12 Å at its narrowest, and ~22 Å at its widest (Zhou et al., 2020). More recently, a cryo-EM structure at 2.9 Å resolution of the yeast core TIM23 complex (formed by subunits Tim17, Tim23 and Tim44) shows that Tim23 and Tim17 do not form a water-filled channel (Sim et al., 2023). Instead, these two subunits interact back-to-back, and exhibit separate, membrane-exposed

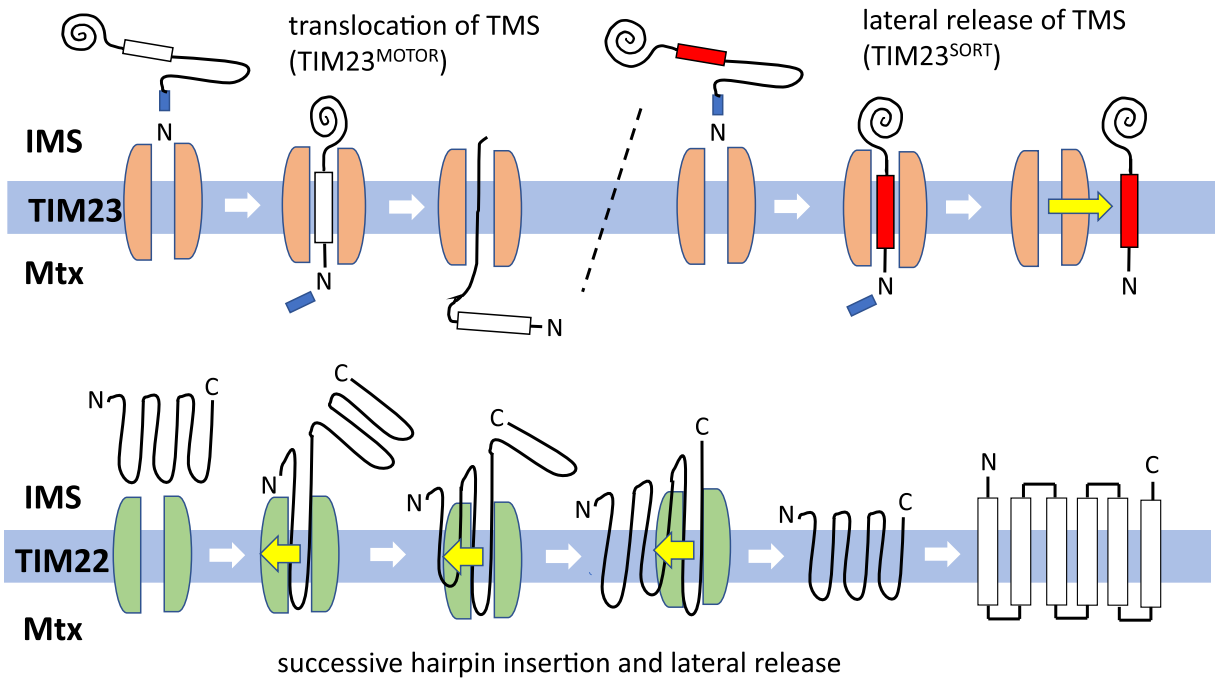

Fig. 2. Protein import mechanisms of the IMM translocators TIM23 and TIM22. For simplicity, the Outer Mitochondrial Membrane is not depicted. Top: TIM23 (pink) exhibits the dual ability to distribute proteins into two different pathways. When following the "conservative sorting" pathway, alpha-helices of relatively low hydrophobicity (white) are translocated by the $TIM23^{MOTOR}$ into the matrix. By contrast, when following the "stop-transfer" pathway, highly hydrophobic alpha-helices (red) usually lacking prolines and flanked by positively charged amino acids in their matrix-exposed end, are arrested by $TIM23^{SORT}$ and released laterally into the IMM. Bottom: the TIM22 complex (green) inserts successively hairpins composed of a pair of TMS into the IMM. Although not exclusively, TIM22 is the main import system for carrier proteins containing six TMS. The mitochondrial inner membrane is represented in light blue. IMS: intermembrane space; Mtx: matrix. N and C termini of protein substrates are indicated, and the blue rectangle indicates the mitochondrial targeting sequence that is cleaved by the matrix peptidase (top panel).

concave cavities that are facing away from each other. Crosslinking experiments suggest that Tim23 probably plays a structural role, while protein translocation occurs through the Tim17 cavity, which appears to be in close contact with the Mgr2 subunit. A cryo-EM structure of another TIM23 subcomplex (formed by subunits Tim17, Tim23 and Mgr2) revealed how Tim23 and Mgr2 shield the polypeptide substrates from the lipid environment (Zhou et al., 2023). Furthermore, both recent 3D structures suggest that the cavity formed by Tim17 is highly conserved, exhibiting a patch of negatively charged residues at the entrance (close to the IMS) and a 10–15 Å long hydrophobic patch in the middle of the translocation pathway (Sim et al., 2023; Zhou et al., 2023). Altogether this novel structural data, along with previous biochemical results (Rehling et al., 2004), strongly indicate that TIM23 handles the translocation of a single TM at a given time.

5. Mitochondrial diseases and their therapeutics

Mitochondrial diseases are prevalent genetic disorders characterized by defects in OXPHOS (La Morgia et al., 2020; Gorman et al., 2016). These diseases can result from mutations in either the nuclear or mitochondrial genomes, with mtDNA mutations accounting for approximately 75 % of the cases in adults and 25 % in children. The nuclear DNA mutations that cause mitochondrial dysfunction (Gorman et al., 2016) are not addressed here. Most patients with mitochondrial diseases harbor heteroplasmic mtDNA mutations, where both mutant and wild type mtDNA versions coexist. The disease phenotype is manifested when the ratio of mutant versus wild type mtDNA copies exceed a certain threshold that depends on the type of mutation, the tissue, and the patient (Russell et al., 2020). Over 300 pathogenic mtDNA mutations have been reported in the well-curated MITOMAP database (https://www.mitomap.org).

Mitochondrial diseases exhibit heterogeneous clinical symptoms and tissue-specificity but typically affect multiple organ systems. The link between a mitochondrial mutation and its pathophysiology is not well understood. Tissues with high energy demands, such as nerves and muscles, are often the most affected. Clinical syndromes range from the muscle disorder Progressive External Ophthalmoplegia (PEO) to multisystemic syndromes such as Myoclonus Epilepsy with Ragged-Red Fibers (MERRF) and Mitochondrial Myopathy, Encephalopathy, Lactic Acidosis, and Stroke-like episodes (MELAS). Leber Hereditary Optic Neuropathy (LHON) is a maternally inherited mitochondrial disorder that affects retinal ganglion cells, causing visual impairment and potential blindness (Carelli et al., 2004). Over the 19 mtDNA mutations associated with LHON, the three most prevalent (G3460A in Nd1, G11778A in Nd4 and T14484C in Nd6) affect subunits of complex I (Wallace et al., 1988; Howell et al., 1991; Jun et al., 1994).

MtDNA mutations fall into three categories: mutations in protein-encoding genes, mutations in structural RNAs (tRNAs and rRNAs), and large-scale mtDNA rearrangements (deletions or duplications). Here, we focus on the 13 genes encoding OXPHOS proteins for which mutations result in severe mitochondrial diseases that currently lack effective treatments. While direct manipulation of human mtDNA is still in development, other strategies for mitochondrial disease therapies have been put forward (DiMauro et al., 2006; Wallace, 2018; Russell et al., 2020; Ng et al., 2021), including mitochondrial delivery of nucleic acids, manipulation of mtDNA heteroplasmy, direct mtDNA editing, and allotopic expression (Di Donfrancesco et al., 2022).

Mitochondrial delivery of nucleic acids involves the use of an adenoassociated virus capsid VP2 fused to an MTS (Yu et al., 2012) or the generation of mitochondrial-targeted transcripts produced in the cytosol and competent in protein translation inside the mitochondrial matrix (Wang et al., 2015). This approach was successfully tested in *Drosophila melanogaster* with the Atp6 subunit encoding transcript (Markantone et al., 2018). Future approaches involve silencing of mitochondrial

translation by importing precursor-morpholino hybrids that could target individual mRNAs at the mitochondrial matrix (Cruz-Zaragoza et al., 2021). Another strategy for manipulating mtDNA heteroplasmy involves the targeted elimination of mutated mtDNA copies using nucleases (Srivastava and Moraes 2001; Bacman and Moraes, 2007; Alexeyev et al., 2008; Xu et al., 2008; Bacman et al., 2013; Gammage et al., 2014; Hashimoto et al, 2015; Bacman et al., 2018; Barrera-Paez and Moraes, 2022). CRISPR-based methods have been used to edit mtDNA (Hussain et al., 2021), although they remain to be substantiated by other studies (Gammage et al., 2018). In addition, advances have been achieved with CRISPR-free mitochondrial base editing of cytosines (Mok et al., 2020; Chen et al., 2022; Nakazato et al., 2022), although this alternative approach also induces undesirable editions in the nuclear genome (Lei et al., 2022). Even though all these approaches show promise, they are still in early stages of development and have not reached mainstream use in gene therapies. Here, we concentrate on allotopic expression, i.e., overcoming mutations in mtDNA-encoded proteins by introducing a wild-type copy of the affected gene in the nucleus and targeting the corresponding cytosol-synthesized protein to mitochondria, thus replacing the defective mitochondrial counterpart (de Grey, 2000; Zullo, 2001; González-Halphen et al., 2004; DiMauro et al., 2006; Kyriakouli et al., 2008).

6. Allotopic expression

Allotopic expression is a strategy to reroute the biogenesis and intracellular transport of a protein (Nagley and Devenish,1989), thus involving the functional activation of an organellar gene in the nucleus (de Grey, 2000). Allotopic expression as therapeutics is intended to overcome mutations in mtDNA-encoded proteins, by placing a modified wild-type copy of the affected gene in the nucleus. If successful, the corresponding protein product can reach the mitochondrion, thereby replacing its dysfunctional counterpart. To achieve this, changes in codon usage must be considered. While the UGA codon is interpreted as tryptophan in mitochondria, it is a termination codon in the nucleus (Macino et al., 1979). Likewise, the AUA codon directs the incorporation of methionine in mitochondria but isoleucine in the nucleus (Takemoto et al., 2009). Prior pioneering research on allotopic expression was carried out in baker's yeast using mitochondrial genes encoding soluble proteins. The first example involved a nuclear version of a cytochrome *b* gene intron encoding the soluble mitochondrial bI4 maturase, which was able to restore respiratory competence to a strain defective in the mtDNA-encoded version of the maturase protein (Banroques et al., 1986; 1987). A similar approach was used in yeast for the soluble Var1 protein, a subunit of the mitoribosome encoded in a mitochondrial gene (Sanchirico et al. 1995). In the plant *Nicotiana sylvestris,* another successful allotopic production of a soluble protein was achieved by targeting the cytosol-synthesized subunit Nd7 (subunit 7 of complex I) to its mitochondrion. Such expression restored complex I biosynthesis in plants lacking a functional mitochondrial *nd7* gene (Pineau et al., 2005). Allotopic expression of genes encoding soluble proteins can be considered trivial, since it is usually achieved after codon optimization and the addition of a sequence encoding an adequate MTS. Undeniably, attempts to direct cytosol-synthesized membrane-bound proteins to mitochondria represents a more significant challenge. A successful allotopic expression requires that the cytosol-synthesized membrane protein gets internalized into mitochondria, inserted in the IMM in its correct topology, and functionally assembled within its corresponding OXPHOS complex. Before describing the specific strategies to achieve allotopic expression in different experimental systems, we discuss examples of mitochondrial genes, encoding membrane proteins, which have been transferred to the nucleus in nature.

7. Examples of mitochondrial gene transfer to the nucleus

Several hypotheses on why mitochondria have retained a genome have been formulated (Daley and Whelan, 2005; Wang, 2012; Allen, 2015). One pioneering hypothesis suggested that, since the protein export machinery of the ER was already in existence when mitochondria appeared, only those genes whose protein products were not highly hydrophobic could have been successfully transferred to the nucleus (von Heijne, 1986). Indeed, hydrophobic stretches, especially those located at the N-terminus of proteins, act as export signals because they are recognized by the Signal Recognition Particle (SRP) and target the protein to the ER (Björkholm et al., 2015). As demonstrated by selective ribosome profiling experiments carried out in *Escherichia coli*, SRP sometimes fails to bind the first TMS and binds instead a TMS located more closely to the C-terminus of the nascent protein. When this happens, the second TMS tends to exhibit a higher hydrophobicity (i.e., a more negative Gibbs free energy difference of membrane insertion ΔG_{app}) (Schibich et al., 2016). So even when the N-terminal TMS is skipped, there will be another one recognized by SRP more internally, and at the end SRP will triage the protein to the ER. Experimental support for the hypothesis that cytosol-synthesized mitochondrial proteins may be mis-targeted to the ER via the SRP was provided with the finding that synthesis of all 13 human mitochondrial-encoded OXPHOS subunits with strong mitochondrial-targeting sequences in the cytosol of human cells, resulted in their transport to the ER, except for Atp8 (Björkholm et al., 2015). Thus, the hydrophobicity of the TMS in the mitochondrial proteins was hypothesized to be a critical limiting factor. In general, mitochondrial proteins whose genes have been relocated to the nucleus exhibit a diminished average hydrophobicity relative to their mtDNA-encoded counterparts (Funes et al., 2002a). A diminished hydrophobicity of proteins synthesized in the cytosol and destined to mitochondria may be a key feature to avoid misrouting to the ER and enable the internalization in the mitochondria (Claros et al., 1995; Daley et al., 2002a,2002b; González-Halphen et al., 2004; Cardol et al., 2006).

In some organisms, mitochondrial genes encoding membrane proteins have been transferred to the nucleus. For example, the genes *atp6*, *cox2*, *cox3, nd3,* and *nd4L*, are absent in the mtDNA of *Chlamydomonas reinhardtii* and related algae (Vahrenholz et al., 1993; Denovan-Wright et al., 1998; Fan and Lee, 2002), and have been functionally relocated to the nucleus. Their corresponding protein products are synthesized by cytosolic ribosomes, post-translationally or co-translationally imported into mitochondria, and functionally assembled into the appropriate OXPHOS complex (Pérez-Martínez et al., 2000; Pérez-Martínez et al., 2001; Funes et al., 2002a). Through evolutionary time the transferred genes have undergone extensive sequence modification to become functional, including mutagenesis, capture of introns, promoters, 5′ and 3′ UTRs, and nucleotide sequences encoding MTS. Addition of MTS may occur by duplication of already existing targeting sequences in instances where functional transfer has already taken place (Kadowaki et al., 1996). In certain lineages the acquired MTS are atypically long, ranging from 100 to 140 residues (Pérez-Martínez et al., 2002; González-Halphen et al., 2004). These long MTS could either promote the binding of precursors to the mitochondrial import machinery or facilitate protein unfolding to enhance its importability (Claros and Vincens, 1996; Claros et al., 1995). When the import rates of artificial precursors containing MTS of varying lengths were measured, it was found that the unfolding of a precursor at the mitochondrial surface is accelerated if the MTS is long enough to span both the OMM and the IMM, enabling the MTS to interact with mtHsp70 in the mitochondrial matrix (Matouschek et al., 1997). Moreover, the synergy between two distinct alpha-helices in a long MTS may stimulate the internalization of some precursors, as demonstrated for the mammalian glutamate dehydrogenase (Kalef-Ezra et al., 2016). In the sections below, we describe examples of natural gene transfer of genes encoding OXPHOS subunits in different organisms.

7.1. The atp6 gene

A gene that is mtDNA-localized in almost all eukaryotic taxa is *atp6*, which encodes subunit 6 of F_1F_o-ATP synthase (Atp6 or subunit a).

Prominent exceptions are found in the malarial parasite *Plasmodium* and the ciliates *Tetrahymena* and *Paramecium*, where the *ATP6* gene is localized in the nucleus (Feagin et al., 1992; Pritchard et al., 1990).

The chlorophycean green alga *Chlamydomonas reinhardtii* also has a nucleus encoded *ATP6* gene (Funes et al., 2002a). The Atp6 precursor with a large MTS of 107 amino acids is synthesized in the cytosol. The algal Atp6 subunit differs from its bovine homolog in that it lacks the first TMS, as observed when comparing the 3D structures of both proteins (Spikes et al., 2021; Murphy et al., 2019) (Suppl Fig. 5). In mammals, Atp6 is mitochondria-synthesized and has five TMS, the first of which is proposed to be cotranslationally inserted into the IMM, followed by the subsequent insertion of two hairpins (Suppl Fig. 1), a process most probably mediated by the Oxa1 insertase. In contrast, during the biogenesis of a cytosol synthesized, algal Atp6 subunit, it is proposed that four TMS are fully translocated into the matrix using $TIM23^{MOTOR}$. Once inside, they are embedded in the IMM as two hairpins via an Oxa1-dependent process (Suppl Fig. 6). It is assumed that the lack of TMS1 in the algal cytosol synthesized Atp6 subunit may facilitate its import into mitochondria.

Subunit *a* (ATP6) is also encoded in the nuclear genome of the apicomplexan parasite *Toxoplasma gondii* (Mühleip et al., 2021). In most eukaryotes, Atp6 typically exhibits a structure with six helices. However, in the case of *T. gondii*, this subunit is distinct, since it lacks helices 1–4 (aH1-4), as revealed by its 3D structure (Suppl Fig 5). Only the helices aH5 and aH6 were found to interact with the *c*-ring (an oligomer of Atp9 subunits), which serves as one of the rotary components in all ATP synthases. The absence of helices 1–4 appears to be compensated by the independent subunits ATPTG16 and ATPG17. Consequently, *T. gondii* Atp6 exhibits a simplified structure with only two TMS. This structural divergence may explain why the cytosol synthesized Atp6 subunit of this parasite can be imported into the mitochondria. Split ATP6 subunits have been also identified in *Trypanosoma brucei* and in other members of the Euglenozoa lineage (Wong et al., 2023).

7.2. The atp8 gene

The *atp8* gene usually resides in the mtDNA, although some exceptions have been reported. The absence of *atp8* is common in rotifers, commonly called wheel animals (Nie et al., 2016). Although the *atp8* gene was originally thought to be absent in some bivalve species, this may not be the case (Breton et al., 2010). In addition, *atp8* seems to be absent from the mtDNA of the chlorarachniophyte alga *Lotharella oceanica* as well, albeit not detected in the nuclear genome either (Tanifuji et al., 2016). In parasitic red algae, the *atp8* gene has either become a pseudogene or disappeared completely from the mtDNA (Hancock et al., 2010). In general, *atp8* may be absent from the mitochondrial genomes because it has migrated to the nucleus or because its encoded protein is no longer a constituent of mitochondrial ATP synthase (i.e., the enzymes from chlorophycean algae typically lack the Atp8 subunit). Nevertheless, to the best of our knowledge, no *atp8* gene that was functionally transferred to the nucleus has been reported.

7.3. The cox1 gene

The *cox1* gene seems to be invariably located in the mtDNA. However, in some organisms, a small fragment of the gene has been transferred to the nucleus. In the amoeboid *Acanthamoeba castellanii* and some other protists, a small, hydrophilic C-terminal portion of Cox1 of only 36 residues, lacking a TMS, has been found to be encoded in the nucleus. The mtDNA-encoded hydrophobic Cox1 large fragment retaining 12 TMS, lacks this C-terminus, but is still encoded in mtDNA (Gawryluk and Gray, 2010). Thus, at some point in evolution, the protist mitochondrial *cox1* gene was fragmented, with the nucleotide sequence encoding the C-terminus of Cox1 functionally integrated into the nuclear genome. This example shows that hydrophobicity limits the transfer of mitochondrial genes to the nucleus, as only the gene encoding the hydrophilic part of Cox1 was successfully relocated.

7.4. The cox2 gene

The Cox2 subunit is usually synthesized in the mitochondrial matrix, (Suppl Fig 2) and embedded in the IMM by the concerted action of the Oxa1 insertase (He and Fox, 1997) and the peripheral IMM protein Mss2 (Broadley et al., 2001). In some species, the *cox2* gene has been transferred to the nucleus, either as a full-length gene (as in leguminous plants) or as a split gene (*COX2A* and *COX2B* in green algae and apicomplexan parasites) (Nugent and Palmer, 1991; Covello et al., 1992; Adams et al., 1999; Pérez-Martínez et al., 2001; Gardner et al., 2002; Funes et al., 2002b). Legumes provide an illustrative example that gene transfer from mitochondria to the nucleus is still occurring. While many species in this clade contain orthodox, mitochondrial *cox2* genes, others show nucleus-localized *cox2* genes, and yet others possess both the mitochondrial and the nuclear versions of the gene (Adams et al., 1999). While in certain instances only one of the versions is active, in others both the nuclear and mitochondrial copies are expressed, strongly suggesting that transfer of mitochondrial genes to the nucleus is an ongoing evolutionary process.

In several chlorophycean algae, the mitochondrial *cox2* gene underwent a fragmentation event, giving rise to the *COX2A* and *COX2B* genes (encoding the hydrophobic domain of Cox2 with its two TMS, and the hydrophilic domain that binds the binuclear copper center, respectively). In some of these green algae, like *Scenedesmus obliquus*, the *cox2a* gene was retained in the mtDNA, while the *COX2B* migrated to the nucleus. In other algal species, like *C. reinhardtii*, *Volvox carteri*, and *Polytomella parva*, both genes were relocated to the nucleus and integrated into different chromosomes (Pérez-Martínez et al., 2001). A similar split in *COX2A* and *COX2B* genes has also been described in apicomplexan parasites (Funes et al., 2002a), and the genes were found to be present in the nuclear genome. All examples of natural, cytosol synthesized Cox2 subunits, i.e., in legumes, chlorophycean algae, and apicomplexan parasites, exhibit low hydrophobicity in their TMS1 and a slightly increased hydrophobicity in their TMS2. Thus, it is suggested that TIM23 may allow the transit of TMS1 toward the matrix (through the conservative sorting pathway) while retaining TMS2 and subsequently releasing it laterally into the IMM (through the stop-transfer pathway) (Daley et al. 2002a; Jiménez-Suárez et al. 2012; Rubalcava-Gracia et al., 2018). The proposed mechanism is the only one that provides a suitable explanation as to why the cytosol-synthesized Cox2 acquires the same final topology as its mitochondria-synthesized counterpart, with both its N- and C-termini exposed to the IMS (Fig. 1 and Suppl Fig. S2).

7.5. The cox3 gene

In several chlorophycean species, closely related to the green alga Chlamydomonas, the *cox3* gene is absent from the mtDNA (Vahrenholz et al., 1993; Denovan-Wright et al., 1998; Fan and Lee, 2002) and resides in the nucleus instead (Pérez-Martínez et al., 2000, 2001, 2002; Watanabe and Ohama, 2001; Merchant et al., 2007; Prochnik et al., 2010). Therefore, the algal Cox3 subunit is synthesized in the cytosol as a precursor containing an unusually large MTS of 98 residues that directs it to mitochondria, where it gets internalized, and functionally assembled into cytochrome *c* oxidase. The mature Cox3 subunit, lacking its MTS, is present in the isolated complex IV of the chlorophycean alga *Polytomella* sp. (Pérez-Martínez et al., 2000). Since Cox3 is a component of the catalytic core of cytochrome oxidase, the knock-down of the nuclear *COX3* gene leads to loss of complex IV assembly, as demonstrated in *C. reinhardtii* (Remacle et al., 2010). *In vitro* experiments have shown that the Cox3 precursor is also readily internalized in isolated *Polytomella* mitochondria and assembled into cytochrome *c* oxidase (Vázquez-Acevedo et al., 2014). In ciliates, for a long time it was considered that their mtDNA did not contain a *cox3* gene, but upon re-

examination it was found that the gene was present but fused to a *cox1* gene that has undergone many variations in its sequence (Degli Esposti et al, 2014).

7.6. The nd3 and nd4L genes

The *ND3 and ND4L* genes are localized in the nucleus in *Chlamydomonas* and other closely related chlorophycean algae. The Nd3 and Nd4L subunits, exhibiting three TMS each, are synthesized in the cytosol as precursors containing MTS of 160 and 130 residues respectively. Both polypeptides show lower hydrophobicity compared to their mitochondrion-encoded counterparts found in other organisms (Cardol et al., 2006). These subunits are eventually processed by the MPP in the mitochondrial matrix, giving rise to the mature subunits that will ultimately integrate into complex I.

7.7. The nd4, nd5 and nd6 genes

To the best of our knowledge, no report of nucleus encoded Nd4, Nd5, and Nd6 exists. This is scarcely surprising, considering the number of TMS in these subunits and their overall high hydrophobicity.

8. Which cytosol synthesized OXPHOS proteins may integrate and reach their correct topology in the IMM? The $\mu\Delta G_{app}$ of each TMS may be the limiting factor

To date, all designs of OXPHOS subunits allotopically produced for import into mitochondria include adding an MTS, since these engineered precursors are expected to be sorted by the TIM23 translocon. As discussed above, a large core of data suggests that TIM23 manages a single alpha-helix at a time, which can either be fully translocated into the matrix or arrested and then released laterally into the IMM. Thus, the average hydrophobicity must be a key parameter that determines through which pathway (conservative or stop-transfer) TIM23 directs a given alpha-helix in an imported protein substrate. To quantify how the hydrophobicity of each alpha-helix governs the insertion of membrane proteins by TIM23, Botelho et al., (2011) took advantage of the nucleus-encoded yeast Mgm1, a membrane protein with two TMS (TMS1 and TMS2) that exhibits an alternative topogenesis and produces two isoforms (large and small). Upon import of the Mgm1 precursor into the mitochondria, TIM23 may laterally release TMS1 into the IMM, giving rise to the large isoform of Mgm1 which remains membrane bound. Alternatively, TMS1 is translocated into the matrix and TMS2 is laterally released into the IMM, where it will be proteolytically processed, giving rise to the small isoform of Mgm1, which will remain as a soluble protein in the IMS (Herlan et al., 2003). For a given population of cytosol synthesized Mgm1 precursors, a mixture of membrane-anchored and soluble isoforms will be formed, where nearly 30–40 % will represent the large isoform of Mgm1 (Botelho et al., 2013). Both isoforms can be resolved according to their different apparent molecular masses in denaturing electrophoresis (SDS-PAGE). By replacing the single TMS of Mgm1 with sequences of varying hydrophobicity, followed by quantification of the ratios of the two Mgm1 isoforms, an apparent free energy of membrane insertion ΔG^{X}_{app} was estimated for each of the 20 amino acids. Thus, for yeast mitochondria, a "biological scale" was constructed, providing ΔG^{X}_{app} values for each residue, ranging from −0.20 (leucine, highly hydrophobic) to +3.01 kcal/mol (arginine, highly hydrophilic). Making use of this tool, the average apparent free energy of membrane insertion $\mu\Delta G_{app}$ can be estimated for any TMS based on its amino acid composition and used as a prediction for TIM23-dependent translocation into the matrix or arrest and lateral release into the IMM.

Table1 lists the calculated $\mu\Delta G_{app}$ values for the TMS of three proteins that are known to be in this threshold scenario: the TMS1 of the yeast Mgm1 protein (Botelho et al., 2013); the TMS1 of the yeast Cox2 subunit (Supekova et al., 2010); and the TMS1 of soybean Cox2 subunit (Daley et al., 2002a). Based on Table 1, we can predict that TMS with $\mu\Delta G_{app}$ values below 0.54 kcal/mol will probably be arrested and released laterally by TIM23, those with $\mu\Delta G_{app}$ values above 0.62 kcal/mol will probably be translocated, and those with $\mu\Delta G_{app}$ values between 0.54 and 0.62 kcal/mol are in a threshold zone and can be either translocated or arrested like the TMS1 in Mgm1. For simplicity, we developed a "traffic-light" color code for each TMS, intended to graphically illustrate which one may be fully transferred (green light), which ones will be presumably arrested and released laterally (red light), and the ones which are in the threshold zone (yellow-light) (Fig. 3). It must be underscored that besides this "traffic-light" color, the choice of pathway through which each alpha-helix in the TMS will be directed does not depend exclusively on its hydrophobicity, but also on other determinants such as its proline content and the presence/absence of charged residues flanking the TMS. Here, we used the biological scale to estimate the $\mu\Delta G_{app}$ values of all TMS present in the 13 mitochondria encoded OXPHOS proteins (Suppl Table S1) and of all the naturally nucleus encoded, membrane-embedded subunits of complexes I, III, IV and V (Suppl Table S2). All 13 mitochondria encoded OXPHOS proteins were found to contain from 1 to 15 "red light" TMS in their sequence (Fig. 4). This result indicates that if allotopically produced, the transfer into the matrix through TIM23 will be hampered and ultimately impede that the proteins reach their final, functional topology. In sharp contrast, the 34 naturally occurring, nucleus-encoded, membrane-embedded subunits of OXPHOS complexes exhibit mainly "green light" TMS, and few of them "red" or "yellow light" (Suppl Table S2). Altogether, the data suggest that the TMS of the nucleus encoded subunits are on average less hydrophobic than the TMS of their mitochondria encoded counterparts (Fig. 3). Although the traffic-light color is a good predictor of the feasibility of TIM23 to sort a given TMS, it reveals some outliers. Of the six nucleus-encoded proteins exhibiting TMS with "red lights", four consist either of a sole TMS or harbor the TMS exhibiting high hydrophobicity as the last one. Conceivably, such TMS would not pose challenge for their insertion into the membrane. The two remaining proteins, have two predicted arrested TMS indicating that our prediction is not absolute. Alternatively, it is possible that these proteins rely on specialized factors that could facilitate their insertion. As illustrated in Fig. 5, the $\mu\Delta G_{app}$ of each TMS must be considered when designing a

Table 1
$\mu\Delta G_{app}$ values for TMS that are in the threshold of being either translocated by TIM23 or arrested and released laterally.

SOURCE	PROTEIN	SEQUENCE OF TMS1	$\mu\Delta G_{app}$ (kcal/mol)	TRAFFIC LIGHT
YEAST	nu Mgm1 (CAA99426.1)	**IISKIIRLPIYVGGGMAAAGSYIAYKM**	0.61	*TRANSLOCATED 40 %*
YEAST	mt Cox2 (NP_009326.1)	**GILELHDNIMFYLLVILGLVSWMLYTIVMTYS**	**0.51**	**ARRESTED**
YEAST	Allotopic Cox2 (W56R mutant)	**GILELHDNIMFYLLVILGLVSRMLYTIVMTYS**	0.57	*TRANSLOCATED*
SOYBEAN	mt Cox2 (NP_001276209.2)	**MMQGIIDLHHDIFFFLILILVFVSWILVRALWHF**	**0.53**	**ARRESTED**
SOYBEAN	nu Cox2 (YP_007516925.1)	**IMQGIIDLHHDIFFFVIQIGVFVSWVLLRALWHF**	0.63	*TRANSLOCATED*
SOYBEAN	Allotopic Cox2 (L169Q/L171G mutant)	**MMQGIIDLHHDIFFFLIQIGVFVSWILVRALWHF**	0.62	*TRANSLOCATED*

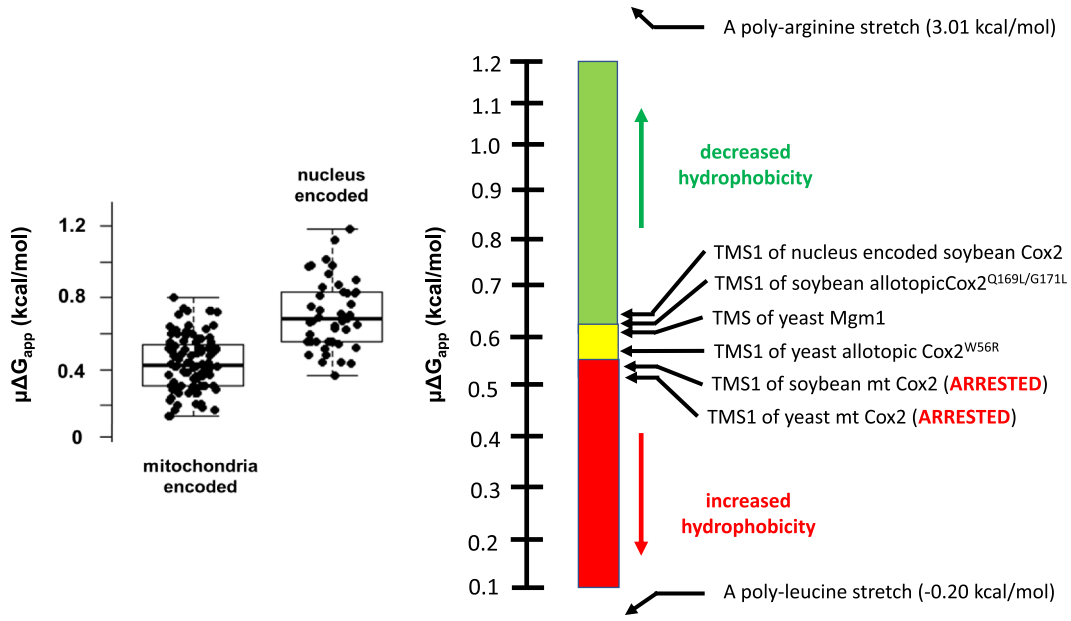

Fig. 3. $\mu\Delta G_{app}$ values for TMS of membrane embedded OXPHOS proteins. The $\mu\Delta G_{app}$ values of various TMS were calculated using the biological scale (Botelho et al., 2011). Boxplots on the left show $\mu\Delta G_{app}$ values for all the TMS of OXPHOS subunits listed on Suppl Table 1 (mitochondria-encoded) and Suppl Table 2 (nucleus-encoded). TMS from mitochondrial encoded subunits exhibit $\mu\Delta G_{app}$ values between 0.14 and 0.80 kcal/mol, with a mean value of 0.44, a median of 0.43 and a mode of 0.31 kcal/mol. In contrast, the TMS from nucleus encoded OXPHOS components tend to be less hydrophobic, exhibiting $\mu\Delta G_{app}$ values between 0.36 and 1.2 kcal/mol, with a mean of 0.70, a median of 0.68 and a mode of 0.55 kcal/mol. Shown on the right is an expanded view of the same biological scale. The upper limit with an $\mu\Delta G_{app}$ value of 3.01 kcal/mol, corresponds to a highly hydrophilic stretch of arginines, whereas the lower limit with an $\mu\Delta G_{app}$ value of −0.20 kcal/mol would represent a highly hydrophobic stretch of leucines. Based on their calculated $\mu\Delta G_{app}$ values, TMS were assigned a "traffic light" color: red, for highly hydrophobic ($\mu\Delta G_{app}$ values below 0.54 kcal/mol), yellow for moderately hydrophobic ($\mu\Delta G_{app}$ values between 0.54 and 0.62 kcal/mol) and green for marginally hydrophobic or highly hydrophilic ($\mu\Delta G_{app}$ values above 0.62 kcal/mol). Arrows indicate $\mu\Delta G_{app}$ values for the single TMS of Mgm1, TMS1 of the wild-type yeast Cox2 subunit, TMS1 of the yeast $Cox2^{W56R}$ subunit variant, TMS1 of the wild-type soybean Cox2 subunits (mitochondria and nucleus encoded) and TMS1 of the soybean $Cox2^{Q169L/G171L}$ subunit variant. Boxplots were built using the R graphics package (version 4.1.0, Vienna, Austria) (R Core Team, 2021).

protein precursor that will be allotopically synthesized.

Our rationale here assumes that the biological scale of Botelho, experimentally determined for yeast mitochondria, also applies to mitochondria from other eukaryotes (note for example, that the $\mu\Delta G_{app}$ values for TMS1 of the wild-type and mutant yeast Cox2 are very similar to the ones of soybean Cox2, as shown in Table 1). Our demonstration that mimicking the naturally occurring mutations that lower the hydrophobicity of soybean Cox2 in its yeast counterpart allows the allotopic expression of Cox2, suggest that $\mu\Delta G_{app}$ extends to mitochondria in other organisms (Rubalcava-Gracia et al. 2019). However, this case may not be generalized, and further experimentation is required considering the variation from organism to organism. For example, the yeast m-AAA protease, that is known to dislocate substrate proteins from the IMM (Korbel et al., 2004), can modulate the threshold hydrophobicity of a given hydrophobic segment being translocated through TIM23. Thus, the pulling force exerted by the m-AAA protease during protein biogenesis may determine whether a hydrophobic segment will form a TMS in the IMM or not (Botelho et al., 2013).

9. Allotopic expression of human OXPHOS related genes

Allotopic expression is considered as one of the promising strategies to develop gene therapies for diseases linked to mtDNA mutations in protein-encoding genes (Zullo, 2001; González-Halphen et al., 2004; DiMauro et al., 2006; Kyriakouli et al., 2008; Scarpelli et al., 2010; Cwerman-Thibault et al., 2010; Tischner and Wenz 2015). To date, all reports of allotopic expression in human cells share two minimal requirements: *i)* the recoding of mitochondrial genes to mirror the genetic code and the codon bias of nuclear genes (Lewis et al., 2020) and *ii)* the addition of a nucleotide sequence encoding an MTS, usually from a precursor protein already known to be targeted to mitochondria (Artika, 2019). In principle, these two modifications should suffice to successfully target, import, and restore OXPHOS activity by any gene expressed allotopically (Gearing and Nagley, 1986; Manfredi et al., 2002; Bonnet et al., 2007; Ojaimi et al., 2002). The choice of an adequate MTS sequence is relatively simple, i.e., the fusion of the MTS of either the beta subunit of ATP synthase (Atp2), the iron-sulfur Rieske protein (ISP) of complex III, or subunit IV of cytochrome *c* oxidase (Cox4) were sufficient to provide access to the allotopically produced bacteriorhodopsin of the archaeon *Halobacterium salinarum* into the mitochondria of the yeast *Schizosaccharomyces pombe* (Hoffmann et al., 1994). In other cases, MTS duplication may increase import efficiency (Galanis et al.,1991; Chin et al., 2018). The addition of untranslated regions, e.g., a 3′-UTR sequence, has been considered as a parameter to enhance allotopic expression (Kaltimbacher et al. 2006). However, an unbiased screening comparing a wide variety of 3′-UTR sequences has shown that their role is not as critical as that of the MTS (Chin et al., 2018).

Here, we underscore the concept that the key constraint for the allotopic expression of a given mitochondrial gene is the hydrophobicity of its encoded protein precursor. There is a large body of evidence suggesting that the high hydrophobic nature of the proteins whose final destination is the IMM hinders the functional, nuclear relocalization of their cognate mitochondrial genes, either by natural gene transfer or by experimental design (Popot & de Vitry 1990; Claros et al. 1995; Claros & Vincens 1996; Adams & Palmer 2003; Ojaimi et al. 2002; Daley et al., 2002; Oca-Cossio et al. 2003; González-Halphen et al. 2004; Figueroa-Martínez et al. 2011; Neupert 2015; Björkholm et al. 2015; Johnston & Williams 2016). As shown in some instances, increasing the $\mu\Delta G_{app}$ (which indicates a decrease of the hydrophobicity) of certain TMS may facilitate the import of proteins into mitochondria (Claros et al., 1995; González-Halphen et al., 2004). Indeed, changing one or two residues in the Cox2 protein was shown to be sufficient to allow its *in vivo* import in yeast (Supekova et al., 2010) or its *in vitro* import into isolated soybean

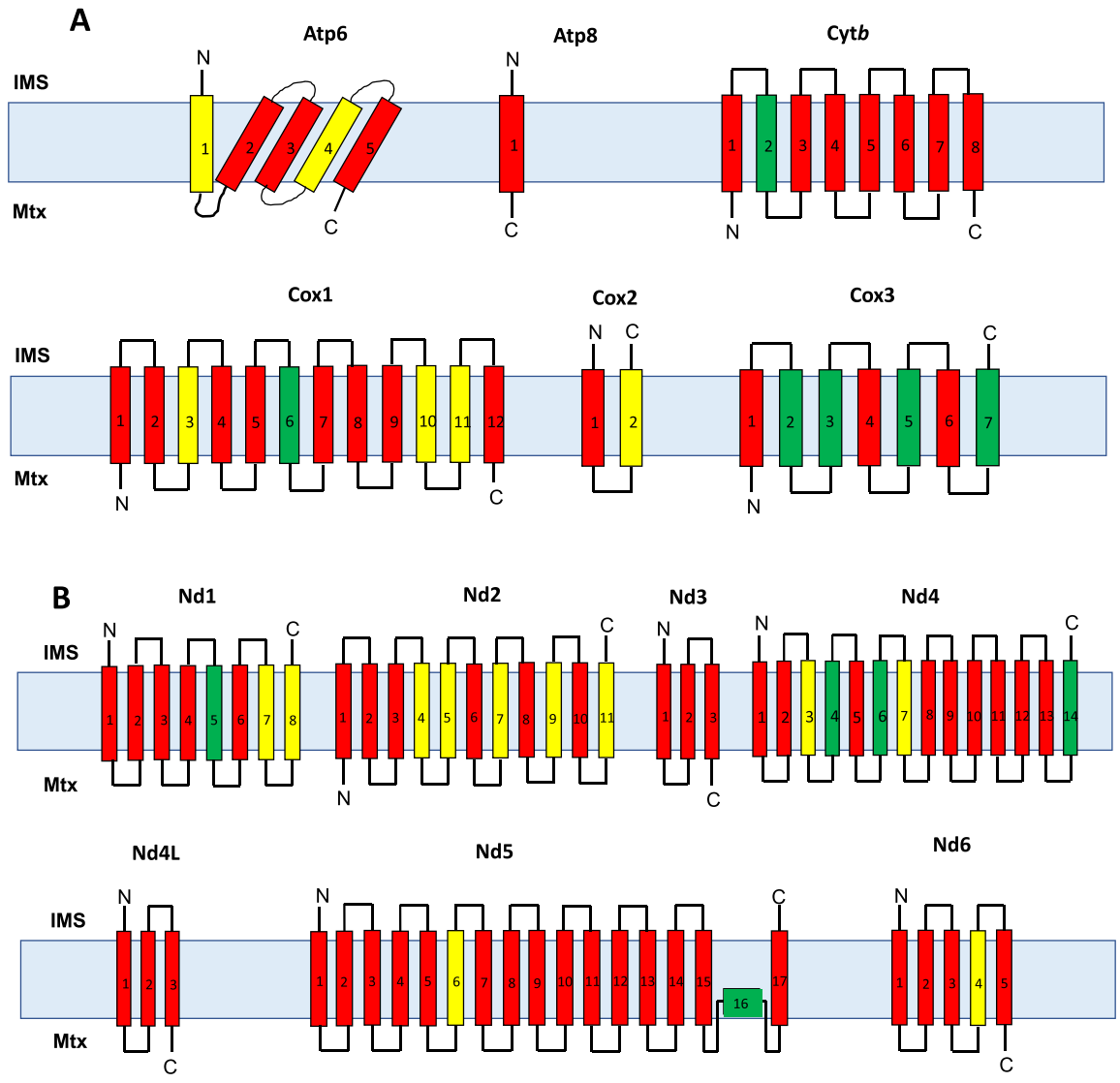

Fig. 4. "Traffic light" color code for all the TMS of the 13 mitochondria encoded OXPHOS subunits. (A) Topological arrangement of the mitochondria-encoded subunits corresponding to complexes III, IV and V, and the "traffic-light" color code assigned to each TMS. (B) Topological arrangement of the mitochondria-encoded subunits of complex I with TMS colored accordingly. Red TMS are predicted to be arrested and released into the IMM by TIM23^{SORT}. The $\mu\Delta G_{app}$ values used to assign the "traffic-light" colors (Fig. 3) were taken from Table S1. The mitochondrial inner membrane is represented as a light blue rectangle. IMS: intermembrane space; Mtx: matrix. N and C termini of each represented protein are indicated.

mitochondria (Daley et al., 2002a). Reports of allotopic expression of genes encoding OXPHOS components have been listed in a recent comprehensive review (Saravanan et al., 2022) and are critically discussed here.

9.1. *The atp6 gene*

More than 12 pathogenic mutations identified in the *atp6* gene have been implicated in several mitochondrial diseases, including LHON, Neuropathy, Ataxia, and Retinitis Pigmentosa (NARP), Parkinson's disease, multiple sclerosis (MS), and systemic lupus erythematosus (SLE) (Ganetzky et al, 2019). Moreover, the protein product of *atp6* is part of the proton channel of complex V and is thus essential for ATP synthesis. Hence, several efforts have been directed to accomplish the allotopic expression of this gene (Kucharczyk et al., 2019). However, the highly hydrophobic nature of Atp6 makes its allotopic production challenging. The proposed mechanism for the internalization into mitochondria of a cytosol synthesized Atp6 subunit (N_{out}-C_{in}) implies the complete translocation of five TMS (Fig. 4) followed by the insertion of two hairpins and an additional TMS into the IMM, probably mediated by the Oxa1 insertase (Suppl Fig. 7).

Allotopic expression of the *atp6* gene in human cells was described in several reports (Manfredi et al., 2002; Zullo et al., 2005; Kaltimbacher et al., 2006; Bonnet et al., 2007). The *atp6* gene was re-designed for nuclear expression, and several MTS were tested, such as the one from Cox8, a nucleus-encoded subunit of complex IV, or from the P1 isoform of subunit *c* of ATP synthase (Manfredi et al., 2002; Oca-Cossio et al., 2003). In other constructs, the MTS of superoxide dismutase 2 (SOD2) was used, along with the addition of the 3′-UTR from the same gene inserted at the end of the transcriptional unit (Kaltimbacher et al., 2006; Bonnet et al., 2007). In these reports, the presence of the Atp6 subunit inside mitochondria was detected by immunofluorescence or immunodetection of a FLAG epitope engineered in the allotopic construct. However, no direct evidence for the allotopically produced subunit assembling into complex V was provided.

Restoration of ATPase activity was reported in cells transformed with the *atp6* gene from human and from the green alga *C. reinhardtii* (Ojaimi et al., 2002) using transiently transfected HEK293T cells, and JCP213 or

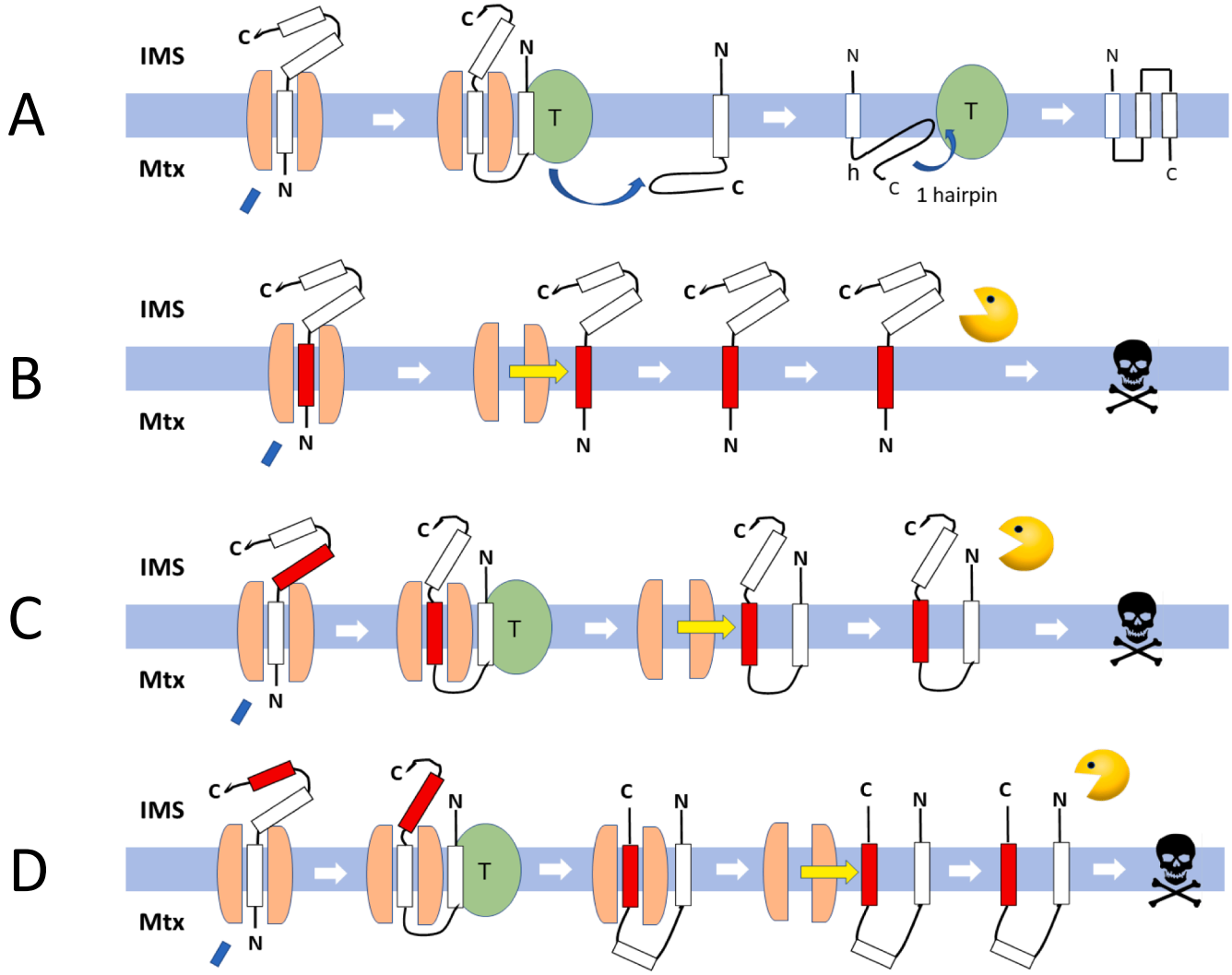

Fig. 5. When things go wrong with allotopic expression and protein import. (A) Diagram representing the import by TIM23 of a cytosol-synthesized membrane protein containing three TMS (that could correspond to Nd3 or Nd4L subunits). For the allotopic protein to adopt a topology identical to the one reached by its mitochondria encoded counterpart, the three TMS must be initially fully translocated into the matrix. If the first (B), second (C) or third TMS (D) is highly hydrophobic (red), TIM23 will laterally release the corresponding alpha-helix into the IMM, and the protein will acquire an anomalous topology. Proteins with an improper folding in the bilayer are recognized by mitochondrial proteases and degraded. The higher the number of red traffic light TMS in a protein, the greater the probability that it will be folded into an inappropriate conformation. The mitochondrial inner membrane is represented as a light blue rectangle. IMS: intermembrane space; Mtx: matrix. N and C termini of each represented protein are indicated.

JCP216 cybrids for stable transfection. The Atp6 subunits were immunodetected as part of a high molecular weight species that was interpreted to be complex V following blue native electrophoresis (BN-PAGE). However, independent experiments by other investigators carried out with the same human and *C. reinhardtii atp6* constructs, showed that both subunits failed to integrate into ATP synthase, and aggregated instead into a high molecular weight species (Bokori-Brown and Holt, 2006). Also, in this report, human and algal constructs were optimized for import into mitochondria of human cell lines (i.e., HEK293T for transient transfection, and JCP2116 cybrid and human osteosarcoma cell line 143B for stable transfection) using the human and the algal MTS of the beta subunit from ATP synthase.

In an independent approach, the human *atp6* gene was engineered as a chimeric human-*C. reinhardtii* construct including the algal MTS and several amino acid substitutions in the TMS to mimic the algal sequence. This chimeric construct was expressed in homoplasmic human mutant cells carrying the T8993G mutation in the mitochondrial *atp6* gene (Figueroa-Martínez et al., 2011). Although the Atp6 subunit chimera was successfully internalized into mitochondria as judged by fluorescence microscopy, the construct failed to increase ATP synthesis.

Zullo et al. (2005) reported that the Atp6 subunit from Chinese Hamster Ovary (CHO) cells could be imported *in vitro* into isolated yeast mitochondria. The construct used in this work was modified to enable the usage of the nuclear genetic code and included a sequence coding the MTS of ornithine transcarbamylase, which was known to direct the import of dihydrofolate reductase (Horwich et al.,1985). A mature form of Atp6 was assumed to be internalized into mitochondria because it exhibited resistance to protease treatments. Nonetheless, these authors did not provide evidence that mitochondrial import was dependent on the electrochemical gradient, i.e., that it could be suppressed by uncouplers or OXPHOS inhibitors; and proof that the allotopic Atp6 was incorporated into Complex V was not given.

The pathogenic human T8993G mutation in *atp6* (NARP mutation) was used as a case study with transgenic mice (Dunn and Pinkert, 2012; Dunn and Pinkert, 2021). Two constructs were designed, one carrying the human EF1α promoter plus sequences encoding the MTS of human Cox8 followed by either the human wild-type *atp6* gene or the one carrying the T8993G mutation, plus a region encoding a C-terminal myc

epitope tag. Transgenic mice expressing either construct were subjected to several neuromuscular and motor tests that yielded mixed results. Mutant mice exhibited motor deficiencies like those observed in NARP patients in some tests, but enhanced performance in others. Biochemical assays to assess the restoration of OXPHOS included quantification of serum lactate concentrations, mitochondrial Manganese superoxide dismutase (MnSOD) levels, ATP synthesis rate, and oxygen uptake rates. Mice from both transgenic lines did not differ substantially from non-transgenic controls, except for lower lactate concentrations in the mice expressing wild-type human *atp6*. Although the presence of the allotopic proteins in mitochondria was assayed by immunostaining striatum sections with gold particles, the delivery of proteins to mitochondria was not quantified, and no evidence was provided that the labeled, allotopically produced Atp6 subunits were assembled into the ATP synthase complex. In these systems, the mitochondrial Atp6 subunit is still efficiently synthesized inside mitochondria, competing against incoming allotopic proteins from the cytosol.

An automated, quantitative, and unbiased screening platform was set up to evaluate protein localization and mitochondrial morphology. This approach entailed generating 124 plasmids with different combinations of 31 MTS and 15 3′-UTRs that were assayed for their ability to localize OXPHOS subunits Atp6, Atp8, Cox2, Cox3, Nd1, Nd3, Nd4 and Nd6 to the mitochondrion (Chin et al., 2018). While the different 3′-UTR sequences did not significantly alter the localization of these proteins, distinct MTS exhibited a superior capability to direct these proteins into mitochondria. In particular, the MTS of maize 4-hydroxybenzoate polyprenyltransferase (encoded by the LOC100282174 gene), either by itself or combined in tandem with another MTS, yielded the highest localization for the allotopically expressed proteins. Chemically modified mRNAs with enhanced stability encoding an optimized allotopic expression construct for *atp6* carrying the MTS of LOC100282174 could functionally rescue a cell line harboring the T8993G point mutation in the mitochondrial *atp6* gene. Although no biochemical evidence showing the presence of the allotopic Atp6 subunit in ATP synthase was provided, expression of the construct in transiently transfected HeLa cells restored respiratory function and ATP synthase functionality. The report by Chin et al. highlights the importance of MTS selection in designing constructs for the allotopic expression of OXPHOS-related genes.

9.2. The atp8 gene

The mitochondrial *atp8* gene encodes subunit Atp8 (also known as subunit A6L in the bovine enzyme), a small hydrophobic polypeptide of 48 amino acids with a single TMS (Fig. 4) that is an essential component of the F_0 sector of the mitochondrial F_1F_0-ATP synthase (Hong and Pedersen, 2004). The group of Philip Nagley in Australia led pioneering efforts in the field achieving the allotopic expression of the yeast *atp8* gene, after optimizing its codon usage for nuclear expression. These experiments made use of two different MTS-encoding sequences, one from the fungus *Neurospora crassa* Atp9 subunit (NcAtp9) and the other from the yeast Cox6 subunit. Whereas the MTS of NcAtp9 (66 residues) promoted the import of Atp8, the MTS of subunit Cox6 did not (Gearing and Nagley, 1986). Furthermore, when the MTS of the NcAtp9 subunit was duplicated in tandem, the import efficiency of the yeast Atp8 subunit was notably increased (Galanis et al., 1991). The successful import into mitochondria of the Atp8 subunit was corroborated by direct sequencing of radiolabeled methionine residues in the imported protein. In another study, the role of the three positively charged residues at the C-terminus of Atp8 was explored using a series of truncated variants, in which the most distal K47 residue was found to be dispensable for Atp8 importability (Nero et al., 1990). This time, the structural and functional assembly of Atp8 and its truncated K47 variant into complex V was demonstrated by its ability to restore respiratory growth to an *atp8*-null yeast strains and by the immunochemical detection of the produced proteins (Grasso et al, 1991; Nagley et al., 1988; Law et al. 1990). Moreover, expression of the *atp8* gene in the nucleus of yeast *atp8* null mutants restored respiration to levels like that of the wild-type strain (Roucou et al., 1999). Altogether, these results show the successful allotopic expression of the yeast *atp8* gene.

The human mitochondrial *atp8* gene was optimized for nuclear codon usage and expressed allotopically in human cells (Oca-Cossio et al., 2003). For this purpose, a recombinant sequence harboring the Atp8 subunit encoding sequence appended with the sequences corresponding to the MTS of Cox8 and a hemagglutinin (HA) C-terminal tag was designed. Although the incorporation of Atp8 into mitochondrial ATP synthase was not examined, the subunit was successfully targeted to mitochondria after transfection of the COS and HeLa cells with the engineered construct, as evidenced by the colocalization of Mitotracker fluorescence and the HA tag detected via immunofluorescence.

In a separate report, all 13 human mitochondrial OXPHOS proteins with sequences carrying the strong MTS of Cox8 were synthesized in the cytosol of human HeLa cells when produced from recoded gene constructs. A FLAG tag sequence at the 3′-terminal end of each gene construct was introduced to enable localization of the synthesized proteins by immunofluorescence confocal microscopy (Björkholm et al., 2017). Only Atp8 was successfully internalized into mitochondria, while the other 12 OXPHOS proteins were all found in the ER, indicating that subcellular protein mistargeting was the reason for lack of functional allotopic expression.

Furthermore, the mouse Atp8 recoded and bearing the MTS of the mouse ATP6G1 subunit and a Myc-FLAG epitope at the C-terminus was produced. A doxycycline dependent induction system was used in C57/BL6$^{(mtFVB)}$ mouse fibroblast cybrids bearing the G7778T mutation in the mitochondrial *atp8* gene. BN-PAGE showed that the allotopically-expressed Atp8 subunit integrated into Complex V and increased the viability of the cybrids (Lewis et al., 2020).

Boominathan et al. (2016) used an homoplasmic cell line harboring the G8529A mutation in the overlap region of the *atp8* and *atp6* genes. This mutation causes premature truncation of the Atp8 subunit but also reduced levels of Atp6 and yields complex V deficiency. Mutant cells were transfected with constructs enabling the synthesis of either Atp8 or Atp6 subunits carrying the MTS of human ATP6G1 fused to a FLAG-tag at their C-termini. Transfections were also carried out with a modified construct containing both genes (*atp8* and *atp6*) in tandem. While the allotopic expression of either the *atp6* or the *atp8* gene had negligible effects, the simultaneous expression of both genes partially recovered complex V assembly and around 55 % of its enzymatic activity.

Overall, there is a large body of experimental evidence indicating that Atp8 subunit has been allotopically expressed successfully in various systems. Since the Atp8 subunit has a single TMS (N_{out}-C_{in}) (Fig. 1), the proposed mechanism for the internalization into mitochondria is relatively simple, involving the complete translocation of this TMS into the matrix followed by its insertion into the IMM, allowing the protein to expose its N-terminus to the IMS.

9.3. The cox1 gene

Although the *cox1* gene, which encodes subunit I of cytochrome *c* oxidase (with 12 TMS) is invariably found in mtDNA, several claims of successful allotopic production have been made. The bovine *cox1* gene was modified to encode Cox1 carrying the MTS of the nucleus-encoded subunit Cox4 and an hexahistidine (6xHis) tag at the C-terminus. The genes encoding wild type and variant versions (D51N) of Cox1 were cloned in a mammalian expression vector under the control of the human cytomegalovirus promoter, which was then used to transfect HeLa cells to obtain stable transfectants. The presence of the Cox1 subunit in complex IV was demonstrated by immunodetection, asserting that both wild-type and mutant subunits formed hybrid enzymes along with the other 12 human subunits of cytochrome *c* oxidase in the transfected HeLa cells (Tsukihara et al., 2003; Shimokata et al., 2007). It is unlikely that the hydrophobicity barrier was overcome by the

allotopically produced Cox1 subunit (N_{in}-C_{in}) (Fig. 1) in these experiments, since the mechanism by which this cytosol synthesized subunit is imported into mitochondria must involve the entire translocation of twelve TMS by TIM23 followed by the insertion of six hairpins by Oxa1 (Suppl Fig. 8). Allotopic expression would probably require reducing the hydrophobicity of at least eight "red light" TMS (Fig. 4). Finally, as part of another approach, the human *cox1* gene, including both the wild-type and the mutant version W494R responsible for a mitochondrial disease, were allotopically expressed in HEK293T cells. Even though the allotopically produced wild-type and variant Cox1 subunits were reported to be located to mitochondria, the allotopically produced proteins appeared to aggregate, and no evidence for their functional integration into complex IV was obtained (Singh et al., 2019).

9.4. The cox2 gene

As discussed above (see section 7.4), the *cox2* gene has been naturally transferred to the nucleus in several legumes, i.e., soybean contains both mitochondria-encoded and nucleus-encoded versions of the Cox2 subunit. In soybean, the nucleus encoded Cox2 precursor exhibits a long MTS of 136 residues, which is required for internalizing the protein into mitochondria. Comparison of the sequences of mitochondria and nucleus encoded Cox2 sequences unveiled significant differences in residues present in the first TMS of the protein. With an MTS and two-point mutations (L169Q and L171G) that together lower the hydrophobicity of the first TMS, the mitochondrial version of the Cox2 protein could be imported into isolated soybean mitochondria (Daley et al., 2002a). This result was a proof-of-concept that hydrophobicity of TMS1 is a key parameter for the allotopic expression of mitochondrial OXPHOS subunits. This is further substantiated by the fact that allotopically produced Cox2 subunit successfully complemented a respiration deficient yeast *cox2*-null mutant when tryptophan was replaced with arginine at position 56 in the first TMS of the protein (Supekova et al., 2010). The W56R mutation was isolated following PCR-prone mutagenesis of a recoded *cox2* gene encoding an MTS from either Atp9 or Oxa1 and shown to restore respiratory growth of a *cox2*-null strain. Also, the W56R mutation increases the $\mu\Delta G_{app}$ of the first TMS of $COX2^{W56R}$, thereby allowing its import into mitochondria and its assembly into complex IV (Fig. 3). Subsequent experiments have shown that other variants of the Cox2 yeast subunit like $Cox2^{W56K}$ and $Cox2^{W56Q}$ are also imported into mitochondria, albeit less efficiently than $Cox2^{W56R}$ (Rubalcava-Gracia et al., 2018). It is assumed that the higher $\mu\Delta G_{app}$ of $COX2^{W56R}$ TMS1 enables its transfer into the mitochondrial matrix by the TIM23 translocon, while $COX2^{W56R}$ TMS2, exhibiting a lower $\mu\Delta G_{app}$, will be retained by TIM23 and released laterally into the IMM (Qualmann et al., 2003; Rubalcava-Gracia et al., 2018) (Suppl Fig. 9). Complementing the *Δcox2* mutant with a cytosol synthesized $Cox2^{W56R}$ (N_{out}-C_{out}) only yields partial recovery of the respiratory proficiency (Supekova et al., 2010). This partial complementation could be due to the lower activity of cytochrome *c* oxidase carrying the W56R mutation or reduced steady-state accumulation levels of this enzyme. The specific enzymatic activity of the purified complex IV from both the wild-type strain and the $Cox2^{W56R}$ mutant was almost equivalent, suggesting that the W56R mutation does not affect the intrinsic complex IV activity. However, in-gel activity and spectroscopic quantification revealed that only 40–60 % of cytochrome *c* oxidase accumulates in the strain producing the $Cox2^{W56R}$ protein (Cruz-Torres et al., 2012). This suggests that the W56R mutation affects complex IV biogenesis, leading to lower steady state levels of the enzyme.

In yeast, defects in mitochondrial Cox2 synthesis impact Cox1 synthesis (Naithani et al., 2003; Barrientos et al., 2004; Pérez-Martinez et al., 2009; García-Villegas et al., 2017), but the allotopically expressed $Cox2^{W56R}$ precursor subunit can restore the mitochondrial synthesis of Cox1 in a *Δcox2* mutant to wild-type levels. In addition, a strain synthesizing $Cox2^{W56R}$ from a mitochondrial *cox2W56R* gene which followed a canonical biogenesis of subunit Cox2, exhibited normal levels of functional cytochrome *c* oxidase (Rubalcava-Gracia et al., 2018). This suggests that the W56R substitution does not affect complex IV activity. Instead, the import of the $Cox2^{W56R}$ precursor through TIM23 could be the limiting step of complex IV biogenesis. Furthermore, when both the cytosolic $Cox2^{W56R}$ and the mitochondrial Cox2 were co-expressed, each protein assembled into complex IV independently from its genetic origin, resulting in a mixed population of this complex, most of which contained the mitochondria-synthesized version (Rubalcava-Gracia et al., 2018).

9.5. The cox3 gene

The human *cox3* gene was re-designed to facilitate the mitochondrial import of its gene product by emulating the structural properties of the corresponding nucleus-encoded algal proteins from *C. reinhardtii.* The algal MTS from Cox3 was used, including multiple algal-like amino acid substitutions to reduce TMS hydrophobicity. The resulting human-algal chimeric *cox3* gene was expressed in a CHO cell line carrying an homoplasmic 15 bp deletion in the mitochondrial gene (Figueroa-Martínez et al., 2011). The chimeric Cox3 protein re-designed for nuclear expression was targeted to the mitochondria but failed to integrate into complex IV. To our knowledge, no further attempts to achieve allotopic expression of the *cox3* gene have been described. The predicted insert pathway of an allotopic Cox3 subunit (N_{in}-C_{out})(Fig. 1) requires the full translocation of six TMS (Fig. 4) by TIM23 (three of which are "red light") followed by the lateral release of TMS7 into the IMM and insertion of three hairpins into the IMM.

9.6. The cytb gene

Cytochrome *b* of complex III, a subunit with six TMS (Fig. 4), is invariably encoded in the mitochondrial genome. Several attempts to engineer the *cytb* gene for allotopic expression have been documented. In a pioneering study, hybrid proteins containing different combinations of the cytochrome *b* transmembrane domains fused to both the MTS of the *N. crassa* Atp9 subunit at the N-terminus and a cytoplasmic version of the bI4 RNA maturase at the C-terminus were produced. The bI4 RNA maturase was used as a reporter to assess the efficiency of mitochondrial import of the different combination of TMS. All TMS from Cyt*b*, either alone or in combination, were found to be internalized into mitochondria, but no more than four TMS could be imported at once (Claros et al., 1995), an indication that overall hydrophobicity was a constraint. It was proposed that the entire protein hydrophobicity and the local TMS hydrophobicity were the limiting factors for Cyt*b* import into mitochondria (Lewis et al., 2020).

In other experiments, different MTS (from the Cox8 subunit, P1 isoform of subunit *c* of ATP synthase, and Nicotinamide Nucleotide Transhydrogenase) were attached to the full-length cytochrome *b* precursor to target the protein to the mitochondria. The resulting allotopically synthesized cytochromes *b* were found to aggregate in fiber-like structures in the periphery of mitochondria, indicating that hydrophobicity was a physical impediment for internalization into the organelle (Oca-Cossio et al., 2003). The case of cytochrome *b* illustrates the difficulties in achieving the correct import and functional integration of a highly hydrophobic membrane protein into its appropriate mitochondrial complex. Indeed, the proposed theoretical mechanism for the import of a cytosol synthesized Cyt*b* subunit (N_{in}-C_{in}) (Fig. 1) involves the complete translocation of its eight TMS (Fig. 4) into the mitochondrial matrix by TIM23, seven of which are "red-light", followed by the insertion of four hairpins by Oxa1.

9.7. The nd1 gene

The human *nd1* gene, encoding subunit Nd1 of complex I (8 TMS), was claimed to be allotopically produced (Bonnet et al., 2008). A construct containing the *nd1* gene with an appended sequence encoding

the MTS from Cox10 protein was used to stably transfect cultured skin fibroblasts from LHON patients (carrying the mutation G3460A). The transfected fibroblasts were restored for growth on galactose, complex I activity, and the rate of ATP synthesis.

A similar construct with additional 3′-UTR from the *COX10* gene was used to transform 43B osteosarcoma-derived cybrids harboring a mostly homoplasmic mutation in the *nd1* gene. Immunoblotting analysis revealed the presence of the Nd1 subunit in transfected cells that also exhibited partial recovery of bioenergetic competence (Calabrese et al., 2013; Iommarini et al., 2018). Nonetheless, since only 8 % of the ATP synthesis was recovered, this suggests that only a small proportion of the imported subunit reaches its final compartment or is functionally incorporated into complex I.

In a recent study the *nd1* gene was engineered for codon optimization to obtain a robust and efficient expression (Lewis et al., 2020). A homoplasmic cybrid cell line containing the mutation m.3571insC which is an insertion of an additional cytosine resulting in a premature stop codon, truncation of the Nd1 subunit, and failure of complex I to assemble, was used as recipient cell line. This recipient cell-line was used for the allotopic production of a FLAG-tagged human ND1 protein fused to the MTS of human ATP5G1 subunit. Allotopically produced Nd1 was immunodetected using anti-FLAG antibodies in a high molecular weight complex following BN-PAGE. However, the integration efficiency of the allotopic Nd1 subunit was suboptimal and insufficient to restore complex I activity to wild-type levels.

The proposed mechanism for a cytosol-synthesized Nd1 subunit (N_{out}-C_{out}) (Fig. 1) implies translocation of the protein first TMS followed by its insertion into the IMM, such that the N-terminus is exposed to the IMS. After that, full translocation of the seven remaining TMS through TIM23 must occur. Finally, three hairpins will be inserted into the IMM, followed by the insertion of TMS8 (Suppl Fig. 10).

9.8. The nd2 gene

Despite the lack of reports describing the allotopic expression of the *nd2* gene, the proposed mechanism for the Nd2 subunit (N_{in}-C_{out}, 11 TMS, Fig. 4) internalization involves the full translocation of ten TMS (six "red-light", Fig. 4) and the lateral release of TMS11 into the IMM, followed by the insertion of five hairpins.

9.9. The nd3 and nd4L genes

Although no claims for the allotopic expression of the *nd3* and *nd4L* genes have been put forth, the theoretical insertion pathway of Nad3 and Nad4L (N_{out}-C_{in}, each one carrying three "red-light" TMS, Fig. 4) involves the full translocation of the three TMS, followed by the insertion of TMS1 and 1 hairpin into the IMM.

9.10. The nd4 gene

The *nd4* gene encoding the membrane-bound subunit Nd4 of complex I has been the subject of efforts to achieve its allotopic expression, mostly because a point mutation in the *nd4* gene (G11778A) is responsible for about 70 % of LHON cases (Manickam et al., 2017).

Pioneering attempts involved expressing constructs encoding the Nd4 subunit fused to the MTS of the Cox8 subunit and tagged either with a HA or a green fluorescent protein (GFP) in COS-7 or HeLa cells. As a result, the Nd4 protein (14 TMS) aggregated, forming fiber-like structures around mitochondria. Similar results were reported when C-terminal truncated forms of the Nd4 subunit (with only 6 or 8 TMS) were allotopically produced (Oca-Cossio et al., 2003). In contrast, successful allotopic expression in human cells has been reported for the *nd4* gene (Bonnet et al., 2007; Bonnet et al., 2008; Guy et al., 2002; Ellouze et al., 2008). In a set of experiments, the recoded *nd4* gene attached to a sequence encoding the MTS of the P1 isoform of subunit c of human ATP synthase (Atp9) and a sequence encoding a short FLAG epitope tag for import detection was used. Complementation of G11778A cybrids with this construct showed a threefold increase in ATP synthesis (Guy et al., 2002). In other independent constructs, the MTS from either mitochondrial SOD2 or COX10 were added to the Nd4 subunit. Immunodetection of the FLAG epitope confirmed the presence of the Nd4 subunit inside mitochondria, but no direct evidence for the allotopically produced subunit assembling into complex I was provided (Bonnet et al., 2007). Also, a human variant Nd4 subunit was expressed allotopically in a murine model. Constructs encoding a synthetic wildtype human Nd4 subunit and a variant Nd4 subunit corresponding to the LHON R340H mutation, carrying the MTS of the Atp9 subunit, were delivered to the mouse visual system. The effects of the variant Nd4 subunit on the optic nerve were assessed by electron microscopy, magnetic resonance imaging, and immunohistochemistry. While the variant Nd4 subunit disrupted mitochondrial architecture and elevated reactive oxygen species, severely affecting the retina ganglion cells, the wild-type Nd4 subunit had no apparent deleterious effects (Qi et al., 2007). Subsequent works used the nuclear-encoded human Nd4 subunit fused to the P1 isoform of subunit c (Atp9) of ATP synthase MTS and FLAG epitope with a self-complementary adeno-associated virus to induce an efficient synthesis of the human Nd4 subunit in the mouse visual system, although no evidence for integration of Nd4 into complex I was provided (Koilkonda et al., 2010).

More recently, efficient delivery of the Nd4 subunit into mitochondria was claimed after ocular administration of a recombinant adeno-associated viral vector containing the human *nd4* gene sequence to adult rats (Cwerman-Thibault et al., 2015). The construct expressed the Nd4 subunit attached to the MTS of the Cox10 subunit and a triple HA tag. An electrophoretically resolved species of about 54 kDa, present in treated retinas but not in the untreated, was identified using an anti-HA antibody. This species was assumed to be the Nd4 subunit (51.7 kDa) fused to a 27-residue segment corresponding to three contiguous HA1 epitopes (about 3 kDa). However, in preparations of complex I from bovine heart mitochondria, Nd4, which is a highly hydrophobic subunit, migrates in SDS-PAGE with a substantial lower apparent molecular mass of about 39 kDa, due to its high hydrophobicity (Fearnley et al., 1991). The discrepancy in apparent molecular masses deserves further experimentation to establish unambiguously if the observed human 51.7 kDa band indeed corresponds to the allotopically-produced Nd4.

It has been claimed that sustained expression of the human *nd4* gene does not lead to harmful effects and that the human Nd4 subunit is efficiently imported into mitochondria and assembled into complex I (Vignal et al., 2018; Vignal-Clermont et al., 2021). Furthermore, in this experimental model of LHON retinal ganglion cell degeneration was prevented, while visual function and complex I activity in optic nerves were preserved. Surprisingly, m.11778G > A LHON patients treated with rAAV2/2-ND4 exhibited an improvement in visual acuity for more than 4 years after vision loss (Newman et al., 2021; 2023). In this regard, GenSight Biologics (Paris/New York) is currently conducting clinical trials using Nd4 in an allotopic expression strategy to treat LHON patients. Since the proposed mechanism for import of the Nd4 subunit (N_{out}-C_{out}) into mitochondria involves the full translocation of 14 TMS (nine of which are "red light"), followed by insertion of TMS1 and 6 hairpins into the IMM, probably mediated by Oxa1, such results in patients are unexpected, and unambiguous proof for successful allotopic production of the subunit must be provided.

9.11. The nd5 gene

To date, the allotopic expression of the *nad5* gene has not been reported. The proposed theoretical mechanism for the import into mitochondria and insertion into the IMM of an allotopic Nd5 subunit (N_{out}-C_{out}) (Fig. 1) involves the entire translocation of 17 TMS (15 of which are "red-light", Fig. 4), the insertion of TMS1 and 7 hairpins, followed by the insertion of TMS16 and the translocation of TMS17.

9.12. The nd6 gene

The mouse mitochondrial *nd6* gene was optimized for nuclear expression and sequences encoding the MTS from Cox8, and an HA epitope were integrated in a construct designed for allotopic production. Transfection of a mice KO mutant line exhibiting a cytosine 13887deletion in mtDNA with the construct showed that the Nd6 subunit was mainly located outside of mitochondria, although complex I activity seemed to be restored. Further experimentation showed that the selected clones were revertants for the mitochondrial *nd6* mutation (Perales-Clemente et al., 2010). No further reports claiming the allotopic expression of the *nd6* gene are currently available. The proposed mechanism for the import of a cytosol synthesized Nd6 (N_{out}-C_{in}) (Fig. 1) involves the full translocation of 5 TMS (4 of which are "red-light", Fig. 4) and the insertion of TMS1 and two hairpins.

10. Allotopic expression of the atp9 gene, a gene not present in human mtDNA

Although the *atp9* gene (encoding *c* subunit, a constituent of ATP synthase rotary *c*-ring) is absent from the mtDNA of mammals, we will briefly discuss its allotopic expression in yeast as the results are relevant here. In early experiments, the yeast *atp9* gene recoded for nuclear expression fused to a sequence encoding the MTS of the *atp9* gene from *N. crassa* was tested (Law et al., 1988). The resulting fusion protein was imported in purified yeast mitochondria and adequately processed. The import of yeast Atp9 was less efficient than the import observed for the yeast Atp8 subunit attached to the same MTS in parallel import experiments (Farrell et al., 1988). Furthermore, duplication in tandem of *N. crassa* Atp9 MTS notably increased its import efficiency (Galanis et al., 1991).

More recently, Bietenhader et al. (2012), developed a strategy that involved relocating the mitochondrial *atp9* gene of *S. cerevisiae* by using the version of *atp9* from the fungus *Podospora anserina*, which naturally carries the *ATP9* gene in its nuclear genome. A notable difference between *P. anserina* and yeast Atp9 proteins is the reduced hydrophobicity of TMS1 in the former, as indicated both by hydropathy plots and its diminished resistance to extraction by detergents. *In vivo*, the *P. anserina* Atp9 subunit was successfully imported into mitochondria and restored the respiratory function of a yeast *atp9*-null strain, restoring fully functional OXPHOS. Nevertheless, these experiments also illustrated other limitations of allotopic expression: the production of Podospora Atp9 in yeast perturbed cellular morphology and activated the heat shock response, as revealed by transcription profiling.

11. Discussion

While several allotopic expressions of mitochondrial genes in human or mammalian cell lines have been reported (Manfredi et al., 2002, Ojaimi et al., 2002; Guy et al., 2002), some of the initially described reports could not be reproduced by other investigators (Oca-Cossio et al., 2003; Bokori-Brown and Holt, 2006). In some of these studies, the apparent improvements in OXPHOS performance may not have resulted from allotopic expression. This is due to the inherent difficulties of working with cultures in which cells with apparently identical genotypes can exhibit clone-to-clone variability (King and Attardi, 1989). In one case, the apparent complementation of a mtDNA mutation by an allotopically produced subunit of ATP synthase was due to a reversion of the original mutation in the cell line used for the experiment (Perales-Clemente et al., 2010). In addition, experimentalists must be mindful of the fact that nonmitochondrial tags could hinder mitochondrial proteins from reaching their correct topology (Sickmann et al., 2003). In our view, the publication of negative data has been instrumental in advancing the field since it has allowed researchers to avoid repeating unsuccessful experimental approaches.

Here, we discussed the factors that limit the import of cytosol-synthesized polytopic membrane proteins impacting the allotopic expression of OXPHOS-related genes, underscoring the importance of the $\mu\Delta G_{app}$ of each TMS. Synthesis of membrane proteins inside mitochondria and their incorporation into the IMM is undoubtedly, on the surface, less complicated than that of their cytosol-synthesized counterparts. The latter follow a multi-step and seemingly more complex biogenesis: import through the TOM/TIM23 translocators, protease-dependent maturation, incorporation into the IMM, and assembly into a multi-subunit complex. When the original mitochondrial gene is still functional, allotopically expressed proteins must outcompete, at least to a functional threshold, the defective endogenous proteins which are continuously synthesized inside mitochondria and that follow their canonical biogenesis pathway. Therefore, complete recovery of OXPHOS after allotopic expression, as reported for the Atp6 and Nad4 subunits (Bonnet et al., 2007,2008), is not necessarily expected, since it implies that all ATP synthase or complex I enzymes preferably incorporate allotopically produced subunits, entirely replacing all endogenous, mutant ones. More likely, a mixed population of OXPHOS complexes coexists, some carrying the allotopically-produced protein and others bearing the mitochondria-synthesized mutant subunit. Indeed, when mtDNA-encoded and allotopically expressed Cox2 proteins were coexpressed in yeast, each protein could assemble into a complex, resulting in a mixed population of complex IV, with most complexes containing the mtDNA-encoded version (Rubalcava-Gracia et al., 2018). In the case of biological models with null mutations (or equivalent to null) in their mtDNA, this competition problem is circumvented.

Another challenge in allotopic expression is selecting appropriate promoters and genome loci to control protein levels. High doses of allotopically expressed proteins could be counterproductive, since they may aggregate outside the organelle or clog the mitochondrial import machinery (Boos et al., 2019; Rubalcava-Gracia et al., 2019).

As suggested before, claims of allotopic production of respiratory chain components should be ideally supported by biochemical evidence showing that imported proteins were fully integrated and functionally assembled into their appropriate complex (Kyriakouli et al., 2008; Perales-Clemente et al., 2010), especially for membrane proteins with two or more TMS. Demonstration should be unambiguous and include multiple experimental approaches such as immunodetection, regain of function, and if possible, biochemical purification and identification of the allotopic subunit by mass spectrometry. This is of utmost importance, especially in instances where allotopic expression approaches are used in human clinical trials to treat mitochondrial diseases (Lam et al., 2010,2022; Newman et al., 2023). It is our opinion that in non-human species, only three reports provide unequivocal functional and biochemical evidence of incorporation of allotopically expressed OXPHOS proteins into their respective complexes, namely Atp8, Atp9, and Cox2 in yeast (Law et al., 1990; Supekova et al., 2010; Bietenhader et al., 2012). These three proteins share some crucial features: *(i)* they are membrane proteins with just one or two TMS, *(ii)* they are products of genes for which examples of naturally re-localized gene versions to the nuclear genome exist in several species, and *(iii)* the allotopic expression was carried out in a mutant organism where the original mitochondrial gene was inactivated entirely, thus avoiding competition between the assembly of the nucleus-encoded version and its mitochondrial counterpart. As for humans, several lines of evidence suggest a successful allotopic expression for the Atp8 subunit (Oca-Cossio et al., 2003; Björkholm et al., 2017; Lewis et al., 2020). In addition, a report describing the expression of an Atp6 construct in cultured mutant HeLa cells carrying the T8993G mutation, showed an evident partial restoration of coupled respiration, which strongly suggests that the allotopic Atp6 subunit was successfully integrated into complex V (Chin et al., 2018).

From a large scale bioinformatic analysis using 150,000 organellar DNA sequences and over 300 whole nuclear genome sequences (Giannakis et al., 2022), four universal features that seem to determine gene retention in organelles were postulated: *(i)* hydrophobicity of the

organelle-encoded protein; *(ii)* the centrality of the encoded subunit within its protein complex; *(iii)* enrichment of residues with a higher carboxyl pKa in the organelle-encoded protein; and *(iv)* the GC content of its cognate gene. Hydrophobicity of the protein product was therefore confirmed to be a reliable predictor for gene retention in mitochondria, and as an inevitable corollary, hindering both transfer to the nucleus and successful allotopic expression of certain organellar genes. We conclude that several mitochondrial genes like *cox1*, *cytb*, *nd1, nd2, nd4, nd5 and nd6*, whose protein products are highly hydrophobic and mistargeted to the ER when synthesized in the cytosol (Björkholm et al., 2017), do not lend themselves to allotopic expression, unless extensive modifications designed to increase the $\mu\Delta G_{app}$ of certain TMS are incorporated in the original design of their expression constructs. In addition, even if precursors are targeted to the mitochondrion, the presence of one or more TMS exhibiting a low $\mu\Delta G_{app}$, may cause the TIM23 translocator to misguide them into an inappropriate sorting route, thus blocking their ability to reach their final functional topology (Fig. 4).

The existence of hydrophilic pathways with lateral opening gates, representing potential paths for preprotein sorting, is a common feature of many protein translocons, such as SecY on the bacterial inner membrane (Ma et al., 2019), Sec61 and Hrd1 complex on the ER membrane (Wu et al., 2019, 2020), TIM22 on the mitochondrial inner membrane (Qi et al., 2021) and the chloroplast TIC complex (Jin et al., 2022; Liu et al., 2023). As discussed above, TIM23 sorts alpha helices either translocating them into the matrix or releasing them laterally into the IMM. Constrained by this sorting mechanism, all the TMS of the allotopically produced membrane proteins ***must*** be fully translocated into the mitochondrial matrix (by $TIM23^{MOTOR}$) and ***then*** incorporated into the IMM (except for the last TMS, which in certain proteins could be laterally released into the IMM (by $TIM23^{SORT}$). Inevitably, physical limitations in importing a cytosol-synthesized membrane protein must augment as the number of TMS increases (Claros et al., 1995). Hence it is expected that major hurdles may be encountered when the Nd6 (5 TMS), Cyt*b* (8 TMS), Nd1 (8 TMS), Nd2 (11 TMS), Cox1 (12 TMS), Nd4 (14 TMS), and Nd5 (17 TMS) subunits are expressed allotopically (Fig. 1). The key challenge in designing constructs for allotopic expression is to include mutations that increase the $\mu\Delta G_{app}$ of certain TMS without altering protein function, as exemplified by the yeast Cox^{W56R} allotopic subunit. While the W56R mutation allows the internalization of the protein into mitochondria, its effect on cytochrome *c* activity is negligible (Rubalcava-Gracia et al., 2018). By contrast, other OXPHOS genes, mainly those that have been transferred to the nucleus in some organisms and encode relatively few "red-light" TMS (Fig. 4), may be viable candidates to attempt allotopic expression in humans, namely: *atp8, cox2 and cox3*. As a general strategy, it might be conceivable to mimic the structural changes that the protein products have undergone, i.e., point mutations replacing hydrophobic amino acids with more polar residues in the first TMS of the protein as in the yeast and algal Cox2, or the loss of a TMS as in the algal Atp6 and Cox3 proteins. Alternatively, the sequence of a complete TMS could be exchanged by the TMS of the same protein pertaining to a closely related organism whose $\mu\Delta G_{app}$ exhibits a higher value. The fragmentation of genes, as illustrated above for Cox2a and Cox2b, each encoding one of the two complementary subunits, may also represent an alternative strategy. Split subunits, each one containing a small number of TMS, may enter mitochondria more efficiently and functionally associate in the IMM after import. There are several examples of genes encoding OXPHOS components that have undergone natural fragmentation including the *cox1*, *cox2, nad1*, *nad2*, and *sdhB* genes (Szafranski, 2017). Alternative approaches could also involve mutations in the TIM/TOM import apparatus or overexpression of certain factors that could enhance the import of allotopic proteins into mitochondria.

The arguments presented above largely rest upon the available data on 3D structures of OXPHOS proteins and the known mechanisms of protein import into mitochondria. In this work, one critical assumption was made: that the biological hydrophobicity scale of Botelho et al. (2011), originally determined in yeast mitochondria, may be extrapolated to other organisms including humans. Further experimentation in human cells will clarify this issue, but at present, we find it to be a reasonable assumption. Two of the approaches used in the past to modify genes for allotopic expression, i.e., codon optimization and the addition of a sequence encoding an MTS, are necessary but not sufficient to ensure a successful outcome. Here, we have argued that three additional elements should be considered: *i)* the $\mu\Delta G_{app}$ of the TMS of proteins destined to reside in the IMM; *ii)* the final topology of each OXPHOS subunit and the number of TMS they contain; and *iii)* the mechanism by which TIM23 distributes cytosol-synthesized precursors. The last two factors are intimately related, since the $\mu\Delta G_{app}$ value will determine the biogenesis pathway by which TIM23 will direct a given TMS. Despite all its caveats, allotopic expression remains a promising, intellectually challenging strategy to develop gene-based therapies for mitochondrial diseases.

Declaration of Competing Interest

The authors declare that they have no known competing financial interests or personal relationships that could have appeared to influence the work reported in this paper.

Acknowledgements

The authors acknowledge the technical expertise that Miriam Vázquez-Acevedo (IFC, UNAM), Laura Carmona Salazar (Facultad de Química, UNAM), and José Luis Santillán Torres (IFC, UNAM) provided to our ongoing projects on allotopic expression. We are immensely grateful to Doctors Johannes Herrmann (University of Kaiserslautern, Germany); Gunnar von Heijne (Stockholm University, Sweden); Jaime Flores-Riveros (Amerstem Inc., California, USA); Mauro Degli Esposti (Centro de Ciencias Genómicas, UNAM); and Ruy Pérez-Montfort (IFC, UNAM) for critically reviewing this manuscript and providing useful suggestions. This review is dedicated to the late Professor Georges Dreyfus (IFC, UNAM), dear friend and colleague. D.G.-H. laboratory received financial support from grants CF2019-21856 (Frontiers of Science, CONACyT, Mexico) and IN209220 (PAPIIT, DGAPA, UNAM). F. N.-P. is a Ph.D. student at Programa de Maestría y Doctorado en Ciencias Bioquímicas (UNAM) and recipient of a CONACyT fellowship (CVU 700670). P.P.H. received a PREI fellowship from DGAPA, UNAM to carry a research stay in Mexico.

Appendix A. Supplementary data

Supplementary data to this article can be found online at https://doi.org/10.1016/j.mito.2023.09.004.

References

Adams, K.L., Palmer, J.D., 2003. Evolution of mitochondrial gene content: gene loss and transfer to the nucleus. Mol. Phylogen. Evol. 29, 380–395. https://doi.org/10.1016/S1055-7903(03)00194-5.

Adams, K.L., Song, K., Roessler, P.G., Nugent, J.M., Doyle, J.L., Doyle, J.J., Palmer, J.D., 1999. Intracellular gene transfer in action: dual transcription and multiple silencings of nuclear and mitochondrial cox2 genes in legumes. PNAS 96, 13863–13868. https://doi.org/10.1073/pnas.96.24.13863.

Alexeyev, M.F., Venediktova, N., Pastukh, V., Shokolenko, I., Bonilla, G., Wilson, G.L., 2008. Selective elimination of mutant mitochondrial genomes as therapeutic strategy for the treatment of NARP and MILS syndromes. Gene Ther. 15, 516–523. https://doi.org/10.1038/gt.2008.11.

Allen, J.F., 2015. Why chloroplasts and mitochondria retain their own genomes and genetic systems: Colocation for redox regulation of gene expression. PNAS 112, 10231–10238. https://doi.org/10.1073/pnas.1500012112.

Anderson, S., Bankier, A.T., Barrell, B.G., de Bruijn, M.H., Coulson, A.R., Drouin, J., Eperon, I.C., Nierlich, D.P., Roe, B.A., Sanger, F., Schreier, P.H., Smith, A.J., Staden, R., Young, I.G., 1981. Sequence and organization of the human mitochondrial genome. Nature 290, 457–465. https://doi.org/10.1038/290457a0.

Andersson, S.G., Zomorodipour, A., Andersson, J.O., Sicheritz-Pontén, T., Alsmark, U.C., Podowski, R.M., Näslund, A.K., Eriksson, A.S., Winkler, H.H., Kurland, C.G., 1998.

The genome sequence of *Rickettsia prowazekii* and the origin of mitochondria. Nature 396, 133–140. https://doi.org/10.1038/24094.
Artika, I.M., 2019. Allotopic expression of mitochondrial genes: Basic strategy and progress. Genes Dis. 7, 578–584. https://doi.org/10.1016/j.gendis.2019.08.001.
Attardi, G., Schatz, G., 1988. Biogenesis of mitochondria. Annu. Rev. Cell Biol. 4, 289–333. https://doi.org/10.1146/annurev.cb.04.110188.001445.
Bacman, S.R., Moraes, C.T., 2007. Transmitochondrial technology in animal cells. Meth. Cell Biol. 80, 503–524. https://doi.org/10.1016/S0091-679X(06)80025-7.
Bacman, S.R., Williams, S.L., Pinto, M., Peralta, S., Moraes, C.T., 2013. Specific elimination of mutant mitochondrial genomes in patient-derived cells by mitoTALENs. Nat. Med. 19, 1111–1113. https://doi.org/10.1038/nm.3261.
Bacman, S.R., Kauppila, J.H.K., Pereira, C.V., Nissanka, N., Miranda, M., Pinto, M., Williams, S.L., Larsson, N.G., Stewart, J.B., Moraes, C.T., 2018. MitoTALEN reduces mutant mtDNA load and restores tRNAAla levels in a mouse model of heteroplasmic mtDNA mutation. Nat. Med. 24, 1696–1700. https://doi.org/10.1038/s41591-018-0166-8.
Banroques, J., Delahodde, A., Jacq, C., 1986. A mitochondrial RNA maturase gene transferred to the yeast nucleus can control mitochondrial mRNA splicing. Cell 46, 837–844. https://doi.org/10.1016/0092-8674(86)90065-6.
Banroques, J., Perea, J., Jacq, C., 1987. Efficient splicing of two yeast mitochondrial introns controlled by a nuclear-encoded maturase. EMBO J. 6, 1085–1091. https://doi.org/10.1002/j.1460-2075.1987.tb04862.x.
Barrera-Paez, J.D., Moraes, C.T., 2022. Mitochondrial genome engineering coming-of-age. Trends Genet. 38, 869–880. https://doi.org/10.1016/j.tig.2022.04.011.
Barrientos, A., Zambrano, A., Tzagoloff, A., 2004. Mss51p and Cox14p jointly regulate mitochondrial Cox1p expression in *Saccharomyces cerevisiae*. EMBO J. 23, 3472–3482. https://doi.org/10.1038/sj.emboj.7600358.
Bensasson, D., Zhang, D., Hartl, D.L., Hewitt, G.M., 2001. Mitochondrial pseudogenes: evolution's misplaced witnesses. Trends Ecol. Evol. 16, 314–321. https://doi.org/10.1016/s0169-5347(01)02151-6.
Berg, O.G., Kurland, C.G., 2000. Why mitochondrial genes are most often found in nuclei. Mol. Biol. Evol. 17, 951–961. https://doi.org/10.1093/oxfordjournals.molbev.a026376.
Bietenhader, M., Martos, A., Tetaud, E., Aiyar, R.S., Sellem, C.H., Kucharczyk, R., Clauder-Münster, S., Giraud, M.F., Godard, F., Salin, B., Sagot, I., Gagneur, J., Déquard-Chablat, M., Contamine, V., Hermann-Le Denmat, S., Sainsard-Chanet, A., Steinmetz, L.M., di Rago, J.P., 2012. Experimental relocation of the mitochondrial ATP9 gene to the nucleus reveals forces underlying mitochondrial genome evolution. PLoS Genet. 8, e1002876.
Birky Jr., C.W., 2001. The inheritance of genes in mitochondria and chloroplasts: laws, mechanisms, and models. Annu. Rev. Genet. 35, 125–148. https://doi.org/10.1146/annurev.genet.35.102401.090231. PMID: 11700280.
Björkholm, P., Harish, A., Hagström, E., Ernst, A.M., Andersson, S.G., 2015. Mitochondrial genomes are retained by selective constraints on protein targeting. PNAS 112, 10154–10161. https://doi.org/10.1073/pnas.1421372112.
Björkholm, P., Ernst, A.M., Hagström, E., Andersson, S.G., 2017. Why mitochondria need a genome revisited. FEBS Lett. 591, 65–75. https://doi.org/10.1002/1873-3468.12510.
Bohnert, M., Rehling, P., Guiard, B., Herrmann, J.M., Pfanner, N., van der Laan, M., 2010. Cooperation of stop-transfer and conservative sorting mechanisms in mitochondrial protein transport. Curr. Biol. 20, 1227–1232. https://doi.org/10.1016/j.cub.2010.05.058.
Bokori-Brown, M., Holt, I.J., 2006. Expression of algal nuclear ATP synthase subunit 6 in human cells results in protein targeting to mitochondria but no assembly into ATP synthase. Rejuven. Res. 9, 455–469. https://doi.org/10.1089/rej.2006.9.455.
Bonnefoy, N., Chalvet, F., Hamel, P., Slonimski, P.P., Dujardin, G., 1994. OXA1, a *Saccharomyces cerevisiae* nuclear gene whose sequence is conserved from prokaryotes to eukaryotes controls cytochrome oxidase biogenesis. J. Mol. Biol. 239, 201–212. https://doi.org/10.1006/jmbi.1994.1363.
Bonnet, C., Kaltimbacher, V., Ellouze, S., Augustin, S., Bénit, P., Forster, V., Rustin, P., Sahel, J.A., Corral-Debrinski, M., 2007. Allotopic mRNA localization to the mitochondrial surface rescues respiratory chain defects in fibroblasts harboring mitochondrial DNA mutations affecting complex I or V subunits. Rejuven. Res. 10, 127–144. https://doi.org/10.1089/rej.2006.0526.
Bonnet, C., Augustin, S., Ellouze, S., Bénit, P., Bouaita, A., Rustin, P., Sahel, J.A., Corral-Debrinski, M., 2008. The optimized allotopic expression of ND1 or ND4 genes restores respiratory chain complex I activity in fibroblasts harboring mutations in these genes. Biochim. Biophys. Acta 1783, 1707–1717. https://doi.org/10.1016/j.bbamcr.2008.04.018.
Boominathan, A., Vanhoozer, S., Basisty, N., Powers, K., Crampton, A.L., Wang, X., Friedricks, N., Schilling, B., Brand, M.D., O'Connor, M.S., 2016. Stable nuclear expression of ATP8 and ATP6 genes rescues a mtDNA Complex V null mutant. Nucl. Acids Res. 44, 9342–9357. https://doi.org/10.1093/nar/gkw756.
Boore, J.L., Fuerstenberg, S.I., 1999. *Entamoeba histolytica*: a derived, mitochondriate eukaryote? Trends Microbiol. 7, 426–428. https://doi.org/10.1016/s0966-842x(99)01606-6.
Boos, F., Krämer, L., Groh, C., Jung, F., Haberkant, P., Stein, F., Wollweber, F., Gackstatter, A., Zöller, E., van der Laan, M., Savitski, M.M., Benes, V., Herrmann, J.M. 2019. Publisher Correction: mitochondrial protein-induced stress triggers a global adaptive transcriptional programme. Nat. Cell Biol. 2019 Jun;21: 793-794. doi: 10.1038/s41556-019-0326-1.
Botelho, S.C., Osterberg, M., Reichert, A.S., Yamano, K., Björkholm, P., Endo, T., von Heijne, G., Kim, H., 2011. TIM23-mediated insertion of transmembrane α-helices into the mitochondrial inner membrane. EMBO J. 30, 1003–1011. https://doi.org/10.1038/emboj.2011.29.
Botelho, S.C., Tatsuta, T., von Heijne, G., Kim, H., 2013. Dislocation by the m-AAA protease increases the threshold hydrophobicity for retention of transmembrane helices in the inner membrane of yeast mitochondria. J. Biol. Chem. 288, 4792–4798. https://doi.org/10.1074/jbc.M112.430892.
Breton, S., Stewart, D.T., Hoeh, W.R., 2010. Characterization of a mitochondrial ORF from the gender-associated mtDNAs of Mytilus spp. (Bivalvia: Mytilidae): identification of the "missing" ATPase 8 gene. Mar. Genom. 3, 11–18. https://doi.org/10.1016/j.margen.2010.01.001.
Broadley, S.A., Demlow, C.M., Fox, T.D., 2001. Peripheral mitochondrial inner membrane protein, Mss2p, required for export of the mitochondrially coded Cox2p C tail in *Saccharomyces cerevisiae*. Mol. Cell Biol. 21, 7663–7672. https://doi.org/10.1128/MCB.21.22.7663-7672.2001.
Calabrese, F.M., Balacco, D.L., Preste, R., Diroma, M.A., Forino, R., Ventura, M., Attimonelli, M., 2017. NumtS colonization in mammalian genomes. Sci. Rep. 7, 16357. https://doi.org/10.1038/s41598-017-16750-2.
Calabrese, C., Iommarini, L., Kurelac, I., Calvaruso, M.A., Capristo, M., Lollini, P.L., Nanni, P., Bergamini, C., Nicoletti, G., Giovanni, C.D., Ghelli, A., Giorgio, V., Caratozzolo, M.F., Marzano, F., Manzari, C., Betts, C.M., Carelli, V., Ceccarelli, C., Attimonelli, M., Romeo, G., Fato, R., Rugolo, M., Tullo, A., Gasparre, G., Porcelli, A. M., 2013. Respiratory complex I is essential to induce a Warburg profile in mitochondria-defective tumor cells. Cancer Metab. 1, 11. https://doi.org/10.1186/2049-3002-1-11.
Callegari, S., Cruz-Zaragoza, L.D., Rehling, P., 2020. From TOM to the TIM23 complex - handing over of a precursor. Biol. Chem. 401, 709–721. https://doi.org/10.1515/hsz-2020-0101.
Cardol, P., Lapaille, M., Minet, P., Franck, F., Matagne, R.F., Remacle, C., 2006. ND3 and ND4L subunits of mitochondrial complex I, both nucleus encoded in *Chlamydomonas reinhardtii*, are required for activity and assembly of the enzyme. Eukaryot. Cell 5, 1460–1467. https://doi.org/10.1128/EC.00118-06.
Carelli, V., Ross-Cisneros, F.N., Sadun, A.A., 2004. Mitochondrial dysfunction as a cause of optic neuropathies. Prog. Retin. Eye Res. 23, 53–89. https://doi.org/10.1016/j.preteyeres.2003.10.003.
Chacinska, A., Lind, M., Frazier, A.E., Dudek, J., Meisinger, C., Geissler, A., Sickmann, A., Meyer, H.E., Truscott, K.N., Guiard, B., Pfanner, N., Rehling, P., 2005. Mitochondrial presequence translocase: switching between TOM tethering and motor recruitment involves Tim21 and Tim17. Cell 120, 817–829. https://doi.org/10.1016/j.cell.2005.01.011.
Chacinska, A., Koehler, C.M., Milenkovic, D., Lithgow, T., Pfanner, N., 2009. Importing mitochondrial proteins: machineries and mechanisms. Cell 138, 628–644. https://doi.org/10.1016/j.cell.2009.08.005.
Chacinska, A., van der Laan, M., Mehnert, C.S., Guiard, B., Mick, D.U., Hutu, D.P., Truscott, K.N., Wiedemann, N., Meisinger, C., Pfanner, N., Rehling, P., 2010. Distinct forms of mitochondrial TOM-TIM supercomplexes define signal-dependent states of preprotein sorting. Mol. Cell Biol. 30, 307–318. https://doi.org/10.1128/MCB.00749-09.
Chen, X., Liang, D., Guo, J., Zhang, J., Sun, H., Zhang, X., Jin, J., Dai, Y., Bao, Q., Qian, X., Tan, L., Hu, P., Ling, X., Shen, B., Xu, Z., 2022. DdCBE-mediated mitochondrial base editing in human 3PN embryos. Cell Discov. 8, 8. https://doi.org/10.1038/s41421-021-00358-y.
Chin, R.M., Panavas, T., Brown, J.M., Johnson, K.K., 2018. Optimized mitochondrial targeting of proteins encoded by modified mRNAs rescues cells harboring mutations in mtATP6. Cell Rep. 22, 2809–2817. https://doi.org/10.1016/j.celrep.2018.02.059.
Claros, M.G., Vincens, P., 1996. Computational method to predict mitochondrially imported proteins and their targeting sequences. Eur. J. Biochem. 241, 779–786. https://doi.org/10.1111/j.1432-1033.1996.00779.x.
Claros, M.G., Perea, J., Shu, Y., Samatey, F.A., Popot, J.L., Jacq, C., 1995. Limitations to in vivo import of hydrophobic proteins into yeast mitochondria. The case of a cytoplasmically synthesized apocytochrome b. Eur. J. Biochem. 228, 762–771. https://doi.org/10.1111/j.1432-1033.1995.0762m.x.
Covello, P.S., Gray, M.W., Weil, J.-H., 1992. Silent mitochondrial and active nuclear genes for subunit 2 of cytochrome c oxidase (cox2) in soybean: evidence for RNA-mediated gene transfer. EMBO J. 1, 3815–3820. https://doi.org/10.1016/0168-9525(93)90062-M.
Cruz-Torres, V., Vázquez-Acevedo, M., García-Villegas, R., Pérez-Martínez, X., Mendoza-Hernández, G., González-Halphen, D., 2012. The cytosol-synthesized subunit II (Cox2) precursor with the point mutation W56R is correctly processed in yeast mitochondria to rescue cytochrome oxidase. Biochim. Biophys. Acta 1817, 2128–2139. https://doi.org/10.1016/j.bbabio.2012.09.006. Epub 2012 Sep 15 PMID: 22985601.
Cruz-Zaragoza, L.D., Dennerlein, S., Linden, A., Yousefi, R., Lavdovskaia, E., Aich, A., Falk, R.R., Gomkale, R., Schöndorf, T., Bohnsack, M.T., Richter-Dennerlein, R., Urlaub, H., Rehling, P., 2021. An in vitro system to silence mitochondrial gene expression. Cell 184, 5824–5837.e15. https://doi.org/10.1016/j.cell.2021.09.033.
Cwerman-Thibault, H., Sahel, J.A., Corral-Debrinski, M., 2010. Mitochondrial medicine: to a new era of gene therapy for mitochondrial DNA mutations. J. Inherit. Metab. Dis. 34, 327–344. https://doi.org/10.1007/s10545-010-9131-5.
Cwerman-Thibault, H., Augustin, S., Lechauve, C., Ayache, J., Ellouze, S., Sahel, J.A., Corral-Debrinski, M., 2015. Nuclear expression of mitochondrial ND4 leads to the protein assembling in complex I and prevents optic atrophy and visual loss. Mol. Ther. Methods Clin. Dev. 2, 15003. https://doi.org/10.1038/mtm.2015.3.
Daley, D.O., Adams, K.L., Clifton, R., Qualmann, S., Millar, A.H., Palmer, J.D., Pratje, E., Whelan, J., 2002b. Gene transfer from mitochondrion to nucleus: novel mechanisms for gene activation from Cox2. Plant J. 30, 11–21. https://doi.org/10.1046/j.1365-313x.2002.01263.x.

Daley, D.O., Whelan, J., 2005. Why genes persist in organelle genomes. Genome Biol. 6, 110. https://doi.org/10.1186/gb-2005-6-5-110.
Daley, D.O., Clifton, R., Whelan, J., 2002a. Intracellular gene transfer: reduced hydrophobicity facilitates gene transfer for subunit 2 of cytochrome *c* oxidase. PNAS 99, 10510–10515. https://doi.org/10.1073/pnas.122354399.
de Grey, A.D., 2000. Mitochondrial gene therapy: an arena for the biomedical use of inteins. Trends Biotechnol. 18, 394–399. https://doi.org/10.1016/s0167-7799(00)01476-1.
Degli Esposti, M., Chouaia, B., Comandatore, F., Crotti, E., Sassera, D., Lievens, P.M., Daffonchio, D., Bandi, C., 2014. Evolution of mitochondria reconstructed from the energy metabolism of living bacteria. PLoS One 9, e96566.
Dennerlein, S., Poerschke, S., Oeljeklaus, S., Wang, C., Richter-Dennerlein, R., Sattmann, J., Bauermeister, D., Hanitsch, E., Stoldt, S., Langer, T., Jakobs, S., Warscheid, B., Rehling, P., 2021. Defining the interactome of the human mitochondrial ribosome identifies SMIM4 and TMEM223 as respiratory chain assembly factors. Elife 10, e68213.
Denovan-Wright, E.M., Nedelcu, A.M., Lee, R.W., 1998. Complete sequence of the mitochondrial DNA of Chlamydomonas eugametos. Plant Mol. Biol. 36, 285–295. https://doi.org/10.1023/a:1005995718091.
Di Donfrancesco, A., Massaro, G., Di Meo, I., Tiranti, V., Bottani, E., Brunetti, D., 2022. Gene therapy for mitochondrial diseases: current status and future perspective. Pharmaceutics. 14, 1287. https://doi.org/10.3390/pharmaceutics14061287.
DiMauro, S., Hirano, M., Schon, E.A., 2006. Approaches to the treatment of mitochondrial diseases. Muscle Nerve 34, 265–283. https://doi.org/10.1002/mus.20598.
Dimogkioka, A.R., Lees, J., Lacko, E., Tokatlidis, A., 2021. Protein import in mitochondria biogenesis: guided by targeting signals and sustained by dedicated chaperones. RSC Adv. 11, 32476–32493. https://doi.org/10.1039/d1ra04497d.
Dunn, D.A., Pinkert, C.A., 2012. Nuclear expression of a mitochondrial DNA gene: mitochondrial targeting of allotopically expressed mutant ATP6 in transgenic mice. J. Biomed. Biotechnol. 2012, 541245 https://doi.org/10.1155/2012/541245.
Dunn, D.A., Pinkert, C.A., 2021. Allotopic expression of ATP6 in mouse as a transgenic model of mitochondrial disease. Methods Mol. Biol. 2277, 1–13. https://doi.org/10.1007/978-1-0716-1270-5_1.
Ellouze, S., Augustin, S., Bouaita, A., Bonnet, C., Simonutti, M., Forster, V., Picaud, S., Sahel, J.A., Corral-Debrinski, M., 2008. Optimized allotopic expression of the human mitochondrial ND4 prevents blindness in a rat model of mitochondrial dysfunction. Am. J. Hum. Genet. 83, 373–387. https://doi.org/10.1016/j.ajhg.2008.08.013.
Engelman, D.M., Steitz, T.A., 1981. The spontaneous insertion of proteins into and across membranes: the helical hairpin hypothesis. Cell 23, 411–422. https://doi.org/10.1016/0092-8674(81)90136-7.
Fan, J., Lee, R.W., 2002. Mitochondrial genome of the colorless green alga Polytomella parva: two linear DNA molecules with homologous inverted repeat Termini. Mol. Biol. Evol. 19, 999–1007. https://doi.org/10.1093/oxfordjournals.molbev.a004180.
Farrell, L.B., Gearing, D.P., Nagley, P., 1988. Reprogrammed expression of subunit 9 of the mitochondrial ATPase complex of Saccharomyces cerevisiae. Expression in vitro from a chemically synthesized gene and import into isolated mitochondria. Eur. J. Biochem. 173, 131–137. https://doi.org/10.1111/j.1432-1033.1988.tb13976.x. PMID: 2895707.
Feagin, J.E., Werner, E., Gardner, M.J., Williamson, D.H., Wilson, R.J., 1992. Homologies between the contiguous and fragmented rRNAs of the two Plasmodium falciparum extrachromosomal DNAs are limited to core sequences. Nucleic Acids Res. 20, 879–887. https://doi.org/10.1093/nar/20.4.879.
Fearnley, I.M., Finel, M., Skehel, J.M., Walker, J.E., 1991. NADH:ubiquinone oxidoreductase from bovine heart mitochondria. cDNA sequences of the import precursors of the nuclear-encoded 39 kDa and 42 kDa subunits. Biochem. J 278 (Pt 3), 821–829. https://doi.org/10.1042/bj2780821.
Fiedorczuk, K., Letts, J.A., Degliesposti, G., Kaszuba, K., Skehel, M., Sazanov, L.A., 2016. Atomic structure of the entire mammalian mitochondrial complex I. Nature 538, 406–410. https://doi.org/10.1038/nature19794.
Figueroa-Martínez, F., Vázquez-Acevedo, M., Cortés-Hernández, P., García-Trejo, J.J., Davidson, E., King, M.P., González-Halphen, D., 2011. What limits the allotopic expression of nucleus-encoded mitochondrial genes? The case of the chimeric Cox3 and Atp6 genes. Mitochondrion 11, 147–154. https://doi.org/10.1016/j.mito.2010.09.003.
Fukasawa, Y., Oda, T., Tomii, K., Imai, K., 2017. Origin and evolutionary alteration of the mitochondrial import system in eukaryotic lineages. Mol. Biol. Evol. 34, 1574–1586. https://doi.org/10.1093/molbev/msx096.
Funes, S., Davidson, E., Claros, M.G., van Lis, R., Pérez-Martínez, X., Vázquez-Acevedo, M., King, M.P., González-Halphen, D., 2002a. The typically mitochondrial DNA-encoded ATP6 subunit of the F1F0-ATPase is encoded by a nuclear gene in *Chlamydomonas reinhardtii*. J. Biol. Chem. 277, 6051–6058. https://doi.org/10.1074/jbc.M109993200.
Funes, S., Davidson, E., Reyes-Prieto, A., Magallón, S., Heroin, P., King, M.P., González-Halphen, D., 2002b. A green algal apicoplast ancestor. Science 298, 2155. https://doi.org/10.1126/science.1076003.
Galanis, M., Devenish, R.J., Nagley, P., 1991. Duplication of leader sequence for protein targeting to mitochondria leads to increased import efficiency. FEBS Lett. 282, 425–430. https://doi.org/10.1016/0014-5793(91)80529-c.
Gammage, P.A., Rorbach, J., Vincent, A.I., Rebar, E.J., Minczuk, M., 2014. Mitochondrially targeted ZFNs for selective degradation of pathogenic mitochondrial genomes bearing large-scale deletions or point mutations. EMBO Mol. Med. 6, 458–466. https://doi.org/10.1002/emmm.201303672.
Gammage, P.A., Moraes, C.T., Minczuk, M., 2018. Mitochondrial genome engineering: the revolution may not be CRISPR-Ized. Trends Genet. 34, 101–110. https://doi.org/10.1016/j.tig.2017.11.001.
Ganetzky, R.D., Stendel, C., McCormick, E.M., Zolkipli-Cunningham, Z., Goldstein, A.C., Klopstock, T., Falk, M.J., 2019. MT-ATP6 mitochondrial disease variants: phenotypic and biochemical features analysis in 218 published cases and cohort of 14 new cases. Hum. Mutat. 40, 499–515. https://doi.org/10.1002/humu.23723.
García-Villegas, R., Camacho-Villasana, Y., Shingú-Vázquez, M.Á., Cabrera-Orefice, A., Uribe-Carvajal, S., Fox, T.D., Pérez-Martínez, X., 2017. The Cox1 C-terminal domain is a central regulator of cytochrome *c* oxidase biogenesis in yeast mitochondria. J. Biol. Chem. 292, 10912–10925.
Gardner, M.J., Hall, N., Fung, E., White, O., Berriman, M., Hyman, R.W., Carlton, J.M., Pain, A., Nelson, K.E., Bowman, S., Paulsen, I.T., James, K., Eisen, J.A., Rutherford, K., Salzberg, S.L., Craig, A., Kyes, S., Chan, M.S., Nene, V., Shallom, S.J., Suh, B., Peterson, J., Angiuoli, S., Pertea, M., Allen, J., Selengut, J., Haft, D., Mather, M.W., Vaidya, A.B., Martin, D.M., Fairlamb, A.H., Fraunholz, M.J., Roos, D. S., Ralph, S.A., McFadden, G.I., Cummings, L.M., Subramanian, G.M., Mungall, C., Venter, J.C., Carucci, D.J., Hoffman, S.L., Newbold, C., Davis, R.W., Fraser, C.M., Barrell, B., 2002. Genome sequence of the human malaria parasite *Plasmodium falciparum*. Nature 419, 498–511. https://doi.org/10.1038/nature01097.
Gawryluk, R.M., Gray, M.W., 2010. An ancient fission of mitochondrial Cox1. Mol. Biol. Evol. 27, 7–10. https://doi.org/10.1093/molbev/msp223.
Gearing, D.P., Nagley, P., 1986. Yeast mitochondrial ATPase subunit 8, normally a mitochondrial gene product, expressed in vitro and imported back into the organelle. EMBO J. 5, 3651–3655. https://doi.org/10.1002/j.1460-2075.1986.tb04695.x.
Gebert, M., Schrempp, S.G., Mehnert, C.S., Heißwolf, A.K., Oeljeklaus, S., Ieva, R., Bohnert, M., von der Malsburg, K., Wiese, S., Kleinschroth, T., Hunte, C., Meyer, H. E., Haferkamp, I., Guiard, B., Warscheid, B., Pfanner, N., van der Laan, M., 2012. Mgr2 promotes coupling of the mitochondrial presequence translocase to partner complexes. J. Cell Biol. 197, 595–604. https://doi.org/10.1083/jcb.201110047.
Giannakis, K., Arrowsmith, S.J., Richards, L., Gasparini, S., Chustecki, J.M., Røyrvik, E. C., Johnston, I.G., 2022. Evolutionary inference across eukaryotes identifies universal features shaping organelle gene retention. Cell Syst. 13, 874–884.e5. https://doi.org/10.1016/j.cels.2022.08.007.
Glick, B.S., Brandt, A., Cunningham, K., Müller, S., Hallberg, R.L., Schatz, G., 1992. Cytochromes c1 and b2 are sorted to the intermembrane space of yeast mitochondria by a stop-transfer mechanism. Cell 69, 809–822. https://doi.org/10.1016/0092-8674(92)90292-k.
Gomkale, R., Cruz-Zaragoza, L.D., Suppanz, I., Guiard, B., Montoya, J., Callegari, S., Pacheu-Grau, D., Warscheid, B., Rehling, P., 2020. Defining the substrate spectrum of the TIM22 complex identifies pyruvate carrier subunits as unconventional cargos. Curr. Biol. 30, 1119–1127.e5. https://doi.org/10.1016/j.cub.2020.01.024.
González-Halphen, D., Funes, S., Pérez-Martínez, X., Reyes-Prieto, A., Claros, M.G., Davidson, E., King, M.P., 2004. Genetic correction of mitochondrial diseases: using the natural migration of mitochondrial genes to the nucleus in chlorophyte algae as a model system. Ann. N. Y. Acad. Sci. 1019, 232–239. https://doi.org/10.1196/annals.1297.039.
Gorman, G.S., Chinnery, P.F., DiMauro, S., Hirano, M., Koga, Y., McFarland, R., Suomalainen, A., Thorburn, D.R., Zeviani, M., Turnbull, D.M., 2016. Mitochondrial diseases. Nat. Rev. Dis. Primers. 2, 16080. https://doi.org/10.1038/nrdp.2016.80.
Grasso, D.G., Nero, D., Law, R.H., Devenish, R.J., Nagley, P., 1991. The C-terminal positively charged region of subunit 8 of yeast mitochondrial ATP synthase is required for efficient assembly of this subunit into the membrane F0 sector. Eur. J. Biochem. 199, 203–209. https://doi.org/10.1111/j.1432-1033.1991.tb16110.x.
Gray, M.W., 1989. Origin and evolution of mitochondrial DNA. Annu. Rev. Cell Biol. 5, 25–50. https://doi.org/10.1146/annurev.cb.05.110189.000325.
Gray, M.W., Lang, B.F., Cedergren, R., Golding, G.B., Lemieux, C., Sankoff, D., Turmel, M., Brossard, N., Delage, E., Littlejohn, T.G., Plante, I., Rioux, P., Saint-Louis, D., Zhu, Y., Burger, G., 1998. Genome structure and gene content in protist mitochondrial DNAs. Nucleic Acids Res. 26, 865–878. https://doi.org/10.1093/nar/26.4.865.
Green, D.E., Tzagoloff, A., 1966. The mitochondrial electron transfer chain. Arch. Biochem. Biophys. 116, 293–304. https://doi.org/10.1016/0003-9861(66)90036-1.
Grevel, A., Pfanner, N., Becker, T., 2020. Coupling of import and assembly pathways in mitochondrial protein biogenesis. Biol. Chem. 401, 117–129. https://doi.org/10.1515/hsz-2019-0310.
Gu, J., Zhang, L., Zong, S., Guo, R., Liu, T., Yi, J., Wang, P., Zhuo, W., Yang, M., 2019. Cryo-EM structure of the mammalian ATP synthase tetramer bound with inhibitory protein IF1. Science 364, 1068–1075. https://doi.org/10.1126/science.aaw4852.
Güngör, B., Flohr, T., Garg, S.G., Herrmann, J.M., 2022. The ER membrane complex (EMC) can functionally replace the Oxa1 insertase in mitochondria. PLoS Biol. 20, e3001380.
Guo, R., Zong, S., Wu, M., Gu, J., Yang, M., 2017. Architecture of human mitochondrial respiratory megacomplex I2III2IV2. Cell 170, 1247–1257.e12. https://doi.org/10.1016/j.cell.2017.07.050.
Guy, J., Qi, X., Pallotti, F., Schon, E.A., Manfredi, G., Carelli, V., Martinuzzi, A., Hauswirth, W.W., Lewin, A.S., 2002. Rescue of a mitochondrial deficiency causing Leber Hereditary Optic Neuropathy. Ann. Neurol. 52, 534–542. https://doi.org/10.1002/ana.10354.
Hancock, L., Goff, L., Lane, C., 2010. Red algae lose key mitochondrial genes in response to becoming parasitic. Genome Biol. Evol. 2, 897–910. https://doi.org/10.1093/gbe/evq075.
Hansen, K.G., Herrmann, J.M., 2019. Transport of proteins into mitochondria. Protein J. 38, 330–342. https://doi.org/10.1007/s10930-019-09819-6.
Hartl, F.U., Pfanner, N., Nicholson, D.W., Neupert, W., 1989. Mitochondrial protein import. Biochim. Biophys. Acta 988, 1–45. https://doi.org/10.1016/0304-4157(89)90002-6.
Hashimoto, M., Bacman, S.R., Peralta, S., Falk, M.J., Chomyn, A., Chan, D.C., Williams, S.L., Moraes, C.T., 2015. MitoTALEN: a general approach to reduce mutant

mtDNA loads and restore oxidative phosphorylation function in mitochondrial diseases. Mol. Ther. 23, 1592–1599. https://doi.org/10.1038/mt.2015.126.
He, S., Fox, T.D., 1997. Membrane translocation of mitochondrially coded Cox2p: distinct requirements for export of N and C termini and dependence on the conserved protein Oxa1p. Mol. Biol. Cell 8, 1449–1460. https://doi.org/10.1091/mbc.8.8.1449.
Hell, K., Neupert, W., Stuart, R.A., 2001. Oxa1p acts as a general membrane insertion machinery for proteins encoded by mitochondrial DNA. EMBO J. 20, 1281–1288. https://doi.org/10.1093/emboj/20.6.1281.
Henze, K., Martin, W., 2001. How do mitochondrial genes get into the nucleus? Trends Genet. 17, 383–387. https://doi.org/10.1016/s0168-9525(01)02312-5.
Herlan, M., Vogel, F., Bornhovd, C., Neupert, W., Reichert, A.S., 2003. Processing of Mgm1 by the rhomboid-type protease Pcp1 is required for maintenance of mitochondrial morphology and of mitochondrial DNA. J. Biol. Chem. 278, 27781–27788. https://doi.org/10.1074/jbc.M211311200.
Herrmann, J.M., Neupert, W., Stuart, R.A., 1997. Insertion into the mitochondrial inner membrane of a polytopic protein, the nuclear-encoded Oxa1p. EMBO J. 16, 2217–2226. https://doi.org/10.1093/emboj/16.9.2217.
Herrmann, J.M., Neupert, W., 2003. Protein insertion into the inner membrane of mitochondria. IUBMB Life 55, 219–225. https://doi.org/10.1080/1521654031000123349.
Hewitt, V., Alcock, F., Lithgow, T., 2011. Minor modifications and major adaptations: the evolution of molecular machines driving mitochondrial protein import. Biochim. Biophys. Acta 1808, 947–954. https://doi.org/10.1016/j.bbamem.2010.07.019.
Hoffmann, A., Hildebrandt, V., Heberle, J., Büldt, G., 1994. Photoactive mitochondria: in vivo transfer of a light-driven proton pump into the inner mitochondrial membrane of *Schizosaccharomyces pombe*. PNAS 91, 9367–9371. https://doi.org/10.1073/pnas.91.20.9367.
Hong, S., Pedersen, P.L., 2004. Mitochondrial ATP synthase: a bioinformatic approach reveals new insights about the roles of supernumerary subunits g and A6L. J. Bioenerg. Biomembr. 36, 515–523. https://doi.org/10.1007/s10863-004-8998-y.
Horten, P., Colina-Tenorio, L., Rampelt, H., 2020. Biogenesis of Mitochondrial Metabolite Carriers. Biomolecules 10, 1008. https://doi.org/10.3390/biom10071008.
Horwich, A.L., Kalousek, F., Mellman, I., Rosenberg, L.E., 1985. A leader peptide is sufficient to direct mitochondrial import of a chimeric protein. EMBO J. 4, 1129–1135. https://doi.org/10.1002/j.1460-2075.1985.tb03750.x.
Howell, N., Bindoff, L.A., McCullough, D.A., Kubacka, I., Poulton, J., Mackey, D., Taylor, L., Turnbull, D.M., 1991. Leber hereditary optic neuropathy: identification of the same mitochondrial ND1 mutation in six pedigrees. Am. J. Hum. Genet. 49, 939–950. PMID: 1928099.
Huang, S., Braun, H.P., Gawryluk, R.M.R., Millar, A.H., 2019. Mitochondrial complex II of plants: subunit composition, assembly, and function in respiration and signaling. Plant J. 98, 405–417. https://doi.org/10.1111/tpj.14227.
Hussain, S.A., Yalvac, M.E., Khoo, B., Eckardt, S., McLaughlin, K.J., 2021. Adapting CRISPR/Cas9 system for targeting mitochondrial genome. Front. Genet. 12, 627050 https://doi.org/10.3389/fgene.2021.627050.
Ieva, R., Schrempp, S.G., Opaliński, L., Wollweber, F., Höß, P., Heißwolf, A.K., Gebert, M., Zhang, Y., Guiard, B., Rospert, S., Becker, T., Chacinska, A., Pfanner, N., van der Laan, M., 2014. Mgr2 functions as lateral gatekeeper for preprotein sorting in the mitochondrial inner membrane. Mol. Cell 56 (5), 641–652. https://doi.org/10.1016/j.molcel.2014.10.010.
Inaoka, D.K., Shiba, T., Sato, D., Balogun, E.O., Sasaki, T., Nagahama, M., Oda, M., Matsuoka, S., Ohmori, J., Honma, T., Inoue, M., Kita, K., Harada, S., 2015. Structural insights into the molecular design of flutolanil derivatives targeted for fumarate respiration of parasite mitochondria. Int. J. Mol. Sci. 16, 15287–15308. https://doi.org/10.3390/ijms160715287.
Iommarini, L., Ghelli, A., Tropeano, C.V., Kurelac, I., Leone, G., Vidoni, S., Lombes, A., Zeviani, M., Gasparre, G., Porcelli, A.M., 2018. Unravelling the Effects of the Mutation m.3571insC/MT-ND1 on Respiratory Complexes Structural Organization. Int. J. Mol. Sci. 19, 764. https://doi.org/10.3390/ijms19030764.
Itoh, Y., Andréll, J., Choi, A., Richter, U., Maiti, P., Best, R.B., Barrientos, A., Battersby, B. J., Amunts, A., 2021. Mechanism of membrane-tethered mitochondrial protein synthesis. Science 371, 846–849. https://doi.org/10.1126/science.abe0763.
Iwata, S., Lee, J.W., Okada, K., Lee, J.K., Iwata, M., Rasmussen, B., Link, T.A., Ramaswamy, S., Jap, B.K., 1998. Complete structure of the 11-subunit bovine mitochondrial cytochrome bc1 complex. Science 281, 64–71. https://doi.org/10.1126/science.281.5373.64.
Jiménez-Suárez, A., Vázquez-Acevedo, M., Rojas-Hernández, A., Funes, S., Uribe-Carvajal, S., González-Halphen, D., 2012. In Polytomella sp. mitochondria, biogenesis of the heterodimeric COX2 subunit of cytochrome c oxidase requires two different import pathways. Biochim. Biophys. Acta 1817, 819–827. https://doi.org/10.1016/j.bbabio.2012.02.038.
Jin, Z., Wan, L., Zhang, Y., Li, X., Cao, Y., Liu, H., Fan, S., Cao, D., Wang, Z., Li, X., Pan, J., Dong, M.Q., Wu, J., Yan, Z., 2022. Structure of a TOC-TIC super complex spanning two chloroplast envelope membranes. Cell 185, 4788–4800.e13. https://doi.org/10.1016/j.cell.2022.10.030.
John, U., Lu, Y., Wohlrab, S., Groth, M., Janouškovec, J., Kohli, G.S., Mark, F.C., Bickmeyer, U., Farhat, S., Felder, M., Frickenhaus, S., Guillou, L., Keeling, P.J., Moustafa, A., Porcel, B.M., Valentin, K., Glöckner, G., 2019. An aerobic eukaryotic parasite with functional mitochondria that likely lacks a mitochondrial genome. Sci. Adv. 5, eaav1110. https://doi.org/10.1126/sciadv.aav1110.
Johnston, I.G., Williams, B.P., 2016. Evolutionary inference across eukaryotes identifies specific pressures favoring mitochondrial gene retention. Cell Syst. 2, 101–111. https://doi.org/10.1016/j.cels.2016.01.013.
Jun, A.S., Brown, M.D., Wallace, D.C., 1994. A mitochondrial DNA mutation at nucleotide pair 14459 of the NADH dehydrogenase subunit 6 gene associated with maternally inherited Leber hereditary optic neuropathy and dystonia. PNAS 91, 6206–6210. https://doi.org/10.1073/pnas.91.13.6206.
Kadowaki, K., Kubo, N., Ozawa, K., Hirai, A., 1996. Targeting presequence acquisition after mitochondrial gene transfer to the nucleus occurs by duplication of existing targeting signals. The EMBO Journal 15, 6652–6661. https://doi.org/10.1002/j.1460-2075.1996.tb01055.x.
Kalef-Ezra, E., Kotzamani, D., Zaganas, I., Katrakili, N., Plaitakis, A., Tokatlidis, K., 2016. Import of a major mitochondrial enzyme depends on synergy between two distinct helices of its presequence. Biochem. J 473, 2813–2829. https://doi.org/10.1042/BCJ20160535.
Kaltimbacher, V., Bonnet, C., Lecoeuvre, G., Forster, V., Sahel, J.A., Corral-Debrinski, M., 2006. mRNA localization to the mitochondrial surface allows the efficient translocation inside the organelle of a nuclear recoded ATP6 protein. RNA 12, 1408–1417. https://doi.org/10.1261/rna.18206.
King, M.P., Attardi, G., 1989. Human cells lacking mtDNA: repopulation with exogenous mitochondria by complementation. Science 246, 500–503. https://doi.org/10.1126/science.2814477.
Koilkonda, R.D., Chou, T.H., Porciatti, V., Hauswirth, W.W., Guy, J., 2010. Induction of rapid and highly efficient expression of the human ND4 complex I subunit in the mouse visual system by self-complementary adeno-associated virus. Arch. Ophthalmol. 128, 876–883. https://doi.org/10.1001/archophthalmol.2010.135.
Korbel, D., Wurth, S., Käser, M., Langer, T., 2004. Membrane protein turnover by the m-AAA protease in mitochondria depends on the transmembrane domains of its subunits. EMBO Rep. 5, 698–703. https://doi.org/10.1038/sj.embor.7400186.
Kucharczyk, R., Dautant, A., Gombeau, K., Godard, F., Tribouillard-Tanvier, D., di Rago, J.P., 2019. The pathogenic MT-ATP6 m.8851T>C mutation prevents proton movements within the n-side hydrophilic cleft of the membrane domain of ATP synthase. Biochim. Biophys. Acta Bioenerg. 1860, 562–572. https://doi.org/10.1016/j.bbabio.2019.06.002.
Kummer, E., Ban, N., 2021. Mechanisms and regulation of protein synthesis in mitochondria. Nat. Rev. Mol. Cell Biol. 22, 307–325. https://doi.org/10.1038/s41580-021-00332-2.
Kyriakouli, D.S., Boesch, P., Taylor, R.W., Lightowlers, R.N., 2008. Progress and prospects: gene therapy for mitochondrial DNA disease. Gene Ther. 15, 1017–1023. https://doi.org/10.1038/gt.2008.91.
La Morgia, C., Maresca, A., Caporali, L., Valentino, M.L., Carelli, V., 2020. Mitochondrial diseases in adults. J. Intern. Med. 287, 592–608. https://doi.org/10.1111/joim.13064.
Lai, Y., Zhang, Y., Zhou, S., Xu, J., Du, Z., Feng, Z., Yu, L., Zhao, Z., Wang, W., Tang, Y., Yang, X., Guddat, L.W., Liu, F., Gao, Y., Rao, Z., Gong, H., 2023. Structure of the human ATP synthase. Mol Cell,:S1097–2765(23), 00324–00326. https://doi.org/10.1016/j.molcel.2023.04.029.
Lam, B.L., Feuer, W.J., Abukhalil, F., Porciatti, V., Hauswirth, W.W., Guy, J., 2010. Leber hereditary optic neuropathy gene therapy clinical trial recruitment: year 1. Arch. Ophthalmol. 128, 1129–1135. https://doi.org/10.1001/archophthalmol.2010.201.
Lam, B.L., Feuer, W.J., Davis, J.L., Porciatti, V., Yu, H., Levy, R.B., Vanner, E., Guy, J., 2022. Leber hereditary optic neuropathy gene therapy: adverse events and visual acuity results of all patient groups. Am. J. Ophthalmol. 241, 262–271. https://doi.org/10.1016/j.ajo.2022.02.023.
Law, R.H., Farrell, L.B., Nero, D., Devenish, R.J., Nagley, P., 1988. Studies on the import into mitochondria of yeast ATP synthase subunits 8 and 9 encoded by artificial nuclear genes. FEBS Lett. 236, 501–505. https://doi.org/10.1016/0014-5793(88)80086-3.
Law, R.H., Devenish, R.J., Nagley, P., 1990. Assembly of imported subunit 8 into the ATP synthase complex of isolated yeast mitochondria. Eur. J. Biochem. 188, 421–429. https://doi.org/10.1111/j.1432-1033.1990.tb15419.x.
Lee, S., Lee, H., Yoo, S., Ieva, R., van der Laan, M., von Heijne, G., Kim, H., 2020. The Mgr2 subunit of the TIM23 complex regulates membrane insertion of marginal stop-transfer signals in the mitochondrial inner membrane. FEBS Lett. 594, 1081–1087. https://doi.org/10.1002/1873-3468.13692.
Lei, Z., Meng, H., Liu, L., Zhao, H., Rao, X., Yan, Y., Wu, H., Liu, M., He, A., Yi, C., 2022. Mitochondrial base editor induces substantial nuclear off-target mutations. Nature 606, 804–811. https://doi.org/10.1038/s41586-022-04836-5.
Letts, J.A., Fiedorczuk, K., Sazanov, L.A., 2016. The architecture of respiratory supercomplexes. Nature 537, 644–648. https://doi.org/10.1038/nature19774.
Lewis, C.J., Dixit, B., Batiuk, E., Hall, C.J., O'Connor, M.S., Boominathan, A., 2020. Codon optimization is an essential parameter for the efficient allotopic expression of mtDNA genes. Redox Biol. 30, 101429 https://doi.org/10.1016/j.redox.2020.101429.
Liu, Z., Li, X., Zhao, P., Gui, J., Zheng, W., Zhang, Y., 2011. Tracing the evolution of the mitochondrial protein import machinery. Comput. Biol. Chem. 35, 336–340. https://doi.org/10.1016/j.compbiolchem.2011.10.005.
Liu, H., Li, A., Rochaix, J.D., Liu, Z., 2023. Architecture of chloroplast TOC-TIC translocon supercomplex. Nature 615, 349–357. https://doi.org/10.1038/s41586-023-05744-y.
Lutz-Bonengel, S., Niederstätter, H., Naue, J., Koziel, R., Yang, F., Sänger, T., Huber, G., Berger, C., Pflugradt, R., Strobl, C., Xavier, C., Volleth, M., Weiß, S.C., Irwin, J.A., Romsos, E.L., Vallone, P.M., Ratzinger, G., Schmuth, M., Jansen-Dürr, P., Liehr, T., Lichter, P., Parsons, T.J., Pollak, S., Parson, W., 2021. Evidence for multi-copy Mega-NUMTs in the human genome. Nucleic Acids Res. 49, 1517–1531. https://doi.org/10.1093/nar/gkaa1271.
Lynch, M., 1997. Mutation accumulation in nuclear, organelle, and prokaryotic transfer RNA genes. Mol. Biol. Evol. 14, 914–925. https://doi.org/10.1093/oxfordjournals.molbev.a025834.

Ma, C., Wu, X., Sun, D., Park, E., Catipovic, M.A., Rapoport, T.A., Gao, N., Li, L., 2019. Structure of the substrate-engaged SecA-SecY protein translocation machine. Nat. Commun. 10, 2872. https://doi.org/10.1038/s41467-019-10918-2.

Macino, G., Coruzzi, G., Nobrega, F.G., Li, M., Tzagoloff, A., 1979. Use of the UGA terminator as a tryptophan codon in yeast mitochondria. PNAS 76, 3784–3785. https://doi.org/10.1073/pnas.76.8.3784.

Mahlke, K., Pfanner, N., Martin, J., Horwich, A.L., Hartl, F.U., Neupert, W., 1990. Sorting pathways of mitochondrial inner membrane proteins. Eur. J. Biochem. 192, 551–555. https://doi.org/10.1111/j.1432-1033.1990.tb19260.x.

Manfredi, G., Fu, J., Ojaimi, J., Sadlock, J.E., Kwong, J.Q., Guy, J., Schon, E.A., 2002. Rescue of a deficiency in ATP synthesis by transfer of MTATP6, a mitochondrial DNA-encoded gene, to the nucleus. Nat. Genet. 30, 394–399. https://doi.org/10.1038/ng851.

Manickam, A.H., Michael, M.J., Ramasamy, S., 2017. Mitochondrial genetics and therapeutic overview of Leber's hereditary optic neuropathy. Indian J. Ophthalmol. 65, 1087–1092. https://doi.org/10.4103/ijo.IJO_358_17.

Markantone, D.M., Towheed, A., Crain, A.T., Collins, J.M., Celotto, A.M., Palladino, M.J., 2018. Protein coding mitochondrial-targeted RNAs rescue mitochondrial disease in vivo. Neurobiol. Dis. 117, 203–210. https://doi.org/10.1016/j.nbd.2018.06.009.

Martijn, J., Vosseberg, J., Guy, L., Offre, P., Ettema, T.J.G., 2018. Deep mitochondrial origin outside the sampled alphaproteobacteria. Nature 557, 101–105. https://doi.org/10.1038/s41586-018-0059-5.

Martin, W., Müller, M., 1998. The hydrogen hypothesis for the origin of the first eukaryote. Nature 392, 37–41. https://doi.org/10.1038/32096.

Matouschek, A., Azem, A., Ratliff, K., Glick, B.S., Schmid, K., Schatz, G., 1997. Active unfolding of precursor proteins during mitochondrial protein import. EMBO J. 16, 6727–6736. https://doi.org/10.1093/emboj/16.22.6727.

Matta, S.K., Kumar, A., D' Silva, P., 2020. Mgr2 regulates mitochondrial preprotein import by associating with channel-forming Tim23 subunit. Mol. Biol. Cell 31, 1112–1123. https://doi.org/10.1091/mbc.E19-12-0677.

McDowell, M.A., Heimes, M., Sinning, I., 2021. Structural and molecular mechanisms for membrane protein biogenesis by the Oxa1 superfamily. Nat. Struct. Mol. Biol. 28, 234–239. https://doi.org/10.1038/s41594-021-00567-9.

Meier, S., Neupe,rt, W., Herrmann, J.M., 2005. Proline residues of transmembrane domains determine the sorting of inner membrane proteins in mitochondria. J. Cell Biol. 170, 881-888. doi: 10.1083/jcb.200505126.

Merchant, S.S., Prochnik, S.E., Vallon, O., Harris, E.H., Karpowicz, S.J., Witman, G.B., Terry, A., Salamov, A., Fritz-Laylin, L.K., Maréchal-Drouard, L., Marshall, W.F., Qu, L.H., Nelson, D.R., Sanderfoot, A.A., Spalding, M.H., Kapitonov, V.V., Ren, Q., Ferris, P., Lindquist, E., Shapiro, H., Lucas, S.M., Grimwood, J., Schmutz, J., Cardol, P., Cerutti, H., Chanfreau, G., Chen, C.L., Cognat, V., Croft, M.T., Dent, R., Dutcher, S., Fernández, E., Fukuzawa, H., González-Ballester, D., González-Halphen, D., Hallmann, A., Hanikenne, M., Hippler, M., Inwood, W., Jabbari, K., Kalanon, M., Kuras, R., Lefebvre, P.A., Lemaire, S.D., Lobanov, A.V., Lohr, M., Manuell, A., Meier, I., Mets, L., Mittag, M., Mittelmeier, T., Moroney, J.V., Moseley, J., Napoli, C., Nedelcu, A.M., Niyogi, K., Novoselov, S.V., Paulsen, I.T., Pazour, G., Purton, S., Ral, J.P., Riaño-Pachón, D.M., Riekhof, W., Rymarquis, L., Schroda, M., Stern, D., Umen, J., Willows, R., Wilson, N., Zimmer, S.L., Allmer, J., Balk, J., Bisova, K., Chen, C.J., Elias, M., Gendler, K., Hauser, C., Lamb, M.R., Ledford, H., Long, J.C., Minagawa, J., Page, M.D., Pan, J., Pootakham, W., Roje, S., Rose, A., Stahlberg, E., Terauchi, A.M., Yang, P., Ball, S., Bowler, C., Dieckmann, C. L., Gladyshev, V.N., Green, P., Jorgensen, R., Mayfield, S., Mueller-Roeber, B., Rajamani, S., Sayre, R.T., Brokstein, P., Dubchak, I., Goodstein, D., Hornick, L., Huang, Y.W., Jhaveri, J., Luo, Y., Martínez, D., Ngau, W.C., Otillar, B., Poliakov, A., Porter, A., Szajkowski, L., Werner, G., Zhou, K., Grigoriev, I.V., Rokhsar, D.S., Grossman, A.R., 2007. The Chlamydomonas genome reveals the evolution of key animal and plant functions. Science 318, 245–250. https://doi.org/10.1126/science.1143609.

Mitchell, P., 1961. Coupling of phosphorylation to electron and hydrogen transfer by a chemi-osmotic type of mechanism. Nature 191, 144–148. https://doi.org/10.1038/191144a0.

Mok, B.Y., de Moraes, M.H., Zeng, J., Bosch, D.E., Kotrys, A.V., Raguram, A., Hsu, F., Radey, M.C., Peterson, S.B., Mootha, V.K., Mougous, J.D., Liu, D.R., 2020. A bacterial cytidine deaminase toxin enables CRISPR-free mitochondrial base editing. Nature 583, 631–637. https://doi.org/10.1038/s41586-020-2477-4.

Mossmann, D., Meisinger, C., Vögtle, F.N., 2012. Processing of mitochondrial presequences. Biochim. Biophys. Acta 1819, 1098–1106. https://doi.org/10.1016/j.bbagrm.2011.11.007.

Mühleip, A., Kock Flygaard, R., Ovciarikova, J., Lacombe, A., Fernandes, P., Sheiner, L., Amunts, A., 2021. ATP synthase hexamer assemblies shape cristae of Toxoplasma mitochondria. Nat. Commun. 12, 120. https://doi.org/10.1038/s41467-020-20381-z.

Murphy, B.J., Klusch, N., Langer, J., Mills, D.J., Yildiz, Ö., Kühlbrandt, W., 2019. Rotary substates of mitochondrial ATP synthase reveal the basis of flexible F1-Fo coupling. Science 364(6446), eaaw9128. doi: 10.1126/science.aaw9128.

Nagley, P., Devenish, R.J., 1989. Leading organellar proteins along new pathways: the relocation of mitochondrial genes and chloroplast genes to the nucleus. Trends Biochem. Sci 14, 31–35. https://doi.org/10.1016/0968-0004(89)90087-X.

Nagley, P., Farrell, L.B., Gearing, D.P., Nero, D., Meltzer, S., Devenish, R.J., 1988. Assembly of functional proton-translocating ATPase complex in yeast mitochondria with cytoplasmically synthesized subunit 8, a polypeptide normally encoded within the organelle. PNAS 85, 2091–2095. https://doi.org/10.1073/pnas.85.7.2091.

Naithani, S., Saracco, S.A., Butler, C.A., Fox, T.D., 2003. Interactions among COX1, COX2, and COX3 mRNA-specific translational activator proteins on the inner surface of the mitochondrial inner membrane of *Saccharomyces cerevisiae*. Mol. Biol. Cell 14, 324–333. https://doi.org/10.1091/mbc.e02-08-0490.

Nakazato, I., Okuno, M., Zhou, C., Itoh, T., Tsutsumi, N., Takenaka, M., Arimura, S.I., 2022. Targeted base editing in the mitochondrial genome of *Arabidopsis thaliana*. PNAS 119. https://doi.org/10.1073/pnas.2121177119 e2121177119.

Needs, H.I., Protasoni, M., Henley, J.M., Prudent, J., Collinson, I., Pereira, G.C., 2021. Interplay between mitochondrial protein import and respiratory complexes assembly in neuronal health and degeneration. Life (basel). 11, 432. https://doi.org/10.3390/life11050432.

Nero, D., Ekkel, S.M., Wang, L.F., Grasso, D.G., Nagley, P., 1990. Site directed mutagenesis of subunit 8 of yeast mitochondrial ATP synthase. Functional and import properties of a series of C-terminally truncated forms. FEBS Lett. 270, 62–66. https://doi.org/10.1016/0014-5793(90)81235-g.

Neupert, W., 2015. A perspective on transport of proteins into mitochondria: a myriad of open questions. J. Mol. Biol. 427 (Pt A), 1135–1158. https://doi.org/10.1016/j.jmb.2015.02.001.

Newman, N.J., Yu-Wai-Man, P., Subramanian, P.S., Moster, M.L., Wang, A.G., Donahue, S.P., Leroy, B.P., Carelli, V., Biousse, V., Vignal-Clermont, C., Sergott, R.C., Sadun, A. A., Rebolleda Fernández, G., Chwalisz, B.K., Banik, R., Bazin, F., Roux, M., Cox, E.D., Taiel, M., Sahel, J.A.; LHON REFLECT Study Group, 2023. Randomized trial of bilateral gene therapy injection for m.11778G>A MT-ND4 Leber optic neuropathy. Brain. 146(4):1328-1341. doi: 10.1093/brain/awac421.

Newman, N.J., Yu-Wai-Man, P., Carelli, V., Biousse, V., Moster, M.L., Vignal-Clermont, C., Sergott, R.C., Klopstock, T., Sadun, A.A., Girmens, J.F., La Morgia, C., DeBusk, A.A., Jurkute, N., Priglinger, C., Karanjia, R., Josse, C., Salzmann, J., Montestruc, F., Roux, M., Taiel, M., Sahel, J.A., 2021. Intravitreal gene therapy vs. natural history in patients with leber hereditary optic neuropathy carrying the m.11778G>A ND4 mutation, systematic review and indirect comparison. Front Neurol. 12, 662838 https://doi.org/10.3389/fneur.2021.662838.

Ng, Y.S., Bindoff, L.A., Gorman, G.S., Klopstock, T., Kornblum, C., Mancuso, M., McFarland, R., Sue, C.M., Suomalainen, A., Taylor, R.W., Thorburn, D.R., Turnbull, D.M., 2021. Mitochondrial disease in adults: recent advances and future promise. Lancet Neurol. 20, 573–584. https://doi.org/10.1016/S1474-4422(21)00098-3.

Nie, Z.J., Gu, R.B., Du, F.K., Shao, N.L., Xu, P., Xu, G.C., 2016. Monogonont rotifer, *Brachionus calyciflorus*, possesses exceptionally large, fragmented mitogenome. Plos One. 11, e0168263.

Nugent, J.M., Palmer, J.D., 1991. RNA-mediated transfer of the gene coxII from the mitochondrion to the nucleus during flowering plant evolution. Cell 66, 473–481. https://doi.org/10.1016/0092-8674(81)90011-8.

Oca-Cossio, J., Kenyon, L., Hao, H., Moraes, C.T., 2003. Limitations of allotopic expression of mitochondrial genes in mammalian cells. Genetics 165, 707–720. https://doi.org/10.1093/genetics/165.2.707.

Ojaimi, J., Pan, J., Santra, S., Snell, W.J., Schon, E.A., 2002. An algal nucleus-encoded subunit of mitochondrial ATP synthase rescues a defect in the analogous human mitochondrial-encoded subunit. Mol. Biol. Cell 13, 3836–3844. https://doi.org/10.1091/mbc.e02-05-0306.

Omura, T., 1998. Mitochondria-targeting sequence, a multi-role sorting sequence recognized at all steps of protein import into mitochondria. J. Biochem. 123, 1010–1016. https://doi.org/10.1093/oxfordjournals.jbchem.a022036.

Osterberg, M., Calado Botelho, S., von Heijne, G., Kim, H., 2011. Charged flanking residues control the efficiency of membrane insertion of the first transmembrane segment in yeast mitochondrial Mgm1p. FEBS Lett. 85, 1238–1242. https://doi.org/10.1016/j.febslet.2011.03.056.

Ott, M., Herrmann, J.M., 2010. Co-translational membrane insertion of mitochondrially encoded proteins. Biochim. Biophys. Acta 1803, 767–775. https://doi.org/10.1016/j.bbamcr.2009.11.010.

Ott, M., Prestele, M., Bauerschmitt, H., Funes, S., Bonnefoy, N., Herrmann, J.M., 2006. Mba1, a membrane-associated ribosome receptor in mitochondria. EMBO J. 25, 1603–1610. https://doi.org/10.1038/sj.emboj.7601070.

Papa, S., Martino, P.L., Capitanio, G., Gaballo, A., De Rasmo, D., Signorile, A., Petruzzella, V., 2012. The oxidative phosphorylation system in mammalian mitochondria. Adv. Exp. Med. Biol. 942, 3–37. https://doi.org/10.1007/978-94-007-2869-1_1.

Perales-Clemente, E., Fernández-Silva, P., Acin-Pérez, R., Pérez-Martos, A., Enríquez, J. A., 2010. Allotopic expression of mitochondrial-encoded genes in mammals: achieved goal, undemonstrated mechanism or impossible task? Nucleic Acids Res. 39, 225–234. https://doi.org/10.1093/nar/gkq769.

Pérez-Martínez, X., Vazquez-Acevedo, M., Tolkunova, E., Funes, S., Claros, M.G., Davidson, E., King, M.P., González-Halphen, D., 2000. Unusual location of a mitochondrial gene. Subunit III of cytochrome C oxidase is encoded in the nucleus of Chlamydomonad algae. J. Biol. Chem. 275, 30144–30152. https://doi.org/10.1074/jbc.M003940200.

Pérez-Martínez, X., Antaramian, A., Vazquez-Acevedo, M., Funes, S., Tolkunova, E., d'Alayer, J., Claros, M.G., Davidson, E., King, M.P., González-Halphen, D., 2001. Subunit II of cytochrome c oxidase in Chlamydomonad algae is a heterodimer encoded by two independent nuclear genes. J. Biol. Chem. 276, 11302–11309. https://doi.org/10.1074/jbc.M010244200.

Pérez-Martinez, X., Butler, C.A., Shingú-Vázquez, M., Fox, T.D., 2009. Dual functions of Mss51 couple synthesis of Cox1 to assembly of cytochrome c oxidase in *Saccharomyces cerevisiae* mitochondria. Mol. Biol. Cell 20, 4371–4380. https://doi.org/10.1091/mbc.e09-06-0522.

Pérez-Martínez, X., Funes, S., Tolkunova, E., Davidson, E., King, M.P., González-Halphen, D., 2002. Structure of nuclear-localized cox3 genes in *Chlamydomonas reinhardtii* and in its colorless close relative *Polytomella* sp. Curr. Genet. 40, 399–404. https://doi.org/10.1007/s00294-002-0270-6.

Pfanner, N., Warscheid, B., Wiedemann, N., 2019. Mitochondrial proteins: from biogenesis to functional networks. Nat. Rev. Mol. Cell Biol. 20, 267–284. https://doi.org/10.1038/s41580-018-0092-0.

Pineau, B., Mathieu, C., Gérard-Hirne, C., De Paepe, R., Chétrit, P., 2005. Targeting the NAD7 subunit to mitochondria restores a functional complex I and a wild-type phenotype in the *Nicotiana sylvestris* CMS II mutant lacking nad7. J. Biol. Chem. 280, 25994–26001. https://doi.org/10.1074/jbc.M500508200.

Pinke, G., Zhou, L., Sazanov, L.A., 2020. Cryo-EM structure of the entire mammalian F-type ATP synthase. Nat. Struct. Mol. Biol. 27, 1077–1085. https://doi.org/10.1038/s41594-020-0503-8.

Popot, J.L., de Vitry, C., 1990. On the microassembly of integral membrane proteins. Annu. Rev. Biophys. Biophys. Chem. 19, 369–403. https://doi.org/10.1146/annurev.bb.19.060190.002101.

Preuss, M., Ott, M., Funes, S., Luirink, J., Herrmann, J.M., 2005. Evolution of mitochondrial oxa proteins from bacterial YidC. Inherited and acquired functions of a conserved protein insertion machinery. J. Biol. Chem. 280, 13004–13011. https://doi.org/10.1074/jbc.M414093200.

Pritchard, A.E., Seilhamer, J.J., Mahalingam, R., Sable, C.L., Venuti, S.E., Cummings, D. J., 1990. Nucleotide sequence of the mitochondrial genome of Paramecium. Nucl. Acids Res. 18 (173–1), 80. https://doi.org/10.1093/nar/18.1.173. PMID: 2308823; PMCID: PMC330218.

Prochnik, S.E., Umen, J., Nedelcu, A.M., Hallmann, A., Miller, S.M., Nishii, I., Ferris, P., Kuo, A., Mitros, T., Fritz-Laylin, L.K., Hellsten, U., Chapman, J., Simakov, O., Rensing, S.A., Terry, A., Pangilinan, J., Kapitonov, V., Jurka, J., Salamov, A., Shapiro, H., Schmutz, J., Grimwood, J., Lindquist, E., Lucas, S., Grigoriev, I.V., Schmitt, R., Kirk, D., Rokhsar, D.S., 2010. Genomic analysis of organismal complexity in the multicellular green alga *Volvox carteri*. Science 329, 223–226. https://doi.org/10.1126/science.1188800.

Qi, X., Sun, L., Lewin, A.S., Hauswirth, W.W., Guy, J., 2007. The mutant human ND4 subunit of complex I induces optic neuropathy in the mouse. Invest. Ophthalmol. Vis. Sci. 48, 1–10. https://doi.org/10.1167/iovs.06-0789.

Qi, L., Wang, Q., Guan, Z., Wu, Y., Shen, C., Hong, S., Cao, J., Zhang, X., Yan, C., Yin, P., 2021. Cryo-EM structure of the human mitochondrial translocase TIM22 complex. Cell Res. 31, 369–372. https://doi.org/10.1038/s41422-020-00400-w.

Qualmann, S.R., Daley, D.O., Whelan, J., Pratje, E., 2003. Import pathway of nuclear-encoded cytochrome c oxidase subunit 2 using yeast as a model. Plant Biol. (Stuttg.) 5, 481–490. https://doi.org/10.1055/s-2003-44781.

Rampelt, H., Sucec, I., Bersch, B., Horten, P., Perschil, I., Martinou, J.C., van der Laan, M., Wiedemann, N., Schanda, P., Pfanner, N., 2020. The mitochondrial carrier pathway transports non-canonical substrates with an odd number of transmembrane segments. BMC Biol. 18 (1), 2. https://doi.org/10.1186/s12915-019-0733-6.

Rath, S., Sharma, R., Gupta, R., Ast, T., Chan, C., Durham, T.J., Goodman, R.P., Grabarek, Z., Haas, M.E., Hung, W.H.W., Joshi, P.R., Jourdain, A.A., Kim, S.H., Kotrys, A.V., Lam, S.S., McCoy, J.G., Meisel, J.D., Miranda, M., Panda, A., Patgiri, A., Rogers, R., Sadre, S., Shah, H., Skinner, O.S., To, T.L., Walker, M.A., Wang, H., Ward, P.S., Wengrod, J., Yuan, C.C., Calvo, S.E., Mootha, V.K., 2021. MitoCarta3.0: an updated mitochondrial proteome now with sub-organelle localization and pathway annotations. Nucl. Acids Res. 49, D1541–D1547. https://doi.org/10.1093/nar/gkaa1011.

R Core Team, 2021. R: A Language and Environment for Statistical Computing. R Foundation for Statistical Computing. https://www.R-project.org/.

Rehling, P., Pfanner, N., Meisinger, C., 2003. Insertion of hydrophobic membrane proteins into the inner mitochondrial membrane–a guided tour. J. Mol. Biol. 326, 639–657. https://doi.org/10.1016/s0022-2836(02)01440-7.

Rehling, P., Brandner, K., Pfanner, N., 2004. Mitochondrial import and the twin-pore translocase. Nat. Rev. Mol. Cell Biol. 5, 519–530. https://doi.org/10.1038/nrm1426. PMID: 15232570.

Remacle, C., Coosemans, N., Jans, F., Hanikenne, M., Motte, P., Cardol, P., 2010. Knock-down of the COX3 and COX17 gene expression of cytochrome c oxidase in the unicellular green alga *Chlamydomonas reinhardtii*. Plant Mol. Biol. 74, 223–233. https://doi.org/10.1007/s11103-010-9668-6.

Ricchetti, M., Tekaia, F., Dujon, B., 2004. Continued colonization of the human genome by mitochondrial DNA. PLoS Biol. 2, e273.

Richter, F., Dennerlein, S., Nikolov, M., Jans, D.C., Naumenko, N., Aich, A., MacVicar, T., Linden, A., Jakobs, S., Urlaub, H., Langer, T., Rehling, P., 2019. ROMO1 is a constituent of the human presequence translocase required for YME1L protease import. J. Cell Biol. 218, 598–614. https://doi.org/10.1083/jcb.201806093.

Roger, A.J., Muñoz-Gómez, S.A., Kamikawa, R., 2017. The origin and diversification of mitochondria. Curr. Biol. 27, R1177–R1192. https://doi.org/10.1016/j.cub.2017.09.015.

Roucou, X., Artika, I.M., Devenish, R.J., Nagley, P., 1999. Bioenergetic and structural consequences of allotopic expression of subunit 8 of yeast mitochondrial ATP synthase. The hydrophobic character of residues 23 and 24 is essential for maximal activity and structural stability of the enzyme complex. Eur. J. Biochem. 261, 444–451. https://doi.org/10.1046/j.1432-1327.1999.00289.x.

Rubalcava-Gracia, D., Vázquez-Acevedo, M., Funes, S., Pérez-Martínez, X., González-Halphen, D., 2018. Mitochondrial versus nuclear gene expression and membrane protein assembly: the case of subunit 2 of yeast cytochrome c oxidase. Mol. Biol. Cell 29, 820–833. https://doi.org/10.1091/mbc.E17-09-0560.

Rubalcava-Gracia, D., García-Rincón, J., Pérez-Montfort, R., Hamel, P.P., González-Halphen, D., 2019. Key within-membrane residues and precursor dosage impact the allotopic expression of yeast subunit II of cytochrome c oxidase. Mol. Biol. Cell 30, 2358–2366. https://doi.org/10.1091/mbc.E18-12-0788.

Ruiz-Pesini, E., Montoya, J., Pacheu-Grau, D., 2021. Molecular insights into mitochondrial protein translocation and human disease. Genes (Basel) 12, 1031. https://doi.org/10.3390/genes12071031.

Russell, O.M., Gorman, G.S., Lightowlers, R.N., Turnbull, D.M., 2020. Mitochondrial diseases: hope for the future. Cell 181, 168–188. https://doi.org/10.1016/j.cell.2020.02.051.

Salinas-Giegé, T., Giegé, R., Giegé, P., 2015. tRNA biology in mitochondria. Int. J. Mol. Sci. 16, 4518–4559. https://doi.org/10.3390/ijms16034518.

Sanchirico, M., Tzellas, A., Fox, T.D., Conrad-Webb, Perlman, P.S., Mason, T.L., 1995. Relocation of the unusual VAR1 gene from the mitochondrion to the nucleus. Biochem. Cell Biol. 73, 987–995. https://doi.org/10.1139/o95-106.

Saraste, M., 1999. Oxidative phosphorylation at the fin de siècle. Science 283, 1488–1493. https://doi.org/10.1126/science.283.5407.1488.

Saravanan, S., Lewis, C.J., Dixit, B., O'Connor, M.S., Stolzing, A., Boominathan, A., 2022. The mitochondrial genome in aging and disease and the future of mitochondrial therapeutics. Biomedicines. 10, 490. https://doi.org/10.3390/biomedicines10020490.

Scarpelli, M., Cotelli, M.S., Mancuso, M., Tomelleri, G., Tonin, P., Baronchelli, C., Vielmi, V., Gregorelli, V., Todeschini, A., Padovani, A., et al., 2010. Current options in the treatment of mitochondrial diseases. Recent Pat. CNS Drug Discov. 5, 203–209. https://doi.org/10.2174/157488910793362412.

Schibich, D., Gloge, F., Pöhner, I., Björkholm, P., Wade, R.C., von Heijne, G., Bukau, B., Kramer, G., 2016. Global profiling of SRP interaction with nascent polypeptides. Nature 536, 219–223. https://doi.org/10.1038/nature19070.

Schneider, A., 2022. Evolution and diversification of mitochondrial protein import systems. Curr. Opin. Cell Biol. 75, 102077 https://doi.org/10.1016/j.ceb.2022.102077.

Schwartz, M.P., Matouschek, A., 1999. The dimensions of the protein import channels in the outer and inner mitochondrial membranes. PNAS 96, 13086–13090. https://doi.org/10.1073/pnas.96.23.13086.

Shimokata, K., Katayama, Y., Murayama, H., Suematsu, M., Tsukihara, T., Muramoto, K., Aoyama, H., Yoshikawa, S., Shimada, H., 2007. The proton pumping pathway of bovine heart cytochrome c oxidase. PNAS 104, 4200–4205. https://doi.org/10.1073/pnas.0611627104.

Sickmann, A., Reinders, J., Wagner, Y., Joppich, C., Zahedi, R., Meyer, H.E., Schönfisch, B., Perschil, I., Chacinska, A., Guiard, B., Rehling, P., Pfanner, N., Meisinger, C., 2003. The proteome of *Saccharomyces cerevisiae* mitochondria. PNAS 100, 13207–13212. https://doi.org/10.1073/pnas.2135385100.

Sim, S.I., Chen, Y., Lynch D.L., Gumbart, J.C., Park, E., 2023. Structural basis of mitochondrial protein import by the TIM23 complex. Nature. 2023 Jun 21. doi: 10.1038/s41586-023-06239-6.

Singh, R.K., Saini, S.K., Prakasam, G., Kalairasan, P., Bamezai, R.N.K., 2019. Role of ectopically expressed mtDNA encoded cytochrome c oxidase subunit I (MT-COI) in tumorigenesis. Mitochondrion 49, 56–65. https://doi.org/10.1016/j.mito.2019.07.002.

Singh, A.P., Salvatori, R., Aftab, W., Aufschnaiter, A., Carlström, A., Forne, I., Imhof, A., Ott, M., 2020. Molecular connectivity of mitochondrial gene expression and OXPHOS biogenesis. Mol. Cell 79, 1051–1065.e10. https://doi.org/10.1016/j.molcel.2020.07.024.

Sirrenberg, C., Bauer, M.F., Guiard, B., Neupert, W., Brunner, M., 1996. Import of carrier proteins into the mitochondrial inner membrane mediated by Tim22. Nature 384, 582–585. https://doi.org/10.1038/384582a0. PMID: 8955274.

Spikes, T.E., Montgomery, M.G., Walker, J.E., 2021. Interface mobility between monomers in dimeric bovine ATP synthase participates in the ultrastructure of inner mitochondrial membranes. PNAS 118. https://doi.org/10.1073/pnas.2021012118 e2021012118.

Srivastava, S., Moraes, C.T., 2001. Manipulating mitochondrial DNA heteroplasmy by a mitochondrially targeted restriction endonuclease. Hum. Mol. Genet. 10, 3093–3099. https://doi.org/10.1093/hmg/10.26.3093.

Supekova, L., Supek, F., Greer, J.E., Schultz, P.G., 2010. A single mutation in the first transmembrane domain of yeast COX2 enables its allotopic expression. PNAS 107, 5047–5052. https://doi.org/10.1073/pnas.1000735107.

Szafranski, P., 2017. Intercompartmental piecewise gene transfer. Genes (Basel) 8, 260. https://doi.org/10.3390/genes8100260.

Szyrach, G., Ott, M., Bonnefoy, N., Neupert, W., Herrmann, J.M., 2003. Ribosome binding to the Oxa1 complex facilitates co-translational protein insertion in mitochondria. EMBO J. 22, 6448–6457. https://doi.org/10.1093/emboj/cdg623.

Takemoto, C., Spremulli, L.L., Benkowski, L.A., Ueda, T., Yokogawa, T., Watanabe, K., 2009. Unconventional decoding of the AUA codon as methionine by mitochondrial tRNAMet with the anticodon f5CAU as revealed with a mitochondrial in vitro translation system. Nucl. Acids Res. 37, 1616–1627. https://doi.org/10.1093/nar/gkp001.

Tanifuji, G., Archibald, J.M., Hashimoto, T., 2016. Comparative genomics of mitochondria in chlorarachniophyte algae: endosymbiotic gene transfer and organellar genome dynamics. Sci. Rep. 6, 21016. https://doi.org/10.1038/srep21016.

Telonis, A.G., Kirino, Y., Rigoutsos, I., 2015. Mitochondrial tRNA-lookalikes in nuclear chromosomes: could they be functional? RNA Biol. 12, 375–380. https://doi.org/10.1080/15476286.2015.1017239.

Tischner, C., Wenz, T., 2015. Keep the fire burning: current avenues in the quest of treating mitochondrial disorders. Mitochondrion 24, 32–49. https://doi.org/10.1016/j.mito.2015.06.002.

Truscott, K.N., Kovermann, P., Geissler, A., Merlin, A., Meijer, M., Driessen, A.J., Rassow, J., Pfanner, N., Wagner, R., 2001. A presequence- and voltage-sensitive channel of the mitochondrial preprotein translocase formed by Tim23. Nat. Struct. Biol. 8, 1074–1082. https://doi.org/10.1038/nsb726.

Tsukihara, T., Shimokata, K., Katayama, Y., Shimada, H., Muramoto, K., Aoyama, H., Mochizuki, M., Shinzawa-Itoh, K., Yamashita, E., Yao, M., Ishimura, Y., Yoshikawa, S., 2003. The low-spin heme of cytochrome c oxidase as the driving

element of the proton-pumping process. PNAS 100, 15304–15309. https://doi.org/10.1073/pnas.2635097100.
Vahrenholz, C., Riemen, G., Pratje, E., Dujon, B., Michaelis, G., 1993. Mitochondrial DNA of *Chlamydomonas reinhardtii*: the structure of the ends of the linear 15.8-kb genome suggests mechanisms for DNA replication. Curr. Genet. 24, 241–247. https://doi.org/10.1007/BF00351798.
van der Laan, M., Rissler, M., Rehling, P., 2006. Mitochondrial preprotein translocases as dynamic molecular machines. FEMS Yeast Res. 6, 849–861. https://doi.org/10.1111/j.1567-1364.2006.00134.x.
van der Laan, M., Meinecke, M., Dudek, J., Hutu, D.P., Lind, M., Perschil, I., Guiard, B., Wagner, R., Pfanner, N., Rehling, P., 2007. Motor-free mitochondrial presequence translocase drives membrane integration of preproteins. Nat. Cell Biol. 9, 1152–1159. https://doi.org/10.1038/ncb1635.
Vázquez-Acevedo, M., Rubalcava-Gracia, D., González-Halphen, D. In vitro import and assembly of the nucleus-encoded mitochondrial subunit III of cytochrome c oxidase (Cox3). Mitochondrion. 19 (Pt B): 314-22. doi: 10.1016/j.mito.2014.02.005.
Vercellino, I., Sazanov, L.A., 2022. The assembly, regulation and function of the mitochondrial respiratory chain. Nat. Rev. Mol. Cell Biol. 23, 141–161. https://doi.org/10.1038/s41580-021-00415-0.
Vignal, C., Uretsky, S., Fitoussi, S., Galy, A., Blouin, L., Girmens, J.F., Bidot, S., Thomasson, N., Bouquet, C., Valero, S., Meunier, S., Combal, J.P., Gilly, B., Katz, B., Sahel, J.A., 2018. Safety of rAAV2/2-ND4 gene therapy for leber hereditary optic neuropathy. Ophthalmology 125, 945–947. https://doi.org/10.1016/j.ophtha.2017.12.036.
Vignal-Clermont, C., Girmens, J.F., Audo, I., Said, S.M., Erreram, M.H., Plainem, L., O'Shaughnessym, D., Taiel, M., Sahel, J.A., 2021. Safety of intravitreal gene therapy for treatment of subjects with leber hereditary optic neuropathy due to mutations in the mitochondrial ND4 gene: the REVEAL study. BioDrugs 35, 201–214. https://doi.org/10.1007/s40259-021-00468-9.
von Heijne, G., 1986. Why mitochondria need a genome. FEBS Lett. 198, 1–4. https://doi.org/10.1002/1873-3468.12510.
von Heijne, G., Steppuhn, J., Herrmann, R.G., 1989. Domain structure of mitochondrial and chloroplast targeting peptides. Eur. J. Biochem. 180, 535–545. https://doi.org/10.1111/j.1432-1033.1989.tb14679.x.
Wallace, D.C., 2018. Mitochondrial genetic medicine. Nat. Genet. 50, b1642–b1649. https://doi.org/10.1038/s41588-018-0264-z.
Wallace, D.C., Singh, G., Lott, M.T., Hodge, J.A., Schurr, T.G., Lezza, A.M., Elsas 2nd, L. J., Nikoskelainen, E.K., 1988. Mitochondrial DNA mutation associated with Leber's hereditary optic neuropathy. Science 242, 1427–1430. https://doi.org/10.1126/science.3201231.
Wallace, D.C., Stugard, C., Murdock, D., Schurr, T., Brown, M.D., 1997. Ancient mtDNA sequences in the human nuclear genome: a potential source of errors in identifying pathogenic mutations. PNAS 94, 14900–14905. https://doi.org/10.1073/pnas.94.26.14900.
Wang, X., 2012. Integrate the mitochondrial genome into the nuclear genome. Bioenerg. Open Access 1, 1–3. https://doi.org/10.4172/2167-7662.1000e103.
Wang, P., Dalbey, R.E., 2011. Inserting membrane proteins: the YidC/Oxa1/Alb3 machinery in bacteria, mitochondria, and chloroplasts. Biochim. Biophys. Acta 1808, 866–875. https://doi.org/10.1016/j.bbamem.2010.08.014.
Wang, G., Shimada, E., Nili, M., Koehler, C.M., Teitell, M.A., 2015. Mitochondria-targeted RNA import. Methods Mol. Biol. 1264, 107–116. https://doi.org/10.1007/978-1-4939-2257-4_11.
Watanabe, K.I., Ohama, T., 2001. Regular spliceosomal introns are invasive in *Chlamydomonas reinhardtii*: 15 introns in the recently relocated mitochondrial cox2 and cox3 genes. J. Mol. Evol. 53, 333–339. https://doi.org/10.1007/s002390010223.
Wei, W., Schon, K.R., Elgar, G., Orioli, A., Tanguy, M., Giess, A., Tischkowitz, M., Caulfield, M.J., Chinnery, P.F., 2022. Nuclear-embedded mitochondrial DNA sequences in 66,083 human genomes. Nature 611, 105–114. https://doi.org/10.1038/s41586-022-05288-7.
Wiedemann, N., Pfanner, N., 2017. Mitochondrial machineries for protein import and assembly. Annu. Rev. Biochem 86, 685–714. https://doi.org/10.1146/annurev-biochem-060815-014352.
Williams, C.C., Jan, C.H., Weissman, J.S., 2014. Targeting and plasticity of mitochondrial proteins revealed by proximity-specific ribosome profiling. Science 346, 748–751. https://doi.org/10.1126/science.1257522.
Woischnik, M., Moraes, C.T., 2002. Pattern of organization of human mitochondrial pseudogenes in the nuclear genome. Genome Res. 12, 885–893. https://doi.org/10.1101/gr.227202.
Wong, J.E., Zíková, A., Gahura, O., 2023. The ancestral shape of the access proton path of mitochondrial ATP synthases revealed by a split subunit-a. Mol. Biol. Evol. 40, msad146. https://doi.org/10.1093/molbev/msad146. PMID: 37338543; PMCID: PMC10306403.
Wu, X., Cabanos, C., Rapoport, T.A., 2019. Structure of the post-translational protein translocation machinery of the ER membrane. Nature 566, 136–139. https://doi.org/10.1038/s41586-018-0856-x.
Xu, H., DeLuca, S.Z., O'Farrell, P.H., 2008. Manipulating the metazoan mitochondrial genome with targeted restriction enzymes. Science 321, 575–577. https://doi.org/10.1126/science.1160226.
Yu, H., Koilkonda, R.D., Chou, T.H., Porciatti, V., Ozdemir, S.S., Chiodo, V., Boye, S.L., Boye, S.E., Hauswirth, W.W., Lewin, A.S., Guy, J., 2012. Gene delivery to mitochondria by targeting modified adenoassociated virus suppresses Leber's hereditary optic neuropathy in a mouse model. PNAS 109, E1238–E1247. https://doi.org/10.1073/pnas.1119577109.
Zaremba-Niedzwiedzka, K., Caceres, E.F., Saw, J.H., Bäckström, D.i., Juzokaite, L., Vancaester, E., Seitz, K.W., Anantharaman, K., Starnawski, P., Kjeldsen, K.U., Stott, M.B., Nunoura, T., Banfield, J.F., Schramm, A., Baker, B.J., Spang, A., Ettema, T.J.G., 2017. Asgard archaea illuminate the origin of eukaryotic cellular complexity. Nature 541, 353–358. https://doi.org/10.1038/nature21031.
Zhou, X., Yang, Y., Wang, G., Wang, S., Sun, D., Ou, X., Lian, Y., Li, L. 2023. Molecular pathway of mitochondrial preprotein import through the TOM-TIM23 supercomplex. bioRxiv 2023.06.21.546012; doi: 10.1101/2023.06.21.546012.
Zhou, S., Ruan, M., Li, Y., Yang, J., Bai, S., Richter, C., Schwalbe, H., Xie, C., Shen, B., Wang, J., 2020. Solution structure of the voltage-gated Tim23 channel in complex with a mitochondrial presequence peptide. Cell Res. 31, 821–824. https://doi.org/10.1038/s41422-020-00452-y.
Zong, S., Wu, M., Gu, J., Liu, T., Guo, R., Yang, M., 2018. Structure of the intact 14-subunit human cytochrome c oxidase. Cell Res. 28, 1026–1034. https://doi.org/10.1038/s41422-018-0071-1.
Zullo, S.J., 2001. Gene therapy of mitochondrial DNA mutations: a brief, biased history of allotopic expression in mammalian cells. Semin. Neurol. 21, 327–335. https://doi.org/10.1055/s-2001-17949.
Zullo, S.J., Parks, W.T., Chloupkova, M., Wei, B., Weiner, H., Fenton, W.A., Eisenstadt, J. M., Merril, C.R., 2005. Stable transformation of CHO Cells and human NARP cybrids confers oligomycin resistance (oli(r)) following transfer of a mitochondrial DNA-encoded oli(r) ATPase6 gene to the nuclear genome: a model system for mtDNA gene therapy. Rejuven. Res. 8, 18–28. https://doi.org/10.1089/rej.2005.8.18.

Further reading

Fiumera, H.L., Broadley, S.A., Fox, T.D., 2007. Translocation of mitochondrially synthesized Cox2 domains from the matrix to the intermembrane space. Mol. Cell Biol. 27, 4664–4673. https://doi.org/10.1128/MCB.01955-06.
Flores-Mireles, D., Camacho-Villasana, Y., Lutikurti, M., García-Guerrero, A.E., Lozano-Rosas, G., Chagoya, V., Gutiérrez-Cirlos, E.B., Brandt, U., Cabrera-Orefice, A., Pérez-Martínez, X., 2023. The cytochrome b carboxyl terminal region is necessary for mitochondrial complex III assembly. Life Sci Alliance. 6 https://doi.org/10.26508/lsa.202201858 e202201858.
Gruschke, S., Kehrein, K., Römpler, K., Gröne, K., Israel, L., Imhof, A., Herrmann, J.M., Ott, M., 2011. Cbp3-Cbp6 interacts with the yeast mitochondrial ribosomal tunnel exit and promotes cytochrome b synthesis and assembly. J. Cell Biol. 193, 1101–1114. https://doi.org/10.1083/jcb.201103132.
Gruschke, S., Römpler, K., Hildenbeutel, M., Kehrein, K., Kühl, I., Bonnefoy, N., Ott, M., 2012. The Cbp3-Cbp6 complex coordinates cytochrome b synthesis with bc(1) complex assembly in yeast mitochondria. J. Cell Biol. 199, 137–150. https://doi.org/10.1083/jcb.201206040.
Hell, K., Herrmann, J., Pratje, E., Neupert, W., Stuart, R.A., 1997. Oxa1p mediates the export of the N- and C-termini of pCoxII from the mitochondrial matrix to the intermembrane space. FEBS Lett. 418, 367–370. https://doi.org/10.1016/s0014-5793(97)01412-9.
Herrmann, J.M., Funes, S., 2005. Biogenesis of cytochrome oxidase-sophisticated assembly lines in the mitochondrial inner membrane. Gene 354, 43–52. https://doi.org/10.1016/j.gene.2005.03.017.
Hildenbeutel, M., Hegg, E.L., Stephan, K., Gruschke, S., Meunier, B., Ott, M., 2014. Assembly factors monitor sequential hemylation of cytochrome b to regulate mitochondrial translation. J. Cell Biol. 205, 511–524. https://doi.org/10.1083/jcb.201401009.
Hunte, C., Palsdottir, H., Trumpower, B.L., 2003. Protonmotive pathways and mechanisms in the cytochrome bc1 complex. FEBS Lett. 545, 39–46. https://doi.org/10.1016/s0014-5793(03)00391-0.
Jia, L., Dienhart, M.K., Stuart, R.A., 2007. Oxa1 directly interacts with Atp9 and mediates its assembly into the mitochondrial F1Fo-ATP synthase complex. Mol. Biol. Cell 18, 1897–1908. https://doi.org/10.1091/mbc.e06-10-0925.
Käll, L., Krogh, A., Sonnhammer, E.L., 2005. An HMM posterior decoder for sequence feature prediction that includes homology information. Bioinformatics. Suppl 1, i251–i257. https://doi.org/10.1093/bioinformatics/bti1014.
Kolli, R., Soll, J., Carrie, C., 2018. Plant mitochondrial inner membrane protein insertion. Int. J. Mol. Sci. 19, 641. https://doi.org/10.3390/ijms19020641.
Pfeffer, S., Woellhaf, M.W., Herrmann, J.M., Förster, F., 2015. Organization of the mitochondrial translation machinery studied in situ by cryoelectron tomography. Nat. Commun. 6, 6019. https://doi.org/10.1038/ncomms7019.
Stiburek, L., Fornuskova, D., Wenchich, L., Pejznochova, M., Hansikova, H., Zeman, J., 2007. Knockdown of human Oxa1l impairs the biogenesis of F1Fo-ATP synthase and NADH:ubiquinone oxidoreductase. J. Mol. Biol. 374, 506–516. https://doi.org/10.1016/j.jmb.2007.09.044.

Artículo II.

Aceptado, *en prensa*

Nieto-Panqueva, F., Vázquez-Acevedo, M., Hamel, P. P., & González-Halphen, D. (2024). Identification of factors limiting the allotopic production of the Cox2 subunit of yeast cytochrome c oxidase. *Genetics*, iyae058. Advance online publication. https://doi.org/10.1093/genetics/iyae058

Identification of factors limiting the allotopic production of the Cox2 subunit of yeast cytochrome *c* oxidase

Felipe Nieto-Panqueva[1], Miriam Vázquez-Acevedo[1], Patrice P. Hamel[2] and Diego González-Halphen[1,*]

1) Departamento de Genética Molecular, Instituto de Fisiología Celular, Universidad Nacional Autónoma de México, Apartado Postal 70-243, México 04510, D.F. (Mexico) Instituto de Fisiología Celular, Universidad Nacional Autónoma de México, Mexico City, Mexico

2) Department of Molecular Genetics and Department of Biological Chemistry and Pharmacology, The Ohio State University, 582 Aronoff laboratory, 318 W. 12th Avenue, Columbus, OH 43210, USA, and Vellore Institute of Technology (VIT), School of BioScience and Technology, Vellore, Tamil Nadu, India.

*Corresponding author. Departamento de Genética Molecular, Instituto de Fisiología Celular, Universidad Nacional Autónoma de México, Apartado Postal 70-243, México 04510, D.F. (Mexico) Tel: (+5255) 5622-5620; FAX: (+5255) 5622-5611. E-mail: dhalphen@ifc.unam.mx

RUNNING HEAD: Factors limiting allotopic Cox2

KEY WORDS: protein import into mitochondria, allotopic expression, Cox2, subunit II of cytochrome *c* oxidase, Mgr2 protein, TIM23 translocator, TIM23^{MOTOR}, TIM23^{SORT}

Abstract

Mitochondrial genes can be naturally or artificially relocalized in the nuclear genome in a process known as allotopic expression, such is the case of the mitochondrial *cox2* gene, encoding subunit II of cytochrome *c* oxidase (C*c*O). In yeast, cox2 can be allotopically expressed and is able to restore respiratory growth of a cox2-null mutant if the Cox2 subunit carries the W56R substitution within the first transmembrane stretch. However, the *COX2^{W56R}* strain exhibits reduced growth rates and lower steady-state C*c*O levels when compared to wild-type yeast. Here, we investigated the impact of overexpressing selected candidate genes predicted to enhance internalization of the allotopic Cox2^{W56R} precursor into mitochondria. The overproduction of Cox20, Oxa1, and Pse1 facilitated Cox2^{W56R} precursor internalization, improving the respiratory growth of the *COX2^{W56R}* strain. Overproducing TIM22 components had a limited effect on Cox2^{W56R} import, while overproducing TIM23-related components showed a negative effect. We further explored the role of the Mgr2 subunit within the TIM23 translocator in the import process by deleting and overexpressing the *MGR2* gene. Our findings indicate that Mgr2 is instrumental in modulating the TIM23 translocon to correctly sort Cox2^{W56R}. We propose a biogenesis

pathway followed by the allotopically produced Cox2 subunit based on the participation of the two different structural/functional forms of the TIM23 translocon, $TIM23^{MOTOR}$ and $TIM23^{SORT}$, that must follow a concerted and sequential mode of action to insert $Cox2^{W56R}$ into the inner mitochondrial membrane in the correct N_{out}-C_{out} topology.

Introduction

Mitochondrial cytochrome *c* oxidase (C*c*O or complex IV), is the final electron acceptor of the respiratory chain and functions as an electrogenic proton pump (Wikström, 1989). In the yeast *Saccharomyces cerevisiae* and many other eukaryotic organisms, C*c*O is assembled from mitochondria- and nucleus-encoded subunits (Barrientos et al., 2002). The yeast C*c*O is composed of 11 subunits; the three largest, Cox1, Cox2, and Cox3, are encoded in the mitogenome, synthesized by mitoribosomes, and cotranslationally inserted into the inner mitochondrial membrane (IMM) (Dennerlein et al., 2021). The other eight subunits are nucleus-encoded, synthesized in cytosolic ribosomes, and internalized into mitochondria through the TOM/TIM import machinery (Poyton and Groot, 1975; Fontanesi et al., 2008). The final maturation of C*c*O takes place when its three independent assembly modules join into a functional holoenzyme containing copper (Cu) and heme A prosthetic groups. Each module or assembly intermediate consists of a subcomplex which is named based on the presence of one mitochondrial synthesized CcO subunit: the Cox1, Cox2 and Cox3 modules. These assembly intermediates contain both mitochondria and nucleus synthesized subunits as well as several other biogenesis factors that bind transiently but do not end up being part of the mature C*c*O complex (Bourens et al., 2014; Franco et al., 2020).

The Cox2 subunit has two transmembrane domains (TMS1 and TMS2) embedded in the IMM and exhibits a N_{out}-C_{out} topology, i.e., it exposes both N- and C-termini to the mitochondrial intermembrane space (IMS). The large, hydrophilic, C-terminal domain of the protein that binds the binuclear copper center (Cu_A), also resides in the IMS. Inside mitochondria, Cox2 is synthesized as a precursor containing a natural leader peptide (LP) of 15 residues (Torello et al., 1997). The TMS1 is co-translationally inserted in the inner mitochondrial membrane (IMM) by the concerted action of mitoribosomes, the Oxa1 translocase, and the assembly factors Mba1 and Cox20 (Hell et al. 1997; Herrmann & Bonnefoy 2004; Fiumera et al. 2007). When the N-terminus of Cox2 gets exposed to the IMS, the Imp1 protease removes the LP giving rise to the mature protein (Sevarino & Poyton 1980; Torello et al. 1997). The Cox2 subunit reaches its final topology once the TMS2 and the hydrophilic domain of the protein are translocated across the IMM by the concerted action of Cox18, Pnt1 and Mss2 (Saracco & Fox 2002). Once TMS2 is embedded in the IMM and the large, hydrophilic domain of the protein reaches the IMS, the Sco1/Sco2/Coa6/Cox12 copper relay system assembles the binuclear Cu center of Cox2 (Rigby et al. 2008; Pacheu-Grau et al. 2015; Ghosh et al. 2016; Maghool et al., 2020; Swaminathan et al., 2022). After the Cox2 module binds to the Cox1 module, the newly formed Cox1-Cox2 module integrates the Cox3 module giving rise to the mature C*c*O complex (Franco et al., 2020).

Since the endosymbiotic event that gave rise to mitochondria, many genes from this organelle have naturally migrated to the nuclear genome (Gray, 2000). When the gene transfer is carried out artificially, the procedure is known as allotopic expression. Understanding this process may help understand the evolution after endosymbiosis and how the gene flow from the organellar genome to the nucleus occurred (Nieto-Panqueva

et al., 2023). Previously, the mitochondrial *COX2* gene was allotopically expressed in a yeast mutant lacking a functional mitochondrial gene (Δ*cox2* null mutant) (Supekova et al., 2010). The nuclear *COX2* gene encodes a mitochondrial targeting sequence (MTS) from the Oxa1 protein fused to a recoded *COX2* gene carrying the point mutation resulting in the W56R substitution in the Cox2 subunit. Both the MTS and the mutation promote the translocation and sorting of the allotopic Cox2 subunit through the TOM/TIM import machinery (Callegari et al., 2020). In particular, the W56R substitution, located in the TMS1 of Cox2, diminishes the hydrophobicity of this alpha-helix and facilitates its translocation into the mitochondrial matrix. Thus, a ***Δcox2*** null strain expressing *COX2*^{W56R} is respiratory competent (Supekova et al., 2010), although it exhibited less respiratory capacity and lower C*c*O levels as compared to the wild-type strain (Cruz-Torres et al. 2012).

The allotopic *COX2*^{W56R} gene can be expressed either from a single copy directly inserted in a nuclear chromosome or from an episomal plasmid. When expressed from a multicopy vector with a constitutive promoter, the precursor of the Cox2^{W56R} subunit (***e***Cox2^{W56R}) is produced in high amount and tends to accumulate on the surface of mitochondria (Rubalcava-Gracia et al., 2019). By contrast, when the gene is inserted in the nuclear genome, its expression gives rise to a Cox2^{W56R} subunit (***n***Cox2^{W56R}) that is readily imported, and its precursor does not accumulate at high levels. It was suggested that when the rate of synthesis of the cytosolic Cox2^{W56R} precursor exceeds its rate of import into mitochondria, the protein tends to aggregate on the mitochondrial surface (Rubalcava-Gracia et al., 2019). Thus, we view the accumulation of the Cox2^{W56R} precursor as an indication that the rate of synthesis of the allotopic product supersedes its import rate.

The W56R substitution is necessary and sufficient to allow the allotopically produced yeast Cox2 subunit to be imported into mitochondria. The presence of this substitution does not directly affect C*c*O assembly or activity, since a strain that produces the Cox2^{W56R} protein from an engineered *cox2*^{W56R} in the mitochondrial genome, cannot be distinguished from a wild-type strain in terms of respiratory growth and C*c*O activity (Rubalcava-Gracia et al., 2018). Since the presence of the W56R substitution by itself does not account for the partial complementation of respiratory phenotype by the allotopically produced subunit, the translocation or sorting of the TMS of Cox2^{W56R} by the TIM23 complex is likely to constitute a limiting step in its biogenesis. In this work, we aimed to define the nature of this limiting step.

We reasoned that proteins controlling some aspects of the biogenesis of mitochondrially synthesized Cox2 might be limiting when Cox2 is allotopically produced. We sought to test if overexpression of candidate genes whose protein products may directly or indirectly participate in the biogenesis of Cox2^{W56R} could improve the respiratory growth of a Δ*cox2* strain expressing the *COX2*^{W56R} from the nucleus (producing ***n***Cox2^{W56R}) or from an episomal, multicopy vector (producing ***e***Cox2^{W56R}). Thus, we opted to test genes encoding proteins known to participate in the import, maturation, or assembly of mitochondrial proteins. Some of these candidate genes encode proteins whose function is known, except for the *PSE1* gene, which was originally identified as a multicopy suppressor that enhanced the levels of an allotopic reporter protein targeted to mitochondria (Corral-Debrinski et al., 1999). We found that overexpression of genes encoding the mitochondrial import-related components Cox20, Oxa1, and Pse1 facilitated the internalization of the ***e***Cox2^{W56R} precursor into mitochondria.

We further explored the effect of Mgr2 on the import of Cox2^{W56R}. Mgr2 is a regulator of the TIM23 complex (Gebert et al., 2012) that functions as a quality control factor involved in

the lateral release of TMS into the IMM. We studied the effects that result from either deleting or overexpressing the *MGR2* gene on the respiratory phenotype of the allotopic strain and the steady state levels of the $Cox2^{W56R}$ precursor and of its mature protein. We discovered that Mgr2 is instrumental in the import of the allotopic Cox2 subunit, since either the absence or the overproduction of this factor affects the import process. Based on these results, we propose a model describing the mechanism through which the allotopically-produced Cox2 subunit is translocated and sorted by the TIM23 machinery. This new biogenesis model suggests the participation of the two structural/functional forms of the TIM23 translocon, $TIM23^{MOTOR}$ and $TIM23^{SORT}$, that must follow a concerted and sequential mechanism to internalize the allotopically produced Cox2 subunit and embed it in the IMM. We propose that the required interchange of the two different structural/functional forms of the TIM23 translocator during the import of the allotopically produced Cox2 subunit defines the limiting step of the process. To the best of our understanding, the necessity for the sequential involvement of both $TIM23^{MOTOR}$ and $TIM23^{SORT}$ in the internalization process of a singular membrane protein has not been examined until now. The hypothesized mechanism potentially transcends the special case of the allotopically produced Cox2 subunit and may apply to several other nucleus-encoded precursors destined to mitochondria characterized by possessing an MTS, two TMS, and a N_{out}-C_{out} arrangement within the IMM.

Materials and Methods

Yeast strains and gene constructs

In this study, yeast strains derived from the parental strain D273-10B (Fred Sherman laboratory, ATCC® 24657™) were used. NB40-36A (*MATα lys2 arg8::hisG leu2-3, 112 ura3-52 [rho+]*), (Perez-Martínez et al., 2003) and EHW154 (*MATa arg8::hisG ura3-52 leu 2-3, 112 his3-ΔHindIII [rho+] cox2(1,89-91)::ARG8^{m}*) (Williams and Fox, 2003) were used as wild-type and *cox2*-null strains, respectively. Yeast strains used in this study are listed in Table S1.

To achieve *$Cox2^{W56R}$* allotopic expression in the *Δcox2* mutant we introduced the hygromycin B-resistance based integrative vector pRS306H (Taxis and Knop, 2006), which targets insertion via homologous recombination at the *URA3* locus (*Δcox2* + ***n****$COX2^{W56R}$*). Additionally, we utilized the episomal 2μ *URA3* multicopy plasmid pFL61 (*Δcox2* + ***e****$COX2^{W56R}$*). These two expressions systems allowed us to achieve low (***n***) and high (***e***) levels of allotopically produced $Cox2^{W56R}$.

The *mgr2*-null (*Δmgr2*), strains were generated by replacing the *MGR2* locus (*YPL098C*) through homologous recombination. We used the *kanMX6* cassette from the pFA6a-kanMX6 plasmid (Bähler et al., 1998), which confers resistance to the selective antibiotic G418. The kanMX6 cassette was amplified using the oligonucleotides *mgr2*-kanMX6: 5´-TAGCACAAATAGCGCAACAGCTTCAAGTCCAATATTAAGATATACCAGCTGAAGCTTC GTACGC-3´ and 5´-GAAAACGATGGGGAAGCGTAAATATATGCAAAATTTCCCCCATCGATGAATTCGAGCT CGTT-3´. These oligonucleotides were designated to include ~50bp flanking homologous regions (underlined) upstream and downstream of the *MGR2* locus. The amplified *kanMX6* cassette was designed to replace the entire ORF of *MGR2*.

The yeast strains overexpressing *MGR2* (*MGR2*↑) were generated by introducing the high-copy episomal vector pMK2 which is a pFL61-derivative. The pMK2 plasmid contains the

LEU2 selectable marker instead of the URA3 marker (Minet et al., 1992) and the phosphoglycerate kinase (PGK) promoter with a cloned wild-type *MGR2* locus. The cloning process involved amplifying the *MGR2* gene using the following oligonucleotides MGR2OE: forward, 5´-GCGCGGCCGCATGCCTCCTCTTCCACA-3´; and reverse 5´-GCGCGGCCGCTCAGTCCTTACGTATACCGT-3´. These oligonucleotides were designed to include restriction site sequences for *Not1* to be cloned in the same site in pFL61.

We obtained plasmids overexpressing candidate genes and genes encoding TIM22 and TIM23 translocation subunits from the yeast genomic tiling collection (Jones et al., 2008). The specific plasmids, designated by their respective identifiers) included: *COX20 (YGPM21k21), OXA1 (YGPM14c18)*, *SDH2 (YGPM20g17)*, *TOM70 (YGPM33c09), CIS1 (YGPM8p09), MSP1 (YGPM30f06), HSP104 (YGPM12e18), PSE1 (YGPM18p15), RRP5 (YGPM5p05), TIM22 (YGPM17f03), SDH3 (YGPM317i06), TIM18 (YGPM17d04), TIM54 (YGPM20p13), TIM9 (YGPM25o01), TIM12 (YGPM32o08), TIM10 (YGPM30n09), TIM17 (YGPM4a13), TIM23 (YGPM23p01), MGR2 (YGPM5l18)* and *TIM21 (YGPM21l20).*These plasmids were created by cloning genomic fragments encompassing selected genes into the high-copy plasmid vector pGP564. We confirmed the presence of such genes in all the plasmids used in this study through sequencing the insert borders or through diagnostic PCR.

Yeast transformations were carried out using the one-step yeast transformation protocol (Chen et al.,1992), and the $C_2H_3LiO_2$ and single-stranded DNA as a carrier method (Gietz and Schiestl, 2007).

For cloning experiments and propagation of plasmids, *Escherichia coli* DH5α (F$^-$ *endA1 glnV44 thi-1 recA1 relA1 gyrA96 deoR nupG purB20 φ80dlacZ*ΔM15 Δ(*lacZYA-argF*)U169, hsdR17(*rK*$^-$*mK*$^+$), λ$^-$) and MR32, a *recA*$^-$ derivative of MC1061 (str. K-12 F$^-$ λ$^-$ Δ*(ara-leu)7697* [*araD139*]B/r Δ*(codB-lacI)3 galK16 galE15* e14$^-$ *mcrA0 relA1 rpsL150*(Str^R) *spoT1 mcrB1 hsdR2(r–m+)*) were employed.

Yeast culture conditions

Yeast strains were cultured in either liquid or solid (2.0% agar) media at 30 ºC, unless otherwise specified. The media employed in this study included fermentable media, such as YPDA or YPGal (1.0% yeast extract, 2.0% bacto peptone, and 2.0% dextrose or galactose), as well as non-fermentable media, including YPEG (1.0% yeast extract, 2.0% bacto peptone, 3.0% ethanol and 3.0% v/v glycerol); YPE (1.0% yeast extract, 2.0% bacto peptone, and 2.0% ethanol), and YPLAC (3.0% yeast extract , 1.0% KH_2PO_4, 1.0% NH_4Cl, 0.5% $CaCl_2{\cdot}2H_2O$, 0.5% NaCl, 0.6% $MgSO_4{\cdot}H_2O$, 3.0% $FeCl_3$, and 2.0% (v/v) lactate with pH adjusted to 5.5 with NaOH pellets). Additionally, minimal media SD or SGal (0.17% yeast nitrogen base [lacking amino acids and $(NH_4)_2SO_4$], 0.5% $(NH_4)_2SO_4$, 2% glucose or galactose supplemented with specific amino acids and nucleotides) were used for selection based on restoration of leucine or uracil prototrophy. Antibiotics Hygromycin B (300 µg/ml) and Geneticin (G418) (200 µg/ml) were employed for selection on YPDA. Growth was monitored by measuring optical density at 600 nm ($O.D._{600}$) using a Bio screen C spectrophotometer (Growth Curves, USA).

Growth test by tenfold serial dilutions

Cells were cultured overnight in 3.0 ml liquid YPDA at 30 ºC, with constant agitation at 180 rpm. The following morning, cultures were diluted to reach exponential phase ($O.D._{600}$ 1.0) (approximately 2.5 x 10^7 cells ml^{-1}). Cells were harvested by centrifugation at 8,600 × *g* and washed once with 1.0 ml of sterile water. This suspension was diluted in a 1:10 ratio

five sequential times for each strain using 96-well plates. Drops of approximately 3.5 µl were spotted onto solid fermentable (YPDA) and non-fermentable (YPEG, YPE, YPLAC) media using a multichannel pipette. The plates were then incubated either at 30 ºC or 37 ºC for 4-7 days as indicated.

Protein extraction and immunodetection

Protein extraction was performed using an alkaline treatment method on whole yeast cells cultured in 20 mL of liquid SGal media and in stationary phase ($O.D._{600}$ 2.5). The cells were collected at 2,800 × *g*) in a microcentrifuge for 3 mins and subsequently washed with 500 µl of a solution containing 1.0 mM phenyl-methyl-sulfonyl-fluoride (PMSF) and 50 µM N-α-tosyl-L-lysyl-chloromethyl ketone (TLCK). The resulting pellet was boiled in SDS-PAGE sample buffer as described (Kushnirov, 2000). Gel electrophoresis was performed using an SDS-tricine-PAGE system (Schägger, 1994). Following electrophoresis, the gels were electro-transferred onto nitrocellulose membranes. The membranes were blocked with 3.0% gelatin from bovine skin type B (Sigma), washed and subjected to immuno-decoration. Monoclonal anti-Cox2 antibody (Abcam: 4B12A5) was used at a 1:9000 dilution), and polyclonal anti-Zwf1 antibody (Sigma-Aldrich: A9521) was used at a 1:10000 dilution as a loading control as described (Fujiwara et al., 2016). For secondary antibody labeling, alkaline phosphatase-conjugated goat anti-rabbit and goat anti-mouse antibodies were incubated for 4 h. Dark purple precipitates in the form of bands were formed upon the addition of nitro-blue tetrazolium chloride (NBT) and 5-bromo-4-chloro-3′-indolyl phosphate p-toluidine salt (BCIP). Finally, the colored bands on membranes were captured using an HP Scanjet G4050 image scanner. When indicated, band intensity was estimated using the GelAnalyzer 23.1 freeware (available at www.gelanalyzer.com), developed by Istvan Lazar Jr., PhD and Istvan Lazar Sr., PhD, CSc. Bar plotting and statistical analysis were conducted using GraphPad Prism version 10.1.1(27) for macOS (GraphPad Software, Boston, Massachusetts, USA, www.graphpad.com). A two-way ANOVA followed by Tukey's multiple comparisons test was performed for each subset of samples.

Gel electrophoresis and in-gel enzymatic activities

Blue Native Polyacrylamide Gel Electrophoresis (BN-PAGE) was performed as previously described (Schägger, 1994). Yeast cells were grown in SGal medium, and mitochondria were isolated as described above. Mitochondria were washed with a solution containing 250 mM sorbitol and 50 mM Bis-Tris (pH 7.0). Subsequently, they were centrifuged at 13,500 x *g* for 2 mins at 4°C. The resulting pellet was resuspended in 750 mM aminocaproic acid, 50 mM Bis-Tris (pH 7.0) and solubilized with 2.0 g of n-Dodecyl β-D-maltoside (DDM) per gram of protein for 30 mins at 4°C. Then, the mixture was centrifuged at 63,000 x *g* at 4 ºC for 30 mins. The resulting supernatant was combined with 5 µl of digesting solution (containing 750 mM amino caproic acid, 25 mM Bis-Tris and 5% Serva Blue G 35050) and loaded onto 3-12% polyacrylamide gradient gels (stacking included). In-gel C*c*O activity staining was performed using 3,3'- diaminobenzidine and horse heart cytochrome *c* as described by Wittig et al., (2007). For in-gel ATPase activity staining BN gels were incubated for 3 hours in 270 mM glycine and 35 mM Tris-HCl (pH 8.4). Then, final concentrations of 8.0 mM ATP, 14.0 mM MgSO4, and 0.2% $Pb(NO_3)_2$ were added. When white precipitates of lead phosphate became visible, the reaction was stopped with the addition of methanol so that the final concentration is 50% (v/v) (Zerbetto et al.,1997).

Oxygen uptake measurements

Oxygen consumption was measured in a polarographic assay with whole cells that had been previously fasted in water for 4 to 6 hours. The assay included 20 mM 2- (N-morpholino) ethane sulfonic acid (MES) pH 6.0 (triethanolamine), 50 mM ethanol as substrate and 200 µM NaCN, which was added at the end of the assay to inhibit C*c*O activity (Estabrook, 1967). Oxygen consumption measurements were conducted using a Warner/Strathkelvin Instruments oxygen meter equipped with a Clark type electrode in a 1.0 mL water-jacketed chamber maintained at 30 ºC. Data acquisition was performed using the 782 Oxygen System software (Warner/Strathkelvin Instruments).

In silico analyses

AlphaFold (Jumper et al., 2021) and ColabFoldA (Mirdita et al., 2022) were run on the HMS O2 cluster at the Center for Computational Biomedicine at Harvard Medical School (https://computationalbiomed.hms.harvard.edu/tools-technologies-old/alphafold-colabfold/). PDB files were visualized using Swiss-PdbViewer (https://spdbv.unil.ch/) (Schwede et al., 2003) and figures prepared using Chimera 1.12 (Pettersen et al., 2004). The yeast mitochondria high-resolution complexome (Schulte et al., 2023) was explored at MitCOM (https://www.complexomics.org/datasets/mitcom).

RESULTS

To uncover the factors limiting the ability of cytosol-produced Cox2^{W56R} to fully complement a *cox2*-null mutant, we undertook an "educated guess" approach, *i.e.*, we sought to test if overexpression of certain genes, encoding proteins involved in mitochondrial protein import, could improve the respiratory growth of the *cox2*-null strain expressing *COX2^{W56R}* from the nuclear chromosome (***n****COX2^{W56R}*) or from an episomal, multicopy vector (***e****COX2^{W56R}*). We selected several candidate proteins known to participate in mitochondrial protein import or Cox2 biogenesis, reasoning that overproduction of their corresponding gene products might enhance the import of the allotopic Cox2^{W56R} subunit if these proteins control a limiting step. We therefore tested the overproduction of the following proteins involved in protein import: Tom70 (a subunit of the TOM complex involved in the recognition of incoming precursor proteins [Meisinger et al., 1999; Brix et al., 2000]); Cox20 (a chaperone essential for Cox2 biogenesis and export of its TMS1 across the IMM [Hell et al., 2000]); and Oxa1 (an IMM insertase that mediates the export of the N-terminus of Cox2 from the mitochondrial matrix to the IMS [Hell et al., 1997, 2000]). We also considered the potential indirect impact of overproducing candidate chaperones: Hsp104 (a cytosolic heat shock protein that disassembles protein aggregates; [Krämer et al., 2023], Msp1 (a mitochondrial AAA-ATPase dislocase that extracts mistargeted proteins for proteasomal degradation; [Nakai et al., 1993; Castanzo et al., 2020]), and Cis1 (an associated factor of the TOM complex that helps to reduce accumulation of mitochondrial precursors by interacting with Msp1; [Kabeya et al., 2007]). Additionally, we explored the overproduction of the Pse1 protein, a karyopherin interacting with the nuclear pore complex involved in the export of mRNA, and Rrp5, an RNA-binding protein with a role in the biogenesis of the large ribosomal subunit (Venema et al.,1996). Both the *PSE1* and *RRP5* genes were previously identified in a multicopy suppressor screen as enhancing the production of an allotopic reporter membrane protein targeted to the mitochondria (Torchet et al.,1998; Corral-Debrinski et al., 1999). As a control, we also tested the overexpression of a gene unrelated to Cox2 biogenesis and selected *SDH2*,

which encodes an iron-sulfur subunit of mitochondrial succinate dehydrogenase (complex II).

When we overexpressed the *CIS1*, *COX20, HSP104, MSP1, OXA1*, *PSE1, RRP5, SDH2*, and *TOM70* genes in the strain producing ***n***Cox2^{W56R}, we did not observe major effects on the growth depending on respiratory substrates (data not shown). In contrast, when we overexpressed the same set of genes in the strain producing ***e***Cox2^{W56R}, we observed that *COX20, OXA1*, and *PSE1* had the ability to enhance respiratory growth compared to the strain carrying only the corresponding empty vector. The enhanced respiratory growth was visible when the transformants were grown at 30 °C and could still be observed at 37 °C in lactate media (Figures 1A and 1B). On one hand, enhancement of the respiratory growth is more pronounced for the transformants expressing *OXA1* or *COX20* than for those expressing *PSE1*. On the other hand, overexpression of *MSP1*, *RRP5*, *TOM70*, *SDH2*, *CIS1*, and *HSP104* appears detrimental to the respiratory growth, with *RRP5* and *MSP1* overexpression eliciting the strongest effect. Immunoblotting analysis of the relative precursor and mature levels of the allotopic subunit when the *COX20*, *OXA1* and *PSE1* genes were overexpressed, revealed an increased accumulation of the mature ***e***Cox2^{W56R} protein compared to the levels observed in the strains carrying only the empty vector or overexpressing a gene which does not improve respiratory growth (Figures 1C, 1D, and 1E). In the case of Oxa1, quantification of the bands obtained after immunoblotting (Figure 1C) suggests that overexpression of the *OXA1* gene resulted in a 45% increase in Oxa1 protein levels. Expectedly, the *RRP5* and *MSP1* genes whose overexpression is severely detrimental to the respiratory growth of the strain producing ***e***Cox2^{W56R}, yield a significant decrease in the amount of mature Cox2^{W56R}. These results suggest that the overproduction of Cox20, Oxa1, and Pse1 enhanced the internalization into mitochondria of the allotopic Cox2 subunit.

One of the two primary protein import machineries of the IMM is TIM22, a translocon that specializes in the import of polytopic membrane proteins, mainly those of the large family of carrier proteins and some of the IMM-embedded subunits of the protein translocators (Horten et al., 2020). While the substrate repertoire of TIM22 is well-defined (Chacinska et al., 2009), TIM22 can also insert unconventional cargos such as the pyruvate carrier subunit Mpc1, which exhibits only two TMS (Gomkale et al., 2020). Therefore, in principle, TIM22 could also insert both TMS of Cox2^{W56R} as a hairpin, allowing the allotopic Cox2 protein to reach its characteristic N_{out}-C_{out} topology after a single insertion step into the IMM. Consequently, we studied the effect of overproducing proteins related to the TIM22 translocon on the import of the ***e***Cox2^{W56R} subunit. The core components of the TIM22 translocase, include Tim18, Tim22, Tim54 and Sdh3, as well as the so-called “small TIMs”, a family of chaperones that function in the IMS and interact with hydrophobic membrane proteins to maintain their import-competent state (Weinhäupl et al., 2021), namely Tim9, Tim10, Tim12, and Tim13. Overproduction of the TIM22 components did not result in enhanced respiratory growth in the strain producing ***e***Cox2^{W56R} (Figure S1A) and did not appear to enhance the steady-state levels of the mature Cox2^{W56R}. We concluded that import of the allotopic Cox2 subunit is probably not dependent upon the TIM22 components.

TIM23 is the other main translocator located in the IMM, that imports and sorts all incoming precursors containing an MTS (Herrmann and Bykov, 2023), so we also studied the effect of overproducing proteins related to TIM23 on the import of the ***e***Cox2^{W56R} subunit. We overexpressed the genes encoding four subunits of the TIM23 translocon, Tim17, Tim21, Tim23 and Mgr2, which are recognized for their pivotal role in importing

hydrophobic proteins. Overexpressing *TIM21* and *TIM23* genes had a deleterious effect on the respiratory growth of the ***e***Cox2^{W56R} strain in all the non-fermentable carbon sources assayed. By contrast, the overexpression of *TIM17* and *MGR2* had a milder negative effect (Figure 2A). Immunoblotting analysis indicated that the overexpression of *TIM17*, *TIM21*, *TIM23* and *MGR2* increased the accumulation of the ***e***Cox2^{W56R} precursor. Notably, the accumulation of the mature allotopic subunit was drastically diminished when the *TIM21* and *TIM23* genes were overexpressed (Figures 2B and 2C). That *TIM23* overexpression produces a deleterious effect on respiratory growth and ***e***Cox2^{W56R} import, was taken as an indication that the allotopic Cox2 subunit most likely enters mitochondria through the TIM23 import pathway, as it occurs with all MTS-containing precursors.

Mgr2 has been described as a regulator of TIM23 overseeing the quality control of protein sorting and translocation (Gebert et al., 2012); so, it could also participate in the import of allotopic Cox2. To study the effects of Mgr2 on the import of the allotopic Cox2 protein, we decided to both delete and overexpress the *MGR2* gene. We found that loss of *MGR2* function led to a clear respiratory growth defect at 37°C (Figure S2A). In contrast, and as previously reported (Gebert et al., 2012; Matta et al., 2020), deletion of the *MGR2* gene in an otherwise wild-type background had no observable growth phenotype at 30 °C, whether on fermentable or respiratory substrates. Therefore, the absence of Mgr2 seems to become limiting at higher growth temperatures.

We then examined the polypeptide pattern of solubilized mitochondria isolated from both the wild-type and the *mgr2* null mutant grown at 30 °C. To resolve the mitochondrial proteins, we used Blue Native electrophoresis (BN-PAGE) followed by detection of the C*c*O activity in the *mgr2* null mutant compared to the wild-type strain (Figure S2B). These experiments revealed that the absence of Mgr2 decreases the activity of C*c*O. In agreement with the decrease in C*c*O, loss of Mgr2 impacts the respiratory activity (Table 1). We noted that 1/3 of the respiratory capacity is lost due to the *mgr2*-null mutation. We concluded that the absence of Mgr2 impacts cellular respiration and C*c*O activity even though respiratory growth appears unaffected on non-fermentable carbon sources.

We then explored the effects of overexpressing or deleting the *MGR2* gene in the ***n***Cox2^{W56R} background. Deletion of the *MGR2* gene had no noticeable effect on growth in a fermentable substrate, but substantially affected respiratory growth even at 30 °C (Figure 3A, upper panels). Under these conditions, overexpression of *MGR2* from the multicopy vector pMK2 (***n****COX2*^{W56R} + *MGR2*↑) also negatively impacted growth of the yeast strain. As expected, transformation with the corresponding empty vector (***n****COX2*^{W56R} + EV) had no effect.

The overexpression and deletion of *MGR2* were assessed in the ***e***Cox2^{W56R} background, *i.e.*, where the ***e****COX2*^{W56R} construct was expressed from a multicopy plasmid (Figure 3A, lower panels). Deleting *MGR2* strongly impaired the respiratory growth of the ***e***Cox2^{W56R} strain, indicating that Mgr2 plays an instrumental role in the import of the allotopic subunit. Likewise, overexpression of *MGR2* in the ***e***Cox2^{W56R} strain had a markedly detrimental effect on the respiratory growth, which was more pronounced compared to the ***n***Cox2^{W56R} strain.

To assess changes in the steady-state levels of the different versions of Cox2 and Cox2^{W56R} when Mgr2 was present or absent, total yeast extracts were assayed for the accumulation of the allotopically produced Cox2 subunit, using a specific anti-yeast Cox2

antibody (Figures 3B and 3C). In the Δ*cox2* + ***n****COX2*^{W56R} background, deletion of *MGR2* resulted in a slight accumulation of the ***n***Cox2^{W56R} precursor and diminished levels of the mature form, revealing that the internalization into mitochondria of the allotopic precursor is partially impaired. In contrast, in the Δ*cox2* + ***e****COX2*^{W56R} background, the absence of Mgr2 led to an accumulation of the precursor while the presence of mature Cox2^{W56R} protein was nearly undetectable. As shown in Table 1, strains carrying the allotopic *COX2*^{W56R} gene and overexpressing *MGR2* display a 20-30% decrease of the oxygen uptake. In accord with the respiratory growth phenotype, loss of Mgr2 function in the ***n***Cox2^{W56R} background yields a 50% diminution of oxygen uptake while the *mgr2*-null mutation results in a complete block of respiration in the ***e***Cox2^{W56R} strain. In conclusion, the respiratory growth phenotype, and the steady state of Cox2^{W56R} correlated with the respiratory capacity measured by the oxygen uptake. Loss of Mgr2 function yields a more severe phenotype when the allotopic *COX2*^{W56R} gene is present in multicopy.

The Δ*mgr2* mutant could be complemented when transformed with *MGR2* cloned in a multicopy plasmid. Complementation was not observed when the gene was inserted in an antisense direction (3´-5´) in relation to the *PGK* promoter or when only the empty vector was used for the transformation (Figure 4A). Mitochondria were isolated from the wild-type, the Δ*mgr2* mutant, and the Δ*mgr2* overexpressing the *MGR2* gene (Δ*mgr2* + *MGR2*↑), solubilized with DDM and subjected to BN-PAGE (Figure 4B). In-gel staining of CcO activity revealed diminished activity of the *mgr2*-null mutant compared to the wild-type strain. This CcO activity was restored in the Δ*mgr2* strain complemented by the wild-type gene (Figure 4C). By contrast, the hydrolytic activity of complex V (ATP synthase) remained unaltered in the three strains (Figure 4D). Subsequently, the BN-gels were independently subjected to second dimension electrophoresis in denaturing conditions (2D-SDS-PAGE) and the resulting gels were blotted and immunodecorated using an anti-Cox2 antibody. An evident decrease in the levels of C*c*O was observed in the *mgr2* null mutant as compared to the wild-type strain (around 50%, data not shown); and enhanced levels were recovered upon complementation with the *MGR2* gene (Figure 4E). The results described above strongly indicate that the absence of Mgr2 elicits diminished levels of C*c*O, even if the growth of the *mgr2*-null strain is comparable to that of the wild-type yeast.

DISCUSSION

Oxa1, Cox20 *and* Pse1 *control a limiting step of the biogenesis of allotopic* *Cox2*^{W56R}.

Overexpression of *COX20* and *OXA1* improved the respiratory growth of a yeast strain expressing *COX2*^{W56R} and facilitated the internalization of Cox2^{W56R} subunit into yeast mitochondria when high levels of the Cox2^{W56R} subunit are synthesized (Figure 1). We hypothesize that overexpression of the two tested genes yields enhanced levels of their cognate protein products. That increased levels of Oxa1 or Cox20 improve the respiratory growth of the ***e***Cox2^{W56R} strain, suggests that both proteins control a limiting step of the biogenesis of allotopically produced Cox2.

The Oxa1 translocator is a protein embedded in the IMM (Hell et al., 1997, 2000; Homberg et al., 2023) that inserts mitochondrial membrane proteins during their synthesis by

mitoribosomes (Szyrach et al., 2003), including the Cox1, Cox2 and Cox3 subunits of C*c*O (Bonnefoy et al., 1994; Herrmann and Funes, 2005). Oxa1 is also instrumental in inserting the TMS of cytosol-synthesized membrane proteins that are imported into mitochondria and is essential for the insertion of the TMS1 of the allotopic Cox2^{W56R} subunit (Elliott et al., 2012). Overproduction of Oxa1 may facilitate the recognition of the LP close to the TMS1 of Cox2^{W56R} reaching the mitochondrial matrix and guiding insertion into the IMM more efficiently.

Cox20, an IMM-bound protein with a N_{out}-C_{out} topology is a Cox2-specific chaperone involved in several steps of C*c*O biogenesis (Herrmann and Funes, 2005; Kumar et al., 2015; Keerthiraju et al., 2019). Along with the mitochondrial ribosome receptor Mba1, Cox20 stabilizes the nascent Cox2 polypeptide exiting the mitoribosome, while its TMS1 is inserted from the matrix into the IMM and delivers the subunit to the Cox18-dependent Cox2 tail export machinery (Lorenzi et al., 2016). Subsequently, the Cox18 insertase interacts with Cox2 to promote translocation from the matrix across the inner membrane of the TMS2 and the C-tail of Cox2, the latter containing the Cu binding site for formation of the Cu_A binuclear center (Bourens et al., 2017). Binding of Cox20 to Cox2 on the IMS-facing side of the IMM accelerates dissociation of Cox18 translocase from the newly exported Cox2 protein (Elliot et al., 2012) and promotes subsequent maturation by delivering the subunit to the Cu-inserting system facing the IMS, *i.e.*, the Sco1-Sco2-Coa6 copper metalation module (Hell et al., 2000).

Import of cytosol synthesized Cox2^{W56R} does not require the Cox18 translocase, suggesting that the biogenesis pathway of the allotopically produced subunit does not involve import of TMS2 and the C-tail into the matrix followed by export across the IMM to the IMS (Elliott et al., 2012). Hence, the *COX20*-dependent improvement of the respiratory phenotype of ***e***Cox2^{W56R} strain cannot be attributed to the function of Cox20 in translocating the TMS2 and C-tail of Cox2. Conceivably, overexpression of *COX20* may promote the production of mature Cox2^{W56R} by enhancing the delivery of Cu to the subunit already inserted in the IMM through interaction with the Cu-inserting machinery. In summary, increased levels of Oxa1 and Cox20 may facilitate the overall import rates of ***e***Cox2^{W56R}.

The basis for the *PSE1*-dependent suppression is not obvious but it is likely that *PSE1* overexpression facilitates the import of Cox2^{W56R} into mitochondria, by mediating the nuclear-to-cytoplasm transport of a transcript encoding a factor directly or indirectly required for mitochondrial import of membrane proteins (Lord et al., 2015). Also, overexpression of *RRP5* or *MSP1* in the ***e****COX2*^{W56R} strain appeared to be detrimental to respiratory growth (Figure 1A and 1B). This suggests that overexpression of these genes affects the internalization of Cox2^{W56R} and/or other aspects of mitochondrial respiration. For genes that did not elicit any enhancement of the respiratory growth, we cannot rule out the possibility that there is no overproduction of the corresponding gene product, or that the level of the overproduced protein is not sufficient to enhance respiratory growth.

Mgr2 participates in the biogenesis pathway of the allotopic Cox2^{W56R} subunit.

Mgr2, a small hydrophobic protein with two TMS, was initially identified as a coupling factor of TIM23, the translocase of most cytosol-synthesized proteins containing an MTS and destined to the mitochondrial matrix or the IMM (Gebert et al., 2012; Ieva et al., 2013).

Mgr2 regulates the gating mechanism of TIM23 (Mirzalieva et al., 2019), which has been proposed to exist in the IMM as three distinct structural/functional forms in continuous dynamic interchange: $TIM23^{CORE}$, $TIM23^{MOTOR}$, and $TIM23^{SORT}$ (Popov-Celeketić et al., 2008; Bohnert et al., 2010; Chacinska et al., 2010). Mgr2 provides "quality control" to the lateral release of membrane proteins into the IMM via $TIM23^{SORT}$ (Gebert et al., 2012). In essence, Mgr2 works as a gatekeeper directly interacting with alpha helices (TMS) being sorted by TIM23 (Matta et al., 2020). Pam18 is a scaffold component of $TIM23^{MOTOR}$ crucial for importing proteins into the mitochondrial matrix (Mokranjac et al., 2020). When Pam18 is recruited to the translocase, the main function of its membrane-spanning alpha-helix domain is to obstruct the lateral release of proteins into the IMM. When a hydrophobic TMS gets arrested in the $TIM23^{SORT}$ protein translocation crevice, Pam18 dissociates and allows Mgr2 recruitment (Schendzielorz et al., 2018). The role of Mgr2 in $TIM23^{SORT}$ is to discriminate which alpha-helices should be laterally released into the IMM or translocated through the IMM. The model is that Mgr2 probably acts by sensing hydrophobic signals and allowing stop-transfer signals contained in the hydrophobic TMS to be released into the membrane, but less hydrophobic alpha-helices to get across the IMM into the matrix (Botelho et al., 2011; Lee et al., 2020). Here, we asked if Mgr2 also modulates TIM23 function during the internalization of the allotopically produced subunit and examined the effects of overexpressing and deleting this factor on $Cox2^{W56R}$ import.

Our findings revealed that the overproduction of Mgr2 exhibited a marginal detrimental effect on the internalization of allotopic ***n***$Cox2^{W56R}$, which becomes more pronounced in the case of ***e***$Cox2^{W56R}$. Since Pam18 and Mgr2 compete for the same binding site in the $TIM23^{CORE}$ complex (Schendzielorz et al., 2018), one possible scenario is that production of high levels of Mgr2 might displace Pam18. Conceivably, this might impair the function of $TIM23^{MOTOR}$ and diminish the import of the TMS1 of $Cox2^{W56R}$ into mitochondria.

While previous studies reported the temperature sensitive respiratory growth phenotype of a *mgr2*-null mutant (Matta et al., 2020), there was no additional description of the consequences on the respiratory chain caused by loss of Mgr2 function. Here we show that the absence of Mgr2 in an otherwise wild-type background has no evident effect on yeast growth, but nevertheless, it yields a 30% decrease of both the oxygen consumption and C*c*O activity. Since C*c*O (complex IV) and the bc_1 complex (complex III) are in a high copy number in a yeast cell (67,000 and 83,000 copies/cell respectively) (Morgenstern et al., 2017; Pfanner et al., 2019) a relatively small decrease in the levels of C*c*O should not drastically affect yeast growth, and its deleterious effects can only be observed when a critical, minimum level is reached. Mgr2 may also participate in C*c*O biogenesis even when the Cox2 subunit is synthesized inside the mitochondria, most probably, by controlling the import process of some of the nucleus-encoded subunits of yeast C*c*O that contain one TMS. Indeed, nine nucleus encoded subunits are present in the cryo-EM structure of yeast C*c*O complex (PDB: 6YMY; Berndtsson et al.,2020) and six of them exhibit one TMS oriented with a N_{in}-C_{out} topology (Cox5, Cox7, Cox8, Cox9, Cox13 and Cox26). To reach this final topology, the six subunits must be laterally released into the IMM by $TIM23^{SORT}$, most probably in a Mgr2-dependent manner. The absence of Mgr2 could affect the lateral release of these subunits into the IMM, therefore slightly diminishing the steady-state levels of C*c*O. Nevertheless, Mgr2 becomes crucial when C*c*O assembly depends on allotopically produced Cox2. The absence of Mgr2 negatively impacted respiratory growth and the internalization of both ***n***$Cox2^{W56R}$ and ***e***$Cox2^{W56R}$. One possible scenario is that, in the absence of Mgr2, TMS1 with the W56R substitution is no longer sensed as less hydrophobic and is recognized as a stop-transfer signal. Subsequently, the

TMS1 is laterally released in the IMM instead of being imported into the matrix, leading to a protein embedded in the membrane with an incorrect topology (N_{in}-C_{out} instead of N_{out}-C_{out}). This is supported by the fact that in a *mgr2*-null mutant, TIM23 tends to accelerate lateral release of TMSs into the IMM through the "stop-transfer" pathway (Ieva et al., 2014; Steffen and Koehler, 2014). We conclude that both the deletion and overexpression of *MGR2* affect the import of the allotopically produced Cox2 subunit. The detrimental effects of Mgr2 on $Cox2^{W56R}$ import strongly suggest the participation of $TIM23^{SORT}$ in this process.

A model for the import of the allotopically synthesized $Cox2^{W56R}$ subunit.

Previous models of the biogenesis of the allotopic $Cox2^{W56R}$ subunit postulated the dual functionality of TIM23 in sorting proteins through two different routes: the TMS1 of the protein is translocated into the mitochondrial matrix through the "conservative-sorting" pathway, while the TMS2 is laterally released into the IMM through the "stop-transfer" pathway (Cruz-Torres et al., 2012; Rubalcava-Gracia et al., 2018; Nieto-Panqueva et al., 2023). Here, the finding that Mgr2 is essential for the import of $Cox2^{W56R}$ led us to define our model (Figure 5). $TIM23^{MOTOR}$ translocates the MTS and the TMS1 of $Cox2^{W56R}$ into the matrix, then, TMS2 will get arrested due to its high hydrophobicity and the presence of a stop transfer signal. At this stage, the PAM motor must disassemble from $TIM23^{MOTOR}$ giving rise transiently to $TIM23^{CORE}$ (Tim50/Tim23/Tim17), and immediately thereafter Mgr2, Tim21 and respiratory complexes III and IV could be recruited by $TIM23^{CORE}$ to assemble a functionally competent $TIM23^{SORT}$ complex, that with the help of Mgr2, will laterally release the TMS2 of $Cox2^{W56R}$ into the IMM.

Additional observations support the proposed model: *i)* two high resolution cryo-EM structures of the yeast TIM23 complex indicate that the Tim23 and Tim17 subunits interact back-to-back, and that protein translocation occurs through a cavity in Tim17 (Sim et al., 2021; Zhou et al., 2023) that is found to be in close contact with Mgr2 (Zhou et al., 2023). *ii)* Since Pam18 and Mgr2 compete for the same binding site in Tim17 (Schendzielorz et al., 2018), once Pam18 gets displaced, Mgr2 may bind and facilitate the lateral release into the IMM of the TMS2 of the allotopic Cox2 precursor (Figure S3). *iii)* Recently, using high-resolution complexome profiling, a quantitative map of protein assemblies of more than 90% of the yeast mitochondrial proteome, termed MitCOM, was made available (Schulte et al., 2023). Mining this database, we could identify two independent peaks in these complexome profiles, representing Tim17-Pam18 and Tim17-Mgr2 associations with distinct apparent molecular masses (Figure S4). *iv)* Models of protein complexes built using AlphaFold-Multimer (Jumper et al., 2021) suggest that both Pam18 and Mgr2 independently bind to the same domain of Tim17 (Figure S5).

In summary, we propose that a dynamic exchange of $TIM23^{MOTOR}$ and $TIM23^{SORT}$ is required during allotopic $Cox2^{W56R}$ precursor translocation and sorting. Our model also explains why the biogenesis pathway followed by either a naturally (Adams et al., 1999; Daley et al., 2002) or artificially (Rubalcava-Gracia et al., 2018) nucleus-encoded Cox2 protein is much more complex than the one followed by its mitochondria-synthesized counterpart. Lastly, the model suggests that the limiting step of $Cox2^{W56R}$ import into mitochondria probably occurs when its TMS2 is retained by Tim17, forcing the disassembly of $TIM23^{MOTOR}$ (release of the PAM motor) followed by the building of a functional $TIM23^{SORT}$ complex. We speculate that a "Pam18-Mgr2 switch" could control the $Tim23^{SORT}$ and $TIM23^{MOTOR}$ interchange required for the correct import/sort of IMM-embedded proteins. This translocation machinery disassembly-assembly shift *must* occur while a single $Cox2^{W56R}$ polypeptide is being internalized, and it inevitably implies a major

discontinuity in the import process of the allotopic subunit. We therefore suggest that the limiting step of the $Cox2^{W56R}$ biogenesis is due to the rearrangement $TIM23^{MOTOR} \rightarrow TIM23^{SORT}$. Our model illustrates the complexity of a process required for an allotopically produced $Cox2^{W56R}$ subunit to reach its final, functional N_{out}-C_{out} topology in the IMM, and it also sheds light on the mechanism through which several other nucleus-encoded mitochondrial membrane proteins, exhibiting a MTS, two TMS, and an N_{out}-C_{out} topology, are imported and sorted into the IMM by TIM23.

DATA AVAILABILITY

Strains and plasmids are available upon request. The authors affirm that all data necessary for confirming the conclusions of the article are present within the article, figures, and tables.

ACKNOWLEDGMENTS

The authors are grateful to Dr. Juan García-Rincón, who carried out preliminary experiments for this project, and acknowledge the technical expertise of José Luis Santillán Torres (IFC, UNAM). We are grateful to Dr. Manuel Osorio-Valeriano (Harvard Medical School, USA) for his help in building the AlphaFold2 3D-models and to Prof. Benjamin Podbilewicz (Technion, Israel) for critically reviewing this manuscript. This article is submitted in partial fulfillment of the doctoral requirements of F.N.-P. for a PhD from the Biochemical Sciences program at UNAM (Programa de Maestría y Doctorado en Ciencias Bioquímicas, Universidad Nacional Autónoma de México).

FUNDING

D.G.-H. laboratory received financial support from grants CF2019-21856 (Frontiers of Science, CONACyT, Mexico) and IN207023 (PAPIIT, DGAPA, UNAM). F.N.-P. is a Ph.D. student at Programa de Maestría y Doctorado en Ciencias Bioquímicas (UNAM) and recipient of a CONACyT fellowship (CVU 700670). P.P.H. received a PREI fellowship from DGAPA, UNAM to carry a research stay in Mexico. Molecular graphics and analyses performed with UCSF Chimera, developed by the Resource for Biocomputing, Visualization, and Informatics at the University of California, San Francisco, with support from NIH P41-GM103311.

REFERENCES

Adams KL, Song K, Roessler PG, Nugent JM, Doyle JL, Doyle JJ, Palmer JD. 1999. Intracellular gene transfer in action: dual transcription and multiple silencings of nuclear and mitochondrial cox2 genes in legumes. PROC NATL ACAD SCI U S A. 96(24):13863-8. doi: 10.1073/pnas.96.24.13863.

Bähler J, Wu JQ, Longtine MS, Shah NG, McKenzie A 3rd, Steever AB, Wach A, Philippsen P, Pringle JR. 1998. Heterologous modules for efficient and versatile PCR-based gene targeting in Schizosaccharomyces pombe. YEAST.14(10):943-51. doi: 10.1002/(SICI)1097-0061(199807)14:10<943::AID-YEA292>3.0.CO;2-Y.

Barrientos A, Barros MH, Valnot I, Rötig A, Rustin P, Tzagoloff A. 2002. Cytochrome oxidase in health and disease. GENE. 286(1):53-63. doi: 10.1016/s0378-1119(01)00803-4.

Berndtsson J, Kohler A, Rathore S, Marin-Buera L, Dawitz H, Diessl J, Kohler V, Barrientos A, Büttner S, Fontanesi F, Ott M. 2020. Respiratory supercomplexes enhance electron transport by decreasing cytochrome c diffusion distance. EMBO REP. 21(12): e51015. doi: 10.15252/embr.202051015.

Bohnert M, Rehling P, Guiard B, Herrmann JM, Pfanner N, van der Laan M. 2010. Cooperation of stop-transfer and conservative sorting mechanisms in mitochondrial protein transport. CURR BIOL. 20(13):1227-32. doi: 10.1016/j.cub.2010.05.058.

Bonnefoy N, Chalvet F, Hamel P, Slonimski P, Dujardin G. 1994. OXA1, a *Saccharomyces cerevisiae* nuclear gene whose sequence is conserved from prokaryotes to eukaryotes controls cytochrome oxidase biogenesis. J MOL BIOL. 239(2):201-212. doi:10.1006/jmbi.1994.1363

Botelho S, Osterberg M, Reicher A., Yamano K, Björkholm P, Endo T, von Heijne G, Kim H. 2011. TIM23-mediated insertion of transmembrane α-helices into the mitochondrial inner membrane. EMBO J. 30(6):1003-11. doi: 10.1038/emboj.2011.29.

Bourens M, Boulet A, Leary SC, Barrientos A. 2014. Human COX20 cooperates with SCO1 and SCO2 to mature COX2 and promote the assembly of cytochrome c oxidase. HUM MOL GENET. 23(11):2901-2913. doi:10.1093/hmg/ddu003

Bourens M, Barrientos A. 2017. Human mitochondrial cytochrome c oxidase assembly factor COX18 acts transiently as a membrane insertase within the subunit 2 maturation module. J BIOL CHEM. 292(19):7774-7783. doi: 10.1074/jbc.M117.778514.

Brix J, Ziegler G, Dietmeier K, Schneider-Mergener J, Schulz G, Pfanner N. 2000. The mitochondrial import receptor Tom70: identification of a 25 kDa core domain with a specific binding site for preproteins. J MOL BIOL. 303(4):479-88. doi: 10.1006/jmbi.2000.4120.

Callegari S, Cruz-Zaragoza L, Rehling P. 2020. From TOM to the TIM23 complex - handing over of a precursor. BIOL CHEM. 401(6-7):709-721. doi: 10.1515/hsz-2020-0101.

Castanzo DT, LaFrance B, Martin A. 2020. The AAA+ ATPase Msp1 is a processive protein translocase with robust unfoldase activity. PROC NATL ACAD SCI U S A. 117(26):14970-14977. doi: 10.1073/pnas.1920109117.

Chacinska A, Koehler CM, Milenkovic D, Lithgow T, Pfanner N. 2009. Importing mitochondrial proteins: machineries and mechanisms. CELL. 138(4):628-44. doi: 10.1016/j.cell.2009.08.005.

Chacinska A, van der Laan M, Mehnert C, Guiard B, Mick D, Hutu D, Truscott K, Wiedemann N, Meisinger C, Pfanner N, Rehling P. 2010. Distinct forms of mitochondrial TOM-TIM supercomplexes define signal-dependent states of preprotein sorting. MOL CELL BIOL. 30(1):307-18. doi: 10.1128/MCB.00749-09.

Chen DC, Yang BC, Kuo TT. 1992. One-step transformation of yeast in stationary phase. CURR GENET. 21(1):83-4. doi: 10.1007/BF00318659.

Corral-Debrinski M, Belgareh N, Blugeon C, Claros MG, Doye V, Jacq C. 1999. Overexpression of yeast karyopherin Pse1p/Kap121p stimulates the mitochondrial import of hydrophobic proteins in vivo. MOL MICROBIOL. 31(5):1499-511. doi: 10.1046/j.1365-2958.1999.01295.x.

Cruz-Torres V, Vázquez-Acevedo M, García-Villegas R, Pérez-Martínez X, Mendoza-Hernández G, González-Halphen D. 2012. The cytosol-synthesized subunit II (Cox2) precursor with the point mutation W56R is correctly processed in yeast mitochondria to rescue cytochrome oxidase. BIOCHIMICA ET BIOPHYSICA ACTA, BIOENER. 1817(12) 2128–39. doi: 10.1016/j.bbabio.2012.09.006.

Daley D, Adams K, Clifton R, Qualmann S, Millar A, Palmer J, Pratje E, Whelan J. 2002. Gene transfer from mitochondrion to nucleus: novel mechanisms for gene activation from Cox2. PLANT J. 30(1):11-21. doi:10.1046/j.1365-313x.2002.01263.

Dennerlein S, Poerschke S, Oeljeklaus S, Wang C, Richter-Dennerlein R, Sattmann J, Bauermeister D, Hanitsch E, Stoldt S, Langer T, Jakobs S, Warscheid B, Rehling P. 2021. Defining the interactome of the human mitochondrial ribosome identifies SMIM4 and TMEM223 as respiratory chain assembly factors. ELIFE. 10:e68213. doi: 10.7554/eLife.68213.

Elliott LE, Saracco SA, Fox TD. 2012. Multiple roles of the Cox20 chaperone in assembly of *Saccharomyces cerevisiae* cytochrome c oxidase. GENETICS. 190(2):559-67. doi: 10.1534/genetics.111.135665.

Estabrook R. 1967. Mitochondrial respiratory control and the polarographic measurement of ADP: O ratios. METHODS IN ENZYMOLOGY. Academic Press. Volume 10. Pages 41-47.

Fiumera H, Broadley S, Fox T. 2007. Translocation of mitochondrially synthesized Cox2 domains from the matrix to the intermembrane space. MOL CELL BIOL. 27(13):4664-73. doi: 10.1128/MCB.01955-06.

Fontanesi F, Soto I, Barrientos A. 2008. Cytochrome c oxidase biogenesis: new levels of regulation. IUBMB LIFE. 60: 557-568.

Franco L, Su C, Tzagoloff A. 2020. Modular assembly of yeast mitochondrial ATP synthase and cytochrome oxidase. BIOL CHEM. 401(6-7):835-853. doi: 10.1515/hsz-2020-0112.

Fujiwara S, Kawazoe T, Ohnishi K, Kitagawa T, Popa C, Valls M, Genin S, Nakamura K, Kuramitsu Y, Tanaka N, Tabuchi M. 2016. RipAY, a Plant Pathogen Effector Protein, Exhibits Robust γ-Glutamyl Cyclotransferase Activity When Stimulated by Eukaryotic Thioredoxins. J BIOL CHEM. Mar 25;291(13):6813-30. doi: 10.1074/jbc.M115.678953.

Gebert M, Schrempp S, Mehnert C, Heißwolf A, Oeljeklaus S, Ieva R, Bohnert M, von der Malsburg K, Wiese S, Kleinschroth T, Hunte C, Meyer H, Haferkamp I, Guiard B, Warscheid B, Pfanner N, van der Laan M. 2012. Mgr2 promotes coupling of the mitochondrial presequence translocase to partner complexes. J CELL BIOL. 197(5):595-604. doi: 10.1083/jcb.201110047.

Ghosh A, Pratt A, Soma, S, Theriault S, Griffin A, Trivedi P, Gohil V. 2016. Mitochondrial disease genes COA6, COX6B and SCO2 have overlapping roles in COX2 biogenesis. HUM MOL GENET. 25(4):660-671. doi:10.1093/hmg/ddv503

Gietz RD, Schiestl RH. 2007. High-efficiency yeast transformation using the LiAc/SS carrier DNA/PEG method. NATURE PROTOCOLS 2(1), 31–34. doi: 10.1038/nprot.2007.13.

Gomkale R, Cruz-Zaragoza LD, Suppanz I, Guiard B, Montoya J, Callegari S, Pacheu-Grau D, Warscheid B, Rehling P. 2020. Defining the Substrate Spectrum of the TIM22 Complex Identifies Pyruvate Carrier Subunits as Unconventional Cargos. CURR BIOL. 30(6):1119-1127.e5. doi: 10.1016/j.cub.2020.01.024.

Gray MW. 2000. Mitochondrial genes on the move. NATURE 408(6810):302-3, 305. doi: 10.1038/35042663.

Hell K, Herrmann J, Pratje E, Neupert W, Stuart R. 1997. Oxa1p mediates the export of the N- and C-termini of pCoxII from the mitochondrial matrix to the intermembrane space. FEBS LETT. 418: 367-370. doi: 10.1016/s0014-5793(97)01412-9.

Hell K, Tzagoloff A, Neupert W, Stuart RA. 2000. Identification of Cox20p, a novel protein involved in the maturation and assembly of cytochrome oxidase subunit 2. J BIOL CHEM. 275(7):4571-8. doi: 10.1074/jbc.275.7.4571.

Herrmann J, Bonnefoy N. 2004. Protein export across the inner membrane of mitochondria: the nature of translocated domains determines the dependence on the Oxa1 translocase. J BIOL CHEM. 279(4):2507-2512. doi:10.1074/jbc.M310468200

Herrmann J, Funes S. 2005. Biogenesis of cytochrome oxidase-sophisticated assembly lines in the mitochondrial inner membrane. GENE. 2005 354:43-52. doi: 10.1016/j.gene..03.017.

Herrmann JM, Bykov Y. 2023. Protein translocation in mitochondria: Sorting out the Toms, Tims, Pams, Sams and Mia. FEBS LETT. 597(12):1553-1554. doi: 10.1002/1873-3468.14614.

Homberg B, Rehling P, Cruz-Zaragoza LD. 2023.The multifaceted mitochondrial OXA insertase. TRENDS CELL BIOL. 33(9):765-772. doi: 10.1016/j.tcb.2023.02.001.

Horan S, Bourges I, Taanman JW, Meunier B. 2005. Analysis of COX2 mutants reveals cytochrome oxidase subassemblies in yeast. BIOCHEM J. 390 (Pt 3): 703-708. doi: 10.1042/BJ20050598.

Horten P, Colina-Tenorio L, Rampelt H. 2020. Biogenesis of Mitochondrial Metabolite Carriers. BIOMOLECULES. 10(7):1008. doi: 10.3390/biom10071008.

Ieva R, Heißwolf AK, Gebert M, Vögtle FN, Wollweber F, Mehnert CS, Oeljeklaus S, Warscheid B, Meisinger C, van der Laan M, Pfanner N. 2013. Mitochondrial inner membrane protease promotes assembly of presequence translocase by removing a carboxy-terminal targeting sequence. NAT COMMUN. 4:2853. doi: 10.1038/ncomms3853.

Ieva R, Schrempp S, Opaliński L, Wollweber F, Höß P, Heißwolf A, Gebert M, Zhang Y, Guiard B, Rospert S, Becker T, Chacinska A, Pfanner N, van der Laan, M. 2014. Mgr2 functions as lateral gatekeeper for preprotein sorting in the mitochondrial inner membrane. MOL CELL. 56(5):641-52. doi: 10.1016/j.molcel.2014.10.010.

Jumper J, Evans R, Pritzel A, Green T, Figurnov M, Ronneberger O, Tunyasuvunakool K, Bates R, Žídek A, Potapenko A, Bridgland A, Meyer C, Kohl SAA, Ballard AJ, Cowie A, Romera-Paredes B, Nikolov S, Jain R, Adler J, Back T, Petersen S, Reiman D, Clancy E, Zielinski M, Steinegger M, Pacholska M, Berghammer T, Bodenstein S, Silver D, Vinyals O, Senior AW, Kavukcuoglu K, Kohli P, Hassabis D. 2021. Highly accurate protein structure prediction with AlphaFold. NATURE. 596(7873):583-589. doi: 10.1038/s41586-021-03819-2.

Kabeya Y, Kawamata T, Suzuki K, Ohsumi Y. 2007. Cis1/Atg31 is required for autophagosome formation in Saccharomyces cerevisiae. BIOCHEM. BIOPHYS. RES. COMMUN. 356(2):405-10. doi: 10.1016/j.bbrc.2007.02.150.

Keerthiraju E, Du C, Tucker G, Greetham D. 2019. A Role for COX20 in Tolerance to Oxidative Stress and Programmed Cell Death in Saccharomyces cerevisiae. MICROORGANISMS. 7(11):575. doi: 10.3390/microorganisms7110575.

Krämer L, Dalheimer N, Räschle M, Storchová Z, Pielage J, Boos F, Herrmann JM. 2023. MitoStores: chaperone-controlled protein granules store mitochondrial precursors in the cytosol. EMBO J. Jan 27:e112309. doi: 10.15252/embj.2022112309.

Kumar V, Hart AJ, Keerthiraju ER, Waldron PR, Tucker GA, Greetham D. 2015. Expression of Mitochondrial Cytochrome C Oxidase Chaperone Gene (COX20) Improves Tolerance to Weak Acid and Oxidative Stress during Yeast Fermentation. PLOS ONE. 10(10):e0139129. doi: 10.1371/journal.pone.0139129.

Kushnirov VV. 2000. Rapid and reliable protein extraction from yeast. YEAST.16(9): 857–860. doi: 10.1002/1097-0061(20000630)16:9<857::AID-YEA561>3.0.CO;2-B.

Lee S, Lee H, Yoo S, Ieva R, van der Laan M, von Heijne G, Kim H. 2020. The Mgr2 subunit of the TIM23 complex regulates membrane insertion of marginal stop-transfer signals in the mitochondrial inner membrane. FEBS LETT. 594(6):1081-1087. doi: 10.1002/1873-3468.13692.

Lord C, Timney B, Rout M, Wente S. 2015. Altering nuclear pore complex function impacts longevity and mitochondrial function in *S. cerevisiae*. J CELL BIOL. 208(6):729-44. doi: 10.1083/jcb.201412024.

Lorenzi I, Oeljeklaus S, Ronsör C, Bareth B, Warscheid B, Rehling P, Dennerlein S. 2016. Ribosome-Associated Mba1 Escorts Cox2 from Insertion Machinery to Maturing Assembly Intermediates. MOL CELL BIOL. 36(22):2782-2793. doi: 10.1128/MCB.00361-16.

Maghool S, Ryan MT, Maher MJ. 2020. What Role Does COA6 Play in Cytochrome C Oxidase Biogenesis: A Metallochaperone or Thiol Oxidoreductase, or Both? INT J MOL SCI. 21(19):6983. doi: 10.3390/ijms21196983.

Matta S, Kumar A, D'Silva P. 2020. Mgr2 regulates mitochondrial preprotein import by associating with channel-forming Tim23 subunit. MOL BIOL CELL. 31(11):1112-1123. doi: 10.1091/mbc.E19-12-0677.

Meisinger C, Brix J, Model K, Pfanner N, Ryan MT. 1999.The preprotein translocase of the outer mitochondrial membrane: receptors and a general import pore. CELL MOL LIFE SCI. 56(9-10):817-24. doi: 10.1007/s000180050028.

Minet M, Dufour ME, Lacroute F. 1992. Complementation of *Saccharomyces cerevisiae* auxotrophic mutants by Arabidopsis thaliana cDNAs. PLANT J. 2(3):417-22. doi: 10.1111/j.1365-313x.1992.00417.x.

Mirdita M, Schütze K, Moriwaki Y, Heo L, Ovchinnikov S, Steinegger M. 2022. ColabFold: making protein folding accessible to all. NAT METHODS.19(6):679-682. doi: 10.1038/s41592-022-01488-1.

Mirzalieva O, Jeon S, Damri K, Hartke R, Drwesh L, Demishtein-Zohary, K, Azem A, Dunn C, Peixoto P. 2019. Deletion of Mgr2p Affects the Gating Behavior of the TIM23 Complex. FRONT PHYSIOL. 9:1960. doi:10.3389/fphys.2018.01960

Mokranjac D. 2020. How to get to the other side of the mitochondrial inner membrane - the protein import motor. BIOL CHEM. 401(6-7):723-736. doi: 10.1515/hsz-2020-0106.

Morgenstern M, Stiller SB, Lübbert P, Peikert CD, Dannenmaier S, Drepper F, Weill U, Höß P, Feuerstein R, Gebert M, Bohnert M, van der Laan M, Schuldiner M, Schütze C, Oeljeklaus S, Pfanner N, Wiedemann N, Warscheid B. 2017. Definition of a High-Confidence Mitochondrial Proteome at Quantitative Scale. CELL REP. 19(13):2836-2852. doi: 10.1016/j.celrep.2017.06.014.

Nakai M, Endo T, Hase T, Matsubara H. 1993. Intramitochondrial protein sorting. Isolation and characterization of the yeast MSP1 gene which belongs to a novel family of putative ATPases. J BIOL CHEM. 268(32):24262-9. doi:10.1016/S0021-9258(20)80519-5.

Nieto-Panqueva F, Rubalcava-Gracia D, Hamel PP, González-Halphen D. 2023. The constraints of allotopic expression. MITOCHONDRION. 73:30-50. doi: 10.1016/j.mito.2023.09.004.

Pacheu-Grau D, Bareth B, Dudek , Juris, L, Vögtle FN, Wissel M, Leary SC, Dennerlein S, Rehling P, Deckers M. 2015. Cooperation between COA6 and SCO2 in COX2 maturation during cytochrome c oxidase assembly links two mitochondrial cardiomyopathies. CELL METAB. 21(6):823-833. doi:10.1016/j.cmet.2015.04.012

Perez-Martínez X, Broadley SA, Fox TD. 2003. Mss51p promotes mitochondrial Cox1p synthesis and interacts with newly synthesized Cox1p. EMBO J. 22(21):5951-61. doi: 10.1093/emboj/cdg566.
Pettersen EF, Goddard TD, Huang CC, Couch GS, Greenblatt DM, Meng EC, Ferrin TE. 2004. UCSF Chimera--a visualization system for exploratory research and analysis. J COMPUT CHEM. 25(13):1605-12. doi: 10.1002/jcc.20084.

Pfanner N, Warscheid B, Wiedemann N. 2019. Mitochondrial proteins: from biogenesis to functional networks. NAT REV MOL CELL BIOL. 20(5):267-284. doi: 10.1038/s41580-018-0092-0. Erratum in: NAT REV MOL CELL BIOL. 2021, 22(5):367.

Popov-Celeketić D, Mapa K, Neupert W, Mokranjac D. 2008. Active remodelling of the TIM23 complex during translocation of preproteins into mitochondria. EMBO J. 27(10):1469-80. doi: 10.1038/emboj.2008.79.

Poyton R, Groott G. 1975. Biosynthesis of Polypeptides of Cytochrome c Oxidase by Isolated Mitochondria. PROC. NATL. ACAD. SCI. USA. 72(1):172–176. doi: 10.1073/pnas.72.1.172.

Rigby K, Cobine P, Khalimonchuk O, Winge D. 2008. Mapping the functional interaction of Sco1 and Cox2 in cytochrome oxidase biogenesis. J BIOL CHEM. 283(22):15015-15022. doi:10.1074/jbc.M710072200

Rubalcava-Gracia D, Vázquez-Acevedo M, Funes S, Pérez-Martínez X, González-Halphen D. 2018. Mitochondrial versus nuclear gene expression and membrane protein assembly: The case of subunit 2 of yeast cytochrome c oxidase. MOL BIOL CELL. 29(7):820-833. doi: 10.1091/mbc.E17-09-0560.

Rubalcava-Gracia D, García-Rincón J, Pérez-Montfort R, Hamel P, González-Halphen D. 2019. Key within-membrane residues and precursor dosage impact the allotopic expression of yeast subunit II of cytochrome *c* oxidase. MOL BIOL CELL. 30(18):2358-2366. doi: 10.1091/mbc.E18-12-0788.

Saracco S, Fox T. 2002. Cox18p is required for export of the mitochondrially encoded *Saccharomyces cerevisiae* Cox2p C-tail and interacts with Pnt1p and Mss2p in the inner membrane. MOL BIOL CELL. 13(4):1122-31. doi: 10.1091/mbc.01-12-0580.

Schägger H. 1994. Denaturing Electrophoretic Techniques, in: Separation, Detection, and Characterization of Biological Macromolecules, a Practical Guide to Membrane Protein Purification, Academic Press, Volume 2, , Pages 59-79, doi: 10.1016/B978-0-08-057172-0.50010-3.

Schendzielorz AB, Bragoszewski P, Naumenko N, Gomkale R, Schulz C, Guiard B, Chacinska A, Rehling P. 2018. Motor recruitment to the TIM23 channel's lateral gate restricts polypeptide release into the inner membrane. NAT COMMUN. 9(1):4028. doi: 10.1038/s41467-018-06492-8

Schulte U, den Brave F, Haupt A, Gupta A, Song J, Müller CS, Engelke J, Mishra S, Mårtensson C, Ellenrieder L, Priesnitz C, Straub SP, Doan KN, Kulawiak B, Bildl W, Rampelt H, Wiedemann N, Pfanner N, Fakler B, Becker T. 2023. Mitochondrial complexome reveals quality-control pathways of protein import. NATURE. 614(7946):153-159. doi: 10.1038/s41586-022-05641-w.

Schwede T, Kopp J, Guex N, Peitsch MC. 2003. SWISS-MODEL: An automated protein homology-modeling server. NUCLEIC ACIDS RES. 31(13):3381-5. doi: 10.1093/nar/gkg520.

Sevarino K, Poyton R. 1980. Mitochondrial membrane biogenesis: identification of a precursor to yeast cytochrome c oxidase subunit II, an integral polypeptide. PROC NATL ACAD SCI U S A. 77(1):142-146. doi:10.1073/pnas.77.1.142.

Sim SI, Chen Y, Park E. 2021. Structural basis of mitochondrial protein import by the TIM complex. BIORXIV 10.10.463828; doi: 10.1101/2021.10.10.463828

Steffen J, Koehler CM. 2014. The great escape: Mgr2 of the mitochondrial TIM23 translocon is a gatekeeper Tasked with releasing membrane proteins. MOL CELL. Dec 4;56(5):613-4. doi: 10.1016/j.molcel.2014.11.022.

Supekova L, Supek F, Greer J, Schultz P. 2010. A single mutation in the first transmembrane domain of yeast COX2 enables its allotopic expression. PROC. NATL. ACAD. SCI. USA 107: 5047-5052. doi: 10.1073/pnas.1000735107.

Swaminathan AB, Gohil VM. 2022. The Role of COA6 in the Mitochondrial Copper Delivery Pathway to Cytochrome c Oxidase. BIOMOLECULES. Jan 13;12(1):125. doi: 10.3390/biom12010125.

Szyrach G, Ott M, Bonnefoy N, Neupert W, Herrmann J. 2003. Ribosome binding to the Oxa1 complex facilitates co-translational protein insertion in mitochondria. EMBO J. 22(24):6448-6457. doi:10.1093/emboj/cdg623

Torchet C, Jacq C, Hermann-Le Denmat S. 1998. Two mutant forms of the S1/TPR-containing protein Rrp5p affect the 18S rRNA synthesis in *Saccharomyces cerevisiae*. RNA. 4(12):1636-52. doi: 10.1017/s1355838298981511.

Torello A, Overholtzer M, Cameron V, Bonnefoy N, Fox T. 1997. Deletion of the leader peptide of the mitochondrially encoded precursor of Saccharomyces cerevisiae cytochrome c oxidase subunit II, GENETICS 145: 903-910.doi: 10.1093/genetics/145.4.903.

Venema J, Tollervey D. 1996. RRP5 is required for formation of both 18S and 5.8S rRNA in yeast. EMBO J. 15(20):5701-14. doi:10.1002/j.1460-2075.1996.tb00954.x

Weinhäupl K, Wang Y, Hessel A, Brennich M, Lindorff-Larsen K, Schanda P. 2021. Architecture and assembly dynamics of the essential mitochondrial chaperone complex TIM9·10·12. STRUCTURE. 29(9):1065-1073.e4. doi: 10.1016/j.str.2021.04.009.

Wikström M. 1989. Identification of the electron transfers in cytochrome oxidase that are coupled to proton-pumping. NATURE. 338(6218):776-8. doi: 10.1038/338776a0.

Williams EH, Fox TD. 2003. Antagonistic signals within the COX2 mRNA coding sequence control its translation in Saccharomyces cerevisiae mitochondria. RNA. 9(4):419-31. doi: 10.1261/rna.2182903.

Wittig I, Karas M, Schägger H. 2007. High resolution clear native electrophoresis for in-gel functional assays and fluorescence studies of membrane protein complexes. MOL CELL PROTEOMICS 6(7):1215-25. doi: 10.1074/mcp.M700076-MCP200.

Zerbetto E, Vergani L, Dabbeni-Sala F. 1997. Quantification of muscle mitochondrial oxidative phosphorylation enzymes via histochemical staining of blue native polyacrylamide gels. ELECTROPHORESIS. 18(11):2059-64. doi: 10.1002/elps.1150181131.

Zhou X, Yang Y, Wang G, Wang S, Sun D, Ou X, Lian Y, Li L. 2023. Molecular pathway of mitochondrial preprotein import through the TOM-TIM23 supercomplex. Nat Struct Mol Biol. 2023 Dec;30(12):1996-2008. doi: 10.1038/s41594-023-01103-7.

Figure Legends:

Figure 1. Overexpression of *OXA1*, *COX20* and *PSE1* enhances the respiratory growth of a strain expressing the *COX2*^{W56R} gene from a multicopy plasmid. A) Serial dilution series showing the fermentative (glucose) and respiratory (ethanol/glycerol, ethanol, and lactate) growth phenotype of a wild-type strain (wt), the *cox2*-null strain (Δ*cox2*), the Δ*cox2* + ***e****COX2*^{W56R} strain (***e****COX2*^{W56R}), and the 9 strains overexpressing (↑) the indicated gene or carrying the empty vector pGP564 (Tilling collection, labeled as EV) in the ***e****COX2*^{W56R} background at 30˚C. Photographs were taken on the fourth day of growth. **B)** Same serial dilution series as in A, except that growth was assayed at 37˚C. Photographs were taken on the fourth day of growth. **C, D and E)** Antibodies against Cox2 and Zwf1 were used to immunodetect the corresponding proteins in total cellular extracts of the indicated yeast strains: wild type (wt); the *cox2*-null mutant strain (Δ*cox2*); the Δ*cox2* + ***e****COX2*^{W56R} strain (***e***), the 9 strains overexpressing (↑) the indicated gene on an ***e****COX2*^{W56R} background, and the control strain (***e***) transformed with an empty vector pGP564 (Tilling collection) (***e*** + EV). The precursor and mature forms of Cox2 or Cox2^{W56R} (28 kDa) are indicated as p and m, respectively. The anti-Zwf1 antibody immunoreacts against a 57 kDa band which is used as a loading control. Antibodies against Oxa1, reacts against a 45 kDa band and is use here to show increased accumulation of OXA1 in the ***e*** + *OXA1*↑ strain. Bar plots represent quantification of technical replicates of immunoblots. Results are presented as mean ± SD, n = 3. The mean and SD abundance of the wild-type protein are indicated by black and grey dotted lines, respectively. Δcox2 data is not displayed.

Figure 2. Overexpression of genes related to the TIM23 translocon affects the growth of a strain expressing the *COX2*^{W56R} gene from a multicopy plasmid. A) serial dilution series showing the fermentative (glucose) and respiratory (ethanol/glycerol, ethanol, and lactate) growth phenotypes of a wild-type strain (wt), the *cox2*-null strain (Δ*cox2*), the Δ*cox2* + ***e****COX2*^{W56R} strain (***e****COX2*^{W56R}), and the 4 strains overexpressing (↑) the indicated gene or carrying the empty vector pGP564 (Tilling collection) (EV) in the ***e****COX2*^{W56R} background at 30°C. Photographs were taken on the fourth day of growth. **B) and C)** antibodies against Cox2 and Zwf1 were used to immunodetect the corresponding proteins in total cellular extracts of the indicated yeast strains: wild-type (wt); the cox2-null mutant strain (Δ*cox2*); the Δ*cox2* + ***e****COX2*^{W56R} strain (e), the four strains overexpressing (↑) the indicated gene on an ***e****COX2*^{W56R} background, and the control strain (***e***) transformed with an empty vector pGP564 (Tilling collection) (***e*** + EV). The precursor and

mature forms of the Cox2 or Cox2^{W56R} proteins (28 kDa) are indicated as p and m respectively. The anti-Zwf1 antibody immunoreacts against a 57 kDa band which is used as a loading control. Bar plots represent quantification of technical replicates of immunoblots. Results are presented as mean ± SD, n = 3. The mean and SD abundance of the wild-type protein are indicated by black and grey dotted lines, respectively. Δcox2 data is not displayed.

Figure 3. Overexpression or deletion of the *MGR2* gene affects the growth of the strains expressing the *COX2^{W56R}* gene either from the nucleus or from a multicopy plasmid. A) *Upper panels*: Serial dilution series at 30˚C showing the fermentative (glucose) and respiratory phenotype (ethanol-glycerol, ethanol, or lactate) of a wild-type strain (wt), the *cox2*-null strain (Δ*cox2*), a wild-type strain whose *MGR2* gene was deleted (Δ*mgr2*), the Δ*cox2* + ***n****COX2^{W56R}* strain (***n****COX2^{W56R}*), and the effect over the latter strain of the *MGR2* deletion (***n****COX2^{W56R}* + Δ*mgr2*) or its overexpression from a multicopy plasmid (***n****COX2^{W56R}* + *MGR2* ↑). The effect on growth of the multi copy empty vector (pMK2) is also shown (***n****COX2^{W56R}* + EV). *Lower panels*: Same serial dilution series as in the upper panels, except that growth was assayed in the strain expressing the multicopy plasmid ***e****COX2^{W56R}*. **B)** Antibodies against Cox2 and Zwf1 were used to immunodetect the corresponding proteins in total cellular extracts of the indicated yeast strains: wild-type (wt); a strain whose *MGR2* gene was deleted (Δ*mgr2*), the Δ*cox2* + ***n****COX2^{W56R}* strain (***n***), the effect over the latter strain of the *MGR2* deletion (***n*** + Δ*mgr2*), the effect of overexpressing *MGR2* (***n*** + *MGR2*↑), and the effect of the empty vector pMK2 (***n*** + EV). The precursor and mature forms of Cox2 or Cox2^{W56R} (28 kDa) are indicated as p and m respectively. Antibodies anti-Zwf1 were used as loading control. **C)** Same series of immunoblots as in B but carried with the strain expressing the multicopy plasmid ***e****COX2^{W56R}*.

Figure 4. Expressing the *MGR2* gene restores growth of the *mgr2*-null mutation in a Δ*cox2* + *nCOX2^{W56R}* strain. A) Serial dilution series at 30˚C and 37˚C showing the fermentative (glucose) and respiratory phenotype (ethanol-glycerol, ethanol, or lactate) of the following strains: Δ*cox2* + ***n****COX2^{W56R}* strain carrying a *MGR2* deletion (***n****COX2^{W56R}* + Δ*mgr2*), the latter strain complemented with a multicopy vector carrying the *MGR2* gene in the 5'-3' orientation [***n****COX2^{W56R}* + Δ*mgr2* + *MGR2*↑ (5'-3')], and a strain expressing *MGR2* cloned in the opposite direction [(***n****COX2^{W56R}* + Δ*mgr2* + *MGR2*↑ (3'-5')]. The effect on growth of the multi copy empty vector (pMK2) is also shown (***n****COX2^{W56R}* + Δ*mgr2* + EV). **B, C and D)** BN gels of solubilized mitochondrial proteins. Mitochondria were isolated from the wild-type strain (wt), the *mgr*2-null mutant (Δ*mgr2*) and the complemented mutant (Δ*mgr2* + *MGR2*↑). The gels were stained with Coomassie Brilliant Blue (**B**), C*c*O in gel activity (**C**), and ATPase in gel activity (white precipitates, **D**). The bands for complex IV (C*c*O) and complex V (ATPase) are indicated. Band IV' corresponds to C*c*O lacking the Cox6 subunit (Horan et al., 2005). **C)** Immunoblotting of 2D gels (SDS-PAGE) after BN-PAGE. Slices of the BN gels were incubated in the presence of SDS and added on second dimension SDS gels. After electrophoresis, the resulting 2D gels were transferred to PVDF membranes and decorated with an anti-Cox2 antibody. The spots corresponding to the mature Cox2 or Cox2^{W56R} proteins are indicated as m (28 kDa).

Figure 5. Proposed biogenesis pathway followed by the allotopic Cox2^{W56R} subunit. A) The allotopic Cox2 precursor is translocated by the TOM complex (colored violet) and delivered to TIM23^{MOTOR} (colored yellow and fuchsia). The MTS, the leader peptide (LP)

and the TMS1 ($\mu\Delta G_{app}$ = 0.55 kcal/mol) of the Cox2 precursor (colored in light blue with a red asterix indicating the W56R substitution) are fully translocated by TIM23 ^{MOTOR} into the mitochondrial matrix and the MTS is proteolytically removed by the Matrix Processing Protease (MPP, light green). **B)** TMS2 ($\mu\Delta G_{app}$ = 0.44 kcal/mol) of allotopic Cox2 (colored in dark blue) is arrested in TIM23 and induces the dissociation of the PAM motor (colored fuchsia) and the recruitment of Mgr2 (light green), Tim21 (green) and respiratory complexes III and IV (colored in light blue) to assemble TIM23^{SORT}. Then, TIM23^{SORT} laterally releases the TMS2 of Cox2 into the IMM. **C)** The Oxa1 insertase (colored red) recognizes the LP and embeds TMS1 in the IMM (this step may occur before, simultaneously, or after TMS2 is released into the IMM). Subsequently, the Imp1 protease (IMP1/2), located in the IMS, removes the LP. The rest of the biogenesis pathway is identical to the one followed by a mitochondrion synthesized Cox2 protein: incorporation of the binuclear copper center, assembly with the Cox1 and Cox3 modules, formation of mature C*c*O, assembly into super complex III_2IV_2. $\mu\Delta G_{app}$ values were calculated as in Nieto-Panqueva et al., (2023).

TABLE 1

Oxygen consumption measurements

STRAIN	Oxygen uptake*	Oxygen uptake*	RC	% O_2 uptake vs reference
	no substrate	+ ethanol		
wild-type	66.2 (+/- 8.1)	158.8 (+/- 0.9)	2.4	100
Δ*mgr2*	63.1 (+/- 6.1)	114.9 (+/- 2.3)	1.8	72
nCox2^{W56R}	51.6 (+/- 1.1)	76.7 (+/- 0.9)	1.5	100
nCox2^{W56R}, Δ*mgr2*	49.1 (+/- 0.5)	41.5 (+/- 0.9)	0.8	54
nCox2^{W56R} +*MGR2*↑	65.6 (+/- 6.9)	60.4 (+/- 4.5)	1.0	79
nCox2^{W56R} +EV	53.0 (+/- 0.3)	76.4 (+/- 0.6)	1.4	99.6
eCox2^{W56R}	50.6 (+/- 5.5)	68.6 (+/- 3.2)	1.4	100
eCox2^{W56R} Δ*mgr2*	17.4 (+/- 0.6)	1.5 (+/- 0.03)	0.1	2
eCox2^{W56R} *MGR2*↑	46.1 (+/- 0.6)	46.9 (+/- 0.9)	1.0	68
eCox2^{W56R} EV↑	43.5 (+/- 3.1)	67.7 (+/- 2.7)	1.6	98.7

*Expressed in ng atomic oxygen/min/mg mitochondrial protein.

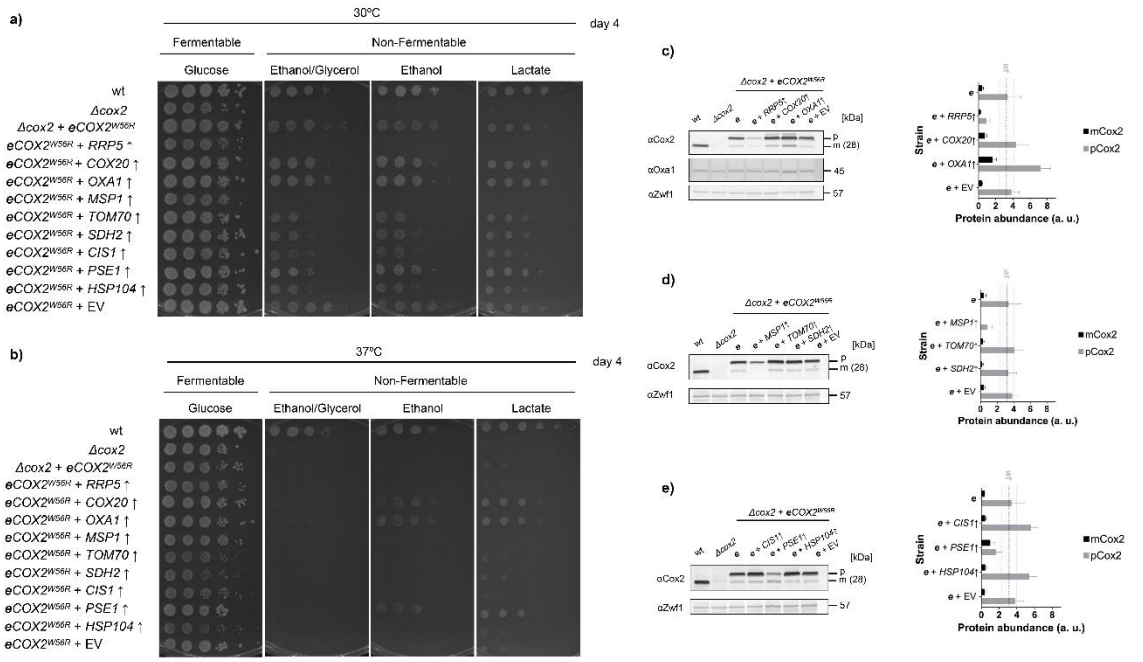

Figure 1
347x206 mm (x DPI)

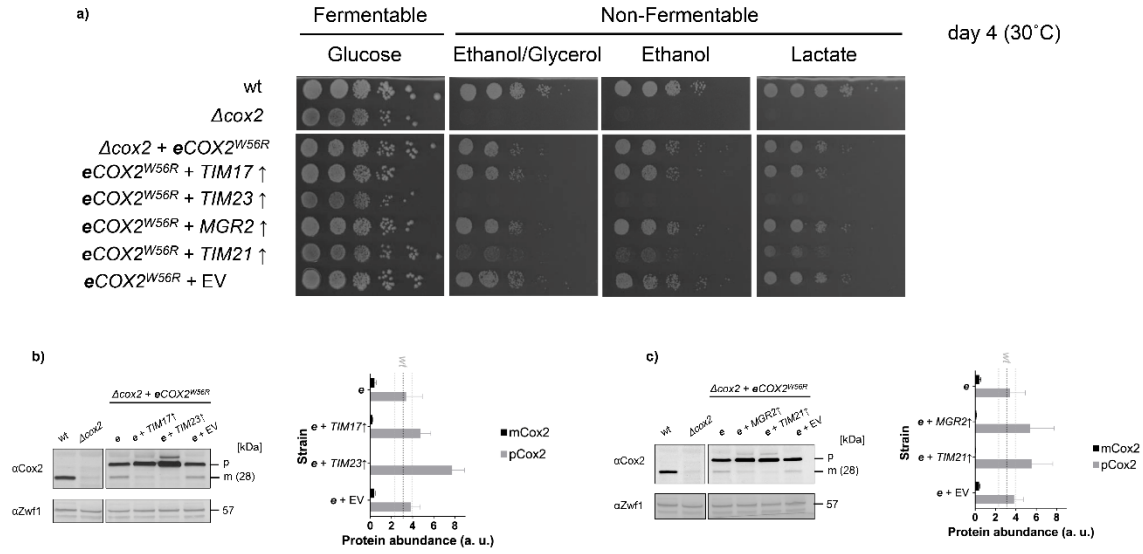

Figure 2
347x206 mm (x DPI)

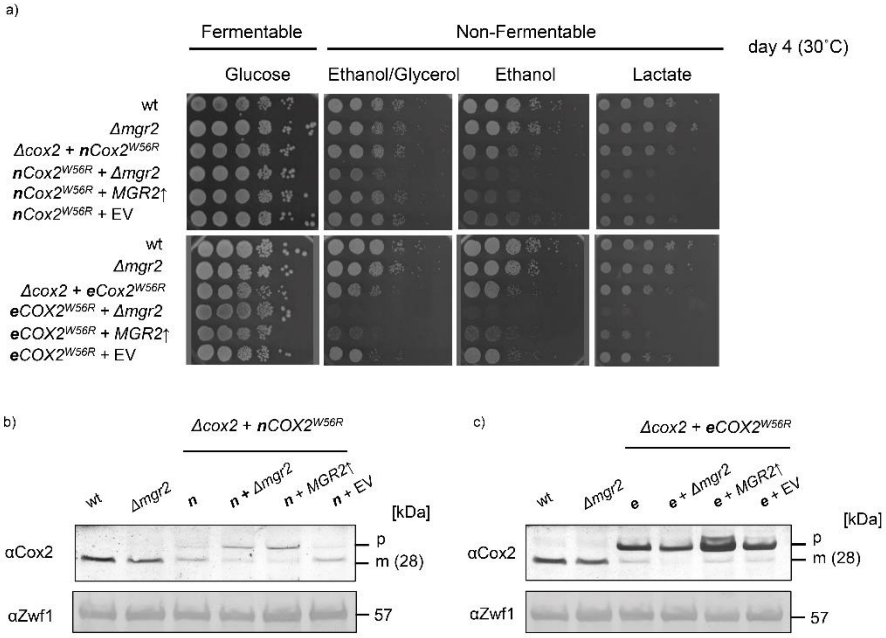

Figure 3
347x206 mm (x DPI)

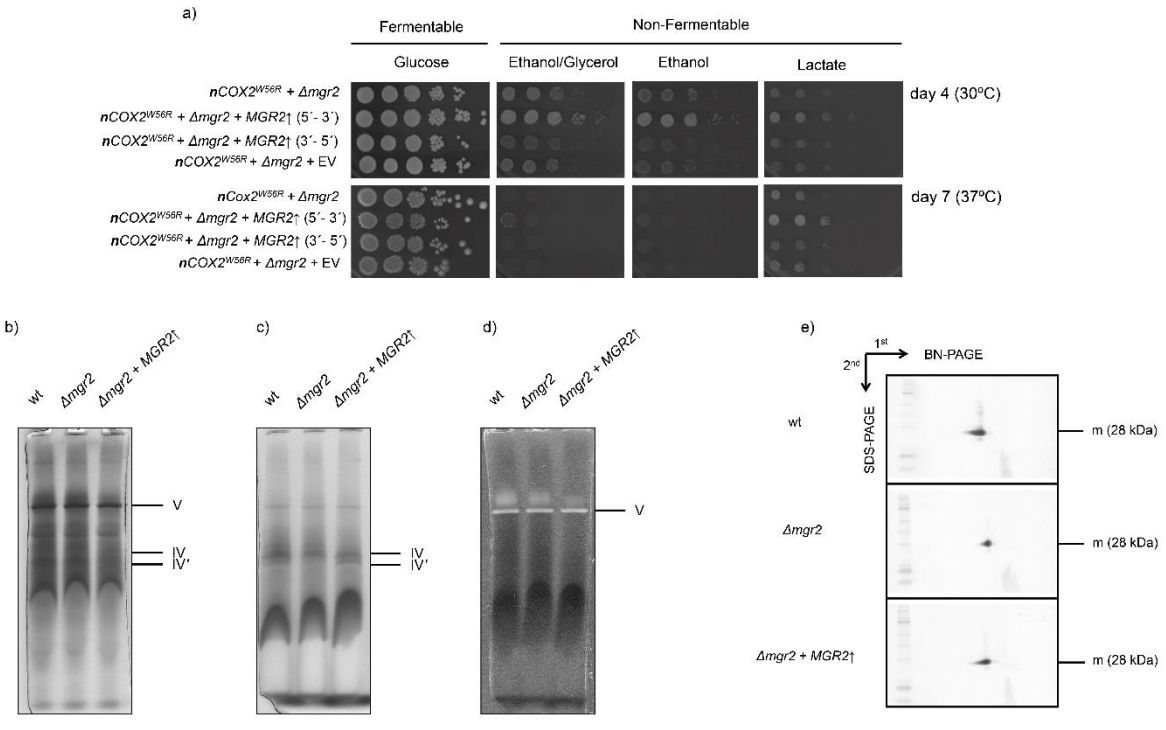

Figure 4
318x195 mm (x DPI)

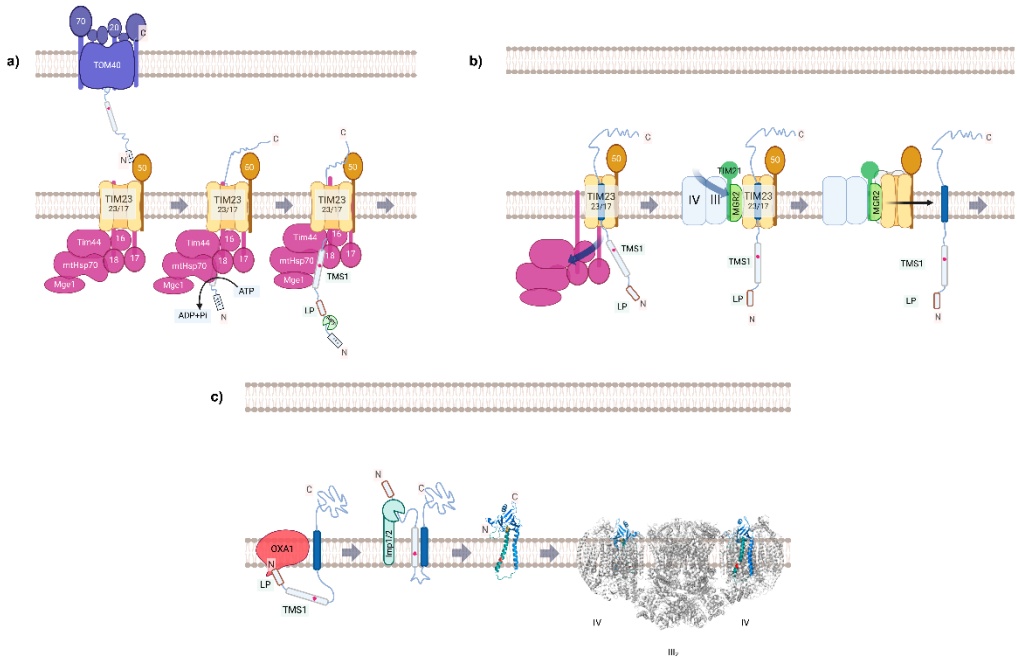

Figure 5
347x206 mm (ax DPI)

Artículo III.

Envíado, *en revisión*

Nieto-Panqueva, F., Vázquez-Acevedo, M., Hamel, P. P., & González-Halphen, D. (2024). A high copy suppressor screen identifies factors enhancing the allotopic production of subunit II of cytochrome *c* oxidase. *G3: Genes, Genomes, Genetics.* N/A.

A high copy suppressor screen identifies factors enhancing the allotopic production of subunit II of cytochrome *c* oxidase.

Felipe Nieto-Panqueva[1], Miriam Vázquez-Acevedo[1], Patrice P. Hamel[2] and Diego González-Halphen[1,*]

1) Instituto de Fisiología Celular, Universidad Nacional Autónoma de México, Mexico City, Mexico

2) Department of Molecular Genetics and Department of Biological Chemistry and Pharmacology, Ohio State University, Columbus, Ohio, USA, and Vellore Institute of Technology (VIT), School of BioScience and Technology, Vellore, Tamil Nadu, India.

*Corresponding author. Departamento de Genética Molecular, Instituto de Fisiología Celular, Universidad Nacional Autónoma de México, Apartado Postal 70-243, México 04510, D.F. (Mexico) Tel: (+5255) 5622-5620; FAX: (+5255) 5622-5611. E-mail: dhalphen@ifc.unam.mx

RUNNING TITLE:

Factors enhancing the allotopic production of Cox2.

ABSTRACT

Allotopic expression refers to the artificial relocation of an organellar gene to the nucleus. Subunit 2 (Cox2) of cytochrome *c* oxidase, a two transmembrane stretches (TMS1 and TMS2) protein with a N_{out}-C_{out} topology, is typically encoded in the mitochondrial *cox2* gene. In the yeast *Saccharomyces cerevisiae*, the *cox2* gene can be allotopically expressed in the nucleus, yielding a functional protein that restores respiratory growth to a Δ*cox2* null mutant. In addition to a mitochondrial targeting sequence followed by its natural 15-residue leader peptide, the cytosol synthesized Cox2 precursor must carry one or several amino acid substitutions that decrease the mean hydrophobicity of TMS1 and facilitate its translocation into the matrix by the TIM23 translocase. Here, using a yeast

strain that contains a *COX2*^{W56R} gene construct inserted in a nuclear chromosome, we searched for genes whose overexpression could facilitate import into mitochondria of the Cox2^{W56R} precursor and increase respiratory growth of the corresponding mutant strain. A *COX2*^{W56R} expressing strain was transformed with a multicopy plasmid genomic library, and transformants exhibiting higher growth rates on a respiratory carbon source were selected. We identified three genes whose overexpression facilitates the internalization of the Cox2^{W56R} subunit into mitochondria, namely: *TYE7, RAS2* and *COX12*. *TYE7* encodes a transcriptional factor, *RAS2* a GTP-binding protein, and *COX12* a non-core subunit of cytochrome *c* oxidase. We discuss potential mechanisms by which the gene products of *TYE7*, *RAS2* and *COX12* could facilitate the import and assembly of the Cox2^{W56R} subunit produced allotopically.

KEY WORDS: subunit 2 of cytochrome *c* oxidase, allotopic expression, protein import into mitochondria, TIM23 translocator, *TYE7*, *RAS2* and *COX12*.

INTRODUCTION

Cytochrome *c* oxidase (C*c*O), or complex IV of the mitochondrial respiratory chain, catalyzes electron transfer from cytochrome *c* to molecular oxygen coupled to proton pumping (Rich, 2017). In yeast, C*c*O is formed by polypeptides encoded in two different genomes: three in the mitochondrial DNA and eight in the nucleus (Poyton *et al.*, 1995). The three mitochondria-encoded subunits, Cox1, Cox2, and Cox3, constitute the core of the complex, and are normally synthesized by mitochondrial ribosomes and cotranslationally inserted into the inner mitochondrial membrane (IMM) (Dennerlein et al., 2023). The eight nucleus-encoded subunits, also referred to as non-core subunits, are synthesized in the cytosol as precursors that usually carry a mitochondrial targeting sequence (MTS), imported into mitochondria, proteolytically matured, and assembled into C*c*O (Poyton and Groot, 1975; Fontanesi et al., 2018). Subunit Cox2 is a membrane-embedded protein with two transmembrane stretches (TMS1 and TMS2) and a C-terminal, hydrophilic domain that binds a catalytic binuclear copper center facing the mitochondrial intermembrane space (IMS). Usually, Cox2 is synthesized by mitochondrial ribosomes as a precursor containing a leader peptide of 15 residues (Torello et al., 1997). The TMS1 of the protein is inserted co-translationally into the inner mitochondrial membrane (IMM) by the combined action of the mitoribosomes, the IMM-located Oxa1 insertase, and the assembly factors Mba1 and Cox20 (Hell et al. 1997; Herrmann & Bonnefoy 2004; Fiumera et al. 2007). When the N-terminus of Cox2 reaches the mitochondrial intermembrane space (IMS), the leader peptide is removed by the Imp1 protease (Sevarino & Poyton 1980; Torello et al. 1997). By contrast, TMS2 and the large, hydrophilic domain of the protein are translocated across the IMM by Cox18, Pnt1 and Mss2, a process by which the Cox2 subunit exposes the C-terminus to the IMS, thus reaching its characteristic N_{out}-C_{out} topology (Saracco & Fox 2002).

Previously, the mitochondrial *cox2* gene was artificially relocated to the nucleus in yeast (Supekova et al., 2010). The expression of a *COX2* gene construct from the nucleus complemented a null ***Δcox2*** yeast strain, restoring growth in non-fermentable carbon sources. Thus, the cytosol synthesized Cox2 subunit ($Cox2^{ALLOTOPIC}$) was successfully directed to mitochondria and functionally assembled into C*c*O. To be internalized into mitochondria, the allotopically produced Cox2 precursor must exhibit some characteristics: a mitochondrial targeting sequence (MTS) followed by the natural leader peptide of the yeast mitochondrial Cox2 precursor, and the presence of amino acid substitutions in TMS1, that can be either W56R, W56K, W56Q or the double V49Q/L51G mutation (Rubalcava-Gracia et al., 2018). As expected, the allotopically produced Cox2 protein follows a different biogenesis pathway than the mitochondria synthesized Cox2 subunit, entering mitochondria through the TOM translocator and subsequently sorted by the TIM23 translocator. The amino acid substitutions diminish the mean hydrophobicity of TMS1, promoting its full translocation into the mitochondrial matrix by TIM23. Once the MTS reaches the matrix, it is selectively removed by the mitochondrial processing protease (MPP). Then, the Oxa1 insertase recognizes the leader peptide and inserts the TMS1 of the protein into the IMM. When the N-terminus of Cox2 gets exposed to the IMS, Cox20 stabilizes TMS1 and the IMS-localized Imp1 protease removes the leader peptide.

Paralleling this process, the highly hydrophobic TMS2 domain of Cox2^{ALLOTOPIC} is retained by the TIM23 complex and released laterally into the IMM, along with the hydrophilic C-terminal domain of the protein, which becomes exposed to the IMS. Thus, the allotopically produced Cox2 subunit reaches the same functional N_{out}-C_{out} topology (Nieto-Panqueva et al., 2023) attained by its Cox2 counterpart synthesized on mitoribosomes (Rubalcava-Gracia et al., 2018). In contrast to the Cox2 protein synthesized in mitochondria, the biogenesis of Cox2^{ALLOTOPIC} does not require the participation of Cox18, which controls the translocation of the TMS2 (Elliott and Fox, 2012). Once the allotopically produced Cox2 protein is inserted in the IMM, it must probably follow the same maturation steps than the Cox2 protein synthesized inside mitochondria: acquisition of a binuclear CuA center (Rigby et al. 2008; Pacheu-Grau et al. 2015; Ghosh et al. 2016; Pacheu-Grau et al. 2020) and its functional assembly into the C*c*O complex (Franco et al., 2020).

Although allotopic production of a yeast Cox2 subunit is clearly viable, strains expressing *COX2^{W56R}* exhibit lower steady-state levels of C*c*O and diminished rates of oxygen uptake when compared to wild-type yeast (Cruz-Torres et al. 2012). This phenotype was not due to the presence of the W56R substitution, because when the mutant Cox2^{W56R} protein was synthesized inside mitochondria, the resulting activity and levels of C*c*O were found to be equivalent to those of a wild-type strain (Rubalcava-Gracia et al., 2018). Thus, the inability of allotopically produced Cox2^{W56R} protein to restore full C*c*O function was attributed to a limiting step during the translocation and sorting of the Cox2^{W56R} precursor by TIM23 (Rubalcava-Gracia et al., 2019).

Here, using a multicopy genomic library, we undertook a search for multicopy suppressors that could enhance the respiratory growth of the yeast strain expressing the *COX2^{W56R}* gene construct from the nucleus (***n****COX2^{W56R}*). Overexpression of three genes, *COX12, RAS2* and *TYE7,* were found to facilitate growth on non-fermentable carbon sources and enhanced levels of mature Cox2^{W56R} subunit in mitochondria. We suggest possible mechanisms by which the independent overexpression of these three genes promote the internalization into mitochondria of the allotopically produced Cox2^{W56R}.

MATERIALS AND METHODS

Yeast culture conditions

The yeast strains were cultivated in liquid or solid media containing 2% agar, maintained at 30 ºC, unless otherwise specified. Media compositions used throughout the study were: YPDA (1% yeast extract, 2% bactopeptone, and 2% dextrose) as fermentable media, YPEG (1% yeast extract, 2% bacto peptone, 3% ethanol and 3% v/v glycerol); YPE (1% yeast extract, 2% bacto peptone, 2% ethanol), and YPLAC (3% yeast extract , 1% KH_2PO_4, 1% NH_4Cl, 0.5% $CaCl_2{\cdot}2H_2O$, 0.5% NaCl, 0.6% $MgSO_4{\cdot}H2O$, 3% $FeCl_3$, 2% (v/v) lactate, pH 5.5), as non-fermentable media. Minimal media SD or SGal (0.17% yeast nitrogen base [lacking amino acids and $(NH_4)_2SO_4$], 0.5% $(NH_4)_2SO_4$, 2% glucose or 2% galactose accordingly, supplemented with specific amino acids and nucleotides), and hygromycin B (300 µg/ml) were used for selection purposes. To monitor growth, optical density at 600 nm (O.D.600) was measured using a Bioscreen C spectrophotometer (Growth Curves, USA).

Yeast strains and gene constructs

Yeast strains used in this study are derived from the parental strain D273-10B (Fred Sherman lab, ATCC® 24657TM). As a wild-type strain we used NB40-36A 36A (*MATα* ; *lys2* ; *arg8::his ; leu2-3*, *11 ; ura3-52* ; [rho^+]) (Pérez-Martínez et al., 2003) and as a *cox2*-null strain we used EHW154 (*MATa* ; *arg8::hisG* ; *ura3-52* ; *leu 2-3, 112* ; *his3-ΔHindIII*, [rho^+] *cox2(1,89-91)::ARG8m*) (Williams and Fox, 2003). For $COX2^{W56R}$ allotopic expression in the Δcox2 mutant, we utilized two approaches. Firstly, we introduced the hygromycin B selectable plasmid pRS306H to target insertion via homologous recombination at the URA3 locus (designated as Δcox2 + nCox2W56R), and the episomal 2µ URA3 multicopy plasmid pFL61 (termed Δcox2 + eCox2W56R) (Rubalcava-Gracia et al., 2019). The strains used in this work are listed in Table S1.

Yeast strains overexpressing *TYE7*, *RAS2*, and *COX12* (designated as *TYE7*↑, *RAS2*↑, and *COX12*↑) were constructed by introducing of the high copy episomal vector pMK2 (M. Karamoko, personal communication) containing each of the three genes. The wild-type *TYE7*, *RAS2*, and *COX12* ORFs were cloned at the NotI site in pMK2 between the phosphoglycerate kinase (*PGK*) promoter and terminator. The ORFs were PCR-amplified using each corresponding chromosomal fragment and the following oligonucleotides with NotI sequences flanking the plasmid multicloning site:
TYE7OE: 5´-GCGCGGCCGCATGAACTCTATTTTAGACA-3´ and 5´-GCGCGGCCGCTTATTTTTGGTCTTGTT-3´;
RAS2OE: 5´-GCGCGGCCGCATGCCTTTGAACAAGTC-3´ and 5´-GCGCGGCCGCTTAACTTATAATACAACAGCCACC-3´;

COX12OE: 5´-GCGCGGCCGCATGGCTGATCAAGAAAA-3´ and 5´-GCGCGGCCGCTTAGTCTGAGTTGATATCAC-3´.

The pMK2 plasmid, a derivative of pFL61, features LEU2 as a selectable marker instead of URA3 (Minet et al., 1992). The plasmid was constructed by self-ligation of *Bgl*II-cut pFL61, which resulted in the deletion of the *URA3* marker. A 2.8 kb *Bgl*II fragment containing the *LEU2* marker was excised from pFL36 (Bonneaud et al., 1991) cloned into the *Bgl*II site of the pFL61 derived plasmid with no *URA3* marker.

Yeast transformations were conducted employing the one-step yeast transformation protocol outlined by Chen et al. (1992). Additionally, we utilized the CH3Li method along with single-stranded DNA as a carrier, following the approach described by Gietz and Schiestl (2007).

Plasmid manipulation and cloning procedures were used with Escherichia coli DH5α (F– endA1 glnV44 thi-1 recA1 relA1 gyrA96 deoR nupG purB20 φ80dlacZΔM15 Δ(lacZYA-argF)U169, hsdR17(rK–mK+), λ–) and MR32, a recA– derivative of MC1061 (str. K-12 F– λ– Δ(ara-leu)7697 [araD139]B/r Δ(codB-lacI)3 galK16 galE15 e14– mcrA0 relA1 rpsL150(StrR) spoT1 mcrB1 hsdR2(r–m+)) according to published protocols (Sambrook, 2001).

Multicopy genomic library

The Δcox2 + nCox2W56R was transformed with a yeast genomic library constructed in the pFL44L vector (Bach et al., 1979; Oulmouden and Karst, 1990). Out of 307,000 primary transformants, 55 colonies displayed enhanced respiratory growth and after re-testing 10 colonies (#3 to #12, now named MS01 to MS10) exhibited a significant improvement in their ability to grow on a respiratory substrate (glycerol pH:7.0). For co-segregation experiments, each transformant was grown into liquid YPDA and subcloned to single colony on solid YPDA medium, which was replicated in minimal medium lacking uracil and YPEG medium. The plasmids were recovered from the strains by the glass bead method adapted from Robzyk and Kassir, (1992) in E. coli MR32. At least two independent bacterial clones resulting from transforming the MR32 strain with the extracted DNA from the yeast transformants were selected and the plasmids profiled by restriction digest. Digestion profiles were determined using SalI, SphI, and BglII, which are present in pFL44L. One profile (profile 1) defines plasmids from suppressors MS01, MS02, MS03, MS08, MS04 and MS05, a second profile (profile 2) is found in suppressors MS06 and MS07, and plasmid extracted from MS09 defines a third (profile 3) distinct profile. Despite numerous attempts, the plasmid contained in the MS10 transformant could never be recovered. The border of the genomic insert contained in the nine pFL44L-based plasmids recovered from the transformants was sequenced using M13-40 forward and M13-48 reverse primers.

UV mutagenesis

One UV-induced respiratory-competent revertant was selected from the DRG103 EHW154 strain. The UV-induced suppressor was isolated from cells grown to stationary phase, which were plated on YPDA medium and stored in the cold overnight before mutagenesis. UV mutagenesis was performed using a UV source (254 nm) placed at 12 cm from yeast cells. Plates were then irradiated in the dark for 10 s, incubated for 3 days in the dark at 28 °C, and replica plated on YPEG. One single revertant was recovered from 2 x 10^9 irradiated cells at an irradiation time causing 30% lethality. The *COX2* ORF in the nucleus was amplified in the suppressed strain using primers PGK-F (5'-CAGATCATCAAGGAAGTAATTATC-3') and PGK-R (5'-CTATTATTTTAGCGTAAAGGATG-3') and sequenced to identify the mutation leading to the W56R substitution.

Growth assessment by tenfold serial dilutions

Yeast cells were grown overnight in 3 mL of liquid YPDA at 30 ºC with constant agitation. The next day, the cultures were diluted and grown to exponential phase (O.D.600 1.0). Cells were centrifugated at 8600 × g, followed by a single wash with 1 mL of sterile water. This suspension was stepwise diluted five times in a 1:10 ratio for each strain and dispensed onto 96-well plates. Using a multichannel pipette, small droplets of roughly 3.5 µl were dispensed onto solid fermentable (YPDA) and non-fermentable (YPEG, YPE, YPLAC) media, and plates were incubated at 30ºC for a duration of 4-7 days, as specified.

Protein extraction and immunodetection

Alkaline extraction was employed for protein extraction from whole yeast cells cultivated in 20 ml of liquid SGal media, reaching the stationary phase (O.D.600 2.5). The cells were then collected at 2800 × g in a microcentrifuge for 3 minutes. Cells were then washed using a 500 µl solution containing 1 mM phenylmethylsufonyl fluoride (PMSF) and 50 mM N-α-tosyl-L-lysyl-Chloromethyl Ketone (TLCK). The pellet was boiled in SDS-PAGE sample buffer (100 mM Tris-HCl pH 6.8, 10% SDS, 30% glycerol, 4% β-mercaptoethanol, 0.3% bromophenol blue) following the protocol by Kushnirov, (2000). Gel electrophoresis was performed using an SDS-tricine-PAGE system as described by Schägger, (1994). After electrophoresis, the gels were transferred onto nitrocellulose membranes which were blocked with 1% bovine skin type B gelatin (Invitrogen), followed by washing and subsequent immuno-decoration. The monoclonal αCox2 antibody (Abcam: 4B12A5) was used at a 1:9000 dilution, as detailed in Ghosh et al. (2020). As a loading control, a polyclonal αZwf1 antibody (Sigma-Aldrich: A9521) was employed at a 1:10000 dilution, as detailed in Fujiwara et al. (2016). Secondary antibody labeling involved a 4-hour incubation with alkaline phosphatase-conjugated goat anti-rabbit and

goat anti-mouse antibodies. The appearance of dark purple precipitates in band form was observed after adding nitro-blue tetrazolium chloride (NBT) and 5-bromo-4-chloro-3′-indolyl phosphate p-toluidine (BCIP) salt. An HP Scanjet G4050 image scanner was utilized to capture the colored bands formed by the precipitate on the membranes. The intensity of the colored bands was estimated using the GelAnalyzer 23.1 freeware developed by Istvan Lazar Jr., PhD and Istvan Lazar Sr., PhD, CSc. (www.gelanalyzer.com). For bar plotting and statistical analysis GraphPad Prism version 10.1.1(27) for macOS (GraphPad Software, Boston, Massachusetts, USA, www.graphpad.com) was used. For each subset of samples, a two-way ANOVA followed by Tukey's multiple comparisons test was carried out.

***In silico* analyses**

The genes networks up-regulated by the transcription factor Tye7 were searched in YEASTRACT (Yeast Search for Transcriptional Regulators And Consensus Tracking), a curated repository of regulatory associations between transcription factors (TF) and target genes in *Saccharomyces cerevisiae* (http://yeastract.com/index.php) (Teixeira et al., 2023). Physical and genetic interactions of Tye7 were explored in the yeast interactome (Cherry et al., 1997) at the Saccharomyces Genome Database (https://www.yeastgenome.org/).

RESULTS

To uncover the factors limiting the ability of cytosol-produced *Cox2*^{W56R} to fully complement a *cox2*-null mutant, we searched for high-copy suppressors that could improve the respiratory growth of a strain expressing an allotopic *COX2*^{W56R} construct from the nucleus (***n***Cox2^{W56R}). For this purpose, the ***n****COX2*^{W56R} strain was transformed with a yeast genomic library containing chromosomal fragments inserted into the multicopy pFL44L vector. Out of an estimated number of 307,000 primary transformants, 55 colonies were found to display enhanced respiratory growth, and after retesting, ten colonies (named as Multicopy Suppressors MS01 to MS10) were selected, since they exhibited a significant improvement in their ability to grow on non-fermentable carbon sources when compared to the ***n****COX2*^{W56R} original strain (Figure 1A). Some transformants exhibited an improved respiratory growth on ethanol/glycerol but not on lactate. The reason for this carbon source dependent difference in respiratory growth is not obvious. Immunoblotting analysis revealed that overexpression of the chromosomal fragments in the 10 transformants increased the levels of both the precursor and mature forms of Cox2^{W56R} (Figures 1B and 1C) when compared to a strain carrying the empty vector (***n*** + EV).

For each multicopy suppressor transformant (MS01 to MS10), a colony which had lost the plasmid (-ura) was tested again for the presence of the *arg8m* and *hph* markers and enhanced respiratory growth. The ten colonies were uracil auxotrophs, and concomitantly,

had lost the enhanced respiratory growth phenotype (not shown). By contrast, all plasmid containing colonies displayed enhanced respiratory growth compared to the recipient strain (***n****COX2*^{W56R}), suggesting that this trait was plasmid-borne for all the isolated multicopy suppressors (not shown). Altogether, these co-segregation experiments showed that the enhanced respiratory ability was indeed conferred by a multicopy plasmid originating from the pFL44L-based genomic library.

Plasmid DNA was recovered from 9 of the 10 yeast multicopy suppressors (MS01 to MS09) and three different restriction profiles were identified. The first profile was found in suppressors MS01 to MS05 and in MS08. The second profile was found in suppressors MS06 and MS07. A third one was present in MS09 and appeared to be a re-arranged plasmid. The borders of the inserts contained in five of the multicopy plasmids were sequenced and four chromosomal fragments were identified, along with the ORFs present in each one of them (Figure 2). This analysis allowed the identification of three candidate ORFs conferring the suppression in the chromosomal fragments: *TYE7* (YOR344C) present in the plasmid contained in transformants MS01 to MS05 and in MS08; *RAS2* (YNL098C) present in transformants MS06 and MS07; and *COX12* (YLR038C) present in transformant MS09.

To assess if the three candidate genes were indeed responsible for causing the observed phenotype, i.e., enhanced respiratory growth, the three ORFs were cloned in front of a strong and constitutive promoter (*PGK*) in a different multicopy plasmid (pMK2). Thus, the original ***n****COX2*^{W56R} strain was independently transformed with the three candidate genes cloned in the pMK2 vector. The growth of the non-transformed ***n****COX2*^{W56R} strain and the three transformants overexpressing *TYE7*, *RAS2* and *COX12* were compared. Unexpectedly, none of the overexpressing genes caused a significant growth improvement on respiratory media (Figure S1). We reasoned that the original strain containing the ***n****COX2*^{W56R} gene construct integrated in the nucleus could have been silenced, or could had evolved over a period, reaching maximal growth efficiency, which did not enhance further upon the independent overexpression of the three candidate genes. This finding led us to generate a new allotopic strain. For this purpose, a yeast strain carrying the mitochondrial *cox2* null mutation and a nucleus localized wild-type *COX2* gene (lacking the mutation corresponding to the W56R substitution) was subjected to UV irradiation. One mutant strain that was able to grow on respiratory was recovered, and we hypothesized that the UV induced mutation was in the *COX2* gene. Sequence analysis showed that indeed, UV light treatment induced a mutation in the *COX2* gene that gave rise to a W56R substitution in the corresponding protein product. The ***n****^{uv}COX2*^{W56R} strain was also independently transformed with pMK2 plasmids containing the three candidate genes. The growth of the non-transformed ***n****^{uv}COX2*^{W56R} strain and the three transformants overexpressing *TYE7*, *RAS2* and *COX12* were compared, as well as the ***n****^{uv}COX2*^{W56R} strain transformed with an empty pMK2 plasmid. The transformants overexpressing the candidate genes exhibited a significant improvement in their growth in respiratory media (Figure 3A). In addition, immunoblotting analysis revealed that overexpression of the three candidate genes in the ***n****^{uv}COX2*^{W56R} strain led to increased levels of the mature form of Cox2^{W56R} (Figure 3B).

To test if the high-copy suppressors improved the growth of *COX2*^{W56R} strain, we also transformed a strain expressing the *COX2*^{W56R} construct from a centromeric plasmid (***cen****COX2*^{W56R}) which should generate levels of cytosolic Cox2 precursor protein like those present in an ***n****COX2*^{W56R} strain. Thus, the strain ***cen****COX2*^{W56R} was independently transformed with the three candidate genes cloned in the pMK2 vector. The growth of the non-transformed *COX2*^{W56R} strain and the three transformants overexpressing *TYE7*, *RAS2* and *COX12* were compared, as well as a ***cen****COX2*^{W56R} transformed with an empty pMK2 plasmid. The transformants overexpressing the candidate genes exhibited a reproducible and significant improvement in their growth in respiratory media (Figure 4A). In addition, immunoblotting analysis revealed that the three high-copy suppressors in the ***cen****COX2*^{W56R} strain increased the levels of the mature form of Cox2^{W56R} (Figure 4B).

It was previously shown that directing high doses of allotopically synthesized Cox2 subunit to mitochondria (i.e., using an expression system with a multicopy vector) could be deleterious because the subunit aggregates at the mitochondrial surface (Rubalcava-Gracia et al., 2019). Following the same line of reasoning concerning dosage of the cytosolically produced Cox2^{W56R} protein, we also explored the effect of overexpressing the *TYE7*, *RAS2* and *COX12* genes on an ***e****COX2*^{W56R} background, i.e., a strain expressing the allotopic gene from a multicopy plasmid. Only the transformants overexpressing the *TYE7* and the *RAS2* genes induced enhanced growth of the strain on lactate (Supp Fig S2A), which correlated with lower levels of the Cox2^{W56R} precursor and higher levels of its mature form (Supp Fig S2B).

The finding that *COX12*, *RAS2* and *TYE7* did not enhance the respiratory growth of the ***n***Cox2^{W56R} (Supp Fig 1) prompted us to re-examine the respiratory growth of this strain along with that of ***n***^{uv}*COX2*^{W56R}. As shown in Supp Fig 3, the respiratory growth of ***n***Cox2^{W56R} is enhanced compared to that of ***n***^{uv}COX2^{W56R} and this is correlated to elevated levels of mature Cox2. This results suggest that the **n**Cox2^{W56R} evolved over time, possibly through the acquisition of second site mutations.

DISCUSSION

In this work, we identified three genes (*TYE7*, *RAS2* and *COX12*) whose overexpression promotes higher respiratory growth of a *COX2*^{W56R} strain, which correlates with enhanced levels of mature allotopic Cox2^{W56R} protein inside mitochondria. We suggest possible mechanisms through which the protein products encoded in these overexpressed genes could enhance the internalization of the allotopic subunit into mitochondria.

Overexpression of the TYE7 gene facilitates the internalization of the allotopic Cox2^{W56R} *subunit into mitochondria.*

Overexpression of the *TYE7* gene increased the levels of mature Cox2^{W56R} in mitochondria. *TYE7* encodes a 33 kDa member of the basic region/helix-loop-helix/leucine-zipper (bHLH) protein family that exhibits a N-terminal region extremely rich in serine and a C-terminal sequence that has similarity with Myc and Max proteins

(Löhning and Ciriacy, 1994). The Tye7 protein functions as a transcriptional activator in retrotransposon Ty1-mediated gene expression (Servant et al., 2012; Gui et al., 2021). Through binding to E-boxes, Tye7 activates several genes encoding glycolytic enzymes like Enolase I, 3-phosphoglycerate kinase, pyruvate kinase, glyceraldehyde-3-phosphate dehydrogenase, phosphoglycerate mutase, and triosephosphate isomerase (Nishi et al., 1995; Sato et al., 1999; Robinson and Lopes, 2000). Tye7 is also predicted to activate a series of genes encoding components related to the mitochondrial protein import machinery (Holland et al., 2019; Horak et al., 2002; Reimand et al., 2010) including the Oxa1 insertase, Cox18 involved in the biogenesis of the mitochondrial Cox2 protein; Tom40, a component of the TOM complex; Tim50 and Ssc1, two components of the TIM23 complex; as well as several chaperones of the HSP70 family, i.e., Sse2, Ssb1 and Mdj1 (Table S2). This suggests that overexpression of *TYE7* may promote Cox2^{W56R} internalization into mitochondria through an indirect mechanism, possibly by activating the expression of several genes whose protein products are involved in mitochondrial protein import.

Overexpression of the RAS2 gene raises the levels of the allotopic Cox2^{W56R} subunit in mitochondria.

Overexpression of the *RAS2* gene was also found to increase the growth of yeast strains producing the allotopic Cox2^{W56R} subunit encoded either in a gene inserted in the nucleus, in a centromeric, or in a multicopy plasmid. The Ras superfamily comprises more than 150 small GTPases that share structural and biochemical properties, mediating multiple metabolic responses and acting as key regulators in different signaling routes (Broach and Deschenes, 1990; Goitre et al., 2014), including control of mitochondrial biogenesis and function (Hlavatá and Nyström, 2003). When yeast grows using glucose as a carbon source, Ras proteins (the two isoforms Ras1 and Ras2) accumulate preferably in both the plasma membrane and in the nucleus. Nevertheless, in the absence of glucose, Ras proteins tend to accumulate in mitochondria (Broggi et al., 2013). Furthermore, deletion of the *RAS2* gene impedes yeast growth in non-fermentable carbon sources (Tatchell et al., 1985). The Ras2 protein activates adenylyl cyclase and other protein kinases that rely on cAMP (Cannon et al., 1987), like the mitochondria-localized protein kinase A (PKA) (Papa et al., 1996). Nutrient availability and the signaling route RAS/cAMP play a critical role in the cellular growth of *S. cerevisiae* (Matsumoto et al.,1983). Early on, it was observed that in yeast, cAMP reverses the glucose repression on mitochondrial biogenesis (Fang and Butow,1970), and activates mitochondrial genes encoding C*c*O subunits and other OXPHOS components (Chandrasekaran and Jayaraman, 1978). Therefore, along with PKA, cAMP seems to govern mitochondrial transcription (Müller and Bandlow, 1987), by acting on a *cis*-regulatory element present in mitochondrial DNA (Iqbal et al., 1996). In mammals, the cAMP/PKA pathway was shown to regulate the biogenesis, assembly, and catalytic activity of respiratory complex I (Papa et al., 2012). In addition, *RAS2* overexpression suppresses a mutation of citrate synthase (*CIT2*), a participant of the glyoxylate cycle (Swiegers et al., 2006) and suppresses a mutation in a non-catalytic site of the alpha subunit (atp1-2) of mitochondrial ATP synthase (Mabuchi et al., 2000). Also, RAS2^{Val19} cells exhibiting an overactive RAS/protein kinase A (PKA) signaling abrogate

activity of the mitochondrial ATP/ADP carrier (Hlavatá et al., 2007). Some of these findings seem to be related to an induced expression of ribosomal protein genes (Neuman-Silberberg, et al., 1995) linked to an increased transcription rate of nuclear genes encoding mitochondrial proteins. Overall, the Ras/adenylate cyclase/PKA pathway is involved in the regulation of metabolism, adaptation to glucose, proliferation, cell growth, stress resistance, in mediating the response to the availability of nutrients, and controlling cytosolic cAMP levels and PKA activity (Tisi et al., 2014). This signaling route also regulates proteins involved in other mitochondria-related phenomena like apoptosis and mitochondrial fission (Cribbs and Strack, 2007; Ould Amer et al., 2018). In yeast mutants exhibiting alterations in this signaling pathway, it was shown that high intracellular levels of cAMP increase the relative abundance of OXPHOS complexes and the mitochondrial respiratory activity (Dejean et al., 2002). Thus, a tight link exists between the activity of the Ras/adenylate cyclase/PKA pathway and the levels of OXPHOS complexes (Bouchez and Devin, 2019). The increased cell levels of cAMP enhance the stability of the transcriptional co-activator Hap4p, a key regulator of the HAP complex (Bouchez et al., 2020). HAP transcriptional complex is an instrumental factor for yeast growth on respiratory substrates, since it controls mitochondrial translation, reprogramming the yeast cell from fermentation to respiration and serving as a coordinator of mitochondrial and nuclear gene expression (Buschlen et al., 2003). Overall, an increase in the activity of the cAMP pathway positively regulates mitochondrial biogenesis (Yoboue et al., 2012). Due to the wide range of effects that Ras proteins regulatory pathways have on several mitochondrial enzymes, we propose that overexpression of *RAS2* may promote increased transcription of several mitochondrial OXPHOS genes, including the mitochondrial *cox1* and *cox3* genes encoding subunits 1 and 3 of CcO, with the concomitant increase in the levels of Cox1 and Cox3 modules in the IMM. These modules may readily integrate incoming allotopic $Cox2^{W56R}$ subunits to form fully assembled C*c*O complexes. We suggest that the favored incorporation of the allotopically produced $Cox2^{W56R}$ subunits into these preformed modules may promote increased overall levels of C*c*O and further internalization of the allotopic precursor.

Overexpression of the COX12 gene facilitates the internalization of the allotopic $Cox2^{W56R}$ subunit into mitochondria.

The *COX12* gene encodes subunit VIb (also known as Cox12), a loosely bound and soluble subunit of C*c*O facing the IMS (LaMarche et al., 1992; Ing et al., 2022). The Cox12 subunit is required for the formation of active C*c*O and its absence results in the assembly of an optically detectable C*c*O with a markedly diminished activity. Cox12 interacts with both Rcf1 and Rcf2, which are required for respiratory complex biogenesis and act mainly by regulating the assembly and enzyme activity of complex IV within supercomplexes, suggesting a role for this C*c*O subunit in super complex formation (Das et al., 2021). A function of Cox12 in the insertion of the binuclear copper center in the Cox2 subunit along with Coa6, an assembly factor has emerged from recent genetic studies. While loss of Coa6 or Cox12 can be rescued by copper supplementation, the simultaneous elimination of Coa6 and Cox12 abrogates Cox2 biogenesis completely, and copper supplementation fails to rescue Cox2 levels (Ghosh et al., 2014, 2016). The overproduction of the *COX12*

gene partially rescued the *coa6* null mutant. Physical interactions were observed between Coa6, Cox2, Cox12 and the Sco proteins, which are involved in copper delivery to Cox2. It is possible that the overexpression of the *COX12* gene suppresses the Δ*coa6* mutant by stabilizing and enhancing the formation of the binuclear CuA site. Copper insertion into the metal center is probably a limiting step during Cox2 biogenesis, due to the several factors that participate in the formation of its metal center, that must also minimize the production of reactive C*c*O assembly intermediates (Nývltová et al., 2022). We therefore suggest that high levels of the Cox12 subunit in the IMS could speed-up copper delivery and assembly of the CuA center, facilitating the subsequent incorporation of $Cox2^{W56R}$ into C*c*O, and simultaneously enhancing the internalization rate of its precursor into mitochondria.

In summary, we identified three yeast genes that when overexpressed, facilitate the internalization of the allotopically produced $Cox2^{W56R}$ protein into mitochondria. Although the suggested mechanisms by which the Tye7, Ras2 and Cox12 independently exert their effect are different, they all seem to facilitate either the internalization or the assembly line of the allotopic Cox2 subunit.

DATA AVAILABILITY

Strains and plasmids are available upon request. The authors affirm that all data necessary for confirming the conclusions of the article are present within the article, figures, and tables.

ACKNOWLEDGEMENTS

The authors are grateful to Dr. Juan García-Rincon, Erick Castillo (IFC, UNAM), and Till Bokern (Berlin Technical University), who carried out preliminary experiments for this project. We also acknowledge the technical expertise of José Luis Santillán Torres (IFC, UNAM). D.G.-H. laboratory received financial support from grants CF2019-21856 (Frontiers of Science, CONACyT, Mexico) and IN207023 (PAPIIT, DGAPA, UNAM). F.N.-P. is a Ph.D. student at Programa de Maestría y Doctorado en Ciencias Bioquímicas (UNAM) and recipient of a CONACyT fellowship (CVU 700670). P.P.H. received a PREI fellowship from DGAPA, UNAM to carry a research stay in Mexico.

REFERENCES

Bach ML, Lacroute F, Botstein D. 1979. Evidence for transcriptional regulation of orotidine-5'-phosphate decarboxylase in yeast by hybridization of mRNA to the yeast structural gene cloned in *Escherichia coli*. PROC NATL ACAD SCI (U S A). 76(1):386-90. doi: 10.1073/pnas.76.1.386.

Bonneaud N, Ozier-Kalogeropoulos O, Li GY, Labouesse M, Minvielle-Sebastia L, Lacroute F. 1991. A family of low and high copy replicative, integrative and single-stranded S. cerevisiae/E. coli shuttle vectors. YEAST. 7(6):609-15. doi: 10.1002/yea.320070609.

Bouchez C, Devin A. 2019. Mitochondrial Biogenesis and Mitochondrial Reactive Oxygen Species (ROS): A Complex Relationship Regulated by the cAMP/PKA Signaling Pathway. CELLS. 8(4):287. doi: 10.3390/cells8040287.

Bouchez CL, Yoboue ED, de la Rosa Vargas LE, Salin B, Cuvellier S, Rigoulet M, Duvezin-Caubet S, Devin A. 2020. "Labile" heme critically regulates mitochondrial biogenesis through the transcriptional co-activator Hap4p in *Saccharomyces cerevisiae*. J BIOL CHEM. 295(15):5095-5109. doi: 10.1074/jbc.RA120.012739.

Brix J, Ziegler GA, Dietmeier K, Schneider-Mergener J, Schulz GE, Pfanner N. 2000. The mitochondrial import receptor Tom70: identification of a 25 kDa core domain with a specific binding site for preproteins. J MOL BIOL. 303(4):479-88. doi: 10.1006/jmbi.2000.4120.

Broach JR, Deschenes RJ. 1990. The function of ras genes in *Saccharomyces cerevisiae*. ADV CANCER RES.; 54:79-139. doi: 10.1016/s0065-230x(08)60809-x.

Broggi S, Martegani E, Colombo S. 2013. Live-cell imaging of endogenous Ras-GTP shows predominant Ras activation at the plasma membrane and in the nucleus in *Saccharomyces cerevisiae*. INT J BIOCHEM CELL BIOL. 45(2):384-94. doi: 10.1016/j.biocel.2012.10.013.

Buschlen S, Amillet JM, Guiard B, Fournier A, Marcireau C, Bolotin-Fukuhara M. 2003. The *S. Cerevisiae* HAP complex, a key regulator of mitochondrial function, coordinates nuclear and mitochondrial gene expression. COMP FUNCT GENOMICS. 4(1):37-46. doi: 10.1002/cfg.254.

Cannon JF, Tatchell K. 1987. Characterization of *Saccharomyces cerevisiae* genes encoding subunits of cyclic AMP-dependent protein kinase. MOL CELL BIOL. 7(8):2653-63. doi: 10.1128/mcb.7.8.2653-2663.1987.

Chandrasekaran K, Jayaraman J. 1978. Effect of cyclic AMP on the biogenesis of cytochrome oxidase in yeast. FEBS LETT. 87, 52– 54. doi: 10.1016/0014-5793(78)80131-8.

Cherry JM, Ball C, Weng S, Juvik G, Schmidt R, Adler C, Dunn B, Dwight S, Riles L, Mortimer RK, Botstein D.1997. Genetic and physical maps of *Saccharomyces cerevisiae*. NATURE. 387(6632 Suppl):67-73. PMID: 9169866

Corral-Debrinski M, Belgareh N, Blugeon C, Claros MG, Doye V, Jacq C. 1999. Overexpression of yeast karyopherin Pse1p/Kap121p stimulates the mitochondrial import of hydrophobic proteins *in vivo*. MOL MICROBIOL. 31(5):1499-511. doi: 10.1046/j.1365-2958.1999.01295.x.

548 Cribbs JT, Strack S. 2007. Reversible phosphorylation of Drp1 by cyclic AMP-dependent
549 protein kinase and calcineurin regulates mitochondrial fission and cell death. EMBO REP.
550 8: 939–944. doi: 10.1038/sj.embor.7401062..

551 Cruz-Torres V, Vázquez-Acevedo M, García-Villegas R, Pérez-Martínez X, Mendoza-
552 Hernández G, González-Halphen D. 2012. The cytosol-synthesized subunit II (Cox2)
553 precursor with the point mutation W56R is correctly processed in yeast mitochondria to
554 rescue cytochrome oxidase. BIOCHIM BIOPHYS ACTA. 1817(12):2128-39. doi:
555 10.1016/j.bbabio.2012.09.006.

556 Das S, Mukherjee S, Bedi M, Ghosh A. 2021. Mutations in the Yeast Cox12 Subunit
557 Severely Compromise the Activity of the Mitochondrial Complex IV. BIOCHEMISTRY
558 (MOSC). 86(12):1607-1623. doi: 10.1134/S0006297921120105.

559 Dejean L, Beauvoit B, Bunoust O, Guérin B, Rigoulet M. 2002. Activation of Ras cascade
560 increases the mitochondrial enzyme content of respiratory competent yeast. BIOCHEM
561 BIOPHYS RES COMMUN. 293(5):1383-8. doi: 10.1016/S0006-291X(02)00391-1.

562 Dennerlein S, Rehling P, Richter-Dennerlein R. 2023. Cytochrome c oxidase biogenesis -
563 from translation to early assembly of the core subunit COX1. FEBS LETT. 597(12):1569-
564 1578. doi: 10.1002/1873-3468.14671.

565 Elliott LE, Saracco SA, Fox TD. 2012. Multiple roles of the Cox20 chaperone in assembly
566 of *Saccharomyces cerevisiae* cytochrome c oxidase. GENETICS, 190(2):559-67. doi:
567 10.1534/genetics.111.135665.60

568 Fang M, Butow RA. 1970. Nucleotide reversal of mitochondrial repression in
569 *Saccharomyces cerevisiae*. BIOCHEM. BIOPHYS. RES. COMMUN. 41, 1579-1583. doi:
570 10.1016/0006-291x(70)90568-1.

571 Fiumera HL, Broadley SA, Fox TD. 2007. Translocation of mitochondrially synthesized
572 Cox2 domains from the matrix to the intermembrane space. MOL CELL BIOL.
573 27(13):4664-73. doi: 10.1128/MCB.01955-06.
574
575 Fontanesi F, Soto IC, Barrientos A. 2008. Cytochrome c oxidase biogenesis: new levels of
576 regulation. IUBMB LIFE. 60: 557-68. doi: 10.1002/iub.86.
577
578 Franco LVR, Su CH, Tzagoloff A. 2020. Modular assembly of yeast mitochondrial ATP
579 synthase and cytochrome oxidase. BIOL CHEM. 401(6-7):835-853. doi: 10.1515/hsz-
580 2020-0112.
581
582 Ghosh A, Trivedi PP, Timbalia SA, Griffin AT, Rahn JJ, Chan SS, Gohil VM. 2014. Copper
583 supplementation restores cytochrome c oxidase assembly defect in a mitochondrial
584 disease model of COA6 deficiency. HUM MOL GENET. 23(13):3596-606. doi:
585 10.1093/hmg/ddu069.

Ghosh A, Pratt AT, Soma S, Theriault SG, Griffi AT, Trivedi PP, Gohil VM. 2016. Mitochondrial disease genes COA6, COX6B and SCO2 have overlapping roles in COX2 biogenesis. HUM MOL GENET. 25(4):660-71. doi: 10.1093/hmg/ddv503.

Goitre L, Trapani E, Trabalzini L, Retta SF. 2014. The Ras superfamily of small GTPases: the unlocked secrets. METHODS MOL BIOL. 1120:1-18. doi: 10.1007/978-1-62703-791-4_1.

Gui W, Xue L, Yue J, Kuang Z, Jin Y, Niu L. 2021. Crystal structure of the complex of DNA with the C-terminal domain of TYE7 from *Saccharomyces cerevisiae*. ACTA CRYSTALLOGR F STRUCT BIOL COMMUN. 77(Pt 10):341-347. doi: 10.1107/S2053230X21009250.

Hell K, Herrmann J, Pratje E, Neupert W, Stuart RA. 1997. Oxa1p mediates the export of the N- and C-termini of pCoxII from the mitochondrial matrix to the intermembrane space. FEBS LETT. 418(3):367-70. doi: 10.1016/s0014-5793(97)01412-9.

Hell K, Tzagoloff A, Neupert W, Stuart RA. 2000. Identification of Cox20p, a novel protein involved in the maturation and assembly of cytochrome oxidase subunit 2. J BIOL CHEM. 275(7):4571-8. doi: 10.1074/jbc.275.7.4571.

Herrmann JM, Bonnefoy N. 2004. Protein export across the inner membrane of mitochondria: the nature of translocated domains determines the dependence on the Oxa1 translocase. J BIOL CHEM. 279(4):2507-12. doi: 10.1074/jbc.M310468200.

Herrmann JM, Funes S. 2005. Biogenesis of cytochrome oxidase-sophisticated assembly lines in the mitochondrial inner membrane. GENE. 354:43-52. doi: 10.1016/j.gene.2005.03.017.

Hlavatá L, Nachin L, Jezek P, Nyström T. 2008. Elevated Ras/protein kinase A activity in *Saccharomyces cerevisiae* reduces proliferation rate and lifespan by two different reactive oxygen species-dependent routes. AGING CELL. 7(2):148-57. doi: 10.1111/j.1474-9726.2007.00361.x.

Hlavatá L, Nyström T. 2003. Ras proteins control mitochondrial biogenesis and function in *Saccharomyces cerevisiae*. FOLIA MICROBIOL (PRAHA). 48(6):725-30. doi: 10.1007/BF02931505.

Holland P, Bergenholm D, Börlin CS, Liu G, Nielsen J. 2019. Predictive models of eukaryotic transcriptional regulation reveal changes in transcription factor roles and promoter usage between metabolic conditions. NUCLEIC ACIDS RES. 47(10):4986-5000. doi: 10.1093/nar/gkz253.

Horak CE, Luscombe NM, Qian J, Bertone P, Piccirrillo S, Gerstein M, Snyder M. 2002. Complex transcriptional circuitry at the G1/S transition in *Saccharomyces cerevisiae*. GENES DEV. 16(23):3017-33. doi: 10.1101/gad.1039602.

Ing G, Hartley AM, Pinotsis N, Maréchal A. 2022. Cryo-EM structure of a monomeric yeast *S. cerevisiae* complex IV isolated with maltosides: Implications in supercomplex formation. BIOCHIM BIOPHYS ACTA BIOENERG. 1863(7):148591. doi: 10.1016/j.bbabio.2022.148591.

Iqbal J,Ge'rard HC, Rahman MU, Hudson AP. 1996. A probable cis-regulatory element on yeast mitochondrial DNA responsible for cAMP-mediated transcription. CURR. GENET. 30, 493– 501. doi: 10.1007/s002940050161.

LaMarche AE, Abate MI, Chan SH, Trumpower BL. 1992. Isolation and characterization of COX12, the nuclear gene for a previously unrecognized subunit of *Saccharomyces cerevisiae* cytochrome *c* oxidase. J BIOL CHEM. 267(31): 22473-80. PMID: 1331057.

Löhning C, Ciriacy M. 1994. The TYE7 gene of *Saccharomyces cerevisiae* encodes a putative bHLH-LZ transcription factor required for Ty1-mediated gene expression. YEAST. 1994 Oct;10(10):1329-39. doi: 10.1002/yea.320101010.

Mabuchi T, Ichimura Y, Takeda M, Douglas MG. 2000. ASC1/RAS2 suppresses the growth defect on glycerol caused by the atp1-2 mutation in the yeast Saccharomyces cerevisiae. J BIOL CHEM. 275(14):10492-7. doi: 10.1074/jbc.275.14.10492.

Matsumoto K., Uno I., Ishikawa T. 1983. Control of cell division in *Saccharomyces cerevisiae* mutants defective in adenylate cyclase and cAMP-dependent protein kinase. EXP CELL RES.146(1):151-61. doi: 10.1016/0014-4827(83)90333-6.

Müller G, Bandlow W. 1987. Protein phosphorylation in yeast mitochondria: cAMP-dependence, submitochondrial localization and substrates of mitochondrial protein kinases. YEAST. 3(3):161-74. doi: 10.1002/yea.320030304.

Neuman-Silberberg FS,Bhattacharya S, Broach JR. 1995. Nutrient availability and the RAS/cyclic AMP pathway both induce expression of ribosomal protein genes in *Saccharomyces cerevisiae* but by different mechanisms. MOL CELL BIOL. 15:3187–3196. doi: 10.1128/MCB.15.6.3187.

Nishi K, Park CS, Pepper AE, Eichinger G, Innis MA, Holland MJ. 1995. The GCR1 requirement for yeast glycolytic gene expression is suppressed by dominant mutations in the SGC1 gene, which encodes a novel basic-helix-loop-helix protein. MOL CELL BIOL. 15(5):2646-53. doi: 10.1128/MCB.15.5.2646.

Nývltová E, Dietz JV, Seravalli J, Khalimonchuk O, Barrientos A. 2022. Coordination of metal center biogenesis in human cytochrome c oxidase. NAT COMMUN.13(1):3615. doi: 10.1038/s41467-022-31413-1.

669 Ould Amer Y, Hebert-Chatelain E. 2018. Mitochondrial cAMP-PKA signaling: What do we
670 really know? BIOCHIM BIOPHYS ACTA BIOENERG. 1859(9):868-877. doi:
671 10.1016/j.bbabio.2018.04.005.

672 Oulmouden A, Karst F. 1990. Isolation of the ERG12 gene of *Saccharomyces cerevisiae*
673 encoding mevalonate kinase. GENE. 88(2):253-7. doi: 10.1016/0378-1119(90)90039-t.

674 Pacheu-Grau D, Bareth B, Dudek J, Juris L, Vögtle FN, Wissel M, Leary SC, Dennerlein S,
675 Rehling P, Deckers M. 2015. Cooperation between COA6 and SCO2 in COX2 maturation
676 during cytochrome c oxidase assembly links two mitochondrial cardiomyopathies. CELL
677 METAB. 21(6):823-33. doi: 10.1016/j.cmet.2015.04.012.

678 Pacheu-Grau D, Wasilewski M, Oeljeklaus S, Gibhardt CS, Aich A, Chudenkova M,
679 Dennerlein S, Deckers M, Bogeski I. Warscheid B, Chacinska A, Rehling P. 2020. COA6
680 Facilitates Cytochrome c Oxidase Biogenesis as Thiol-reductase for Copper
681 Metallochaperones in Mitochondria. J MOL BIOL. 432(7): 2067-2079. doi:
682 10.1016/j.jmb.2020.01.036.

683 Papa S, Sardanelli AM, Cocco T, Speranza F, Scacco SC, Technikova-Dobrova Z. 1996.
684 The nuclear-encoded 18 kDa (IP) AQDQ subunit of bovine heart complex I is
685 phosphorylated by the mitochondrial cAMP-dependent protein kinase. FEBS LETT.
686 379(3): 299-301. doi: 10.1016/0014-5793(95)01532-9.

687 Papa S, Rasmo DD, Technikova-Dobrova Z, Panelli D, Signorile A, Scacco S. Petruzzella
688 V, Papa F, Palmisano, G, Gnoni A, Micelli L, Sardanelli AM. 2012. Respiratory chain
689 complex I, a main regulatory target of the cAMP/PKA pathway is defective in different
690 human diseases. FEBS LETT. 586(5): 568-77. doi: 10.1016/j.febslet.2011.09.019.

691 Poyton RO, Groot GS. 1975. Biosynthesis of polypeptides of cytochrome c oxidase by
692 isolated mitochondria. PROC NATL ACAD SCI (U S A). 72(1): 172-6. doi:
693 10.1073/pnas.72.1.172.
694
695 Poyton RO, Goehring B, Droste M, Sevarino KA, Allen LA, Zhao XJ. 1995. Cytochrome-c
696 oxidase from *Saccharomyces cerevisiae*. METHODS ENZYMOL. 260:97-116. doi:
697 10.1016/0076-6879(95)60133-3.

698 Reimand J, Vaquerizas JM, Todd AE, Vilo J, Luscombe NM. 2010. Comprehensive
699 reanalysis of transcription factor knockout expression data in *Saccharomyces cerevisiae*
700 reveals many new targets. NUCLEIC ACIDS RES. 38(14): 4768-77. doi:
701 10.1093/nar/gkq232.

702 Rich PR. 2017. Mitochondrial cytochrome *c* oxidase: catalysis, coupling and controversies.
703 BIOCHEM SOC TRANS. 45(3): 813-829. doi: 10.1042/BST20160139.

Rigby K, Cobine PA, Khalimonchuk O, Winge DR. 2008. Mapping the functional interaction of Sco1 and Cox2 in cytochrome oxidase biogenesis. J BIOL CHEM. 283(22):15015-22. doi: 10.1074/jbc.M710072200.

Robinson, K.A., Lopes, J.M. 2000. SURVEY AND SUMMARY: *Saccharomyces cerevisiae* basic helix-loop-helix proteins regulate diverse biological processes. NUCLEIC ACIDS RES., 28(7):1499-505. doi: 10.1093/nar/28.7.1499.

Robzyk K, Kassir Y. 1992. A simple and highly efficient procedure for rescuing autonomous plasmids from yeast. NUCLEIC ACIDS RESEARCH, 20(14): 3790. doi: 10.1093/nar/20.14.3790.

Rubalcava-Gracia D, Vázquez-Acevedo M, Funes S, Pérez-Martínez X, González-Halphen D. 2018. Mitochondrial versus nuclear gene expression and membrane protein assembly: the case of subunit 2 of yeast cytochrome c oxidase. MOL BIOL CELL. 29(7): 820-833. doi: 10.1091/mbc.E17-09-0560.

Rubalcava-Gracia D, García-Rincón J, Pérez-Montfort R, Hamel PP, González-Halphen D. 2019. Key within-membrane residues and precursor dosage impact the allotopic expression of yeast subunit II of cytochrome c oxidase. MOL BIOL CELL. 30(18):2358-2366. doi: 10.1091/mbc.E18-12-0788.

Saracco SA, Fox TD. 2002. Cox18p is required for export of the mitochondrially encoded *Saccharomyces cerevisiae* Cox2p C-tail and interacts with Pnt1p and Mss2p in the inner membrane. MOL BIOL CELL. 2002 13(4):1122-31. doi: 10.1091/mbc.01-12-0580.

Saini PK, Dawitz H, Aufschnaiter A, Bondarev S, Thomas J, Amblard A, Stewart J, Thierry-Mieg N, Ott M, Pierrel F. 2022. The [PSI^{+}] prion modulates cytochrome *c* oxidase deficiency caused by deletion of *COX12*. MOL BIOL CELL. 33(14):ar130. doi: 10.1091/mbc.E21-10-0499.

Sambrook J 2001. Molecular Cloning : a Laboratory Manual. Cold Spring Harbor, N.Y., Cold Spring Harbor Laboratory Press.

Sato T, Lopez MC, Sugioka S, Jigami Y, Baker HV, Uemura H. 1999. The E-box DNA binding protein Sgc1p suppresses the gcr2 mutation, which is involved in transcriptional activation of glycolytic genes in *Saccharomyces cerevisiae*. FEBS LETT. 463(3) :307-11. doi: 10.1016/s0014-5793(99)01654-3.

Servant G, Pinson B, Tchalikian-Cosson A, Coulpier F, Lemoine S, Pennetier C, Bridier-Nahmias A, Todeschini AL, Fayol H, Daignan-Fornier B, Lesage P. 2012. Tye7 regulates yeast Ty1 retrotransposon sense and antisense transcription in response to adenylic nucleotides stress. NUCLEIC ACIDS RES., 40(12): 5271-82. doi: 10.1093/nar/gks166.

748 Sevarino KA, Poyton RO. 1980. Mitochondrial Membrane Biogenesis: Identification of a
749 Precursor to Yeast Cytochrome c Oxidase Subunit II, an Integral Polypeptide.
750 PROCEEDINGS OF THE NATIONAL ACADEMY OF SCIENCES (USA) 77:142–146. doi:
751 10.1073/pnas.77.1.142.
752
753 Stettler S, Chiannilkulchai N, Hermann-Le Denmat S, Lalo D, Lacroute F, Sentenac A,
754 Thuriaux P. 1993. A general suppressor of RNA polymerase I, II and III mutations in
755 *Saccharomyces cerevisiae*. MOLECULAR & GENERAL GENETICS 239(1-2): 169–176.
756 doi: 10.1007/BF00281615.
757
758 Supekova L, Supek F, Greer JE, Schultz PG. 2010. A single mutation in the first
759 transmembrane domain of yeast COX2 enables its allotopic expression. PROC. NATL.
760 ACAD. SCI. (USA) 107: 5047-5052. doi: 10.1073/pnas.1000735107.

761 Swiegers JH, Pretorius IS, Bauer FF. 2006. Regulation of respiratory growth by Ras: the
762 glyoxylate cycle mutant, cit2Delta, is suppressed by RAS2. CURR GENET. 50(3):161-71.
763 doi: 10.1007/s00294-006-0084-z.

764 Tatchell K, Robinson LC, Breitenbach M. 1985. RAS2 of *Saccharomyces cerevisiae* is
765 required for gluconeogenic growth and proper response to nutrient limitation.
766 PROCEEDINGS OF THE NATIONAL ACADEMY OF SCIENCES (USA). 82(11):3785–
767 3789. doi: 10.1073/pnas.82.11.3785.

768 Teixeira MC, Viana R, Palma M, Oliveira J, Galocha M, Mota MN, Couceiro D, Pereira
769 MG, Antunes M, Costa IV, Pais P, Parada C, Chaouiya C, Sá-Correia I, Monteiro PT.
770 2023. YEASTRACT+: a portal for the exploitation of global transcription regulation and
771 metabolic model data in yeast biotechnology and pathogenesis. NUCLEIC ACIDS RES.
772 51(D1): D785-D791. doi: 10.1093/nar/gkac1041.

773 Tisi R, Belotti F, Martegani E. 2014. Yeast as a model for Ras signaling. METHODS MOL
774 BIOL. 1120:359-390. doi: 10.1007/978-1-62703-791-4_23.
775
776 Torello AT, Overholtzer MH, Cameron VL, Bonnefoy N, Fox TD. 1997. Deletion of the
777 leader peptide of the mitochondrially encoded precursor of *Saccharomyces cerevisiae*
778 cytochrome *c* oxidase subunit II, GENETICS 145: 903-910. doi:
779 10.1093/genetics/145.4.903.
780
781 Yoboue ED, Augier E, Galinier A, Blancard C, Pinson B, Casteilla L, Rigoulet M, Devin A.
782 2012. cAMP-induced mitochondrial compartment biogenesis: role of glutathione redox
783 state. J BIOL CHEM. 287(18):14569-14578. doi: 10.1074/jbc.M111.302786.
784

785 **LEGENDS TO FIGURES**

786 Figure 1. **Ten transformants (MS01 to MS10) exhibited a significant improvement in**
787 **their respiratory growth and increased levels of mature Cox2 subunit. A)** Serial
788 dilution series at 30 ˚C showing the fermentative (glucose) and respiratory

(ethanol/glycerol and lactate) growth phenotype of a wild-type strain (wt), the Δ***cox2*** + ***n****COX2*^{W56R} strain (***n****COX2*^{W56R}), and the 10 strains (MS01 to MS10) obtained after transformation with the multicopy genomic library. Photographs were taken on the fourth day of growth. **B and C)** Antibodies against Cox2 and Zwf1 were used to immunodetect the corresponding proteins in total cellular extracts of the indicated yeast strains: the Δ***cox2*** + ***n****COX2*^{W56R} strain (***n***), the control strain transformed with an empty vector (***n*** + EV), and the 10 transformants (MS01 to MS10). The precursor (p) and mature (m) forms of Cox2^{W56R} are indicated. The anti-Zw1 antibody immunoreacts against a 57 kDa band which is used as a loading control.

Figure 2. **Three distinct chromosomal fragments are present in the multicopy plasmids in transformants M01 to M09.** The scheme depicts the genomic fragments from chromosomes XV, XIV and XII (with corresponding coordinates) cloned in pFL44L-based plasmids carried by the selected transformants and the ORFs present in each one of them (gray and light blue boxes). The three candidate ORFs selected for further analysis are shown in light blue color *TYE7*, *RAS2*, and *COX12*.

Figure 3. **Overexpression of the *TYE7*, *RAS2*, and *COX12* genes affects the growth of a strain expressing the *COX2*^{W56R} gene from the nucleus. A)** Serial dilution series showing the fermentative (glucose) and respiratory (ethanol/glycerol, ethanol, and lactate) growth phenotypes of a wild-type strain (wt), the Δ***cox2*** + ***n***^{uv}*COX2*^{W56R} strain (***n***^{uv}*COX2*^{W56R}) obtained after UV mutagenesis, and the three strains overexpressing (↑) the indicated gene or carrying the empty vector (EV) in the ***n***^{uv}*COX2*^{W56R} background at 30 °C. Photographs were taken on the fourth day (upper panels) and on the seventh day of growth (lower panels). **B)** Antibodies against Cox2 and Zwf1 were used to immunodetect the corresponding proteins in total cellular extracts of the indicated yeast strains: wild type (wt); the Δ***cox2*** + ***n***^{uv}*COX2*^{W56R} strain (***n***), the three strains overexpressing (↑) the indicated gene on a ***n***^{uv}*COX2*^{W56R} background, and the control strain transformed with an empty vector (***n*** ^{uv}+ EV). The mature proteins Cox2 or Cox2^{W56R} (28 kDa) are indicated. The anti-Zw1 antibody immunoreacts against a 57 kDa band which is used as a loading control. Quantification of technical replicates of immunoblots are represented by bar plots (mean ± SD, n = 3). Black and grey dotted lines indicate the mean and SD abundance of the wild-type protein. ***Δcox2*** data is not displayed.

Figure 4. **Overexpression of the *TYE7*, *RAS2*, and *COX12* genes enhance the respiratory growth of a strain expressing the *COX2*^{W56R} gene from a centromeric plasmid. A)** Serial dilution series showing the fermentative (glucose) and respiratory (ethanol/glycerol, ethanol, and lactate) growth phenotypes of a wild-type strain (wt), the Δ***cox2*** + ***cen****COX2*^{W56R} strain (***cen****COX2*^{W56R}), and the three strains overexpressing (↑) the indicated gene or carrying the empty vector (EV) in the ***cen****COX2*^{W56R} background at 30 °C. Photographs were taken on the fourth day (upper panels) and on the seventh day of growth (lower panels). **B)** Antibodies against Cox2 and Zwf1 were used to immunodetect the corresponding proteins in total cellular extracts of the indicated yeast strains: wild type (wt); the Δ***cox2*** + ***cen****COX2*^{W56R} strain (***cen***), the three strains overexpressing (↑) the indicated gene on a ***cen****COX2*^{W56R} background, and the control strain transformed with an empty vector (***cen*** + EV). The mature proteins Cox2 or Cox2^{W56R} (28 kDa) are indicated. The anti-Zw1 antibody immunoreacts against a 57 kDa band which is used as a loading control. Quantification of technical replicates of immunoblots are represented by bar plots (mean ± SD, n = 3). Black and grey dotted lines indicate the mean and SD abundance of the wild-type protein. ***Δcox2*** data is not displayed.

LEGENDS TO SUPPLEMENTARY FIGURES:

Figure S1. **Overexpression of the *TYE7*, *RAS2*, and *COX12* genes does not improve the growth of a strain expressing the *COX2*^{W56R} gene from the nucleus.** Serial dilution series showing the fermentative (glucose) and respiratory (lactate) growth phenotypes of a wild-type strain (wt), the Δ*cox2* + ***n****COX2*^{W56R} strain (***n****COX2*^{W56R}), and the three strains overexpressing (↑) the indicated gene cloned in the pMK2 vector or carrying the empty vector (EV) in the ***n****COX2*^{W56R} background at 30 °C. Photographs were taken on the seventh day of growth. Only lactate-dependent growth is shown, but no improvement was observed on ethanol/glycerol.

Figure S2. **Overexpression of the *TYE7*, *RAS2*, and *COX12* genes affects the growth of a strain expressing the *COX2*^{W56R} gene from a multicopy plasmid. A)** Serial dilution series showing the fermentative (glucose) and respiratory (ethanol/glycerol and lactate) growth phenotypes of a wild-type strain (wt), the Δ*cox2* + ***e****COX2*^{W56R} strain (***e****COX2*^{W56R}) expressing the allotopic construct from a multicopy vector and the three strains overexpressing (↑) the indicated gene or carrying the empty vector (EV) in the ***e****COX2*^{W56R} background at 30 °C. Photographs were taken on the fourth (*upper panels*) and on the seventh day of growth (*lower panels*). **B)** Antibodies against Cox2 and Zwf1 were used to immunodetect the corresponding proteins in total cellular extracts of the indicated yeast strains: wild type (wt); the Δ*cox2* + ***e****COX2*^{W56R} strain (***e***), the three strains overexpressing (↑) the indicated gene on a ***e****COX2*^{W56R} background, and the control strain transformed with an empty vector (***e*** + EV). The precursor and mature proteins Cox2 or Cox2^{W56R} (28 kDa) are indicated. The anti-Zw1 antibody immunoreacts against a 57 kDa band which is used as a loading control. Quantification of technical replicates of immunoblots are represented by bar plots (mean ± SD, n = 3). Black and grey dotted lines indicate the mean and SD abundance of the wild-type protein. ***Δcox2*** data is not displayed.

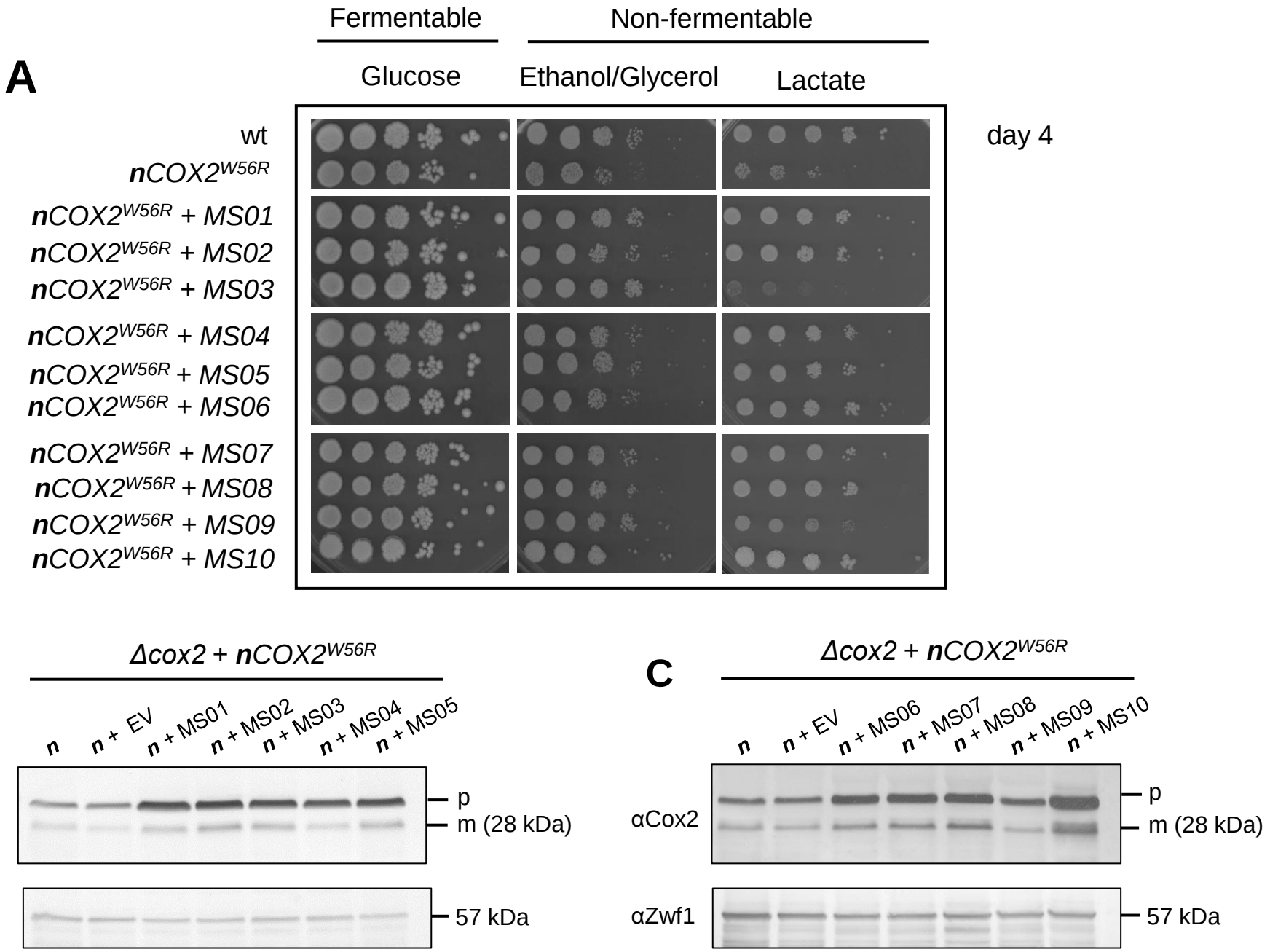
A
Fermentable
Non-fermentable
Glucose
Ethanol/Glycerol
Lactate
wt
nCOX2W56R
nCOX2W56R + MS01
nCOX2W56R + MS02
nCOX2W56R + MS03
nCOX2W56R + MS04
nCOX2W56R + MS05
nCOX2W56R + MS06
nCOX2W56R + MS07
nCOX2W56R + MS08
nCOX2W56R + MS09
nCOX2W56R + MS10
day 4
B
Δcox2 + nCOX2W56R
n
n + EV
n + MS01
n + MS02
n + MS03
n + MS04
n + MS05
αCox2
p
m (28 kDa)
αZwf1
57 kDa
C
Δcox2 + nCOX2W56R
n
n + EV
n + MS06
n + MS07
n + MS08
n + MS09
n + MS10
αCox2
p
m (28 kDa)
αZwf1
57 kDa

Figure 1

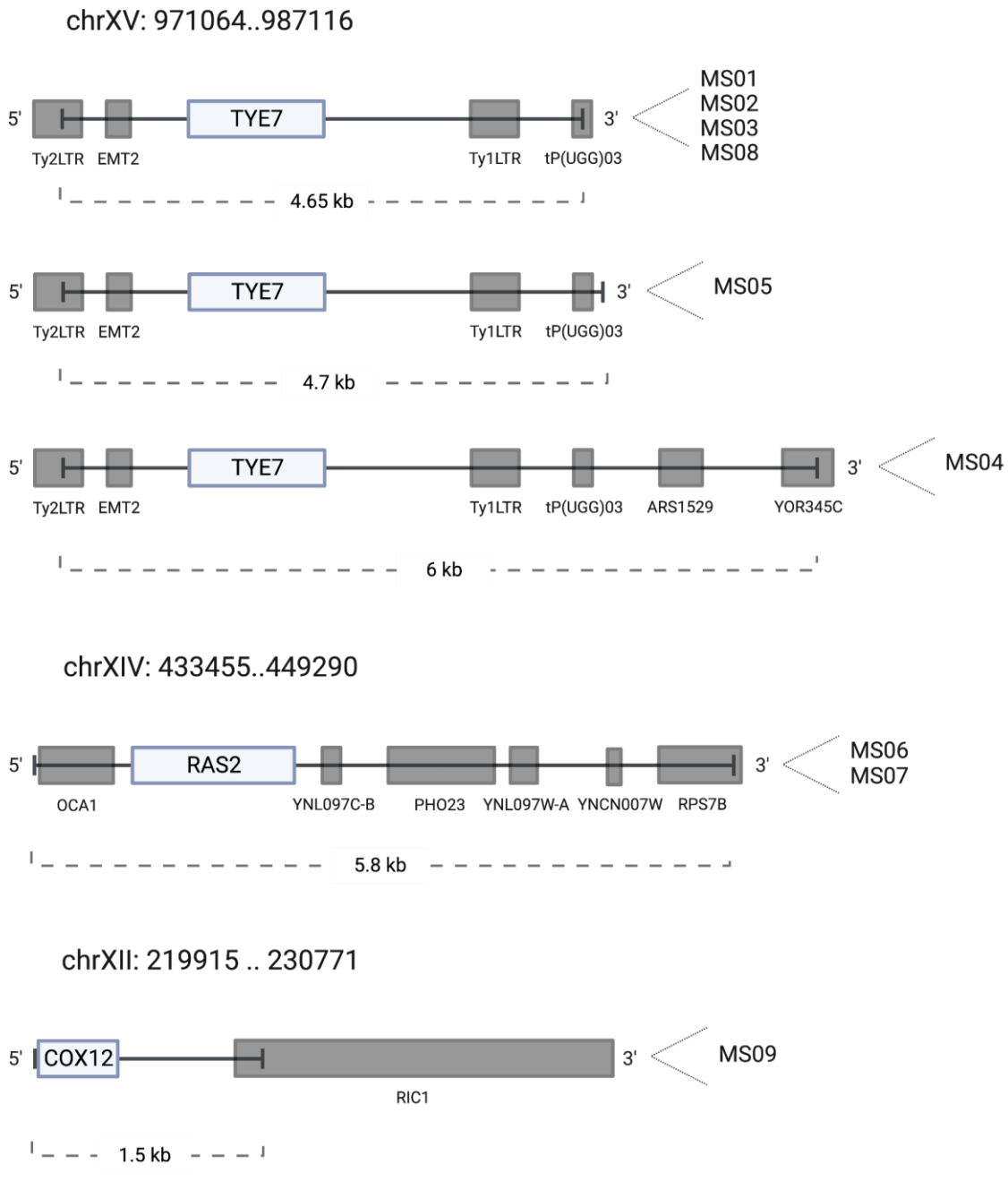
chrXV: 971064..987116
5'
TYE7
3'
MS01
MS02
MS03
MS08
Ty2LTR
EMT2
Ty1LTR
tP(UGG)03
4.65 kb
5'
TYE7
3'
MS05
Ty2LTR
EMT2
Ty1LTR
tP(UGG)03
4.7 kb
5'
TYE7
3'
MS04
Ty2LTR
EMT2
Ty1LTR
tP(UGG)03
ARS1529
YOR345C
6 kb
chrXIV: 433455..449290
5'
RAS2
3'
MS06
MS07
OCA1
YNL097C-B
PHO23
YNL097W-A
YNCN007W
RPS7B
5.8 kb
chrXII: 219915 .. 230771
5'
COX12
3'
MS09
RIC1
1.5 kb

Figure 2

A

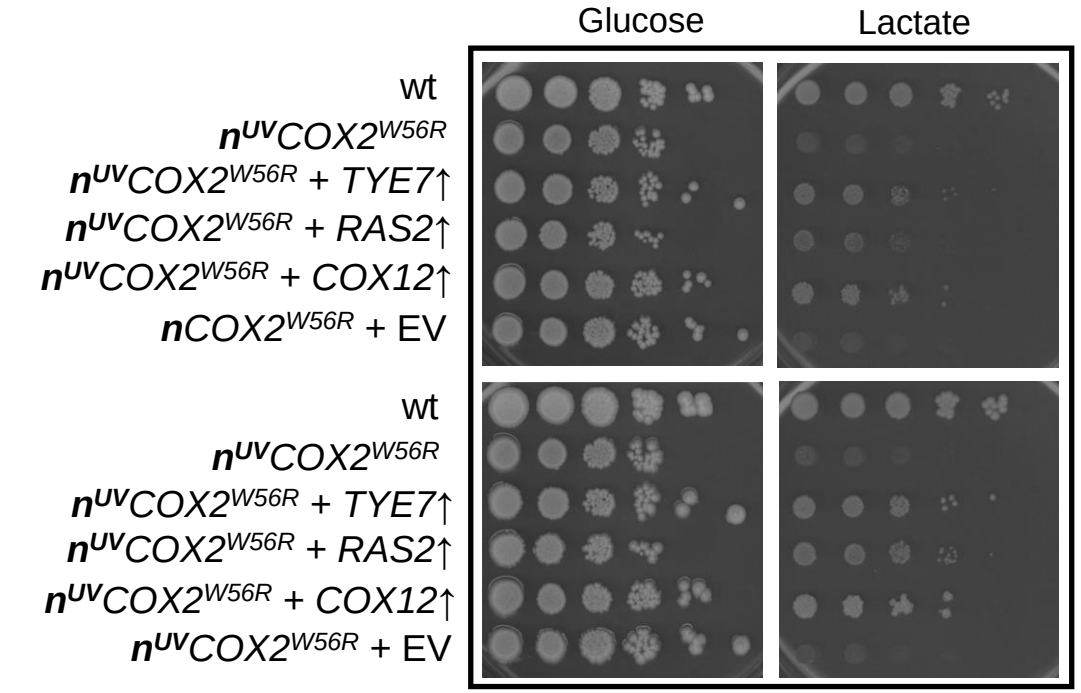
Glucose
Lactate
wt
n^UV COX2^W56R
n^UV COX2^W56R + TYE7↑
n^UV COX2^W56R + RAS2↑
n^UV COX2^W56R + COX12↑
nCOX2^W56R + EV
day 4
wt
n^UV COX2^W56R
n^UV COX2^W56R + TYE7↑
n^UV COX2^W56R + RAS2↑
n^UV COX2^W56R + COX12↑
n^UV COX2^W56R + EV
day 7

B

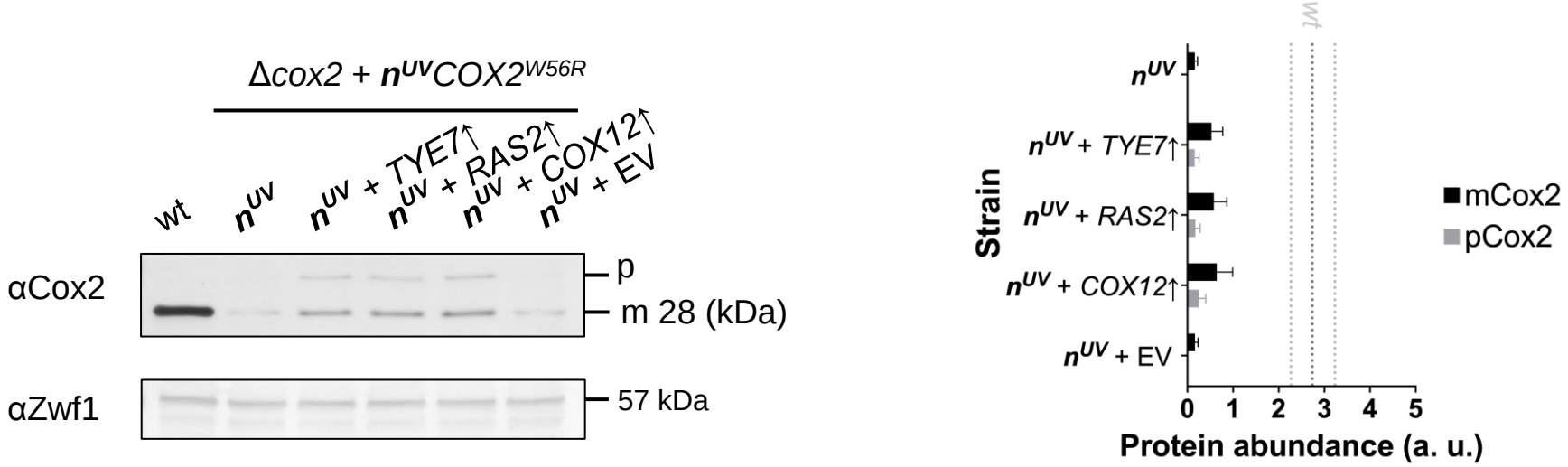
Δcox2 + n^UV COX2^W56R
wt
n^UV
n^UV + TYE7↑
n^UV + RAS2↑
n^UV + COX12↑
n^UV + EV
αCox2
p
m 28 (kDa)
αZwf1
57 kDa
wt
Strain
n^UV
n^UV + TYE7↑
n^UV + RAS2↑
n^UV + COX12↑
n^UV + EV
mCox2
pCox2
0 1 2 3 4 5
Protein abundance (a. u.)

Figure 3

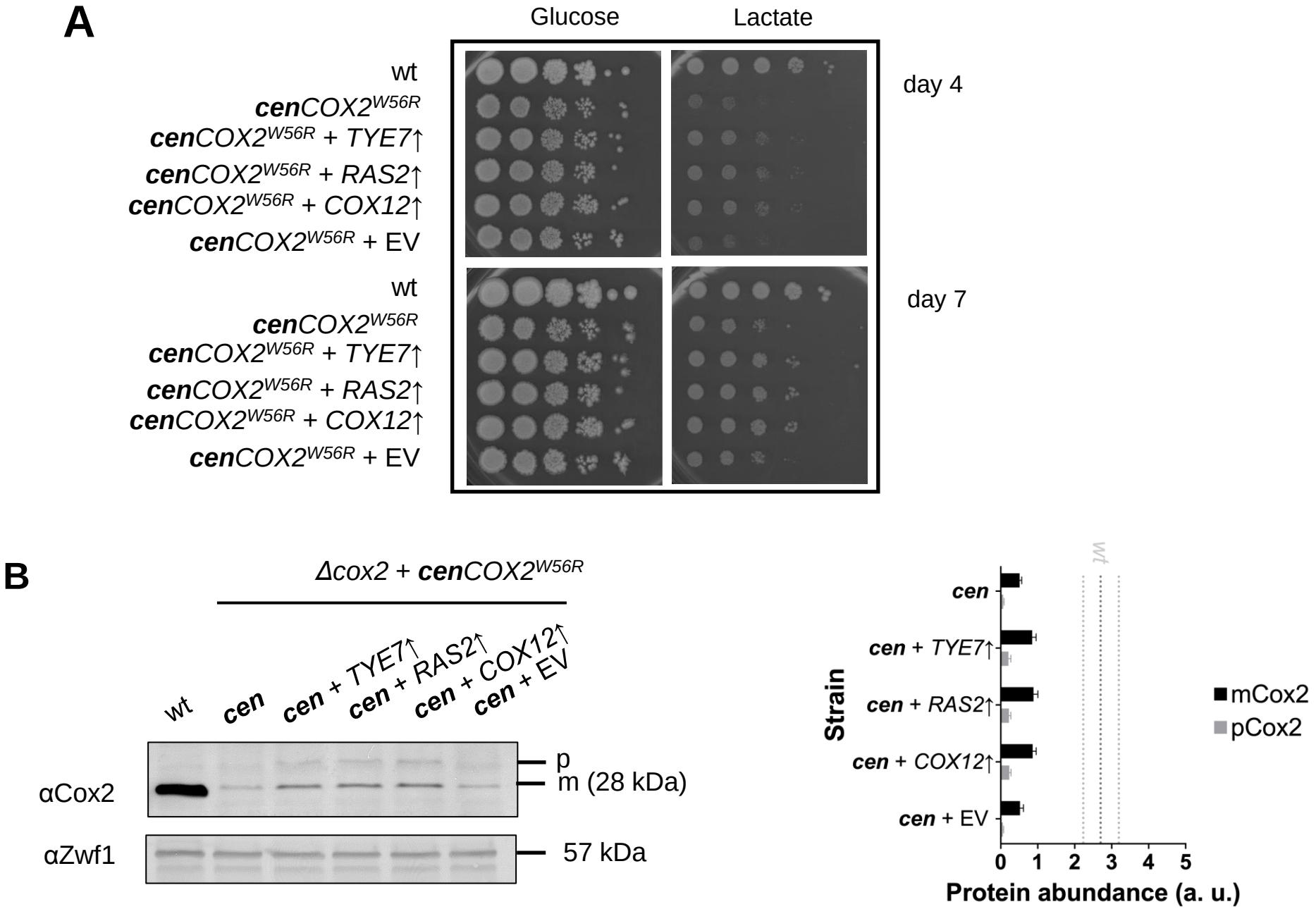
A
Glucose
Lactate
wt
cenCOX2W56R
cenCOX2W56R + TYE7↑
cenCOX2W56R + RAS2↑
cenCOX2W56R + COX12↑
cenCOX2W56R + EV
day 4
wt
cenCOX2W56R
cenCOX2W56R + TYE7↑
cenCOX2W56R + RAS2↑
cenCOX2W56R + COX12↑
cenCOX2W56R + EV
day 7
B
Δcox2 + cenCOX2W56R
wt
cen
cen + TYE7↑
cen + RAS2↑
cen + COX12↑
cen + EV
αCox2
αZwf1
p
m (28 kDa)
57 kDa
wt
cen
cen + TYE7↑
cen + RAS2↑
cen + COX12↑
cen + EV
Strain
0 1 2 3 4 5
Protein abundance (a. u.)
mCox2
pCox2

Figure 4